Sustainable Convergence of Electricity and Transport Sectors in the Context of Integrated Energy Systems

by

Amirhossein Hajimiragha

A thesis
presented to the University of Waterloo
in fulfillment of the
thesis requirement for the degree of
Doctor of Philosophy
in
Electrical and Computer Engineering

Waterloo, Ontario, Canada, 2010

I hereby declare that I am the sole author of this thesis. This is a true copy of the thesis, including any required final revisions, as accepted by my examiners.

I understand that my thesis may be made electronically available to the public.

Abstract

Transportation is one of the sectors that directly touches the major challenges that energy utilities are faced with, namely, the significant increase in energy demand and environmental issues. In view of these concerns and the problems with the supply of oil, the pursuit of alternative fuels for meeting the future energy demand of the transport sector has gained much attention.

The future of transportation is believed to be based on electric drives in fuel cell vehicles (FCVs) or plug-in electric vehicles (PEVs). There are compelling reasons for this to happen: the efficiency of electric drive is at least three times greater than that of combustion processes and these vehicles produce almost zero emissions, which can help relieve many environmental concerns. The future of PEVs is even more promising because of the availability of electricity infrastructure. Furthermore, governments around the world are showing interest in this technology by investing billions of dollars in battery technology and supportive incentive programs for the customers to buy these vehicles. In view of all these considerations, power systems specialists must be prepared for the possible impacts of these new types of loads on the system and plan for the optimal transition to these new types of vehicles by considering the electricity grid constraints.

Electricity infrastructure is designed to meet the highest expected demand, which only occurs a few hundred hours per year. For the remaining time, in particular during off-peak hours, the system is underutilized and could generate and deliver a substantial amount of energy to other sectors such as transport by generating hydrogen for FCVs or charging the batteries in PEVs. This thesis investigates the technical and economic feasibility of improving the utilization of electricity system during off-peak hours through alternative-fuel vehicles (AFVs) and develops optimization planning models for the transition to these types of vehicles. These planning models are based on decomposing the region under study into different zones, where the main power generation and electricity load centers are located, and considering the major transmission corridors among them.

An emission cost model of generation is first developed to account for the environmental impacts of the extra load on the electricity grid due to the introduction of AFVs. This is followed by developing a hydrogen transportation model and, consequently, a comprehensive optimization model for transition to FCVs in the context of an integrated electricity and hydrogen system. This model can determine the optimal size of the hydrogen production plants to be developed in different zones in each year, optimal hydrogen transportation routes and ultimately bring about hydrogen economy penetration. This model is also extended to account for optimal transition to plug-in hybrid electric vehicles (PHEVs). Different aspects of the proposed transition models are discussed on a developed 3-zone test system.

The practical application of the proposed models is demonstrated by applying them to Ontario, Canada, with the purpose of finding the maximum potential penetrations of AFVs into Ontario's transport sector by 2025, without jeopardizing the reliability of the grid or developing new infrastructure. Applying the models to this real-case problem requires the development of models for Ontario's transmission network, generation capacity and base-load demand during the planning study. Thus, a zone-based model for Ontario's transmission network is developed relying on major 500 and 230 kV transmission corridors. Also, based on Ontario's Integrated Power System Plan (IPSP) and a variety of information provided by the Ontario Power Authority (OPA) and Ontario's Independent Electricity System Operator (IESO), a zonal pattern of base-load generation capacity is proposed.

The optimization models developed in this study involve many parameters that must be estimated; however, estimation errors may substantially influence the optimal solution. In order to resolve this problem, this thesis proposes the application of robust optimization for planning the transition to AFVs. Thus, a comprehensive sensitivity analysis using Monte Carlo simulation is performed to find the impact of estimation errors in the parameters of the planning models; the results of this study reveals the most influential parameters on the optimal solution. Having a knowledge of the most affecting parameters, a new robust optimization approach is applied to develop robust counterpart problems for planning models. These mod-

els address the shortcoming of the classical robust optimization approach where robustness is ensured at the cost of significantly losing optimality. The results of the robust models demonstrate that with a reasonable trade-off between optimality and conservatism, at least 170,000 FCVs or 900,000 PHEVs with 30 km all-electric range (AER) can be supported by Ontario's grid by 2025 without any additional grid investments.

Acknowledgments

First, I would like to dedicate my sincere thanks to my supervisor Professor Claudio A. Cañizares for his trust, support and guidance at every stage of my PhD studies. I would also like to express my deep gratitude to Professor Michael W. Fowler for all his help and support as my co-supervisor. Their professionalism and dedication have always been inspiring for me, and working with them has been a truly enriching experience.

I would like to acknowledge the following members of my comprehensive or examination committees for their valuable comments and input: Professor Francisco D. Galiana from McGill University; Professor Miguel F. Anjos from the Management Sciences Department at the University of Waterloo, and Professors Kankar Bhattacharya and Mehrdad Kazerani from the Electrical and Computer Engineering Department at the University of Waterloo. I also wish to thank Professor Juan Vera for agreeing to serve on my examination committee.

A very special word of thanks goes to Professors Ali Elkamel and Kankar Bhattacharya for their exceptional understanding, kindness and support as well as the helpful discussions I was privileged to have with them. One of my greatest experiences at the University of Waterloo has been the opportunity to become acquainted with them. I admire their bright wisdom and their strength of character.

I would like to convey my sincere thanks to Ms. Somayeh Moazeni for her constructive comments and for sharing valuable conceptual insights in the area of mathematical programming.

I acknowledge the Natural Sciences and Engineering Research Council (NSERC) of Canada, Mathematics of Information Technology and Complex Systems (MITACS) and Bruce Power for providing the funding necessary to carry out this research.

I extend my most heartfelt gratitude to my beloved mother, father, brother and aunt for their unconditional love and support.

I owe my loving thanks to my wife Sara for being with me in all the ups and downs and for the many sacrifices she has made to support me in undertaking my doctoral studies; thank you Sara for your understanding and your endless love.

I warmly thank my friends in the Electricity Market Simulation and Optimization Lab who have given me a great deal of support and provided a pleasant work environment in the years of my studies. I am tempted to individually thank all of them but as the list might be too long and for fear I might omit someone, it will suffice to mention the name of my dear friend Mohammad, and thank him for his constant presence and kind words.

I wish to express my warm and sincere thanks to Mr. Barazandeh, my high school Mathematics teacher whose kindness and encouragement have kept me going through all these years.

Finally, and most importantly, I would like to thank the Almighty God who has been the major source of strength, knowledge and wisdom to make this thesis possible.

Dedication

This thesis is dedicated to my loving family, including my wife Sara, my mother Esmat, my father Mansour, and my brother Hesam.

Contents

List of Figures

List of Tables

List of Abbreviations

ADI	:	Average Deviation Index
AER	:	All-Electric-Range
AFV	:	Alternative-Fuel Vehicle
AMPL	:	A Modeling Language for Mathematical Programming
BPV	:	Battery-Powered Vehicle
CAD	:	Canadian Dollar
CDM	:	Conservation and Demand Management
CHP	:	Combined Heat and Power
EC	:	Emission Constraint
FCV	:	Fuel Cell Vehicle
FIT	:	Feed-In Tariff
GEGEA	:	Green Energy and Green Economy Act
GHG	:	GreenHouse Gas
GV	:	Gasoline Vehicle
HEV	:	Hybrid Electric Vehicle
HHV	:	Higher Heating Value
HOEP	:	Hourly Ontario Energy Price
HPP	:	Hydrogen Production Plant
HVDC	:	High Voltage Direct Current
ICE	:	Internal Combustion Engine
IESO	:	Independent Electricity System Operator
IPSP	:	Integrated Power System Plan

IRR	:	Internal Rate of Return
LDV	:	Light-Duty Vehicle
MILP	:	Mixed Integer Linear Programming
NE	:	North East
NP	:	Non-deterministic Polynomial-time
NPV	:	Net Present Value
NUG	:	Non-Utility Generation
NW	:	North West
OPA	:	Ontario Power Authority
PEV	:	Plug-in Electric Vehicle
PHEV	:	Plug-in Hybrid Electric Vehicle
PI	:	Profitability Index
PV	:	PhotoVoltaic
SCC	:	Social Cost of Carbon
SIL	:	Surge Impedance Loading
SMES	:	Superconducting Magnetic Energy System
SMR	:	Steam Methane Reforming
SUV	:	Sport Utility Vehicle
SW	:	South West
USD	:	United States Dollar
V2G	:	Vehicle-to-Grid

Nomenclature

Indexes

Symbol	Definition
c	Index for vehicle type
e	Index for constraint under uncertainty
i, j	Index for zones
m	Index for Monte Carlo simulation
v	Index for uncertain parameter
y, k	Index for year
τ, ω	Index for time period
ω_1	Index for the time period corresponding to weekday hours
ω_2	Index for the time period corresponding to weekend hours

Sets

Symbol	Definition
E	Set of constraints subject to uncertainty
L	Set of voltage angle blocks
U	Set of uncertainty
V	Set of total uncertain parameters
V_e	Set of uncertain parameters in constraint e

VT	Set of different types of light-duty vehicles
X	Set of mixed integer feasible solution
Y	Set of planning years
Y_1	Set of planning years excluding the first year
Z	Set of zones
Z^*	Set of hydrogen transfer corridors
Ψ	Set of time periods
Ω	Set of transmission lines

Parameters

Symbol	Definition
AM	Annual mileage (km)
b_{ijy}	Line susceptance (p.u.)
CC_{cab}	Capital cost of cab (CAD)
CC_{tube}	Capital cost of tube trailers (CAD)
Cf_y	Correction factor
CF_{hpp}	Average capacity factor of HPPs (%)
$Chpp_{iy}$	Local required capacity of HPPs (MW)
$\overline{CT}$	Maximum capacity of each compressed gas truck (ton)
d_{ij}	Approximate distance between zones (km)
DR	Discount rate (%)
DT	PHEVs' daily trip running on battery (km)
E_{CO_2}	Constant value of CO_2 emissions from burning gasoline (kg/litre)
ER_{chp_i}	Emission rate of CHP plants (ton/MWh)
ER_{coal_i}	Emission rate of coal plants (ton/MWh)
FE_{fcv}	Fuel economy of the fuel cell vehicle (km/kg)
$FE_{gv_{cy}}$	Fuel economy of the gasoline vehicle (km/litre)
g_{ijy}	Line conductance (p.u.)
h	Number of off-peak hours

h_{wd}	Number of HPPs operation hours in weekdays
h_{we}	Number of HPPs operation hours in weekends
H	Last year of the planning horizon
HHV	Higher heating value of hydrogen (kWh/kg)
LF	Linking factor (ton/day.MW)
LT_{cab}	Lifetime of cab (year)
LT_{tube}	Lifetime of tube trailer (year)
M	Number of Monte Carlo simulations
$Nldv_{iy}$	Total number of light-duty vehicles
OC_y	Operation cost of compressed gas truck (CAD/km)
p_e	Threshold probability of constraint e
P_{e_y}	Total base-load electricity demand (MW)
$P^{\tau}_{e_{iy}}$	Zonal base-load electricity demand (MW)
$\overline{P_{g_{iy}}}$	Maximum available generation power (MW)
$\underline{P_{g_{iy}}}$	Lower bound of zonal generation power (MW)
$\overline{P_{ga_{iy}}}$	Maximum capacity of non-polluting generation resources (MW)
$\overline{P_{gb_{iy}}}$	Maximum capacity of non-polluting plus CHP generation resources (MW)
$\overline{P_{hpp_{iy}}}$	Maximum size of HPPs (MW)
$\overline{P_{miy}}$	Upper bound of imported power (MW)
$\underline{P_{m_{iy}}}$	Lower bound of imported power (MW)
$\overline{P_{xiy}}$	Upper bound of exported power (MW)
$\underline{P_{x_{iy}}}$	Lower bound of exported power (MW)
Pch_{iy}	Total maximum PHEVs charging power
$\overline{Pd_{ijy}}$	Maximum capacity of transmission corridor for direct power flow (MW)
$\overline{Pr_{ijy}}$	Minimum capacity of transmission corridor for reverse power flow (MW)
PS	Planning span (year)
s_{ev}	Scaled deviation
S_{cab_y}	Salvage value of cab (% of initial cost)
S_{tube_y}	Salvage value of tube trailer (% of initial cost)
$SC_{CO_2}p$	Social cost of CO_2 emission in the population area (CAD/ton)

SC_{CO_2g}	Social cost of CO_2 emission of generation (CAD/ton)
$\overline{TH}$	Upper bound of transferred hydrogen (ton/day)
$\underline{TH}$	Lower bound of transferred hydrogen (ton/day)
VS_c	Percent share of vehicle
y_1	First year of the planning horizon
$\alpha_{ijy}(l)$	Slope of the lth block of voltage angle (MW/rad)
γ_i	Annual peak-load demand growth rate (%)
Γ_e	Budget of uncertainty
$\Delta\delta_y$	Upper bound of each angle block (rad)
$\Delta\eta_{hpp}$	Efficiency improvement of the HPPs over the planning horizon
$\overline{\Delta P_{hpp_{iy}}}$	Maximum annual development of HPPs (MW)
ϵ_a, ϵ_b	Small positive numbers
ε_t	Constraint violation probability (%)
η^b_{hpp}	Base efficiency of HPPs at the beginning of the planning horizon
λ_i	Annual base-load demand growth rate (%)
$\bar{\mu}_y$	Maximum possible AFV penetration (%)
π_y	Internal or hourly Ontario energy price (CAD/MWh)
π_{m_y}	Import electricity price (CAD/MWh)
π_{x_y}	Export electricity price (CAD/MWh)
ρ	Size of the relative perturbation (%)
σ	Ratio of base-load to peak-load growth rates

Variables

Symbol	Definition
FF_{iy}	Feasibility factor
K^{τ}_{liy}	Binary variable to denote if the average zonal generation power is located in the lth segment of the emission cost curve ($l = 1, 2, 3$)
N_{ijy}	Integer number of required compressed gas trucks or tube trailers with the capacity of $\overline{CT}$

NT_y	Total number of compressed gas trucks or tube trailers with the capacity of $\overline{CT}$
p_e, q_{ev}, r_v	Additional continuous variables used to develop robust counterpart problems
$P^{\tau}_{g_{iy}}$	Average zonal generation power (MW)
$P^{\tau}_{gl_{iy}}$	Continuous auxiliary variable for the average zonal generation power ($l = 1, 2, 3$)
$P^{\tau}_{l_{iy}}$	Total base-load electricity demand including HPPs or PHEVs (MW)
$P_{m_{iy}}$	Zonal imported power (MW)
$P_{x_{iy}}$	Zonal exported power (MW)
PC_k	Integer number of purchased cabs
Ph_{iy}	Local required capacity of HPPs (MW)
$Phpp_{iy}$	Total installed HPP capacity (MW)
$Ploss_{ij}$	Power loss (MW)
Ps_{ijy}	Contribution of zone i in total required power of HPPs in zone j (MW)
PT_k	Integer number of purchased compressed gas trucks or tube trailers with the capacity of $\overline{CT}$
TH_{ijy}	Transferred hydrogen (ton/day)
V^{τ}_{liy}	Continuous auxiliary variable for $K^{\tau}_{liy}P^{\tau}_{g_{iy}}$ ($l = 1, 2, 3$)
W	Continuous variable used to represent all the uncertain parameters in the constraints of the robust counterpart problem
β_{ijy}	Binary variable to denote if there is transferred hydrogen between zones
δ^{τ}_{iy}	Voltage angle (rad)
δ^{τ}_{ijy}	Voltage angle difference (rad)
$\delta^{\tau}_{ijy}(l)$	Value of the lth block of voltage angle (rad)
$\delta^{\tau+}_{ijy}$, $\delta^{\tau-}_{ijy}$	Nonnegative variables used to linearize the absolute value $\left\|\delta^{\tau}_{iy} - \delta^{\tau}_{jy}\right\|$ (rad)
$\mu^{\tau}_{ijy}(l)$	Binary variable to denote if the value of the lth voltage angle block is equal to its maximum value $\Delta\delta_y$

Chapter 1

Introduction

1.1 Research Motivation

Currently, energy utilities are presented with the challenges of increased energy demand and the need to immediately address environmental concerns such as climate change. Due to population and economic growth, the global demand for energy is expected to increase by 50% over the next 25 years [1, 2]. This significant demand increase along with the dwindling supply of fossil fuels has raised concerns about the environment and the security of the energy supply.

The transport sector is one of the largest and fastest growing contributors to energy demand, urban air pollution and greenhouse gases; for example, in Canada, the transport sector represents almost 35% of the total energy demand and is the second highest source of greenhouse gas emissions [3, 4]. In view of these facts and the challenges associated with the supply of oil, the issue of alternative fuels for meeting the future energy demand of the transport sector has gained notable attention.

Owing to the increased energy demand and environmental concerns, different approaches such as distributed generation and demand-side management have been proposed and are widely being put into practice (e.g., [5]–[8]). However, the optimal

utilization of the existing energy infrastructure is an issue that also ought to be properly addressed to deal with the major challenges that energy utilities are facing; this is the main objective of this thesis. The electric grid, which is a strategic asset, can be mentioned as an example. This infrastructure is designed to meet the highest expected demand, which occurs only a few hundred hours per year, at most about 5% of the time. For the remaining time, in particular during off-peak hours, namely 11 pm to 7 am, the system is underutilized and could generate and deliver a substantial amount of energy to other sectors such as transport without jeopardizing the reliability of the system. This unutilized generation capacity can be used efficiently in hydrogen production for use by fuel cell vehicles (FCVs) or for charging the batteries in plug-in electric vehicles (PEVs), such as hybrid vehicles (PHEVs) or battery-powered vehicles (BPVs), with zero or very low emissions in populated areas; this is the main reason that FCVs and PEVs have received critical attention in recent years.

The introduction of alternative-fuel vehicles (AFVs), such as FCVs and PEVs, improves the utilization and efficiency of the existing electricity grids and also helps for further development of renewable energy resources in the future. The environmental benefits of renewable energy resources such as wind and solar are sometimes overshadowed by their intermittent nature and their consequent low capacity factors; this makes the development of these resources a challenging task. However, the storage capacities of hydrogen in FCVs and batteries in PEVs provide dispersed storage capacity for the whole grid that could help address this intermittency issue.

In view of the challenges associated with the supply of oil and environmental benefits of FCVs and PEVs as well as the technical advantages of electric drives, such as efficiency, the future of transportation is believed to be greatly influenced by these new types of vehicles. In particular, the future of PEVs is even more promising because of the availability of the grid infrastructure. With these facts in mind, the electric grid impacts of AFVs should be analyzed in detail, and appropriate quantitative tools and planning models for a transition to these vehicles should be developed in order to maximize their environmental benefits and to minimize their

corresponding costs and negative impacts.

Motivated by the notion of efficient utilization of the existing infrastructure, this thesis explores optimal potential penetrations of AFVs into the transport sector by considering the electricity grid constraints during off-peak periods. This research is novel as the application of Mathematical programming approaches for deriving optimal transition to AFVs with environmental constraints in both population areas and generation as well as electricity grid constraints, in particular of the transmission system, has not yet been addressed in the literature.

The "big picture" of this research is shown in Figure 1.1, which represents the main sub-models, required data, analytical engine and major results. The region under study is first decomposed into different zones, where the main power generation and electricity load centers are located and where there are major transmission corridors between them. Thereafter, appropriate models for the transmission system and the procurement of generation capacities in each zone during the planning study are developed. Environmental costs and credits are also considered in generation facilities and population areas, respectively, to account for the environmental benefits of AFVs and possible environmental consequences of the extra generated power , which may not be necessarily pollution free. As can be observed in Figure 1.1, the proposed optimization models involve so many parameters that their estimation errors may substantially influence the optimal solution. In order to resolve this problem, this thesis proposes the application of robust optimization approach to deal with uncertainty.

1.2 Literature Review

1.2.1 Hydrogen Economy and FCVs

The hydrogen economy is defined as a future economy in which hydrogen is adopted for mobile applications and electric grid load balancing [9]–[12]. However, the hydrogen economy that is considered in this study is based solely on electrolytic

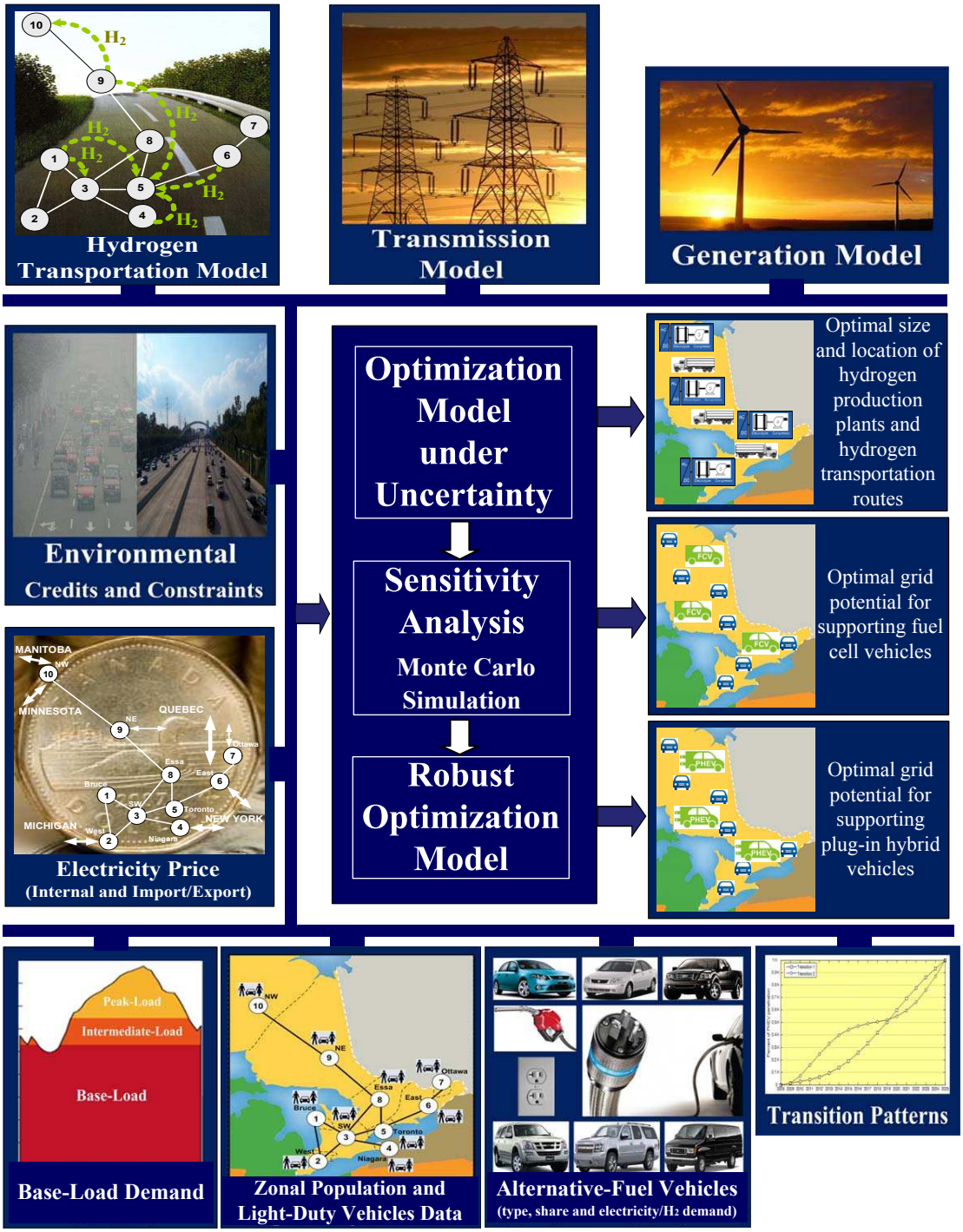

Figure 1.1: The big picture of the research.

hydrogen production during off-peak periods for use of fuel cell vehicles (FCVs). Therefore, grid impacts of electrolytic hydrogen production plants (HPPs) during off-peak hours serving the hydrogen requirement of the transport sector is the main concern of this research.

Economic assessment of electrolytic hydrogen production as a whole, independent of the type of power source for the HPPs, is studied in [13] where electricity prices and fuel taxes are shown to be the two dominant factors influencing the competitive position of electrolytic hydrogen production. The cost of electrolytic hydrogen production, particularly during off-peak periods, has been studied in [14], considering different fluctuating and stable electricity markets. It is shown in [14] that hydrogen production using off-peak electricity, where prices are sufficiently low, can be of interest in those countries that have highly fluctuating electricity spot markets. An economic evaluation of electrolytic hydrogen production during off-peak hours for the real case of Ontario, Canada is also performed in this thesis to demonstrate the feasibility of the idea, given the electricity prices in Ontario.

Solar or wind-based hydrogen production to meet the demands of FCVs has also been studied in a number of papers, e.g., [15]–[18], where the main emphasis is on the role of hydrogen in the transport sector to overcome the intermittency issues of these resources. These studies typically rely on a single type of generation resource and do not consider the mix of different available generation resources to support a hydrogen economy. Although renewable energy resources such as wind and solar can help to meet the requirement of a true hydrogen economy, neglecting the mix of different generation resources, which have low shares of polluting resources, causes power system planners to underestimate the grid potential for covering the hydrogen requirement of FCVs.

Planning the transition to a hydrogen economy has been studied in various locations and reported in the literature [19]–[31]. Each of these plans consider particular aspects of this issue, varying considerably from place to place due to different local limitations and energy policies, and with inadequate attention to the electric grid constraints. This thesis explores a different aspect of a hydrogen economy

transition in the transport sector by developing an optimization planning model that takes into account both electricity and hydrogen networks as one integrated system. Considering the future development of both generation and transmission systems within a planning horizon, this model determines the optimal size of HPPs to be installed in different locations and the optimal hydrogen transportation routes required to achieve optimal hydrogen economy penetrations during this planning framework. Furthermore, based on the reported works (e.g., [21, 25]), planning the transition to a hydrogen economy is usually based on some estimates of hydrogen economy penetrations at a fixed time in the future; however, the optimal values of these penetrations are found in the proposed model via an optimization process. These optimal values are influenced by the electric grid constraints as well as by hydrogen transfer limits. Another novel aspect of the proposed planning model is the application of a new robust optimization approach, which gives the possibility of adjusting the trade-off between optimality and conservatism. Also, the proposed procedure does not jeopardize the reliability of the system through stressing the system at peak demand hours and does not require the development of new and separate infrastructure to cover the electricity requirement of HPPs.

1.2.2 PHEVs

In view of the technical and environmental advantages of PHEVs, the possible impacts on the grid as a result of the PHEV load should be analyzed in detail. Although this is a new area of research, some studies regarding the grid impacts of PHEVs have been reported in the literature. For example, in [32], both PHEV charging and discharging are studied in six geographic regions in the U.S. to examine the grid impacts for different PHEV penetration levels up to a maximum level of 50%. That paper disregards the environmental impacts as well as different types of vehicles, and it assumes a unique average value for the energy requirements of all PHEVs.

Based on different charging scenarios, the authors in [33] evaluate various PHEV-

charging impacts on utility system operations within the Xcel Energy Colorado service territory. Total load impacts, additional generation capacity requirements and incremental generation costs for a large penetration of PHEVs are evaluated under both controlled and uncontrolled charging conditions. Environmental issues are also studied, evaluating different types of emissions and considering the time of charging and the marginal power plant.

The author in [34] evaluates the impact of PHEVs on both generation supply and emissions for the Virginia-Carolinas electric grid in 2018. This study assumes different charging levels and timing (in early evening or at night) and, based on a gradual ramp up of PHEV market share to 25% in 2018, finds the generation shares according to different types of power plants. The analysis in [34] also extends to all regions of the country, finding the marginal power plants in different regions for varied charging patterns.

In [35], the percentage of U.S. light-duty vehicles that could potentially be supplied by the U.S. electricity infrastructure without additional investments in generation, transmission and distribution capacities is estimated in 2007; the impact on overall emissions of criteria gases and GHGs is also studied. Concentrating on the limit of today's grid infrastructure to support a new transportation load, this paper does not consider the growing demands for both electricity and transportation, the need to upgrade of the electricity infrastructure over time, and the gradual penetration of PHEVs.

Smart demand management of power systems integrated with PHEVs has been studied in [36]. This study assumes independent customers whose plugs are not controlled by a utility and therefore they are allowed to charge their PHEVs even at peak times - a practice which may cause grid problems. A smart agent-based demand management scheme is proposed based on nonlinear pricing to assure proper distribution of the available energy to PHEV customers. The suggested approach in [36] assumes a relatively small number of PHEV connections in one urban area modelled as an energy hub, and it does not consider the integration of PHEVs into large electricity systems.

The issue of PHEV charging strategies and their impacts on generation expansion planning is studied in [37]; this study identifies the required generation infrastructure for the future based on an assumed high penetration of PHEVs. Given four PHEV load profiles including uniform charging, home-based charging, off-peak charging and vehicle-to-grid (V2G) operation, the most economical electric capacity expansions by fuel type are found, considering the emission limits.

It can be seen from the above review that an important requirement that has not yet been addressed is the inclusion of transmission system constraints in the analysis process. Furthermore, even at the generation level, the reported works try to either derive the grid potential for supporting PHEVs at the present time or to find the required generation capacity for supporting a target value of PHEVs penetration at a specified future time. These studies do not consider the penetration of PHEVs as a transitional process. Also, to the author's knowledge, the Mathematical programming approach, especially with the consideration of parameter uncertainty, has not yet been used specifically to find the grid potential for supporting PHEVs. This research presents the development of a new robust optimization model to find optimal potential penetrations of PHEVs into the transport sector during a planning horizon, considering that these vehicles can only be charged from the grid in off-peak hours. The proposed techniques, relying on present and planned generation and transmission capacities, allow to determine how the electricity system can be optimally exploited during base-load periods for charging the PHEVs.

1.3 Objectives

Based on the state-of-the-art research discussed above, the main objectives in this thesis are the following:

1. Propose an optimization framework for planning the transition to a hydrogen economy in the context of an integrated electricity and hydrogen system based on a proper model of generation emission costs in order to properly ac-

count for the environmental consequences of AFVs, and a model for hydrogen transportation between different zones of the region under study.

2. Propose a similar optimization framework for planning the transition to PHEVs based on a similar generation emission cost model developed for the FCV transition model.

3. Employ the proposed optimization planning models to the real-case of Ontario, Canada based on a transmission system model for Ontario, a zonal base-load demand model and a zonal pattern of base-load generation capacity in Ontario.

4. Perform a sensitivity analysis using Monte Carlo simulation to determine the most influential parameters of the proposed optimization models on the optimal value.

5. Apply a robust optimization approach using the most influential uncertain parameters to derive optimal potential penetrations of AFVs into Ontario's transport sector by 2025 that properly consider these uncertainties.

1.4 Thesis Outline

This thesis is organized into seven chapters and two appendixes as follows:

Chapter 2 presents a review of the main concepts and tools of interest in this thesis. It describes the concepts of integrated energy systems and energy hubs as well as the main specifications of the hydrogen economy, FCVs and PHEVs. Then, a brief review of Mixed Integer Linear Programming (MILP) models is presented, followed by a discussion of the issue of parameter uncertainty in optimization models, and a review of the classical approaches to deal with this uncertainty. This chapter also reviews the application of a robust optimization approach to properly consider uncertainty.

Chapter 3 presents a novel optimization framework for planning the transition to AFVs. First, environmental aspects of AFVs in both population areas and generation sites are comprehensively discussed. A model for generation emission costs is then developed, followed by a hydrogen transportation model between the zones for optimal transition to FCVs. This model is then modified to study an optimal transition to PHEVs. Finally, the proposed optimization planning models are evaluated on a three-zone test system under a variety of scenarios.

Chapter 4 presents the models required for the application of the planning models for a real-case problem in Ontario, Canada. These models include Ontario's transmission network, zonal pattern of base-load generation capacity and zonal base-load demands during the planning study period. This chapter also discusses the required data in both the electricity and the transport sectors of Ontario as well as the relevant assumptions regarding the transition to both FCVs and PHEVs. An economic assessment of the electrolytic hydrogen production in Ontario during off-peak hours is also presented in this chapter.

Chapter 5 presents the results of the application of the proposed optimization models to Ontario, Canada. In this chapter, optimal potential penetrations of both FCVs and PHEVs into Ontario's transport sector are determined for a variety of scenarios.

Chapter 6 discusses the impact of parameter uncertainty on the optimal potential penetration of AFVs into Ontario's transport sector. It first identifies and ranks the most influential uncertain parameters through a sensitivity analysis using Monte Carlo simulations. These results are then used to develop robust optimization models to study the optimal transition to AFVs in Ontario, Canada, properly accounting for the most relevant uncertainties.

Chapter 7 summarizes the conclusions and main contributions of this thesis and suggests directions for future research work. Finally, Appendixes A and B provides additional data for the test systems.

Chapter 2

Background Review

2.1 Introduction

This chapter presents a review of the concepts and tools on which the research presented in this thesis is based. It first discusses the concepts of integrated energy systems and energy hubs. Major components of the future transport sectors, i.e., hydrogen economy and FCVs as well as PHEVs, are discussed here, highlighting their interactions with the electric grid. A review of MILP models is presented and the issue of parameter uncertainty in optimization models and the classical approaches to deal with this issue are reviewed. Finally the application of robust optimization approach to properly consider uncertainty is discussed.

2.2 Integrated Energy Systems

Different energy sources and carriers, such as natural gas, electricity, heat and hydrogen, are tightly coupled due to the technical and economic interactions among them. For example, a microturbine being fed from natural gas can produce electricity and heat simultaneously, and an electrolyzer being fed from the electricity network can satisfy both hydrogen and heat demands. In view of these interactions,

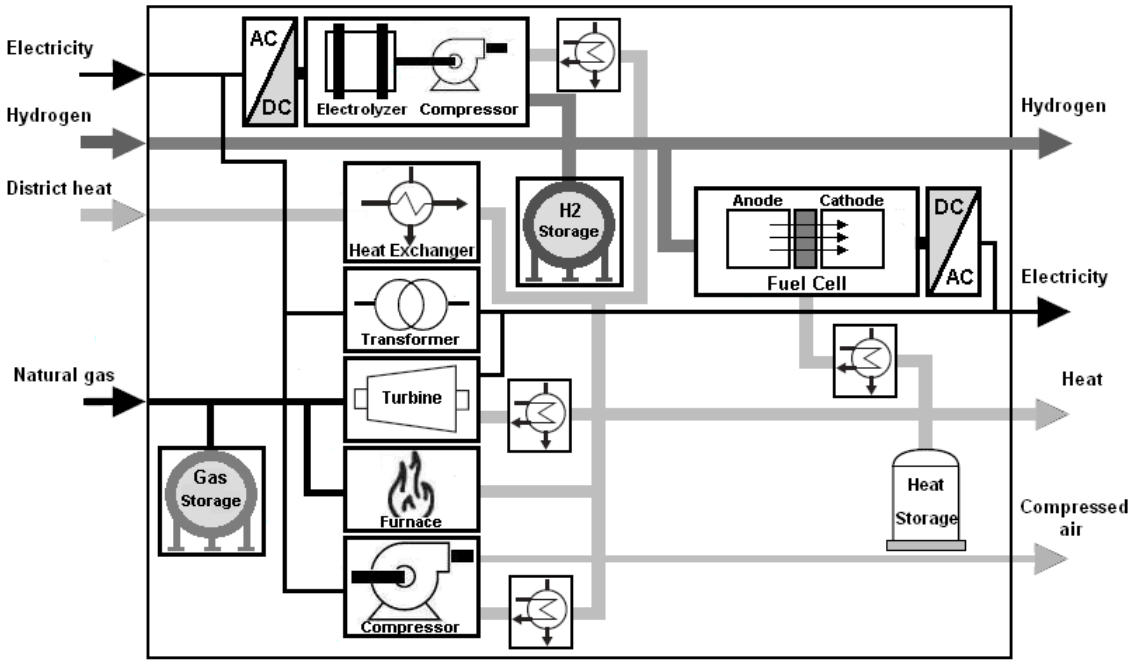

Figure 2.1: Configuration of a comprehensive energy hub.

different energy systems that have typically been planned independently, should be investigated in the context of an integrated energy system. Such a concept provides an opportunity for adequate and coordinated planning and operation of these systems. For example, congestion on a particular transmission path in one energy system can be relieved by shifting part of the energy flow to another energy system [38, 39]. However, more complex problems arise in this integrated approach, because the planning and operation are now transferred to a larger scale system with multiple interactions between various sub-systems.

One of the key concepts, which is established in the context of integrated energy systems is the *energy hub* [40]–[42]. This concept facilitates the study the flow of multiple energy carriers or energy sources and their interactions. An energy hub is an interface between energy loads (e.g., electricity, heat, compressed air, and hydrogen demand for transportation) and primary energy sources and energy carriers (e.g., electricity, natural gas, district heat, and hydrogen). The concept of a node in an electrical system can be generalized or extended to an energy hub in an inte-

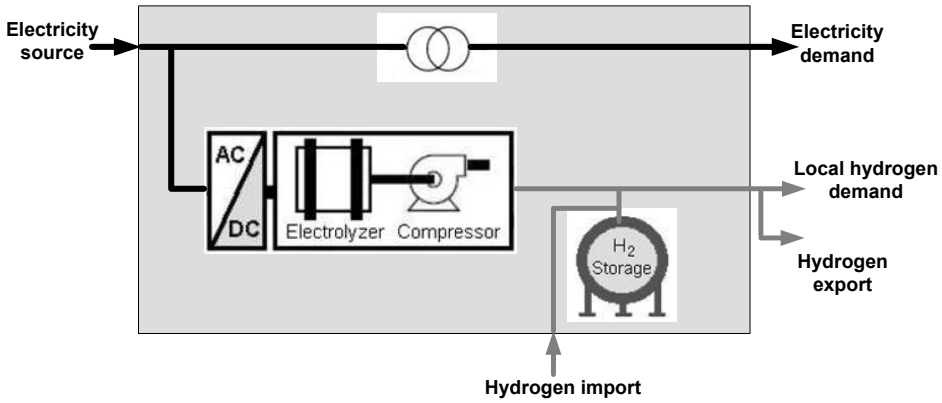

Figure 2.2: Configuration of the energy hubs under study.

grated energy system. Figure 2.1 represents the configuration of a comprehensive energy hub with multiple inputs and outputs and a variety of converters and storage devices. Since the converters inside an energy hub exhibit different characteristics, with particular costs associated with different energy sources and related energy carriers, an optimal dispatch problem can be formulated for the hub and associated energy systems. The integrated energy system considered in this research is composed of two energy carriers, i.e., electricity and hydrogen, with energy hubs as shown in Figure 2.2.

2.3 Hydrogen Economy and Fuel Cell Vehicles

The concept of a *hydrogen economy* which was introduced in the early 1970s has attracted a great deal of attention both in industry and academia. Hydrogen, as an energy carrier, can link or interface multiple energy resources such as fossil fuels, nuclear, and renewables for multiple end-uses; and hence leads to a hydrogen economy. This concept is concerned with the economic aspects associated with the production, distribution, and utilization of hydrogen in energy systems. In this respect, important issues in the hydrogen economy are the costs of production, storage, and delivery to customers of hydrogen as an energy carrier.

The introduction of the hydrogen economy concept originated from environ-

mental concerns. Because of the ecological impacts, mainly smog and greenhouse gas emissions in the transport sector, the ultimate goal is to find a zero emission transportation fuel that can be derived from a wide range of primary energy resources [44]–[47]. The existing technologies for hydrogen production includes the steam reforming of natural gas, and electrolysis. Electrolysis can be based on the electricity provided from coal-fired, biomass, or nuclear power plants, and renewable resources such as wind, hydro and solar PV [48]. It is preferable to generate hydrogen from non-fossil energy resources (e.g., renewables and nuclear); if fossil fuel resources are considered, then carbon sequestration should also be included in the process, but this process can be costly [49, 50].

There is much debate with regard to the hydrogen economy, with strong advocates and opponents [51]–[59]. At the present state of technological development, there are a variety of concerns, regarding the production, distribution, storage, and use of hydrogen. However, many of these concerns should be addressed in the course of time [60], as proper solutions are developed to solve the current challenges of hydrogen as a new energy carrier. By keeping these challenges in mind, the hydrogen economy concept can be considered in the framework of integrated energy systems for the following reasons:

1. **Potential for Energy Storage**

   One physical characteristic of electricity is its lack of storage capacity, at least in large quantities. Consequently, the grid must remain constantly energized with an instantaneous balance between the generated electricity and variable demand. This is especially an issue for the incorporation of renewable energy sources such as wind and solar which are intermittent in nature. Electrical energy storage can relieve this stringent balancing requirement. There are a few alternatives for electrical energy storage, including pumped hydro and compressed air energy storage in underground caverns, flywheels, Superconducting Magnetic Energy Storage (SMES), super-capacitors, and batteries [61, 62]. Hydrogen can be considered as a new alternative for electricity storage (e.g., [63,64]. Onboard use of hydrogen allows for zero emission

fuel cell vehicles with extended range and rapid refueling. Hydrogen production through the electrolysis process has around 60%-80% efficiency, which means that a significant part of the electrical energy can be stored as hydrogen [44, 58].

2. **Decrease in Urban Air Pollution and Greenhouse Gas Emissions**

   If the hydrogen economy concept is properly applied, i.e., assuming non-fossil resources for hydrogen production, it can significantly relieve many environmental concerns. No NO_x, SO_x and CO_2 emissions will be generated by fuel cell vehicles in the urban airshed [48].

3. **Diversification of Energy Production and Security of Supply**

   The economics of production, storage, and the utilization of hydrogen become quite relevant in the context of competitive electricity markets, given the price differences between peak and low price periods [65], and traditional generation plants, which are most efficient when operating at rated load levels. Furthermore, for congestion problems in the electric transmission system during the normal operation of a power grid, the use of hydrogen as an energy carrier to increase the efficiency and reliability of the grid is certainly attractive. Under these conditions, the availability of low-price electricity and unused generation capacity, the generation plant can be efficiently operated for hydrogen production and storage that can later be used by fuel cell vehicles.

It should be noted that the hydrogen economy concept, which is applied in this research, is concentrated on the application of hydrogen-related systems only in the transport sector and not for power generation. Preliminary studies show that electricity production by fuel cells in the grid level may not still be justifiable due to higher efficiencies and lower costs of other energy pathways [63, 64, 66, 67]. In fact, significant electricity price differences between off-peak and on-peak hours and higher efficiencies and lower of fuel cells might make the power generation by fuel cells for the grid economically viable.

2.4 Plug-in Hybrid Electric Vehicles

Hybrid electric-vehicle (HEV) technology presents an option for significant reductions in gasoline consumption as well as smog precursor and GHG emissions. This is achieved through the possibility of downsizing the combustion engine and the ability to recover a substantial amount of the vehicle's kinetic energy in the battery storage system through regenerative braking [68]–[70]. However, EVs still suffer from their dependence on a single hydrocarbon fuel source. The emerging PHEV is somewhat similar to a conventional HEV but features a much larger onboard battery and a plug-in charger; this helps it to achieve a large All-Electric-Range (AER) capability for the a portion of a driving trip. The main advantage of PHEV technology is that the vehicle is not completely dependent on a single fuel source; thus, it can travel 30 km or more on battery power alone, without running the internal combustion engine. This allows the completion of daily trips on battery power alone and thus substantially reduces gasoline consumption as well as cold-start emissions [70]–[73]. However, at the present state of technological development, there are still some concerns regarding the viability of PHEVs; in particular, energy-storage costs, range, and durability are the major challenges that must be overcome [74].

PHEV technology is a prime example of the integration of the transport sector with power systems to improve the efficiency of both. In this case, the integration of the energy demand for electrical power with the energy demand for transportation fuel is of particular interest. Unutilized generation capacity during off-peak hours as well as low electricity prices and demands in these time periods provide a unique opportunity of supporting PHEVs using the electricity grid.

2.5 Mixed Integer Linear Programming Models

Mixed integer linear programming (MILP) is a powerful mathematical framework, which involve both discrete and continuous decision variables in linear programming

problems [75]. An MILP model can generally be represented as follows:

$$\begin{aligned} \min \quad & \mathbf{c}'\mathbf{x} \\ \text{s.t.} \quad & \mathbf{A}\mathbf{x} \geq \mathbf{b}, \\ & \mathbf{l} \leq \mathbf{x} \leq \mathbf{u} \\ & x_e \text{ integral}, e = 1, ..., g, \end{aligned} \tag{2.1}$$

where the input data are the matrices $\mathbf{c}(n \times 1)$, $\mathbf{A}(m \times n)$, $\mathbf{b}(m \times 1)$, $\mathbf{l}(n \times 1)$ and $\mathbf{u}(n \times 1)$, and $\mathbf{x}$ is an n-vector of decision variables with g integer elements ($1 \leq g \leq n$). The ability of including binary or integer decision variables in the model allows modeling a variety of real-world problems. In this research, such discrete variables are used to model emission costs of generation, hydrogen transportation and transmission losses.

The most common method for solving MILP problems is the *branch-and-bound* method; more novel methods include *branch-and-price* and *branch-and-cut* methods [76]–[78]. These methods require solving a sequence of linear programming relaxations of the MILP problem. In particular, the branch-and-cut method is a combination of a cutting plane method with a branch-and-bound algorithm. In the cutting plane method, additional constraints, called cutting planes, are added to tighten the feasibility region. There are powerful software packages, such as CPLEX [79], that can efficiently solve large MILP problems; this is the adopted solver in this research, using the branch-and-cut method to solve the proposed MILP problems.

Since MILPs are classified in the category of *NP-hard* problems [80, 81], computational requirements can grow substantially as the number of integer variables in the model increases; this is a major disadvantage of MILP problems. Therefore, due to theoretical and practical limitations, there is a need to consider trade-off between solution quality and computational time for large-size MILP problems. In CPLEX, this is achieved by choosing an appropriate value for the parameter (directive) `mipgap` which defines how close one is to the optimal solution (e.g., for

`mipgap` equal to 0.01, CPLEX will stop as soon as it finds a solution within 1% of optimality). There is also the possibility of changing the behavior of the MILP problem and improve the performance of CPLEX by defining the values of some other directives such as `mipemphasis` which directs the branch-and-cut algorithm to focus on different balances of optimality and feasibility, or `mipcuts` which increases the cut generation and tightens the feasibility region of the MILP that CPLEX optimizes [79, 82].

2.6 Data Uncertainty in Optimization Models

Optimization models often rely on some input parameters whose values are typically assumed to be definitely known. More precisely, a general mathematical programming problem has the following form:

$$\begin{aligned} \min \quad & f_0(\boldsymbol{x}, \boldsymbol{d}_0) \\ \text{s.t.} \quad & f_e(\boldsymbol{x}, \boldsymbol{d}_e) \geq 0, \forall e \in E, \end{aligned} \tag{2.2}$$

where $\boldsymbol{x}$ is a vector of decision variables and $\boldsymbol{d}_e, e \in E \cup \{0\}$ is the input data or parameter vector of the optimization model. Input parameters usually come from measurement, tests, historical data and various assumptions; hence, they are subject to uncertainty and estimation error. On the other hand, errors in estimating input parameters may severely affect the obtained optimal solution and its actual performance. Thus, as the data take values different than nominal or expected ones, several constraints may be violated, and the optimal solution yielded by the nominal data may no longer be optimal or even feasible. Therefore, due to the impact of data uncertainty on the quality and feasibility of the optimization models, methodologies should be adopted that appropriately deal with the uncertainty of the parameters in the model [83, 84].

Sensitivity analysis and stochastic programming are the classical approaches for dealing with parameter uncertainty in optimization models [85]–[88]. Sensitiv-

ity analyses such as Monte Carlo simulations [89], which are used in this work, measure the sensitivity of a solution to stochastic changes in the input parameters; however, it provides no mechanism by which this sensitivity can be controlled. In this regard, it can be counted as a reactive approach to deal with uncertainty [86]. In the stochastic programming approach, it is assumed that the probability distributions of the uncertain input parameters are known or can be estimated with reasonable accuracy. The goal in this approach is to find a solution that is feasible for all (or almost all) possible instances of the data and to maximize the expectation of some function of the decisions and the random variables. For example, in chance constrained stochastic programming models where the feasibility of a solution is expressed by chance constraints, a feasible solution is not required to satisfy every outcome of the random parameters, but it is required to be feasible with at least some specified probability [90]. Therefore, the corresponding stochastic optimization problem to (2.2) can be expressed as follows:

$$\begin{aligned} \min \quad & k \\ \text{s.t.} \quad & Pr(f_0(\boldsymbol{x}, \widetilde{\boldsymbol{d}}_0) \leq k) \geq p_0, \\ & Pr(f_e(\boldsymbol{x}, \widetilde{\boldsymbol{d}}_e) \geq 0) \geq p_e, \forall e \in E, \end{aligned} \tag{2.3}$$

where $\widetilde{\boldsymbol{d}}_e, e \in E \cup \{0\}$ are the random variables associated with the constraint e and p_e are the threshold probabilities given by the decision-maker.

There are inherent difficulties with the aforementioned approach. First, while the optimal decision variables can be quite sensitive to the distributions of the random parameters, it is difficult, in practice, to accurately estimate these distributions; therefore, the obtained solution can be considered as only an approximation. Secondly, even if the distributions are known, it is still computationally difficult to evaluate the chance constraints. Finally, the convexity of the model can be lost due to the introduction of chance constraints which increases the complexity of the original optimization model [91, 92].

2.7 Robust Optimization

In view of all the difficulties with sensitivity analysis and stochastic programming approaches discussed in the previous section, one of the most attractive approaches of the last decade to deal with parameter uncertainty in the optimization process has been *robust optimization* [93, 94]. The classic robust optimization method presents an uncertainty-immunized solution, which remains feasible in all realizations of the input data, and the value of the objective function at this solution is the guaranteed value of the uncertain objective. The main tools in the classic robust optimization framework are *uncertainty sets* and a *robust counterpart problem*. Thus, uncertainty in the input data is described through uncertainty sets, which contain all or most possible values that may be realized for the uncertain parameters. Also, a deterministic problem, which is called a robust counterpart problem, is associated with the uncertain problem [90]. Given the nonempty uncertainty sets U_e, the robust optimization yields a solution that optimizes the worst-case performance when the input data belong to the uncertainty sets. More specifically, robust optimization solves the following problem:

$$\begin{aligned} \min \quad & \max \quad f_0(\boldsymbol{x}, \boldsymbol{d}_0) \\ \text{s.t.} \quad & f_e(\boldsymbol{x}, \boldsymbol{d}_e) \geq 0, \forall e \in E, \forall \boldsymbol{d}_e \in U_e, \end{aligned} \tag{2.4}$$

where for $e \in E \cup \{0\}$, the set U_e is the uncertainty set of the parameter $\boldsymbol{d}_e$; it is important to highlight that the uncertain parameters are not simultaneously in constraints and objective function. Although this approach provides immunization to parameter uncertainty, its results are perceived to be too conservative for real applications, i.e., robustness is ensured at the cost of significantly losing optimality [84, 91]. To rectify this shortcoming of robust optimization, it has been suggested in the literature (e.g., see [95]–[99]) to intelligently shrink the uncertainty set. One of such techniques was proposed in [83], which is also applicable to discrete optimization models [100]. The main feature of this formulation is that it does not lead to nonlinear models; therefore, the tractability of the problem is not affected.

Also, this approach offers full control on the degree of conservatism desired for any constraint. This approach will be applied in this research to develop robust optimization models for transition to AFVs and is briefly explained next [83, 84, 100].

Consider the following general linear programming model:

$$\begin{aligned} \min \quad & \mathbf{c}'\mathbf{x} \\ \text{s.t.} \quad & \tilde{\mathbf{a}}_e'\mathbf{x} \geq b_e, \quad \forall e \\ & x \in X, \end{aligned} \tag{2.5}$$

where X includes all mixed integer feasible solutions, and uncertainty is assumed without loss of generality to affect only the constraint coefficients $\tilde{\mathbf{a}}_e$, since even problems with uncertainty in the cost vector $\mathbf{c}$ and the right-hand side b_e can also be reformulated so that all uncertainties are only reflected in $\tilde{\mathbf{a}}_e$. It is assumed that every element of the vector $\tilde{\mathbf{a}}_e$, i.e., $\tilde{a}_{ev}$, $v \in [1, n]$ is subject to uncertainty and belongs to a symmetrical interval $[\hat{a}_{ev} - \Delta a_{ev}, \hat{a}_{ev} + \Delta a_{ev}]$, which is known by the decision-maker. This interval is centered at the point forecast $\hat{a}_{ev}$, while Δa_{ev} measures the precision of the estimate. The scaled deviation s_{ev} of parameter $\tilde{a}_{ev}$ from its nominal value can then be defined as:

$$s_{ev} = \frac{\tilde{a}_{ev} - \hat{a}_{ev}}{\Delta a_{ev}}, \tag{2.6}$$

which belongs to [-1,1]. The aggregate scaled deviation for constraint e, $\sum_{v=1}^{n} |s_{ev}|$, which is more accurate than individual ones, can take any value between 0 and n; however, it is unlikely that all of the coefficients $\tilde{a}_{ev}$ will change and consequently the true value taken by $\sum_{v=1}^{n} |s_{ev}|$ will belong to a much narrower range. This point is expressed in mathematical terms as follows:

$$\sum_{v=1}^{n} |s_{ev}| \leq \Gamma_e, \forall e. \tag{2.7}$$

The parameter $\Gamma_e \in [0, n]$ is called the *budget of uncertainty* of constraint e, and

its role is to adjust the robustness against the level of conservatism of the solution. The value of this parameter reflects the attitude of the decision-maker toward uncertainty. Thus, for $\Gamma_e = 0$, there is no "protection" against uncertainty, and $\Gamma_e = n$ yields a very conservative solution because it can be interpreted as all the uncertain parameters' taking their worst-case values at the same time. For any values between 0 and n, the decision-maker makes a trade-off between the protection level of the constraint and the degree of conservatism of the solution. If Γ_e is an integer, it can be interpreted as the maximum number of parameters that can simultaneously deviate from their nominal values.

The uncertainty set U now becomes:

$$U = \{(\tilde{a}_{ev}) \mid \tilde{a}_{ev} = \hat{a}_{ev} + \Delta a_{ev} s_{ev}, \forall e, v, s_{ev} \in S_e\}, \tag{2.8}$$

where:

$$S_e = \left\{ \mathbf{s}_e = [s_{e1}, s_{e2}, ..., s_{en}] \mid |s_{ev}| \leq 1, \forall v, \sum_{v=1}^{n} |s_{ev}| \leq \Gamma_e \right\}. \tag{2.9}$$

Now, a robust optimal solution can be obtained from the following counterpart problem:

$$\begin{aligned} \min \quad & \mathbf{c}'\mathbf{x} \\ \text{s.t.} \quad & \hat{\mathbf{a}}_e'\mathbf{x} + \min_{\mathbf{s}_e \in S_e} \sum_{v=1}^{n} \Delta a_{ev} x_v s_{ev} \geq b_e, \quad \forall e, \\ & \mathbf{x} \in X. \end{aligned} \tag{2.10}$$

It is proved in Theorem 1 of [83] that (2.10) is equivalent to the following problem, which is a linear programming model:

$$\begin{aligned} \min \quad & \mathbf{c}'\mathbf{x} \\ \text{s.t.} \quad & \hat{\mathbf{a}}_e'\mathbf{x} - \Gamma_e p_e - \sum_{v \in V_e} q_{ev} \geq b_e, \forall e \in E, \end{aligned}$$

$$
\begin{aligned}
& p_e + q_{ev} \geq \Delta a_{ev} r_v, && \forall e \in E \wedge v \in V_e, \\
& -r_v \leq x_v \leq r_v, && \forall v \in V, \\
& p_e \geq 0, && \forall e \in E, \\
& q_{ev} \geq 0, && \forall e \in E \wedge v \in V_e, \\
& r_v \geq 0, && \forall v \in V, \\
& \mathbf{x} \in X, && \qquad (2.11)
\end{aligned}
$$

where E is the set of indexes of constraints subject to uncertainty, V is the set of indexes of total uncertain parameters and V_e is the set of indexes of uncertain parameters in constraint e. Observe that this robust formulation requires the determination of a budget of uncertainty $\Gamma_e \in [0, |V_e|]$ for each constraint e subject to uncertainty, as well as the definition of new decision variables p_e, q_{ev} and r_v.

It is probabilistically guaranteed that even if more than a definite number of uncertain coefficients change, then the robust solution will, with high probability, remain feasible. Thus, it is proved that for constraint e with n uncertain parameters to be violated with probability of at most ε_e, it is sufficient to choose a budget of uncertainty Γ_e at least equal to $1 + \Phi^{-1}(1 - \varepsilon_e)\sqrt{n}$, where Φ is the cumulative distribution of a standard normal [83]. Alternatively, the violation probability of constraint e at a given budget of uncertainty Γ_e can be calculated as $1 - \Phi\left(\frac{\Gamma_e - 1}{\sqrt{n}}\right)$.

2.8 Summary

This chapter introduces the concepts of integrated energy systems and energy hubs. Interactions between the electricity grid and the transport sector are discussed through the frameworks of the hydrogen economy, FCVs and PHEVs. This chapter presents a review of MILP problems and also discusses the issue of data uncertainty in optimization models and reviews the classical approaches suggested to address this problem. Finally, the robust optimization approach, which is the method adopted in this research to deal with the problem of data uncertainty, is presented.

Chapter 2. Background Review

The concepts presented in this chapter are used throughout the thesis to study and propose optimization planning models for the transition to AFVs.

Chapter 3

An Optimization Framework for Transition to AFVs Considering Electricity Grid Constraints

3.1 Introduction

This chapter presents a detailed optimization framework for planning the transition to AFVs, with particular attention to electricity grid constraints. The proposed model is based on decomposing the region under study into different zones, where the main power generation and electricity load centers are located, which are assumed to be interconnected through major transmission corridors. Considering the future development of both power generation and transmission capacities as well as future changes to the transport sector, this model seeks to find the optimal levels of the load, in the form of HPPs or PHEVs, that can be supported in each zone during off-peak periods.

In Section 3.2, environmental issues associated with AFVs in both population areas and generation facilities are discussed. This is followed by the development of an emission cost model of generation in Section 3.3. Optimization models for

the transition to AFVs are first developed for FCVs in Section 3.4, and then are extended in Section 3.5 to accommodate PHEVs. In Section 3.6, a small 3-zone test system is developed to analyze the performance of the proposed planning framework.

3.2 Environmental Aspects of AFVs

Many attempts have been made thus far to assign a monetary value to the damage caused by CO_2 emission, which is commonly referred to as the social cost of carbon (SCC). More precisely, it is an estimate of the economic value of the extra or marginal impact caused by the emission of one more tonne of carbon (in the form of CO_2) at any point in time [101]. The SCC can also be interpreted as the marginal benefit of reducing carbon emissions by one tonne [102]. Reported values in the literature for the SCC come in an extremely wide range. As an example, the probability function developed in [103] based on 100 estimates of the SCC from 28 published studies, displays a median of 14 USD/ton of carbon, a mean of 93 USD/ton and a 95th percentile estimate equal to 350 USD/ton. There are also other estimates of the SCC running from less than 1 USD/ton to over 1500 USD/ton of carbon [102]. It is discussed in [103] that much of the uncertainty in the estimates of the SCC corresponds to the following two main assumptions: the discount rate (by which the future costs are discounted back to the year of emission), and the equity weights that are used to aggregate monetized impacts over countries.

Each gasoline or diesel-fuelled vehicle in a population area and fossil fuel plant release CO_2 to the atmosphere; hence, based on the SCC, the monetary value of the damages to the environment caused by such vehicles or generation plants can be estimated. Therefore, an environmental credit is assigned to each FCV or PHEV that can be introduced to the transport sector in this study, whose value depends on the SCC, the fuel economy of the LDV, which is supposed to be replaced by a PHEV or FCV, and the known value of CO_2 emission from burning gasoline (2.3 kg/litre). An environmental cost is also assigned to each polluting generation plant, which is

based on the SCC, the power generation level and the CO_2 emission rates of the plant. Disregarding this type of environmental cost may lead to overestimating the environmental benefits of AFVs. Thus, in order to cover the energy requirement of the FCVs or PHEVs' charging demands, extra power must be generated by generation facilities which may not necessarily be a renewable source of energy; as a consequence, the CO_2 emission in the generation side could increase. Therefore, while adopting FCVs or PHEVs in the transport sector reduces the CO_2 emission in the population area where the vehicle is used, it may increase the CO_2 emission from power generation, depending on the share of fossil fuel in the marginal generation mix.

Although high penetration of AFVs may not necessarily result in emission reductions in all regions, it would help to shift the emission from millions of tailpipes in highly populated areas to a limited number of central generation power plants, thus facilitating more efficient control and management of CO_2 emissions. For example, studies show that PHEVs result in lower emissions compared to conventional gasoline vehicles even for regions with high CO_2 levels from electric generation [33,34,104]. It is also important to highlight that the environmental benefits of AFVs are not limited to CO_2 emission reductions. Urban air emissions and photochemical smog are major issues in densely populated areas [105]; e.g., the estimated number of deaths in Toronto from air pollution is 5,800 annually [106]. These issues could be addressed by the introduction of AFVs into the transport sector. In view of these considerations, the environmental and health damage caused by all emissions such as CO_2, volatile organic compound, particulate matters, NO_x, SO_x and Hg, is much more significant in densely populated areas [107]. Therefore, different values for the social cost of CO_2 emissions in populated areas versus unpopulated areas where most generation power plants are located are considered in this study, to account for the emission impact associated with vehicles.

It should also be noted that assigning environmental costs and credits to polluting generation plants and AFVs, respectively, is particularly justified due to the fact that the optimization models to find the electricity grid potential to support

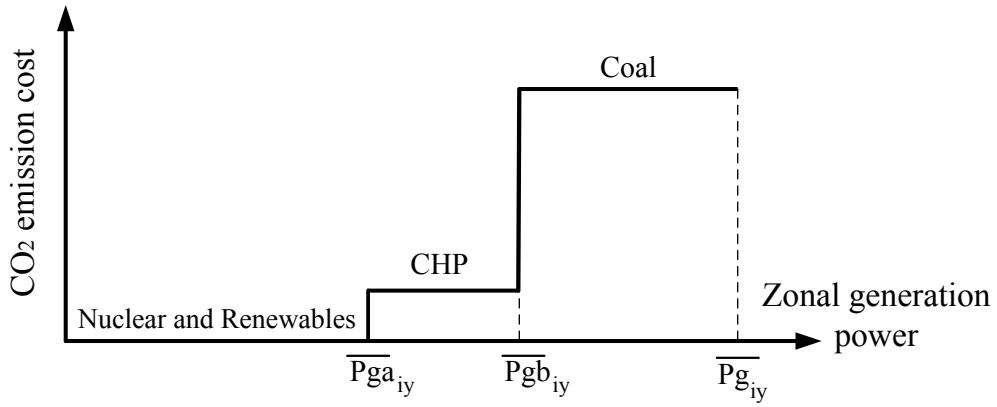

Figure 3.1: Emission cost function of generation.

AFVs are formulated and solved from the viewpoint of the government, which is responsible for the public health care; this is especially the case in Canada. The damaging consequences of emissions caused by internal combustion engine (ICE) vehicles or fossil fuel power plants directly increase the government costs to maintain a standard level of health care.

3.3 Emission Cost Model of Generation

Based on the discussions presented in the previous section, CO_2 emission costs of generation are considered in the optimization models for transition to both FCVs and PHEVs. Figure 3.1 represents a typical emission cost function during off-peak hours, when the contributing generation resources include nuclear, renewables, CHP and coal plants. It is to be noted that the contribution of gas-fired generation is not usually considered during off-peak hours. Also, the emission of nuclear plants, in per unit of electricity ultimately produced, are considered very negligible compared to the emission levels of coal and CHP plants [108, 109].

The emission cost function represented in Figure 3.1 in zone i and year y during the time period of τ, which corresponds to off-peak hours, can be expressed as

follows:

$$EC_{iy}=\begin{cases} 0: & 0 \le P^{\tau}_{g_{iy}} \le \overline{P_{ga_{iy}}}, \\ ER_{chp_i}\left(P^{\tau}_{g_{iy}} - \overline{P_{ga_{iy}}}\right) & \\ \times SC_{CO_2}g \times h \times 365: & \overline{P_{ga_{iy}}} < P^{\tau}_{g_{iy}} \le \overline{P_{gb_{iy}}}, \\ \left[ER_{chp_i}\left(\overline{P_{gb_{iy}}} - \overline{P_{ga_{iy}}}\right) + ER_{coal_i}\left(P^{\tau}_{g_{iy}} - \overline{P_{gb_{iy}}}\right)\right] & \\ \times SC_{CO_2}g \times h \times 365: & \overline{P_{gb_{iy}}} < P^{\tau}_{g_{iy}} \le \overline{P_{g_{iy}}}. \end{cases} \tag{3.1}$$

where:

$P^{\tau}_{g_{iy}}$ is the average generation power during the time period of τ in zone i and year y (in MW);

$\overline{P_{ga_{iy}}}$ is the maximum capacity of non-polluting generation resources in zone i and year y (in MW);

$\overline{P_{gb_{iy}}}$ is the maximum capacity of non-polluting plus CHP generation resources in zone i and year y (in MW);

$\overline{P_{g_{iy}}}$ is the maximum available generation resources in zone i and year y (in MW);

ER_{chp_i} and ER_{coal_i} are the emission rates of CHP and coal plants, respectively (in ton/MWh);

$SC_{CO_2}g$ is the social cost of CO_2 emission of generation (in CAD/ton);

h is the number of off-peak hours.

In order to incorporate this cost function into the optimization model, three sets of binary and continuous auxiliary variables corresponding to three segments of the cost function in Figure 3.1 are defined. Thus, K^{τ}_{1iy}, K^{τ}_{2iy} and K^{τ}_{3iy} are binary variables, which take the value of 1 if the average zonal generation power during the time period τ are located in the first, second and third segments of the emission cost

curve, respectively. Also, $P^{\tau}_{g_{1iy}}$, $P^{\tau}_{g_{2iy}}$ and $P^{\tau}_{g_{3iy}}$ are continuous auxiliary variables for the average zonal generation power $P^{\tau}_{g_{iy}}$ in the time period τ corresponding to each segment of emission cost curve, which are defined as follows:

$$P^{\tau}_{g_{iy}} = \begin{cases} P^{\tau}_{g_{1iy}}: & \text{if } K^{\tau}_{1iy} = 1, \\ P^{\tau}_{g_{2iy}}: & \text{if } K^{\tau}_{2iy} = 1, \\ P^{\tau}_{g_{3iy}}: & \text{if } K^{\tau}_{3iy} = 1. \end{cases} \tag{3.2}$$

Based on the defined sets of binary and continuous auxiliary variables, the incorporation of CO_2 emission costs in the generation side requires the addition of the following cost components into the objective function:

$$\begin{aligned} EC^{*} = \sum_{y}\sum_{i} \Big\{ & ER_{chp_i}\left[K^{\tau}_{2iy}P^{\tau}_{g_{iy}} - K^{\tau}_{2iy}\overline{P_{ga}}_{iy} + K^{\tau}_{3iy}\left(\overline{P_{gb}}_{iy} - \overline{P_{ga}}_{iy}\right)\right] \\ & + ER_{coal_i}\left(K^{\tau}_{3iy}P^{\tau}_{g_{iy}} - K^{\tau}_{3iy}\overline{P_{gb}}_{iy}\right)\Big\} SC_{CO_2} g \times h \times 365 \end{aligned} \tag{3.3}$$

by adding the following constraints:

$$\begin{aligned} & 0 \le P^{\tau}_{g_{1iy}} \le K^{\tau}_{1iy}\overline{P_{ga}}_{iy} \\ & K^{\tau}_{2iy}\left(\overline{P_{ga}}_{iy} + \epsilon_a\right) \le P^{\tau}_{g_{2iy}} \le K^{\tau}_{2iy}\left(\overline{P_{gb}}_{iy} + \epsilon_a\right) \\ & K^{\tau}_{3iy}\left(\overline{P_{gb}}_{iy} + \epsilon_a + \epsilon_b\right) \le P^{\tau}_{g_{3iy}} \le K^{\tau}_{3iy}\left(\overline{P_{g}}_{iy} + \epsilon_a + \epsilon_b\right) \\ & K^{\tau}_{1iy} + K^{\tau}_{2iy} + K^{\tau}_{3iy} \le 1 \\ & P^{\tau}_{g_{iy}} = P^{\tau}_{g_{1iy}} + P^{\tau}_{g_{2iy}} + P^{\tau}_{g_{3iy}} \\ & \forall i \in Z \wedge y \in Y \wedge \tau \in \Psi \end{aligned} \tag{3.4}$$

where Z, Y and Ψ are the sets of zones, planning years and time periods, respectively. Also, ϵ_a and ϵ_a are extremely small positive numbers.

In order to remove non-linear terms in 3.3 to keep the model an MILP problem, i.e., $K^{\tau}_{2iy}P^{\tau}_{g_{iy}}$ and $K^{\tau}_{3iy}P^{\tau}_{g_{iy}}$, they are replaced by new variables V^{τ}_{2iy} and V^{τ}_{3iy},

respectively, by adding the following constraints:

$$
\begin{aligned}
&V^{\tau}_{2iy} \geq P^{\tau}_{g_{iy}} - \overline{P_{g_{iy}}}\left(1 - K^{\tau}_{2iy}\right)\\
&V^{\tau}_{3iy} \geq P^{\tau}_{g_{iy}} - \overline{P_{g_{iy}}}\left(1 - K^{\tau}_{3iy}\right)\\
&V^{\tau}_{2iy} \geq \underline{P_{g_{iy}}} K^{\tau}_{2iy}\\
&V^{\tau}_{3iy} \geq \underline{P_{g_{iy}}} K^{\tau}_{3iy}\\
&\forall i \in Z \wedge y \in Y \wedge \tau \in \Psi
\end{aligned} \tag{3.5}
$$

where $\underline{P_{g_{iy}}}$ are lower bounds of zonal generation power.

3.4 Optimization Model for Transition to FCVs

In this section, an optimization planning model is developed that takes into account both electricity and hydrogen networks as one integrated system. It is assumed that the hydrogen demand for transportation purposes in each zone would be fulfilled by the operation of electrolytic HPPs during off-peak price time intervals. Therefore, the purpose of the proposed optimization model is to determine the optimal size of HPPs to be installed in different zones, as well as to find the optimal hydrogen transportation routes to achieve optimal hydrogen economy penetrations for each year of the planning horizon. This section begins with the development of a hydrogen transportation model, and then the MILP model formulation is described, by starting with the objective function and followed by the description of the required problem constraints.

3.4.1 Hydrogen Transportation Model

In an ideal case, each zone should be able to fulfill its own hydrogen requirement. However, due to resource limitations in a couple of zones, power loss in transmission networks, the assumed level of hydrogen economy penetration or some operational

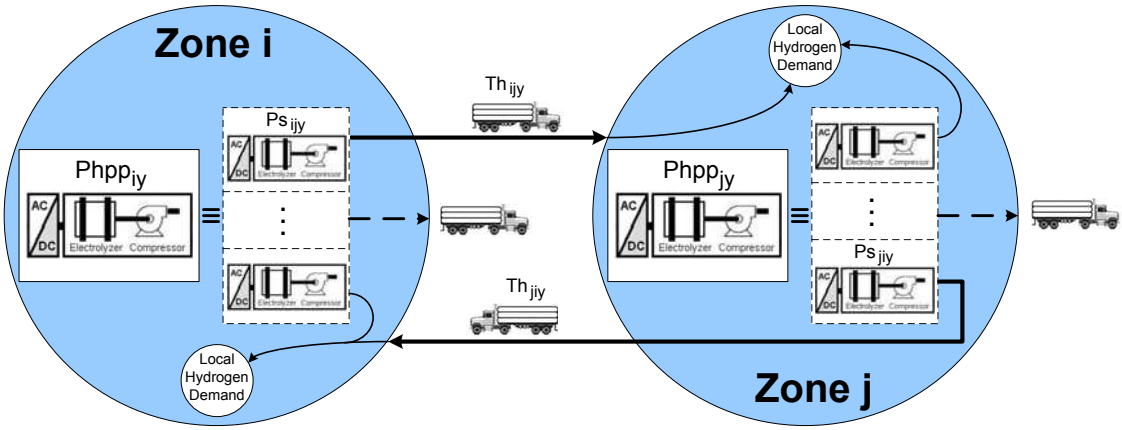

Figure 3.2: Demonstration of the proposed hydrogen transfer concept.

or placement constraints, there may be a need for hydrogen transfer between particular zones in certain years. Among the possible modes of hydrogen transfer, i.e., compressed gas trucks, cryogenic tanker trucks and pipelines [110], the first mode is considered at this stage mainly because of economic considerations and greater availability of the required infrastructure in the near term compared to other options.

A simple demonstration of the proposed hydrogen transfer concept is shown in Figure 3.2, where both hydrogen import and export possibilities exist for each zone. In general, the total installed HPP capacity in zone i, by year y ($Phpp_{iy}$) can be partly utilized for covering the local hydrogen demand as well as the hydrogen requirements of other zones. Hence, the total capacity of an HPP can be decomposed into multiple components, each of which covers a portion of the hydrogen requirement of other zones. For example, the power component Ps_{ijy} in Figure 3.2 can be interpreted as the contribution of zone i in total required power of HPPs in zone j, which should be transferred to zone j by compressed gas trucks. Similarly, other zones such as zone j can share the required power of HPPs in zone i based on a power component Ps_{jiy}. Based on this, the required MW capacity of HPPs for zone i by Year y (Ph_{iy}) which supplies the local hydrogen demand to achieve a certain level of hydrogen economy penetration, can be expressed as follows:

$$Ph_{iy} = Phpp_{iy} - \sum_{j \neq i} Ps_{ijy} + \sum_{j \neq i} Ps_{jiy} \quad \forall i, j \in Z \wedge y \in Y_1 \tag{3.6}$$

where Y_1 is the set of planning years excluding the first year. Also, the total installed HPP in zone i by year y is equal to the previously installed HPP by year $y-1$ and the newly installed HPP in year y ($\Delta Phpp_{iy}$), which is expressed as follows:

$$Phpp_{iy} = Phpp_{iy-1} + \Delta Phpp_{iy} \quad \forall i \in Z \wedge y \in Y_1 \tag{3.7}$$

In general, local required MW capacity of HPPs in zone i and year y for a 100% hydrogen economy penetration can be calculated as follows:

$$Chpp_{iy} = \frac{10^{-3} AM.HHV}{24 \times 365 \eta^b_{hpp}.FE_{fcv}.CF_{hpp}} Cf_y Nldv_{iy} \quad \forall i \in Z \wedge y \in Y \tag{3.8}$$

where:

AM is the annual mileage (in km).

HHV is the higher heating value of hydrogen ($\simeq$39.45 kWh/kg).

η^b_{hpp} is the base efficiency of HPPs at the beginning of the planning horizon.

FE_{fcv} is the fuel economy of the fuel cell vehicles (in km/kg).

CF_{hpp} is the average capacity factor of HPPs (in %).

$Nldv_{iy}$ is the total number of light-duty vehicles in zone i and year y.

Cf_y is the correction factor in year y, which considers the efficiency improvement of the HPPs over the planning years and is calculated as follows:

$$Cf_y = \frac{\eta^b_{hpp}}{\left[\eta^b_{hpp} + \frac{\Delta \eta_{hpp}}{PS} (y - y_1)\right]} \quad \forall y \in Y \tag{3.9}$$

where PS is the planning span, $\Delta\eta_{hpp}$ is the efficiency improvement of the HPPs over the planning horizon, and y_1 is the first year of the planning years.

Based on the definition of $Chpp_{iy}$, the local required MW capacity of HPP to achieve a certain level of hydrogen economy penetration can then be expressed as follows:

$$Ph_{iy} = FF_{iy}\overline{\mu}_y Chpp_{iy} \quad \forall i \in Z \wedge y \in Y \tag{3.10}$$

where:

$\bar{\mu}_y$ is the maximum possible hydrogen economy penetration in year y which is fixed by the system planner based on an assumed transition curve. This transition curve accounts for the time needed for the development of the required infrastructure and specifies the maximum penetration levels that can be realized in each year to achieve a certain penetration level by the end of the planning horizon.

FF_{iy} is the feasibility factor in zone i and year y which determines the percentage of the penetration levels set by the transition curve that is achievable due to electricity grid constraints.

Combining (3.8)-(3.10) with (3.6) results in the following equality constraints in which penetration levels are reflected:

$$\begin{gathered} Phpp_{iy} - \sum_{j\neq i} Ps_{ijy} + \sum_{j\neq i} Ps_{jiy} \\ -\frac{10^{-3} AM.HHV}{24 \times 365 FE_{fcv} CF_{hpp}\left[\eta^b_{hpp} + \frac{\Delta\eta_{hpp}}{PS}(y - y_1)\right]} Nldv_{iy}\overline{\mu}_y FF_{iy} = 0 \\ \forall i \in Z \wedge y \in Y_1 \end{gathered} \tag{3.11}$$

As previously discussed and demonstrated in Figure 3.2, corresponding to each power component Ps_{ijy} (MW) there is a transferred hydrogen component TH_{ijy}

(ton/day); these variables can be coupled together by a linking factor LF_y as follows:

$$TH_{ijy} = LF_y Ps_{ijy} \quad \forall (i,j) \in Z^* \wedge y \in Y_1 \tag{3.12}$$

where $Z^* = \{(i,j) : i,j \in Z, i \neq j\}$ is the set of indexes of hydrogen transfer corridors. This relation means that the Ps_{ijy} (MW) component in zone i is capable of producing $LF_y Ps_{ijy}$ (ton/day) hydrogen to be transferred to zone j by compressed gas trucks. In order to find LF_y, one should note the HHV of hydrogen as well as the efficiency and average capacity factor of HPPs; thus, considering the efficiency improvement of HPPs over time, LF_y can, in general, be expressed as follows:

$$LF_y = \frac{24 CF_{hpp}}{HHV} \left[\eta^b_{hpp} + \frac{\Delta \eta_{hpp}}{PS} (y - y_1) \right] \quad \forall y \in Y_1 \tag{3.13}$$

Average daily transferred hydrogen between zones i and j in each year (TH_{ijy}) should be zero or lie between predefined lower and upper bounds. This requirement can be implemented by defining new binary variables in the following constraint:

$$\beta_{ijy} \underline{TH} \leq TH_{ijy} \leq \beta_{ijy} \overline{TH} \quad \forall (i,j) \in Z^* \wedge y \in Y_1 \tag{3.14}$$

where $\underline{TH}$ and $\overline{TH}$ are the lower and upper bounds of daily transferred hydrogen, respectively, and β_{ijy} are binary variables which take the value of 1 if there is transferred hydrogen between zones i and j in year y.

Depending on the values of transferred hydrogen, appropriate numbers of compressed gas trucks including cabs and tube trailers must be purchased. This can be realized by the following set of constraints:

$$N_{ijy} \geq TH_{ijy} / \overline{CT} \quad \forall (i,j) \in Z^* \wedge y \in Y_1 \tag{3.15}$$

$$NT_y \geq \sum_{(i,j) \in Z^*} N_{ijy} \quad \forall y \in Y_1 \tag{3.16}$$

$$\sum_{k=y_1}^{y} PT_k \geq NT_y \quad \forall y \in Y_1 \tag{3.17}$$

$$\sum_{k=y-LT_{cab}+1}^{y} PC_k = NT_y \quad \forall y \in \{y_1 + LT_{cab} - 1, ..., H\} \tag{3.18}$$

$$\sum_{k=y_1}^{y} PC_k = NT_y \quad \forall y \in \{y_1, ..., y_1 + LT_{cab} - 1\} \tag{3.19}$$

where:

$\overline{CT}$ is the maximum capacity of each compressed gas truck (in ton).

N_{ijy} is the integer number of compressed gas trucks or tube trailers with the capacity of $\overline{CT}$ needed for route (i, j) in year y.

NT_y is the total number of compressed gas trucks or tube trailers with the capacity of $\overline{CT}$ needed in year y.

PT_k is the integer number of purchased compressed gas trucks or tube trailers with the capacity of $\overline{CT}$ in year k.

PC_k is the integer number of purchased cabs in year k.

LT_{cab} is the lifetime of cabs.

y_1 and H are the first and last years of the planning horizon.

Note that the trucks are represented here in two components, i.e., cabs and tube trailers, given the difference in the operational lifetime between them.

The required number of compressed gas trucks is linked to the transferred hydrogen in route (i, j) in year y through the constraints (3.15). Constraints (3.16) state that the total number of required trucks should not be less than the required trucks in all the possible routes. The total number of purchased trucks (tube trailers) by year y is related to the total number of required trucks in year y by constraints (3.17). Constraints (3.18) and (3.19) state that the total number of purchased cabs

in any time interval equal to the lifetime of the cab ending in year y should be equal to the total number of trucks (tube trailers) needed in year y.

3.4.2 Objective Function

The model's objective is to minimize the present value of the net electricity, emission and hydrogen transportation costs. Thus, the objective function consists of electricity generation and imported/exported power cost/revenue components; emission cost and credit components in generation facilities and population areas, respectively; and the hydrogen transportation costs. Therefore, the objective function is expressed as follows:

$$\min \sum_{y \in Y} \frac{1}{(1+DR)^{y-y_1}} \left(C_{1y} - C_{2y} + C_{3y} + C_{4y}\right) \tag{3.20}$$

where DR is the percentage of discount rate used to represent all costs at present value, and $C_{iy}, i \in \{1, ..., 4\}$ are different cost and revenue components, which are defined in the following sections.

Net Electricity Cost

C_{1y} represents the net total electricity costs in year y. Since different time frames for the operation of HPPs during weekdays and weekends are assumed, the electricity cost and revenue components in C_{1y} have two separate terms corresponding to different time frames in weekdays and weekends as follows:

$$\begin{aligned} C_{1y} = \sum_{i \in Z} \Big\{ & (P_{g_{iy}}^{\omega_1} \pi_y^{\omega_1} + P_{m_{iy}}^{\omega_1} \pi_{m_y}^{\omega_1} - P_{x_{iy}}^{\omega_1} \pi_{x_y}^{\omega_1}) \times h_{wd} \times 261 \\ & + (P_{g_{iy}}^{\omega_2} \pi_y^{\omega_2} + P_{m_{iy}}^{\omega_2} \pi_{m_y}^{\omega_2} - P_{x_{iy}}^{\omega_2} \pi_{x_y}^{\omega_2}) \times h_{we} \times 104 \Big\} \end{aligned} \tag{3.21}$$

where:

h_{wd} and h_{we} are the number of HPPs operation hours in weekdays and weekends, respectively.

ω_1 is an identifier of the time period corresponding to weekday hours.

ω_2 is an identifier of the time period corresponding to weekend hours.

$P_{g_{iy}}$, $P_{m_{iy}}$ and $P_{x_{iy}}$ are zonal generation power, imported power and exported power, respectively, in zone i, year y and during the time period ω_1 or ω_2 (in MW).

π_y, π_{m_y} and π_{x_y} are internal, import and export electricity prices, respectively (in CAD/MWh).

Environmental Credit

C_{2y} represents the environmental credits assigned to FCVs in year y and is stated as:

$$C_{2y} = \sum_{i \in Z} \left\{ FF_{iy}.\bar{\mu}_y.Nldv_{iy}.AM.SC_{CO_2}p.E_{CO_2} \times 10^{-3} \sum_{c \in VT} \left(\frac{VS_c}{FE_{gv_{cy}}} \right) \right\} \quad (3.22)$$

where:

VT is the set of indexes corresponding to different types of light-duty vehicles.

$SC_{CO_2}p$ is the social cost of CO_2 emission in the population area (in CAD/ton).

E_{CO_2} is the constant value of CO_2 emissions from burning gasoline ($\simeq 2.3$ kg/litre).

VS_c is the percent share of the vehicle of type c.

$FE_{gv_{cy}}$ is the fuel economy of the gasoline vehicle of type c in year y (in km/litre).

Emission Cost of Generation

C_{3y} represents the environmental costs of generation in year y, and similar to C_{1y}, has two terms corresponding to weekdays and weekends. Based on the Mathematical formulation developed in Section 3.3, this cost component is expressed as follows:

$$\begin{aligned} C_{3y} = \sum_{i \in Z} \Bigg\{ & \Big\{ ER_{chp_i} \Big[V_{2_{iy}}^{\omega_1} - K_{2iy}^{\omega_1} \overline{P_{ga}}_{iy} + K_{3iy}^{\omega_1} \Big(\overline{P_{gb}}_{iy} - \overline{P_{ga}}_{iy} \Big) \Big] \\ & + ER_{coal_i} \Big(V_{3_{iy}}^{\omega_1} - K_{3iy}^{\omega_1} \overline{P_{gb}}_{iy} \Big) \Big\} SC_{CO_2} g \times h_{wd} \times 261 \\ & + \Big\{ ER_{chp_i} \Big[V_{2_{iy}}^{\omega_2} - K_{2iy}^{\omega_2} \overline{P_{ga}}_{iy} + K_{3iy}^{\omega_2} \Big(\overline{P_{gb}}_{iy} - \overline{P_{ga}}_{iy} \Big) \Big] \\ & + ER_{coal_i} \Big(V_{3_{iy}}^{\omega_2} - K_{3iy}^{\omega_2} \overline{P_{gb}}_{iy} \Big) \Big\} SC_{CO_2} g \times h_{we} \times 104 \Bigg\} \end{aligned} \tag{3.23}$$

Hydrogen Transportation Cost

C_{4y} represents total hydrogen transportation costs, including the capital and operating costs of compressed gas trucks, which can be stated as follows:

$$C_{4y} = PC_y.CC_{cab}(1 - S_{cab_y}) + PT_y.CC_{tube}(1 - S_{tube_y}) + \sum_{(i,j) \in Z^*} 2OC_y.d_{ij}.N_{ijy} \times 365 \tag{3.24}$$

where:

CC_{cab} and CC_{tube} are capital cost of cabs and tube trailers, respectively (in CAD).

PC_y and PT_y are integer numbers of purchased cabs and tube trailers, respectively, in year y.

S_{cab_y} and S_{tube_y} are salvage values of cabs and tube trailers, respectively, in year y.

OC_y is the operation cost of compressed gas trucks (in CAD/km).

d_{ij} is the approximate distance between zones i and j (in km).

Based on straight-line depreciation, the salvage values for cab and tube trailers in (3.24) can be calculated as follows, as per the notation defined in Section 3.4.1:

$$S_{cab_y} = \begin{cases} \frac{1}{(1+DR)^{(H-y+1)}} \left(y + LT_{cab} - H - 1\right) / LT_{cab} : & \forall y \geq H - LT_{cab}, \\ 0 : & \text{else .} \end{cases} \tag{3.25}$$

$$S_{tube_y} = \begin{cases} \frac{1}{(1+DR)^{(H-y+1)}} \left(y + LT_{tube} - H - 1\right) / LT_{tube} : & \forall y \geq H - LT_{tube}, \\ 0 : & \text{else .} \end{cases} \tag{3.26}$$

3.4.3 Constraints

Transmission System

The transmission-system model in this study is appropriate for long-term planning studies, which are mainly concerned about generation, transmission, and demand of active power [111,112]. In these studies, reactive power and related voltage issues are usually indirectly represented in the transmission-system constraints by further limiting the amount of active power that can be transferred between relevant areas. Hence, given the nature of the presented studies which only require an approximate representation of the grid, a dc optimal power flow model that accounts for the transmission system losses is adopted here [113]. This model is discussed in detail next.

The power losses in line (i, j) of the electricity network can be approximately calculated as:

$$Ploss_{ij} \cong g_{ij}(\delta_i - \delta_j)^2 \tag{3.27}$$

where g_{ij} is the conductance of the line between buses i and j and δ denotes the corresponding bus-voltage angles. Following the method proposed in [114] with some modifications, a linear approximation of power losses in year y and during the time period of τ can be obtained using L piecewise linear blocks as follows:

$$\delta^{\tau}_{ijy} = \left|\delta^{\tau}_{iy} - \delta^{\tau}_{jy}\right| \tag{3.28}$$

$$\delta^{\tau}_{ijy} = \sum_{l=1}^{L} \delta^{\tau}_{ijy}(l) \tag{3.29}$$

$$Ploss^{\tau}_{ijy} = g_{ijy} \sum_{l=1}^{L} \alpha_{ijy}(l)\delta^{\tau}_{ijy}(l) \tag{3.30}$$

where $\alpha_{ijy}(l)$ and $\delta^{\tau}_{ijy}(l)$ denote the slope and value of the lth block of voltage angle during the time period of τ, respectively. Assuming that each angle block has a constant maximum length $\Delta\delta_y$, the slope of the blocks of angles for all lines (i, j) can be calculated as:

$$\alpha_{ijy}(l) = (2l-1)\Delta\delta_y \quad \forall (i,j) \in \Omega \wedge y \in Y \tag{3.31}$$

where Ω is the set of indexes of transmission lines. Consequently, each block of voltage angle is bounded between zero and $\Delta\delta_y$, as follows:

$$0 \leq \delta^{\tau}_{ijy}(l) \leq \Delta\delta_y \quad \forall (i,j) \in \Omega \wedge y \in Y \wedge \tau \in \Psi \wedge l \in L_1 \tag{3.32}$$

where L_1 is the set of total voltage angle blocks; $L_1 = \{1, ..., L\}$.

To linearize the absolute value in 3.28, the two new nonnegative variables $\delta^{\tau+}_{ijy}$ and $\delta^{\tau-}_{ijy}$ are defined, together with the following constraints [115]:

$$\begin{gathered} \delta^{\tau}_{ijy} = \delta^{\tau+}_{ijy} + \delta^{\tau-}_{ijy} \\ \delta^{\tau}_{iy} - \delta^{\tau}_{jy} = \delta^{\tau+}_{ijy} - \delta^{\tau-}_{ijy} \\ \delta^{\tau+}_{ijy} \geq 0, \delta^{\tau-}_{ijy} \geq 0 \\ \forall (i,j) \in \Omega \wedge y \in Y \wedge \tau \in \Psi \end{gathered} \tag{3.33}$$

The following constraints are also needed to enforce the adjacency of the angle blocks:

$$\mu^{\tau}_{ijy}(l).\Delta\delta_y \leq \delta^{\tau}_{ijy}(l) \quad \forall(i,j) \in \Omega \wedge y \in Y \wedge \tau \in \Psi \wedge l \in L_2 \tag{3.34}$$

$$\delta^{\tau}_{ijy}(l) \leq \mu^{\tau}_{ijy}(l-1).\Delta\delta_y \quad \forall(i,j) \in \Omega \wedge y \in Y \wedge \tau \in \Psi \wedge l \in L_3 \tag{3.35}$$

$$\mu^{\tau}_{ijy}(l) \leq \mu^{\tau}_{ijy}(l-1) \quad \forall(i,j) \in \Omega \wedge y \in Y \wedge \tau \in \Psi \wedge l \in L_4 \tag{3.36}$$

where $\mu^{\tau}_{ijy}(l)$ is a binary variable which adopts the value of one if the value of the lth angle block for the line (i,j) during the time period of τ is equal to its maximum value $\Delta\delta_y$; L_2=$\{1,...,L-1\}$; L_3=$\{2,...,L\}$; and L_4=$\{2,...,L-1\}$.

Considering the line-loss model just described, the net power injected at zone i in year y and during the time period of τ can be represented as:

$$P^{\tau}_{iy} = \sum_{(i,j)\in\Omega} \left[\frac{1}{2} g_{ijy} \sum_{l=1}^{L} \alpha_{ijy}(l) \delta^{\tau}_{ijy}(l) - b_{ijy}(\delta^{\tau}_{iy} - \delta^{\tau}_{jy}) \right] \tag{3.37}$$

where b_{ijy} is the susceptance of the line (i,j) in year y. As a result, the zonal-power-balance constraints can be generally formulated as follows:

$$\begin{gathered} P^{\tau}_{g_{iy}} - P^{\tau}_{l_{iy}} + P^{\tau}_{m_{iy}} - P^{\tau}_{x_{iy}} \\ - \sum_{(i,j)\in\Omega} \left[\frac{1}{2} g_{ijy} \sum_{l=1}^{L} \alpha_{ijy}(l) \delta^{\tau}_{ijy}(l) - b_{ijy}(\delta^{\tau}_{iy} - \delta^{\tau}_{jy}) \right] = 0 \\ \forall i \in Z \wedge y \in Y \wedge \tau \in \Psi \end{gathered} \tag{3.38}$$

where P_l is the total base load in each zone and is comprised of the zonal electricity demand (P_e) and the total installed HPPs as follows:

$$P^{\tau}_{l_{iy}} - P^{\tau}_{e_{iy}} - P_{hpp_{iy}} = 0 \quad \forall i \in Z \wedge y \in Y \wedge \tau \in \Psi \tag{3.39}$$

Transmission Capacity Constraints

Based on the transmission model discussed in the previous section, these constraints are defined as follows:

$$-b_{ijy}(\delta^{\tau}_{iy} - \delta^{\tau}_{jy}) + \frac{1}{2}g_{ijy}\sum_{l=1}^{L}\alpha_{ijy}(l)\delta^{\tau}_{ijy}(l) \leq \overline{Pd}_{ijy}$$

$$b_{ijy}(\delta^{\tau}_{iy} - \delta^{\tau}_{jy}) + \frac{1}{2}g_{ijy}\sum_{l=1}^{L}\alpha_{ijy}(l)\delta^{\tau}_{ijy}(l) \leq \overline{Pr}_{ijy}$$

$$\forall (i,j) \in \Omega \wedge y \in Y \wedge \tau \in \Psi \tag{3.40}$$

where $\overline{Pd}_{ijy}$ and $\overline{Pr}_{ijy}$ are the maximum capacities of the transmission corridor (i,j) in year y for direct and reverse power flows, respectively. These limits are obtained based on thermal and stability considerations such as reactive-power and related-voltage stability issues.

Zonal Power Generation Limits

Zonal power generation in each year is confined by minimum and maximum limits, $\underline{Pg}_{iy}$ and $\overline{Pg}_{iy}$, respectively. These limits are the minimum and maximum effective generation capacities which are available in each zone during the planning years in the time period of τ:

$$\underline{P_g}_{iy} \leq P^{\tau}_{g_{iy}} \leq \overline{P_g}_{iy} \quad \forall i \in Z \wedge y \in Y \wedge \tau \in \Psi \tag{3.41}$$

The lower bounds $\underline{P_g}_{iy}$ may be set based on the operational considerations of the base-load generation resources in each zone.

Zonal Import/Export Power Limits

These limits are stated as:

$$\begin{gathered} \underline{P_{m_{iy}}} \leq P_{m_{iy}}^{\tau} \leq \overline{P_{miy}} \\ \underline{P_{x_{iy}}} \leq P_{xiy}^{\tau} \leq \overline{P_{xiy}} \\ \forall i \in Z \wedge y \in Y \wedge \tau \in \Psi \end{gathered} \tag{3.42}$$

where $\underline{P_{m_{iy}}}$ and $\overline{P_{miy}}$ are the lower and upper bounds of imported power, respectively, and $\underline{P_{x_{iy}}}$ and $\overline{P_{xiy}}$ are exported power minimum and maximum limits, respectively.

HPP Placement Constraints

These constraints are represented by:

$$\begin{gathered} 0 \leq P_{hpp_{iy}} \leq \overline{P_{hpp_{iy}}} \\ 0 \leq \Delta P_{hpp_{iy}} \leq \overline{\Delta P_{hpp_{iy}}} \\ \forall i \in Z \wedge y \in Y_1 \end{gathered} \tag{3.43}$$

where $\overline{P_{hpp_{iy}}}$ is the maximum size of HPPs, which is allowed to be installed in zone i by year y, and $\overline{\Delta P_{hpp_{iy}}}$ is the maximum annual development of HPPs in zone i. $\overline{P_{hpp_{iy}}}$ is equal to zero for the first year of the planning horizon.

Hydrogen Transportation Constraints

As discussed in Section 3.4.1, hydrogen transportation constraints are expressed by (3.7) and (3.11)–(3.19).

Generation Emission Constraints

Based on the model developed in Section 3.3, these constraints are expressed by (3.4) and (3.5).

Penetration Constraints

These constraints are defined as:

$$0 \leq FF_{iy} \leq 1 \quad \forall i \in Z \wedge y \in Y \tag{3.44}$$

$$FF_{iy}\overline{\mu}_y - FF_{iy-1}\overline{\mu}_{y-1} \geq 0 \quad \forall i \in Z \wedge y \in Y_1 \tag{3.45}$$

Constraints (3.44) state that the penetration levels in each year cannot exceed the limits $\overline{\mu}_y$ set by the assumed transition curve, and (3.45) enforce the increase of the ultimate penetration levels over time, so that the total number of FCVs in the transport sector in each year cannot be less than in previous year. Furthermore, the following constraints should be considered in the model for a uniform hydrogen economy penetration in all zones:

$$FF_{iy} - FF_{jy} = 0 \quad \forall i, j \in Z \wedge y \in Y_1 \tag{3.46}$$

3.5 Optimization Model for Transition to PHEVs

Using almost the same methodology as used in Section 3.4, with some modifications, an optimization model for transition to PHEVs is developed based on the following considerations:

- Since there is no integrated energy system in this case, all the variables and constraints corresponding to the hydrogen transportation model are eliminated.
- The charging of batteries is assumed to take place during a similar time frame in both weekdays and weekends. Therefore, all the parameters and variables in the FCVs model, that were defined for different time frames are not needed in this case.

- Annual mileage of PHEVs and FCVs are interpreted differently in the objective function of the optimization models. In FCVs, the only fuel is hydrogen; therefore, the total distance traveled in a year, which is solely based on hydrogen, is considered in the emission credit term of the objective function. However, PHEVs run on both battery and gasoline, and only the electric share of vehicle miles traveled deserve credit in the objective function.

In view of the above considerations, the objective function of the optimization model for transition to PHEVs can be expressed as follows:

$$\min \sum_{y \in Y} \frac{1}{(1+DR)^{y-y_1}} \left(C_{1y} - C_{2y} + C_{3y}\right)$$

$$\begin{aligned}
C_{1y} &= \left(P^{\omega}_{g_{iy}} \pi^{\omega}_{y} + P^{\omega}_{m_{iy}} \pi^{\omega}_{m_y} - P^{\omega}_{x_{iy}} \pi^{\omega}_{x_y}\right) \times h \times 365 \\
C_{2y} &= \sum_{i \in Z} \left\{ FF_{iy}.\bar{\mu}_y.Nldv_{iy}.DT.SC_{CO_2}p.E_{CO_2} \times 0.365 \sum_{c \in VT} \left(\frac{VS_c}{FE_{gv_{cy}}}\right) \right\} \\
C_{3y} &= \sum_{i \in Z} \Big\{ ER_{chp_i} \left[V^{\omega}_{2_{iy}} - K^{\omega}_{2iy} \overline{P_{ga}}_{iy} + K^{\omega}_{3iy} \left(\overline{P_{gb}}_{iy} - \overline{P_{ga}}_{iy}\right)\right] \\
&\qquad + ER_{coal_i} \left(V^{\omega}_{3_{iy}} - K^{\omega}_{3iy} \overline{P_{gb}}_{iy}\right) \Big\} SC_{CO_2} g \times h \times 365
\end{aligned} \tag{3.47}$$

where:

C_{1y}, C_{2y} and C_{3y} are the net total electricity costs, emission credits and emission costs of generation, respectively, in year y.

h is the number of off-peak hours per day in which PHEVs charging takes place.

ω is an identifier kept to relate this model to the FCV transition model, even though is not really needed here.

DT is the PHEVs' daily trip running on battery, which is also referred to as all-electric range (AER) in the literature (in km).

The constraints of this optimization model are almost the same as the ones discussed in Section 3.4.3; however, hydrogen-transportation-related constraints are disregarded, and all the parameters and variables defined for the two periods ω_1 and ω_2 are considered here only for one time period ω. Hence, the zonal-power-balance constraints are represented as follows:

$$P^{\omega}_{g_{iy}} - P^{\omega}_{l_{iy}} + P^{\omega}_{m_{iy}} - P^{\omega}_{x_{iy}} - \sum_{(i,j)\in\Omega} \left[\frac{1}{2} g_{ijy} \sum_{l=1}^{L} \alpha_{ijy}(l) \delta^{\omega}_{ijy}(l) - b_{ijy}(\delta^{\omega}_{iy} - \delta^{\omega}_{jy}) \right] = 0 \quad \forall i \in Z \wedge y \in Y \tag{3.48}$$

where P_l is the total base load in each zone and is comprised of the zonal electricity demand P_e and PHEVs charging power $FF\overline{\mu}Pch$ as follows:

$$P^{\omega}_{l_{iy}} - P^{\omega}_{e_{iy}} - FF_{iy}\overline{\mu}_y Pch_{iy} = 0 \quad \forall i \in Z \wedge y \in Y \tag{3.49}$$

with Pch_{iy} representing the total maximum PHEVs charging power in zone i and year y.

3.6 Test System

In this section, a test system is developed to evaluate the performance and demonstrate the capabilities of the proposed model for transition to FCVs in a planning horizon from 2008 to 2025. This model is the more comprehensive one of the two models due to its hydrogen transportation constraints and hence captures all the properties of the proposed planning framework. Also, the small scale of this test system allows one to better understand and interpret the results and evaluate the impacts of different constraints.

As demonstrated in Figure 3.3, the test system is composed of three zones interconnected by 500 kV transmission corridors and with the possibility of power

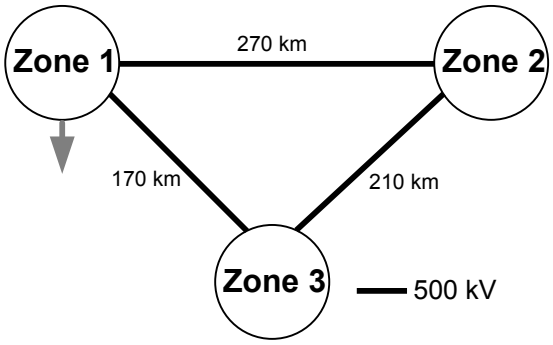

Figure 3.3: 3-zone test system.

export to a neighboring jurisdiction in Zone 1. The approximate distances between the zones are also reflected in this figure; the parameters, which are used to model the electricity network are based on typical values of 500 kV networks, considering these approximate distances. Further assumptions regarding both electricity and transport sectors are discussed in the following sections.

3.6.1 Transport Sector

LDVs

The number of LDVs in Zones 1, 2 and 3 are assumed to be equal to 50,000, 900,000 and 550,000, respectively, with 1% annual rate of increase. These values are selected in proportion of the corresponding zonal electricity demands. Also, the assumed annual mileage of LDVs is 20,000 km.

Disregarding the different types of gasoline-fuelled LDVs, an average fuel economy of 10 km/litre is assumed for all these vehicles. However, in order not to overestimate the environmental credit of FCVs, it is assumed that this average fuel economy will be improved by 20% by the end of the planning horizon.

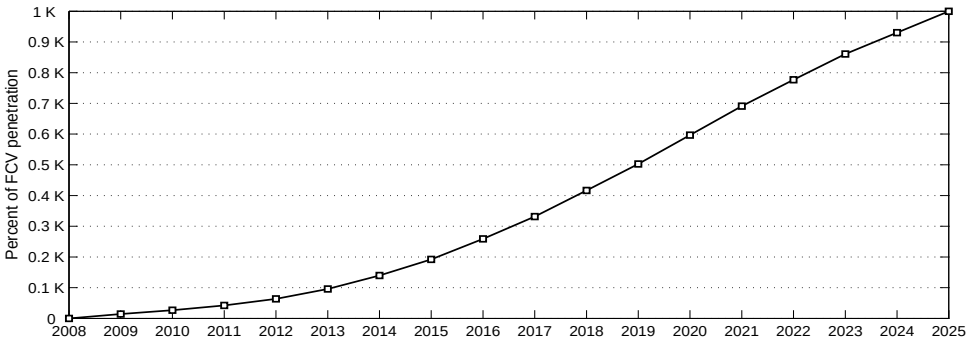

Figure 3.4: Pattern of transition to FCVs in the transport sector.

Transition Pattern

Maximum penetrations of the hydrogen economy into the transport sectors of all three zones ($\bar{\mu}_y$) are assumed to be as shown in Figure 3.4. This curve specifies the maximum possible hydrogen economy penetrations in each year with respect to the ultimate K% penetration by the end of the planning horizon. Numerical values of $\bar{\mu}_y$ in the model are calculated with K=100.

Hydrogen Demand

Based on 20,000 km annual mileage and 100 km/kg average fuel economy of the different types of fuel cell light-duty vehicles [13, 21, 116], the average hydrogen demand of a representative FCV is approximately calculated to be 0.55 kg/day. This number yields the daily hydrogen demand in each zone, considering the number of LDVs and hydrogen economy penetration levels to be realized each year following the transition curve. In this way, the hydrogen demand of all the transport sectors of the 3-zone system amounts to 965 ton/day in 2025 for a 100% FCV penetration.

Hydrogen Transportation

The maximum capacity of each compressed gas truck for the possible transfer of hydrogen between zones is assumed to be equal to 0.4 ton. The lower bound of daily

hydrogen transfer is assumed to be 25% of the maximum capacity of one truck, and the upper bound of daily hydrogen transfer is fixed at 4 ton/day, i.e., at most 10 trucks can be assigned for daily hydrogen transfer along each route.

The investment costs of cabs and tube trailers for compressed gas trucks, for the possible hydrogen transportation between the zones are assumed to be equal to 100,000 and 240,000 CAD, respectively. Also, the operating cost of trucks is assumed as 1 CAD/km, which increases by 2.5% per year during the planning years. Lifetimes of cabs and tube trailers are also assumed to be 5 and 20 years, respectively.

3.6.2 Electricity Sector

Transmission Capacity

Transmission capacities for corridors 1-2, 1-3 and 2-3 are assumed to be 2560, 1940 and 1560 MW, respectively. Also, there is a 2000 MW capacity improvement in 2012 for corridor 1-2 and a 500 MW capacity improvement in 2015 for corridor 1-3.

Generation Capacity

The development of generation capacity during the planning study is assumed to be as shown in Figure 3.5; the MW values reflected in these figures are the effective capacities contributing to the demand during off-peak hours, including the capacity factors. Observe that Zone 1 is the main generation center of the whole system, and Zone 3 is the most polluting zone in generation side because of coal and CHP resources. The increase and decrease of nuclear power capacity in Zone 1 are due to the development of new units and the refurbishment of old ones, respectively. Also, retirement of coal-fired power plants in Zone 2 and partly in Zone 3 explains the decrease of coal power capacity in these zones over the planning years.

CO_2 emission rates of coal and CHP plants in Zones 2 and 3 are assumed to be equal to 1 and 0.25 ton/MWh, respectively. Also, based on the discussions

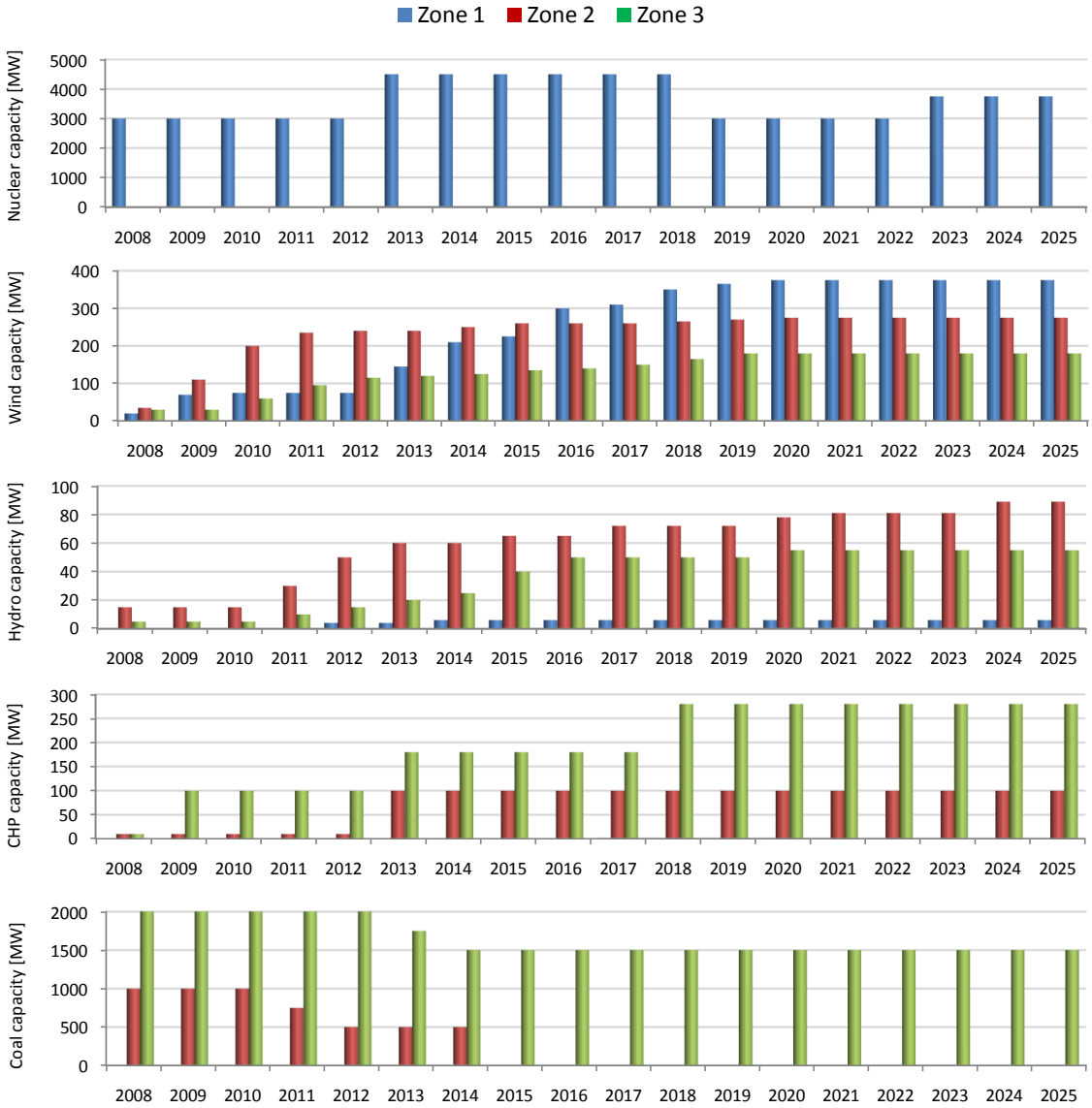

Figure 3.5: Generation capacity developments during the planning horizon.

presented in Section 3.2, a social cost of emission of 35 CAD/ton is assumed for the generation. However, in order to reflect the maximum potential of electricity system to support FCVs, a sufficiently large value of the social cost of emissions for populated areas is assumed; this issue is further discussed in Section 3.7.

Electricity Demand and Price

Average base-load electricity demands in Zones 1, 2 and 3 at the beginning of the planning study are assumed to be equal to 100, 3000 and 1600 MW, respectively, which will increase by 1% each year. It is also assumed that the average load levels for 8 weekday hours and 14 weekend hours are the same; these time frames are the assumed operation times of HPPs. Also, average electricity prices for 8 weekday hours and 14 weekend hours are assumed to be equal to 30 CAD/MWh and 35 CAD/MWh, respectively, and the discount rate is fixed at 8%.

HPP Size

The zonal hydrogen demand during the planning period allows for the determination of the required capacity of the HPPs. For example, based on a HHV of hydrogen, a 70% efficiency for the whole plant and 68 hours of operation per week, including 8 and 14 hours of operation during weekdays and weekends, respectively, the required size of the plant producing an average 1 ton/day of hydrogen is found to be almost equal to 5.8 MW. However, this size reduces over time with the efficiency improvement in the plant. In general, the required MW size of HPPs in different zones over the planning years were determined from (3.8) assuming a 15% efficiency improvement of HPPs by 2025. Based on a 100% FCV penetration, this results in a required size of 4,869 MW of HPPs for the whole system by 2025.

Table 3.1: 3-zone model statistics

Number of continuous variables	7,877
Number of binary variables	6,758
Number of integer variables	161
Number of constraints	21,077
MIP gap (%)	0.05
CPU time (s)	30.531

3.7 Results and Discussion

The proposed model for the transition to FCVs was applied to the 3-zone test system discussed in the previous section. The model was formulated using AMPL [117] modeling language and solved with CPLEX [118], on an IBM eServer xSeries 460 with 8 Intel Xeon 2.8 GHz processors and 3 GB (effective) of RAM. The model statistics are given in Table 3.1; the CPU time reflected in this table corresponds to the non-uniform-penetration case with a 20 MW HPP placement constraint in each zone. This section presents and discusses the results obtained in a variety of scenarios for a non-uniform hydrogen economy penetration; discussion about the uniform-penetration-case will be presented in Chapter 5, where the proposed transition models are applied to a real-case problem. It should also be mentioned that after several simulations it was found that the maximum value of the penetration levels in the optimal solution of the optimization model are achieved based on a sufficiently large value of the social cost of emissions in populated areas. This is expected with the structure of the objective function, where an increase of the penetration levels increases the emission credits and electricity costs simultaneously. Therefore in order to reflect the maximum electricity system potential to support FCVs in the transport sector, the largest value reported in the literature considered for social cost of emissions is selected for this parameter. No further improvements to penetration levels would be achieved by selecting a value beyond this figure for the social cost of emissions.

Table 3.2: Optimal cost and revenue components (CAD) for non-uniform hydrogen economy penetration with and without emission constraints (EC) for generation

Cost/Revenue	without EC	with EC
Power generation	7,558,880,057	6,250,947,498
Power export	-1,347,592,694	-5,893,075
Hydrogen transportation	0	0
Emission credit in transport sector	-2,357,501,142	-2,354,020,183
Emission cost of generation	1,974,115,673	1,363,385,792
Total	5,827,901,894	5,254,420,032

3.7.1 Impact of Emission Constraints for Generation

Optimal cost and revenue components within the whole planning horizon with and without emission constraints for generation are shown in Table 3.2. It is to be mentioned that without the consideration of emission constraints, no component represents the CO_2 cost in the objective function; the corresponding component in Table 3.2 was calculated separately based on emission cost function (3.1) and is included in this table for comparison purposes. he reduction of power generation costs when emission constraints are considered is mainly due to limiting impact of these constraints on the most polluting Zone 3, as can also be observed by considering emission costs. Thus, more power is being supplied by Zone 1 which increases the capacity utilization of transmission corridors 1-2 and 1-3 and ultimately leaves less power in Zone 1 for export. Comparing the emission credit in the transport sector with and without the emission constraints reveals that the total number of FCVs within the entire transport sector is not significantly impacted by these constraints.

Optimal hydrogen economy penetration levels with and without emission constraints for generation are reflected in Figure 3.6. It is observed that the emission constraints reduce the potential penetration level in the most polluting Zone 3; this causes more penetrations in the more environmentally tolerant Zones 1 and 2. The greater increase in the penetration level in Zone 2 compared to Zone 1, due

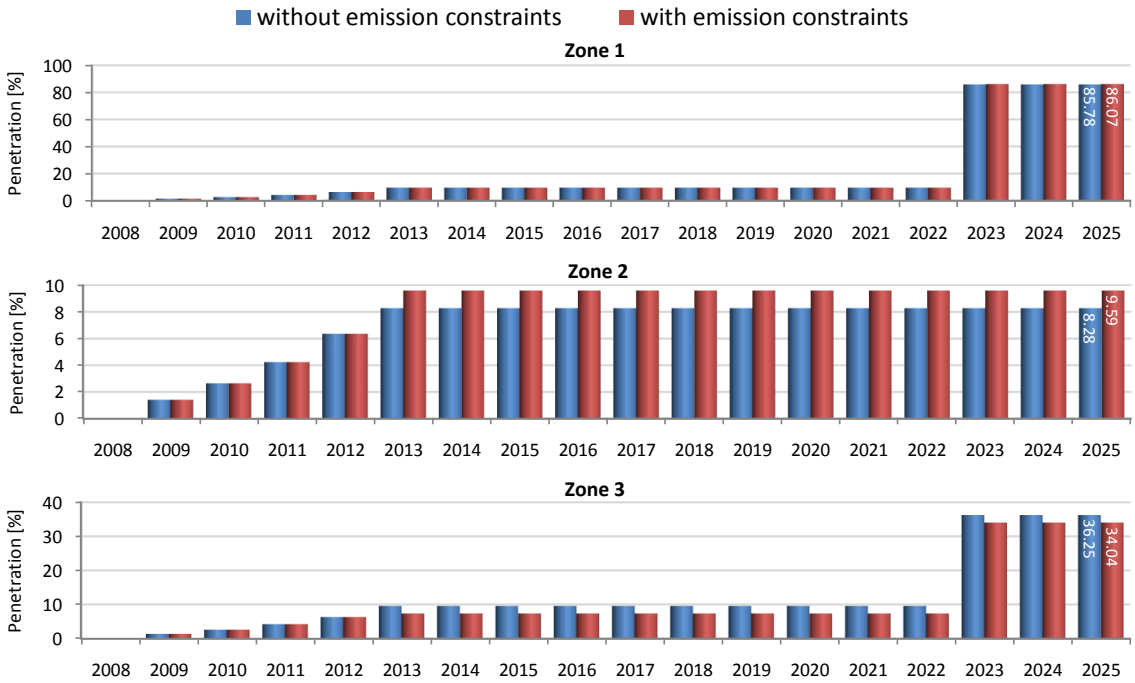

Figure 3.6: Optimal non-uniform hydrogen economy penetration with and without emission constraints of generation.

to emission constraints, can be explained by the fact that this zone has the largest number of LDVs; as a consequence, higher FCV penetration in this zone leads to a larger emission credit while generating low CO_2 emissions since this zone has only a 100 MW effective CHP capacity after 2015.

The potential number of FCVs in different zones that can be supported by the electricity grid are also shown in Figure 3.6, highlighting the important years. It is observed that although the total number of supportable FCVs in the whole transport sector is only slightly impacted by the emission constraints (less than 0.1%), the number of FCVs in the most polluting zone decreases by 14,247, and in the most populated zone it increases by 13,746.

The HPPs developed in different zones are also demonstrated in Table 3.3. Observe that the total developed HPPs in all three zones by 2025 with the emission constraints being considered is slightly reduced by almost 1 MW; however, almost

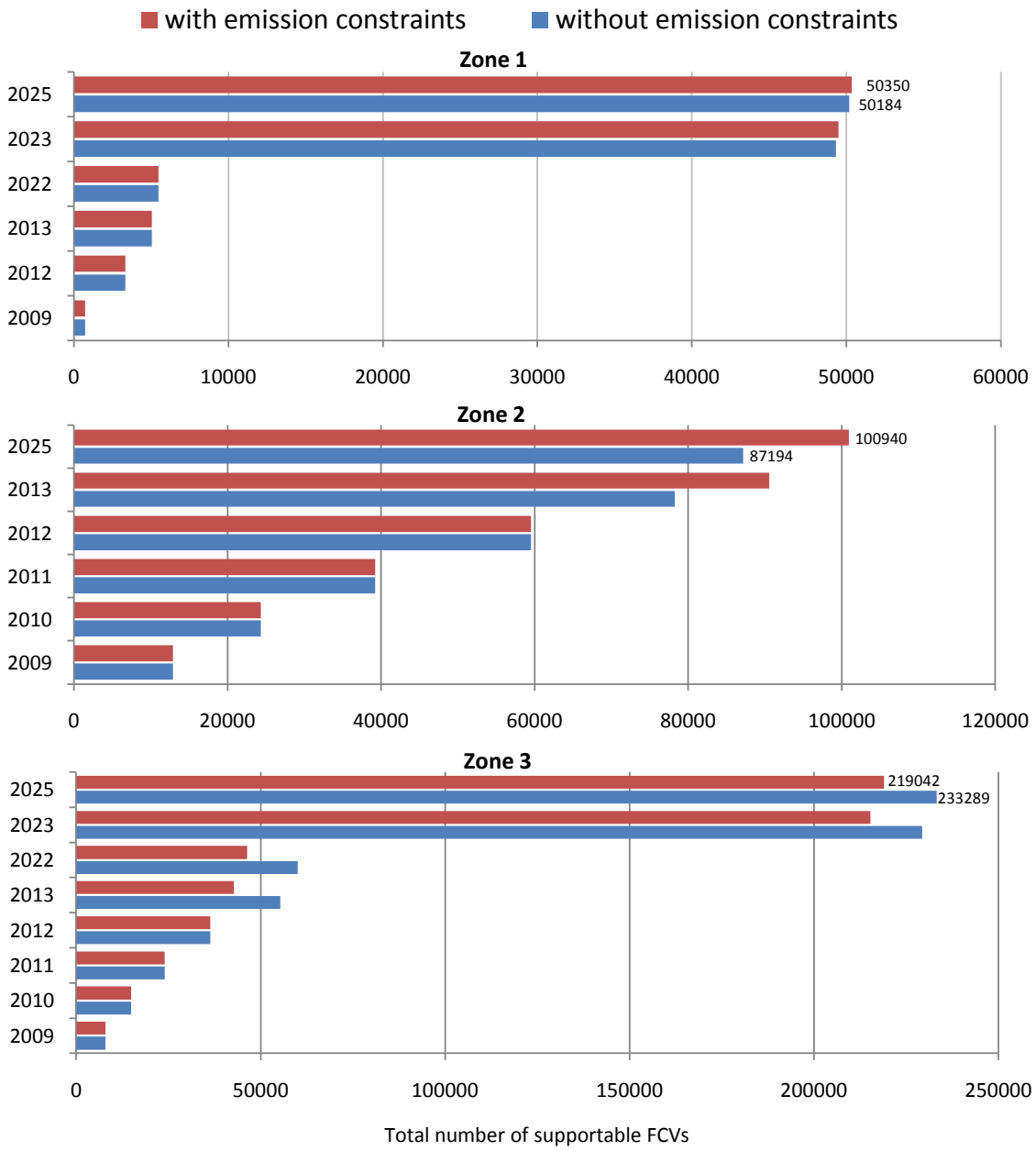

Figure 3.7: Total number of FCVs in different zones with and without emission constraints of generation.

Table 3.3: Optimal HPPs development in different zones with (+) and without (-) emission constraints of generation

	Zone 1		**Zone 2**		**Zone 3**	
	-	+	-	+	-	+
2009	2.26	2.26	40.77	40.77	24.91	24.91
2010	1.97	1.97	35.48	35.48	21.68	21.68
2011	2.54	2.54	45.64	45.64	27.89	27.89
2009	3.42	3.42	61.61	61.61	37.65	37.65
2013	5.19	5.19	55.63	93.33	57.04	18.44
2014	0.02	0.02	0.25	0.29	0.18	0.14
2015	0.02	0.02	0.25	0.29	0.18	0.14
2016	0.02	0.02	0.25	0.28	0.17	0.13
2017	0.02	0.02	0.24	0.28	0.17	0.13
2018	0.02	0.02	0.24	0.28	0.17	0.13
2009	0.02	0.02	0.23	0.27	0.17	0.13
2020	0.01	0.01	0.23	0.27	0.16	0.13
2009	0.01	0.01	0.23	0.26	0.16	0.12
2022	0.01	0.01	0.22	0.26	0.16	0.12
2023	123.48	123.94	0.22	0.25	475.44	474.93
2024	0.12	0.13	0.22	0.25	0.58	0.54
2025	0.12	0.12	0.21	0.25	0.57	0.54
Total	139.24	139.70	241.93	280.07	647.29	607.76

40 MW in planned HPP development is shifted from the most polluting Zone 3 to the more environmentally friendly Zones of 1 and 2. It is also to be mentioned that although the number of light-duty vehicles in Zone 3 is considerably lower than that of Zone 2, Zone 3 has the largest share in total developed HPPs; this is due only to the availability of generation resources in Zone 3. It is also interesting to note that the major HPPs development in all three zones happen before 2014 and after 2023. This can be explained by means of the available generation capacity in Zones 1, 2 and 3, which are at the lowest level between 2019-2022, 2015-2016, and 2014, respectively. Also, Zone 2 with a significantly larger load level has the lowest generation capacity; in particular, its capacity is at minimum levels after 2015 when its coal plant is phased out.

3.7.2 Impact of Transmission Congestion

In this section, the capacity reinforcement of the transmission corridor 1-2 is assumed to take place with a 5-year delay in 2017; the corresponding impacts are investigated here, including emission constraints. The impact of transmission congestion on zonal penetration levels can be studied in Figure 3.8. It is observed that this 5-year delay significantly reduces the potential penetration level in Zone 2 within the overall planning horizon; this also has a limiting impact on the potential penetration level in Zone 3 before 2017 when transmission reinforcement is performed. This is expected since Zone 2 is the main load center with limited local generation capacity and Zone 1 is its main power supplier through transmission corridor 1-2; any limitation on the capacity of this corridor directly influences the potential penetration level in Zone 2. Note that the limiting impact of transmission congestion on the penetration level in Zone 2 results in higher penetration levels in Zones 1 and 3, in particular, after 2017.

It should be emphasized that one of the reasons for the significant reduction in the potential penetration level in Zone 2 when transmission corridor 1-2 is congested corresponds to the 4 ton/day limit on hydrogen transfer between the zones. By relaxing this constraint, higher potential penetration levels in Zone 2 are expected; however, higher hydrogen transportation costs and/or lower penetration levels in other zones in some years are inherent, as shown in Figure 3.9. The impact of hydrogen transfer constraints can be studied further in Table 3.4 where optimal cost and revenue components with and without the 4 ton/day hydrogen transfer limit are demonstrated.

It is observed that without the hydrogen transfer limit, the hydrogen transportation cost increases by almost ten-fold and power export revenue decreases by 22%. This is perceived to be due to increased development of HPPs in Zone 1 and consequently more hydrogen transfer from Zone 1 to other zones, leaving less generation capacity in Zone 1 to export. This is illustrated in Tables 3.5-3.7 where hydrogen transportation details as well as developed HPPs with and without hy-

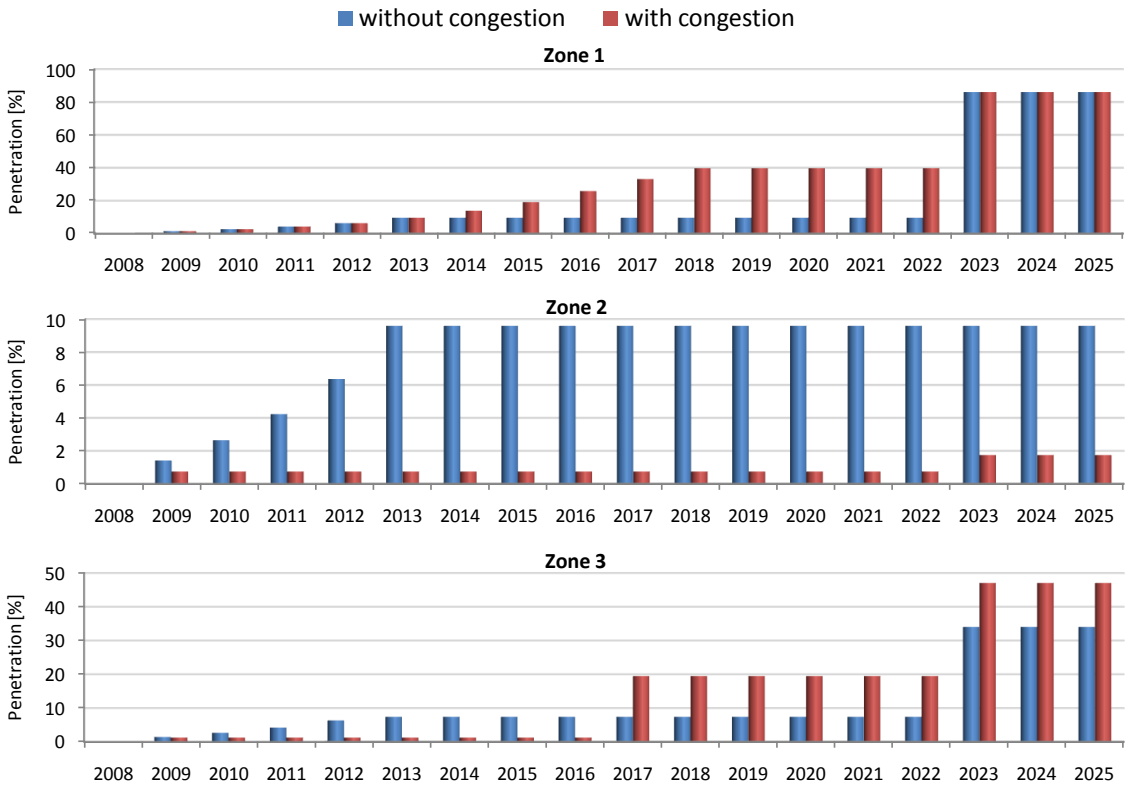

Figure 3.8: Optimal non-uniform hydrogen economy penetration with and without congestion in transmission corridor 1-2 (emission constraints included).

Table 3.4: Optimal cost and revenue components for a congested transmission corridor 1-2, with and without hydrogen transfer limit for non-uniform penetration of FCVs

Cost/Revenue	**without H_2 transfer limit**	**with H_2 transfer limit**
Power generation	6,585,465,296	6,542,223,271
Power export	-354,948,121	-455,470,854
Hydrogen transportation	323,789,608	32,690,479
Emission credit in transport sector	-2,397,833,346	-1,523,337,941
Emission cost of generation	1,728,906,632	1,681,342,400
Total	5,885,380,069	6,277,447,355

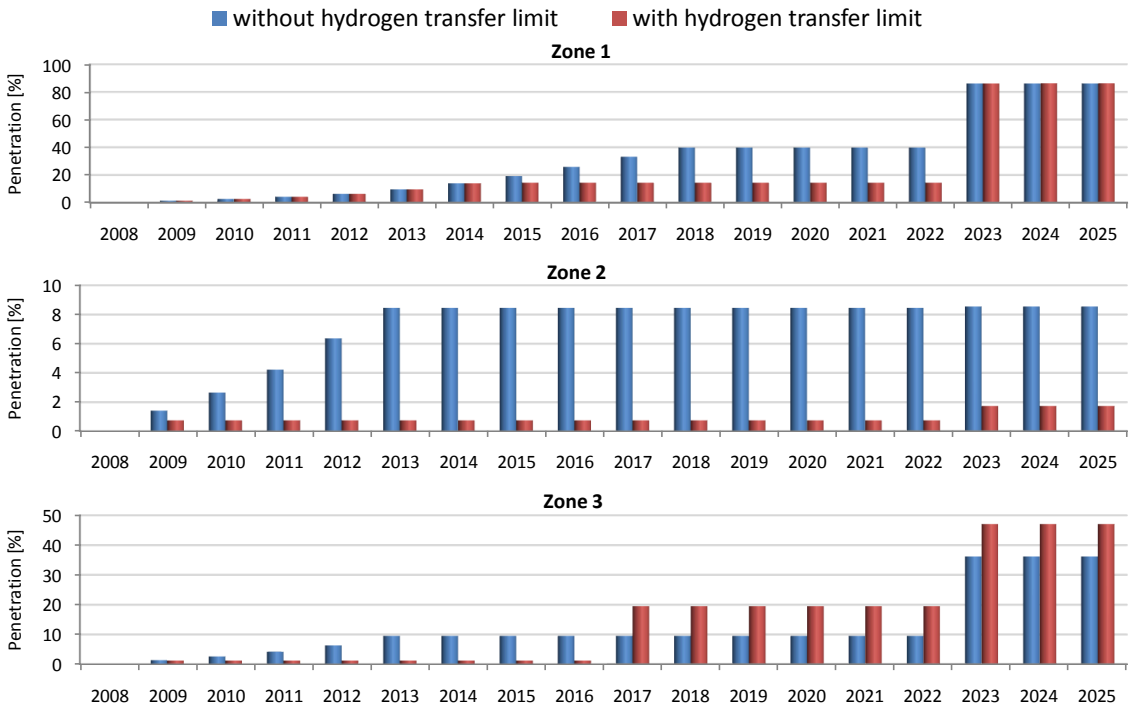

Figure 3.9: Optimal non-uniform hydrogen economy penetration for a congested transmission corridor 1-2, with and without the 4 ton/day hydrogen transfer limit.

drogen transfer limit can be compared; hydrogen export and import in Table 3.5 are distinguished with positive and negative values, respectively. It is observed from these tables that relaxing the hydrogen transfer constraints makes Zone 1 have the largest share of total installed HPPs with all of them being developed before 2016, and with significant hydrogen export to other zones during the planning years. This is expected as this zone has the largest non-polluting generation capacity. It should also be mentioned that relaxing the hydrogen transfer limit has negligible impact on the total number of supportable FCVs in the whole transport sector; it reaches 373,327 with a 0.53% increase. However, the greater emission credit achieved without a hydrogen transfer limit in Table 3.4 is justified by the larger number of FCVs that can be supported in earlier years, in particular, before 2017 as demonstrated in Figure 3.10.

Note that this study is aimed merely at finding the impact of hydrogen transfer

Table 3.5: Hydrogen export and import in ton/day for a congested transmission corridor 1-2 with (+) and without (-) hydrogen transfer limit (emission constraints included)

	Zone 1		**Zone 2**		**Zone 3**	
	-	+	-	+	-	+
2009	11.42	7.58	-7.09	-3.74	-4.33	0.14(-3.98)
2010	21.55	7.66	-13.55(0.17)	-3.78	-8.17	-3.88
2011	34.73	7.73	-21.57	-3.81	-13.17	-3.92
2012	52.75	7.81	-32.75	-3.85	-20	-3.96
2013	74.26	7.88	-43.94	-3.89	-30.32	-4
2014	74.97	7.93	-44.36	-3.93	-30.61	-4
2015	75.58	7.96	-44.78	-3.96	-30.80	-4
2016	76.29	8	-45.20	-4	-31.09	-4
2017	76.90	5.88	-45.55	-1.88	-31.36	-4
2018	77.53	3.92	-45.96	0	-31.56	-3.92
2009	78.15	3.94	-46.38	0	-31.77	-3.94
2020	78.77	3.96	-46.80	0	-31.97	-3.96
2021	79.40	3.98	-47.20	0	-32.20	-3.98
2022	80.02	4	-47.60	0	-32.42	-4
2023	58	0	0	0	-58	0
2024	58.37	0	0	0	-58.37	0
2025	58.80	0	0	0	-58.80	0

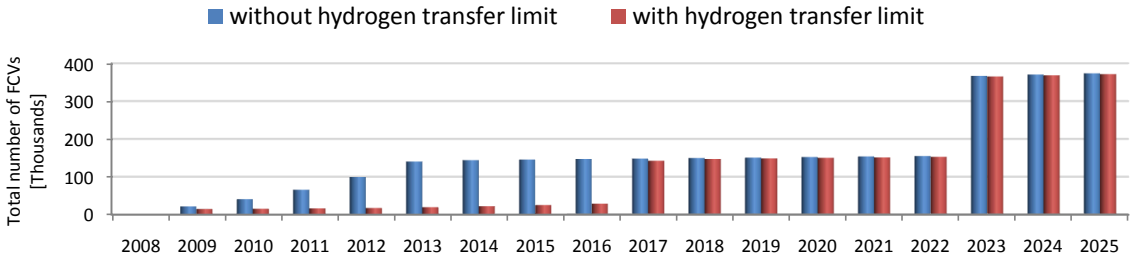

Figure 3.10: Total number of FCVs with and without hydrogen transfer limit (emission constraints included).

Table 3.6: Required number of compressed gas trucks, and purchased tube trailers (0.4 ton capacity) and cabs for a congested transmission corridor 1-2 with (+) and without (-) hydrogen transfer limit (emission constraints included)

	Trucks		**Tube trailers**		**Cabs**	
	-	+	-	+	-	+
2009	29	20	29	20	29	20
2010	55	20	26	0	26	0
2011	87	20	32	0	32	0
2012	132	20	45	0	45	0
2013	186	20	54	0	54	0
2014	188	20	2	0	31	20
2015	189	20	1	0	27	0
2016	191	20	2	0	34	0
2017	193	20	2	0	47	0
2018	195	20	2	0	56	0
2019	196	10	1	0	32	10
2020	197	10	1	0	28	0
2021	199	10	2	0	36	0
2022	201	10	2	0	49	0
2023	145	10	0	0	0	0
2024	146	0	0	0	33	0
2025	147	0	0	0	29	0

constraints on the electricity network as well as optimal hydrogen economy penetration levels, HPP development and hydrogen transportation routes. However, the significant amount of hydrogen exported from Zone 1, which is reflected in the substantial number of compressed gas trucks required shown in Table 3.6, might be operationally infeasible. Removing the hydrogen transfer limit also helps to relieve stress on the electricity system with congestion in transmission corridor 1-2; it is observed in Table 3.8 that total transmission losses within the whole planning horizon are reduced by 7.5% if the hydrogen transfer constraint is relaxed. In this case, stress on the electricity network is shifted to the transport sector by introducing larger numbers of compressed gas trucks transferring hydrogen between the zones.

Table 3.7: Optimal HPPs development in different zones for a congested transmission corridor 1-2, with (+) and without (-) hydrogen transfer limit (emission constraints included)

	Zone 1		**Zone 2**		**Zone 3**	
	-	+	-	+	-	+
2009	67.95	45.88	0	0	0	0
2010	59.13	2.02	0	0	0	0
2011	76.01	2.58	0	0	0.07	0
2012	102.68	3.47	0	0	0	0
2013	122.25	5.23	0	0	0	0
2014	7.46	6.89	0	0	0	0.19
2015	0.68	8.29	0	0	0.53	0.21
2016	0.45	10.62	0	0	0	0.2
2017	0	0	0.39	11.58	0.11	323.29
2018	0	0	0	10.14	0.43	0.94
2009	0	0	0	0.02	0.43	0.40
2020	0	0	0	0.02	0.42	0.39
2009	0	0	0.09	0.02	0.32	0.39
2022	0	0	0.09	0.02	0.32	0.38
2023	0	54.47	248.64	29.07	345.27	511.81
2024	0	0.13	0.22	0.05	0.98	0.75
2025	0	0.12	0.22	0.04	0.69	0.74
Total	436.61	139.70	249.66	50.97	349.57	839.69

3.7.3 Impact of Annual HPP Development

Considering the HPP placement constraints discussed in Section 3.4.3, a 20 MW maximum limit on annual HPP development in each zone is considered in this section. As shown in Figure 3.11 and Table 3.9, this constraint significantly influences the potential penetration levels as well as the pattern of HPP development over time. Observe in Figure 3.11 that a 20 MW limit on annual HPP development reduces the ultimate penetrations in all three zones, the largest impact occurring in Zone 3; however, there are somewhat increased penetration levels in Zones 1 and 3 between 2014 and 2022. Since Zone 2 has the largest number of LDVs, the reduction of potential penetration levels in this zone within the planning years translates into considerable reductions in the total number of supportable FCVs as

Table 3.8: Total transmission losses during the planning horizon for the congested transmission corridor 1-2, with and without hydrogen transfer limit (emission constraints included)

Transmission loss [MWh]		
	without H_2 transfer limit	with H_2 transfer limit
2008	346,528	346,528
2009	341,703	349,330
2010	330,256	350,564
2011	320,505	351,711
2012	317,427	363,364
2013	382,439	382,439
2014	382,095	382,095
2015	369,047	369,047
2016	370,598	370,598
2017	651,895	743,751
2018	654,558	758,710
2019	368,303	427,443
2020	373,181	428,865
2021	379,621	425,856
2022	384,106	431,013
2023	534,027	565,290
2024	531,731	566,589
2025	532,737	571,580
Total	7,570,757	8,184,773

well as emission credits in transport sector. The overall impact of this constraint is the reduction of total developed HPPs and the number of supportable FCVs in the overall transport sector by 40.61%. This annual HPP development constraint causes a substantial amount of hydrogen tranportation between the zones at a total cost of 30,952,067 CAD and Zones 1 and 3 being the main exporter and importer, respectively.

It is observed in Table 3.9 that the total HPPs developed in all three zones are reduced when the 20 MW annual limit is in place; this justifies the reduction of ultimate FCV penetration in all the zones by 2025. Also, major developments of HPPs in Zones 1 and 3 happen in 2023; however, the 20 MW annual limit causes 60

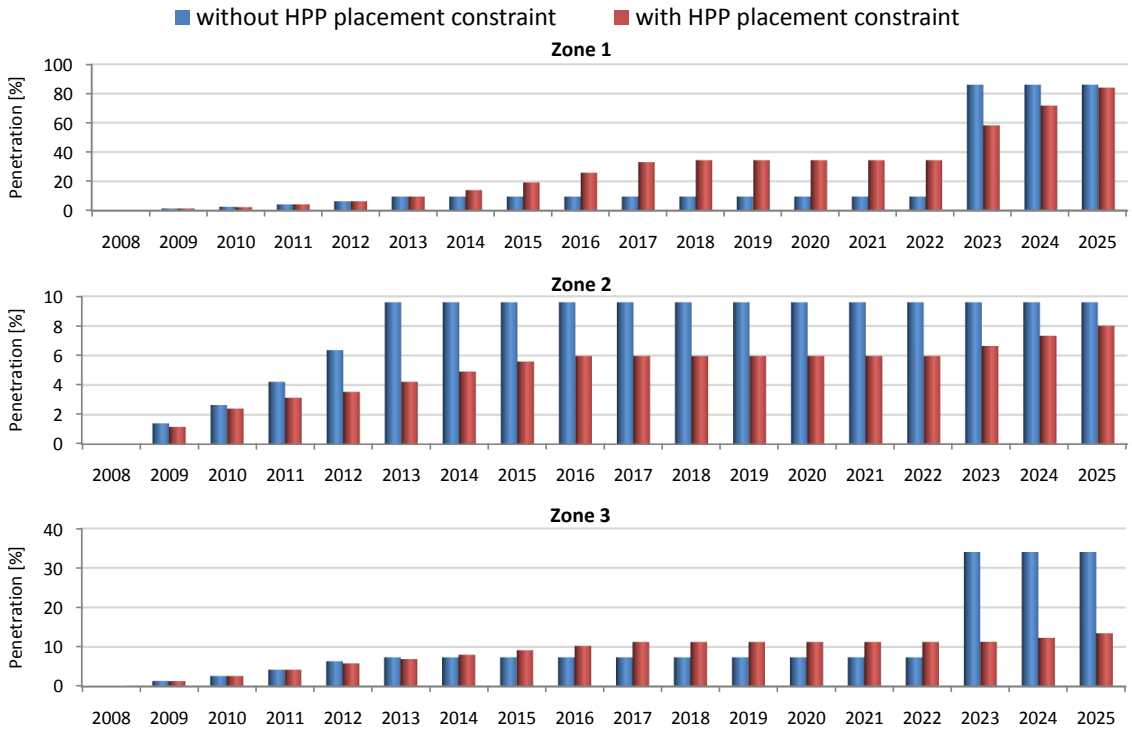

Figure 3.11: Optimal non-uniform hydrogen economy penetration with and without a 20 MW limit on annual HPP development.

MW be developed in both zones after 2023 and the remainder would be developed in previous years, in particular, before 2017. This explains the increase of FCV penetration levels in these zones before 2022. It is interesting to note that more than 475 MW HPPs, planned to be developed in Zone 3 after 2023, is reduced to only 60 MW when the 20 MW annual limit is considered; this justifies the significant reduction of hydrogen economy penetration in Zone 3 after 2023 despite the fact that maximum possible hydrogen import from Zone 1, i.e., 4 ton/day also occurs in 2023.

Table 3.9: Optimal HPPs development in different zones with (+) and without (-) a 20 MW limit on annual HPP development (emission constraints included)

	Zone 1		**Zone 2**		**Zone 3**	
	-	+	-	+	-	+
2009	2.26	20	40.77	20	24.91	20
2010	1.97	20	35.48	20	21.68	20
2011	2.54	11.99	45.64	20	27.89	20
2012	3.42	3.04	61.61	20	37.65	20
2013	5.19	4.81	93.33	20	18.44	20
2014	0.02	6.65	0.29	20	0.14	20
2015	0.02	8.08	0.29	20	0.14	20
2016	0.02	1.75	0.28	20	0.13	20
2017	0.02	0	0.28	11.03	0.13	18.84
2018	0.02	0	0.28	2.32	0.13	0.13
2009	0.02	0	0.27	0.17	0.13	0.25
2020	0.01	0	0.27	0.17	0.13	0.24
2009	0.01	0	0.26	0.16	0.12	0.24
2022	0.01	0	0.26	0.16	0.12	0.24
2023	123.94	20	0.25	20	474.93	20
2024	0.13	20	0.25	20	0.54	20
2025	0.12	20	0.25	20	0.54	20
Total	139.70	136.32	280.07	234.01	607.76	239.94

3.8 Summary

This chapter presents a novel mixed-integer linear optimization framework for planning the transition to AFVs with particular attention to electricity grid constraints in transmission and generation levels. This optimization framework is based on zonal representation of the region under study, with main power generation and electricity load centers. It also takes into consideration the environmental issues in both population areas and generation power plants. The solution of the proposed optimization framework yields optimal potential penetrations of AFVs into the transport sector during the planning study. Also, the optimization model for a transition to FCVs finds the optimal size of HPPs to be developed in each zone over time as well as the optimal hydrogen export/import and transportation routes

to achieve optimal hydrogen economy penetrations during the planning horizon.

A 3-zone test system is developed to demonstrate the capabilities of the proposed optimization framework. Optimal potential penetration of FCVs into transport sector is studied on this test system through a variety of scenarios. The results show how environmental issues as well as operational considerations such as annual HPP development or hydrogen transfer limits can influence the penetration levels. The findings of this chapter demonstrate that the proposed optimization planning framework can be effectively used to study and plan for the transition to AFVs in realistic systems with a zonal structure.

Chapter 4

Ontario's Electricity System and Transport Sector Models

4.1 Introduction

In Chapter 3, comprehensive optimization planning models for the transition to AFVs were presented, and their capabilities were demonstrated on a 3-zone test system. The objective in this thesis is then to apply these models to study the real-case problem of Ontario, Canada; however, an adequate model of Ontario's electricity system should first be developed. Therefore, this chapter concentrates on presenting the different models used in this thesis for the Ontario-based studies, including the transmission network, power generation development, base-load electricity demand as well as power import/export assumptions, which are all common for studying the transition to both FCVs and PHEVs. Furthermore, additional assumptions related to both electricity and transport sectors which are required for planning the transition to AFVs are also discussed; thus, two patterns of the transition to AFVs are considered, and their advantages and disadvantages are discussed from the viewpoints of Ontario's available base-load generation capacity and the speed of infrastructure development. This is followed by an analysis of the required

Table 4.1: Estimated transmission corridor enhancements for simplified grid model.

Year	Corridor	Current MW	Planned MW
2012	Bruce-SW	2560	4560
2012	SW-Toronto	3212	5212
2013	NE-NW	350	550
2015	Bruce-West	1940	2440
2017	Toronto-Essa	2000	2500
2017	Essa-NE	1900	2400

data for each zone of Ontario's transport sector during the planning horizon. Finally, electricity demand and price issues in Ontario and the assumptions made for the operation of HPPs and the charging of PHEVs are discussed.

4.2 Transmission Network Model

Ontario's Independent Electricity System Operator (IESO) represents the Ontario network with ten zones [119]. This same representation is used in this study to develop the 10-bus simplified model of Ontario's network, as shown in Figure 4.1, which considers the main grid load and generation centers and transmission corridors. This model is mostly the 500 kV network, with a 230 kV interconnection between North East (NE) and North West (NW). Hence, the parameters used to model this network are based on typical values of 230 and 500 kV networks, considering the approximate distances between zones, and transmission capacities, as per general information provided by the IESO [119] and line loading limits in per unit of surge impedance loading (SIL) [120]. Based on the existing and planned projects provided by the Ontario Power Authority (OPA) [121, 122], the transmission-capacity enhancements presented in Table 4.1 are assumed for the simplified model used in this study.

Figure 4.1: Simplified model of Ontario's grid.

4.3 Generation Development Model

Based on the Ontario IPSP and a variety of information provided by the OPA and the IESO, a zonal pattern of generation capacity between 2008 and 2025 contributing to base-load energy in Ontario was developed [123]–[129]. The proposed model specifies the total effective generation capacity which is available in each zone to supply the base-load. The mix of base-load generation resources in Ontario considered in this model includes nuclear, wind, hydro (only those units with limited dispatch capability and small scale units less than 10 MW), Combined Heat and Power (CHP), Conservation and Demand Management (CDM), and coal. It is important to mention that the contribution of gas-fired generation to base-load energy has been disregarded in this study, based on the Ontario government's 2006

Supply Mix Directive indicating that natural gas should only be used at peak-load times and in high-efficiency and high-value applications [121]. The details of the generation model are provided in the following sections.

4.3.1 Nuclear

The present installed nuclear capacity in Ontario, located in the Bruce and Toronto zones, is 14000 MW, with 11365 MW in operation, 1500 MW under refurbishment (Bruce A, Units 1 & 2), 1057 MW already refurbished (Pickering A, Units 1 & 4), and about 1100 MW on long-term lay up (Pickering A, Units 2 & 3). Also, the present operating capacity includes 4720 MW in the Bruce zone (Bruce A: 1540 MW, Bruce B: 3180 MW) and 6645 MW in Toronto zone (Pickering A: 1057 MW, Pickering B: 2064 MW, and Darlington: 3524 MW) [123]–[125].

According to the 20-year energy plan set by the Ontario government, nuclear energy capacity should be maintained for base-load operation up to its current level of 14000 MW [121]; this will require that existing nuclear plants be refurbished and/or new plants be built to maintain this capacity. The nuclear power generation pattern in Ontario up to 2025 depicted in Figure 4.2 was developed based on the following facts, figures, and assumptions [123, 125]:

- Bruce A (Units 1 & 2) refurbishment is assumed to be completed by 2010. This should basically increase Bruce A capacity to 3040 MW, and as a consequence total nuclear power generation capacity in the Bruce zone will increase to 6220 MW by 2010. However, refurbishment work on Units 3 & 4 is assumed to start in 2010 and be completed in 2013, which limits the total nuclear capacity of the Bruce zone to 4720 MW until 2013.

- Bruce B refurbishment is assumed to take place in 2018-19 (2 units in 2018 and 2 units in 2019) and will be complete in 2023-24.

- At least half of the capacity of Pickering A (Units 2 & 3) in the Toronto zone is economically unfeasible for refurbishment.

- Pickering B refurbishment is assumed to commence in 2014-15 (2 units in 2014 and 2 units in 2015). This refurbishment is assumed to be completed by 2019-20.

- For the new projected nuclear plant development, the following scenarios have been assumed:

  Scenario 1: 1500 MW new nuclear power will be available in the Toronto zone in 2018. This assumed capacity is somewhat less than the capacity of two Darlington units in this zone.

  Scenario 2: 1500 MW new nuclear power will be available in the Bruce zone in 2018. This assumed capacity is equal to two Bruce A units. It is to be mentioned that, although the capacity of nuclear units in Bruce and Darlington are not the same, the assumed similar development of nuclear capacity in Bruce and Toronto zones in 2018 is merely for comparison purposes.

4.3.2 Wind

The share of wind power to meet the renewable target in 2025 (15700 MW) is 4685 MW. This includes 395 MW of existing wind power in 2007, 1251 MW of committed wind power that will be in service by 2010, and 3039 MW of small and large wind projects which are planned to be in service between 2011-2025 [125]–[127]. As of 2007, total capacity of the existing and signed wind projects was 1312 MW [127]–[129], distributed in SW, Bruce, East, NE, and West with shares of 48%, 15%, 15%, 14%, and 8%, respectively. Since the wind capacity in Ontario in 2008 is 472 MW including 189 MW in NE, 99 MW in West, 108 MW in SW, and 76 MW in Bruce, there is still 1174 MW of committed wind capacity to be developed by 2010. It is assumed here that this capacity will be developed in the same 5 zones between 2008 and 2010 with the same share of capacity development as in 2007.

The priority of wind power development is through small wind projects (1148 MW), which are planned to be in service at a uniform pace over the period from

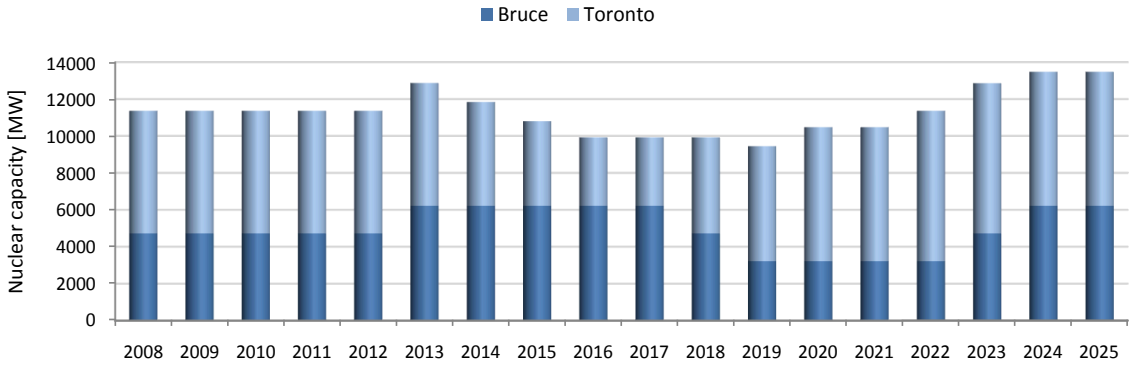

(a) Scenario 1: New nuclear units in the Toronto zone.

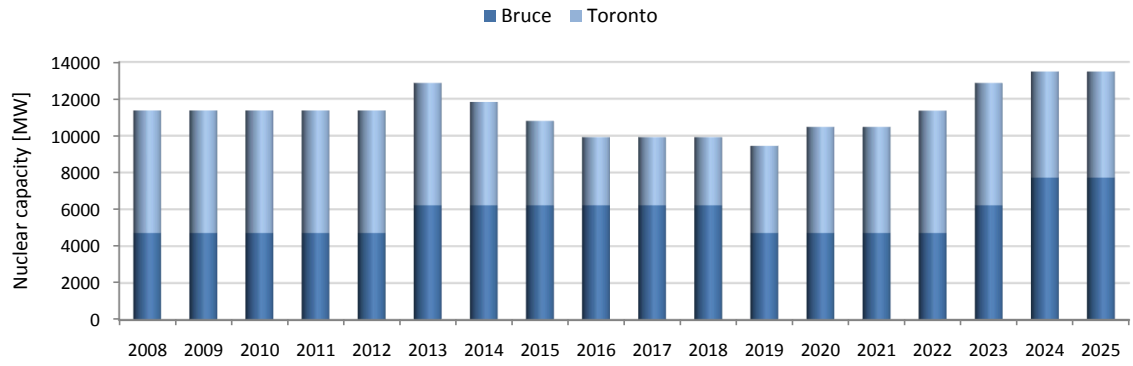

(b) Scenario 2: New nuclear units in the Bruce zone.

Figure 4.2: Nuclear power capacity in Ontario contributing to base-load energy.

2011 to 2020 in almost all the zones except Ottawa. The remainder of the wind power target will be made up of large wind projects (1891 MW) which are planned to be developed in 6 zones including Bruce, NE, East, West, Essa, and SW with shares of 37%, 27%, 14%, 9%, 8% and 5%, respectively. Although the development of large wind projects will also start in 2011 (in West and SW), almost 46% of the projects will come into service after 2015 [127]. Finally, the wind power share of different zones between 2011 and 2025 was extracted from [124]–[129], resulting in wind power distribution for the planning study depicted in Figure 4.3, assuming an average wind power capacity factor of 30% for base-load energy service [125, 130, 131]. Observe that the share of wind power by 2025 in southern zones (mainly

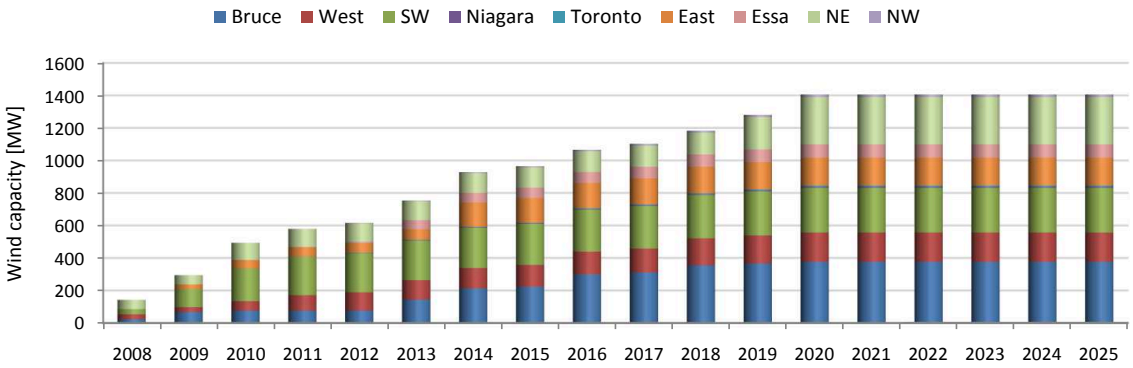

Figure 4.3: Effective wind power capacity in Ontario contributing to base-load energy.

Bruce, SW and West), NE, and NW are 78%, 20% and 2%, respectively.

It should also be mentioned that the wind-power capacity is likely to increase further due to the Feed-in Tariff (FIT) program associated with the recent Green Enery and Green Economy Act (GEGEA) [132, 133]. However, this has not been considered in the wind-power capacity values derived in this study.

4.3.3 Hydro

Currently, there are 7788 MW of hydroelectric capacity in Ontario, of which 3161 MW is provided by run-of-the-river facilities located in the Niagara and East zones that contribute to base-load energy, each with the total capacity of 2116 and 1045 MW, respectively [124,125]. The share of hydroelectric capacity in the target value of renewables in 2025 (15700 MW) is almost 10700 MW, meaning that almost 2912 MW of hydropower is planned to be developed between 2008-2025 [122, 127]. Most of the potential hydroelectric sites in Ontario are located in northern zones, in particular, in the NE; thus, the share of developed hydroelectric by 2025 in southern, NW, and NE zones are 5.08%, 10.17% and 84.75%, respectively [122,127,129]. Most of these planned hydroelectric generations are plants with large storage capacities that have high dispatch flexibility and hence capable of serving peak demand. In this respect, the hydroelectric facilities which are planned to be developed by 2025

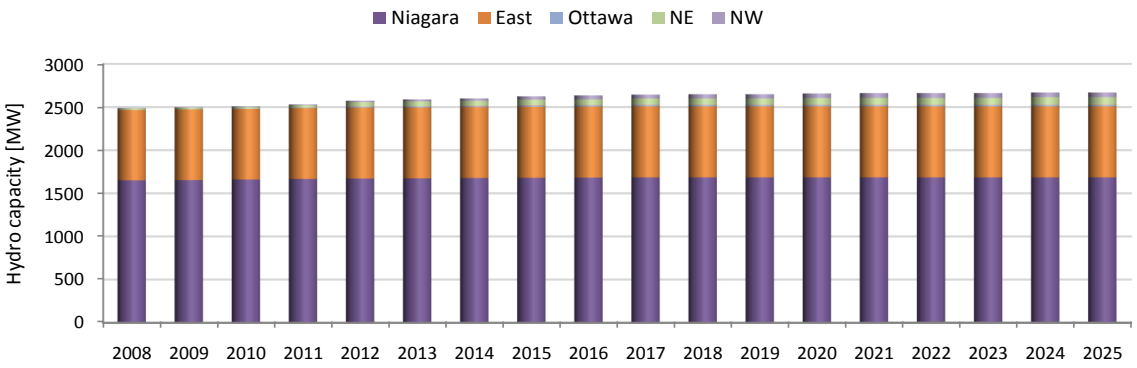

Figure 4.4: Effective hydroelectric capacity in Ontario contributing to base-load energy.

will have a relatively low impact on meeting Ontario's base-load energy requirement; since this study is particularly concerned with base-load time intervals, only the capacity of these plants serving base-load are taken into account here.

All the existing run-of-the-river hydroelectric plants (in Niagara and East zones) plus the 25 MW run-of-the-river unit which is planned to be in service by 2012 in NE are considered here to contribute to base load energy with a 78% capacity factor. Existing and planned small-scale hydro units (10 MW or less in size) that are not run-of-the-river facilities are also assumed to contribute to base-load energy, but with an average capacity factor of 50% [125, 126, 128]. The zonal base-load hydroelectric available power in Ontario during the planning period is illustrated in Figure 4.4.

4.3.4 Combined Heat and Power (CHP)

There are currently 7 new CHP projects with a total capacity of 414 MW under development across Ontario [134]. The projects, which have been planned to be in service by the end of 2008, include 12 MW in SW, 11.5 MW in West, and 7.3 MW in Toronto. Also, 2 projects including 84 MW in West and 63 MW in NE, as well as a 236 MW plant in Niagara will be in service by 2009 and 2010, respectively. Since the OPA has been directed by the Ontario Ministry of Energy to procure 1000 MW

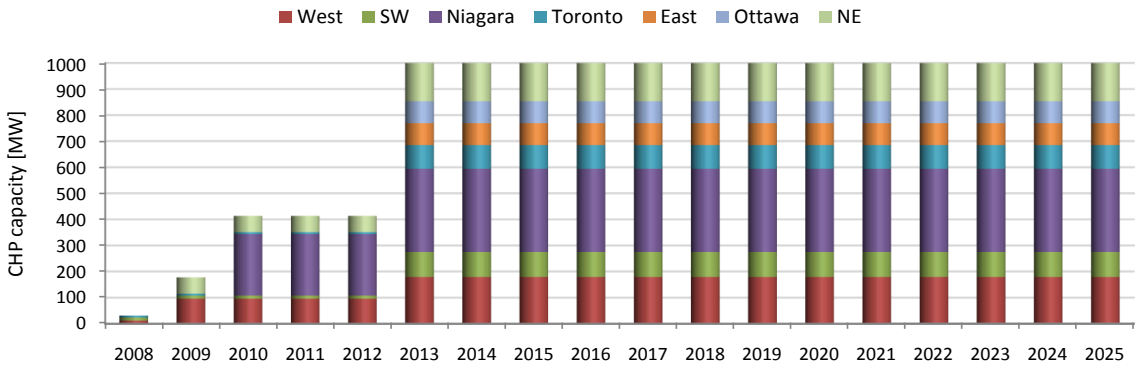

Figure 4.5: Effective CHP capacity in Ontario contributing to base-load energy.

CHP generation [125, 126, 134], there are 586 MW of CHP plants expected to be developed in the future. The OPA has targeted 2013 as the completion date for the planned CHP resources in Ontario [125]. In this study, the planned CHP capacity (586 MW) is equally split between the existing CHP zones, i.e., all the zones except for Bruce, Essa and NW.

It should also be mentioned that there are some CHP facilities in Ontario such as the 140 MW cogeneration plant in the East [124,125], which are under long-term Non-Utility Generation (NUG) power purchase agreements with the Ontario Electricity Financial Corporation. To be conservative, these CHP-NUG facilities have not been considered in the mix of base-load capacity, based on the fact that their contracts will expire over the 2012-2018 period and because there are uncertainties regarding their operation during base-load periods, since some of these facilities are not available due to contract limitations and are uneconomic for supplying base-load energy [125]. Based on all these considerations, the assumed zonal CHP capacity in Ontario during the planning period is depicted in Figure 4.5.

4.3.5 Conservation and Demand Management (CDM)

CDM programs are basically energy saving programs and incentives such as building retrofitting or the use of smart meters to implement time-of-use electricity pricing

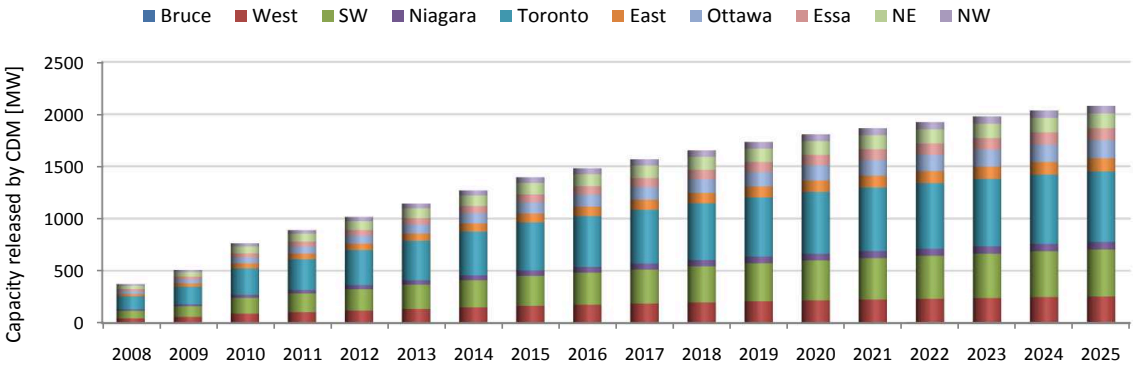

Figure 4.6: CDM released capacity in Ontario contributing to base-load energy.

to encourage customers to manage their electricity consumption. These programs are expected to result in a reduction on demand, and in [121] are considered as a supply resource, giving them the same importance and priority as generation resources such as nuclear, renewables or gas-fired plants. According to the OPA, CDM programs have the potential to offset the expected growth in demand over the next 15 years; therefore, CDM programs are considered here, and as per [121] are assumed to be independent of demand growth.

Based on the Ontario IPSP, the target values for peak-load reduction are 1350 MW by 2010 and another 3600 MW by 2025 [121]; however, the effective capacity released by CDM during base-load time intervals is less than these target values. Thus, both committed (2008–2010) and planned (2010–2025) target values for base-load CDM capacity released are, as per [125], 550 MW and 2587 MW by 2010 and 2025, respectively. In this study, the share of each zone from the released capacity target values is considered to be proportional to the ratio of its base-load demand with respect to the total base-load demand. Furthermore, it is assumed that only 75% of the planned conservation is to be achieved in practice. The CDM values used here are shown in Figure 4.6.

4.3.6 Coal

Currently, there are 4 coal plants operating in Ontario with a total capacity of 6285 MW [124]. These plants, which are located in West (1948 MW), SW (3820 MW), and NW (517 MW), are planned to be phased out by the end of 2014 [121]. The loss of coal-based generation is planned to be made up by renewables, gas fired generation, conservation programs, and imports. Because of the impact of these plants on voltage control and reliability issues, some transmission upgrades, especially in NW and SW zones are to be done before the full retirement of these coal plants.

The assumed retirement process of coal plants in this study is as follows [122,125, 135]: All the coal plants will retain their full capacities by the end of 2010. One coal plant (211 MW) in NW will be completely retired in 2011, and the capacity of the rest will be reduced by 20%, reaching 5000 MW by the end of 2011. For the purpose of system reliability, all the remaining capacities in NW, West, and SW will remain, but will be reduced by 40% during 2012-2014, and finally be completely phased out thereafter. Coal plants in Ontario are neither "base load" nor "peaking" plants and are typically considered in the category of "intermediate load" plants [124]. In this study, the contribution of coal plants to base-load energy is considered with a capacity factor of 50%, which is a typical value in the base-load system studies performed by the OPA [125,126]. The zonal coal power capacity in Ontario during the planning period is depicted in Figure 4.7. Observe that the zero contribution of coal plants to the total base-load energy in Ontario after 2014 helps to meet the requirements of a true hydrogen economy and sustainable transportation based on FCVs and PHEVs.

4.3.7 Total Effective Generation Capacity in Ontario

Considering the previously discussed base load resources in Ontario, total effective generation capacity ($\overline{P_{g_{iy}}}$) which is available in each zone during 2008-2025 is calculated. The corresponding results for both scenarios are illustrated in Figure 4.8.

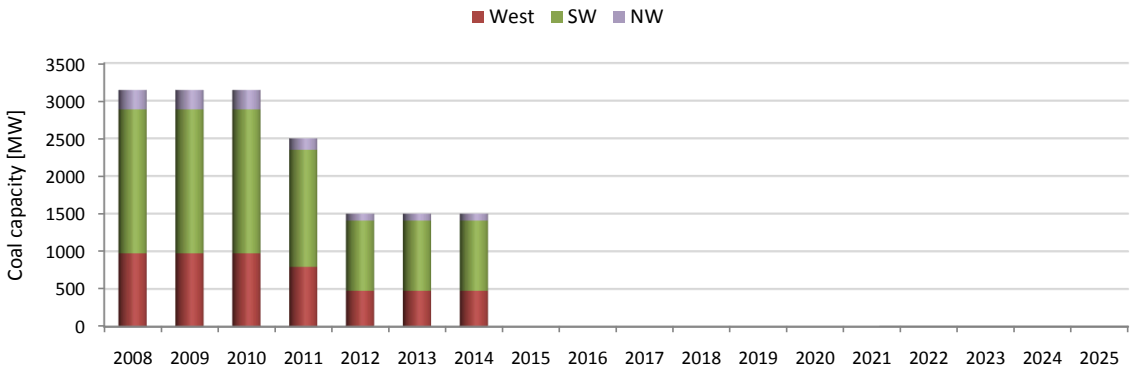

Figure 4.7: Effective coal power capacity in Ontario contributing to base-load energy.

These figures highlight the dominant contribution of both the Toronto and Bruce zones in supplying the base-load requirements of Ontario. Furthermore, observe that the total effective capacities under both scenarios are at their lowest levels from 2016-2021; this is mainly due to coal plants retirements and both Bruce B and Pickering B refurbishments. Also, the availability of the capacity of different generation resources allows to determine $\overline{P_{ga}}_{iy}$ and $\overline{P_{gb}}_{iy}$, which are needed for the generation cost model discussed in Chapter 3.

4.3.8 Environmental Aspects of Generation Resources in Ontario

Fossil-fuel-based resources considered in the mix of Ontario's base-load generation in this study include coal and CHP plants. Considering that coal plants in Ontario are planned to be phased out by the end of 2014, the maximum contributions of coal plants to the total base-load energy in Ontario has been determined in this study to be 17% in 2008–2010, 14% in 2011, 9% in 2012–2014, and none after 2014; thus, the contribution of coal plants to CO_2 emissions is not very significant in the proposed model for the study period. Natural-gas-fuelled power plants also emit CO_2 but at a substantially lower rate per unit of output energy as compared to coal plants, and CHP plants emit an even lower amount of CO_2 due to their high

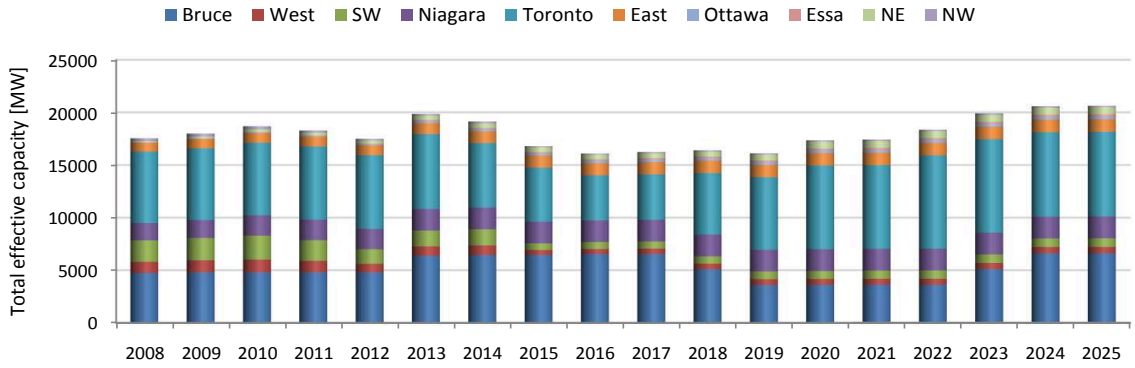

(a) Scenario 1: New nuclear units in the Toronto zone.

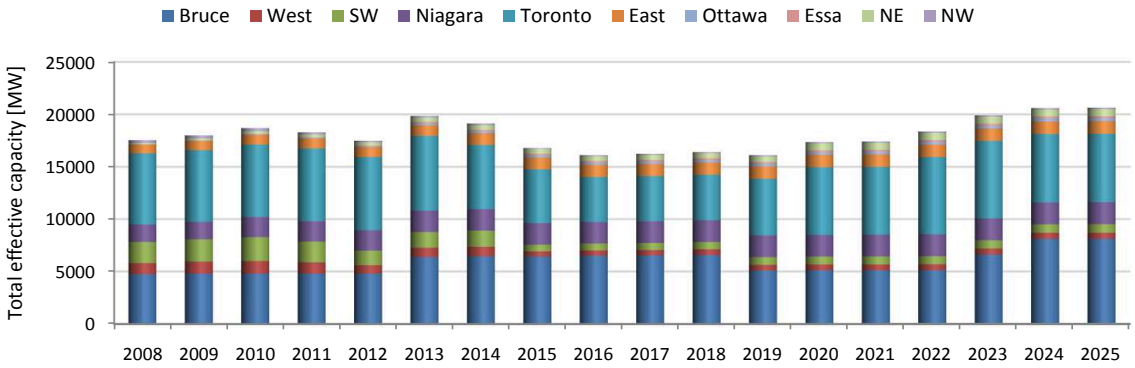

(b) Scenario 2: New nuclear units in the Bruce zone.

Figure 4.8: Total effective generation capacity in Ontario contributing to base-load energy.

efficiencies [136]–[138]. In view of all these considerations, the introduction of FCVs and PHEVs into Ontario's transport sector during the planning horizon does not significantly add to the environmental footprint on the generation side. However, since the emission cost of generation is included in the model, CO_2 emission rates of coal and CHP plants in Ontario should be determined. As per [139] and in 2007 base, the average CO_2 emission rates of coal plants in the West and SW zones are calculated as 0.9553 and 0.9881 ton/MWh, respectively. Moreover, two different emission rates of 1.1536 and 1.1966 ton/MWh are found for the two coal plants located in the NW zone. For simplicity, an average figure of 1.1751 ton/MWh is used for the coal plants in this zone. Also, according to [140, 141], an approximate

Table 4.2: Estimated percent of zonal annual peak-demand growth rates in Ontario.

Zone	Bruce	West	SW	Niagara	Toronto	East	Ottawa	Essa	NE	NW
Annual growth rate [%]	0.78	1.14	1.28	0.41	0.77	0.71	1.42	1.17	-0.33	0.10

CO_2 emission rate of 0.25 ton/MWh is assumed for the CHP plants in Ontario. All these emission rates are considered to be constant during the planning years.

4.4 Base-load Electricity Demand Model

To find the base-load demand of the different zones of Ontario on the various years of the planning horizon, zonal base-load demand growth rates need to be determined based on the available data, which are the zonal peak-demand forecasts from 2007 to 2015 [142], and the average base-load demand in 2007 [143]. The average values of annual peak-demand growth rates shown in Table 4.2 were readily calculated from [142]; it is assumed here that these values are reasonably valid for the whole planning horizon. As per [125, 126], the average base and peak-load values in Ontario from 2007 to 2025 will increase by 21% and 24%, respectively. On average, these load increases translate into 1.11% and 1.26% of base and peak-load annual growth rates respectively for all of Ontario. If the ratio of base-load growth rate to peak-load growth rate is assumed to be constant for all the zones, then it is possible to decompose the base-load growth rate of the whole Ontario into different zones as explained next:

It is assumed that the base-load demand in Ontario in Year y is equal to P_{e_y}, which is expressed as follows:

$$P_{e_y} = \sum_i P_{e_{iy}} \tag{4.1}$$

Considering the annual base-load demand growth rates λ_i, results in the following

base-load demand in Year $y+1$:

$$P_{e_{y+1}} = \sum_i \lambda_i P_{e_{iy}} \tag{4.2}$$

The ratio of base-load growth rate λ_i to peak-load growth rate γ_i is assumed to be constant for all the zones:

$$\sigma = \frac{\lambda_i}{\gamma_i} \tag{4.3}$$

Hence, (4.2) can be stated as:

$$P_{e_{y+1}} = \sum_i \sigma\gamma_i P_{e_{iy}} = \sigma \sum_i \gamma_i P_{e_{iy}} \tag{4.4}$$

On the other hand, if λ is assumed to be the annual base-load growth rate of Ontario's total zones, then the following relation holds:

$$P_{e_{y+1}} = \lambda \sum_i P_{e_{iy}} \tag{4.5}$$

From (4.4) and (4.5), σ can be found as follows:

$$\sigma = \frac{\lambda \sum_i P_{e_{iy}}}{\sum_i \gamma_i P_{e_{iy}}} \tag{4.6}$$

Finally, from (4.3) and (4.6), the zonal annual growth rates of base-load demand can be calculated as follows:

$$\lambda_i = \lambda \left(\frac{\gamma_i \sum_i P_{e_{iy}}}{\sum_i \gamma_i P_{e_{iy}}} \right) \tag{4.7}$$

The zonal annual growth rates obtained from (4.7), along with the Ontario's average base-load demand in 2007 [143], were used to obtain the annual expected base load in different zones of Ontario during the planning years.

Comparing the total effective generation capacity in Ontario with the expected

base load shows that there is a capacity deficit to supply base-load power from 2016 to 2021. This is mainly due to the retirement of coal plants and refurbishments of both Bruce B and Pickering B nuclear units. The possible supply alternatives for covering this power deficit include power imports from neighboring grids, contributions from further conservation, renewable and CHP resources in excess of planned levels, and contributions from intermediate-load resources such as combined-cycle gas turbines [125]. Since there are strong tie lines with New York and Michigan and an Ontario–Quebec HVDC interconnection is scheduled to be operational by 2010 [127], the base-load deficit is assumed here to be mainly supplied by power imports, as discussed in more detail in the next section.

4.5 Power Imports/Exports

As demonstrated in Figure 4.1, power import and export possibilities exist in 6 of Ontario's zones including West, Niagara, East, Ottawa, NE and NW. In general, there is a 4,000 MW import capability in Ontario from Manitoba, Quebec, Michigan, New York and Minnesota, and an additional 1,000-1,250 MW from Quebec is being developed [119, 144]. There is an import capability in the East zone both from New York and Quebec. For the NW, there is also a possibility of import both from Manitoba and Minnestota. No limitation on power export is considered in this study, however, a maximum of 750 MW of power imports from New York and Quebec between 2015-2022 is assumed for both the Ottawa and East zones. Moreover, a maximum of 500 MW of imports in both NE and NW are assumed during the same period. Also, a maximum of 300 MW of imported power in NW is assumed in other years within the planning period. These assumptions are consistent with the operational import limits reflected in [144]; however, an upgrade of the import capability in NE is also assumed in this study. If no upgrade on the import capability of NE occurs by 2015, the assumed import power for this zone from 2015-2022 in excess of the import limit is assumed to be covered by local dispatchable hydro units.

4.6 AFV Transition Assumptions

4.6.1 Transition Pattern

The transition to AFVs in Ontario for the study years is assumed to be as shown in Figure 4.9, where K = 100 represents a 100% AFV penetration into the transport sector. These curves specify the maximum level of AFV penetrations to be realized each year ($\bar{\mu}_y$), as discussed in Chapter 3. Transition 1 shown in Figure 4.9 assumes a sluggish penetration of AFVs, particularly from 2009 to 2015, with a faster slope thereafter to reach the target value in 2025. Sluggish penetration in the first years provides sufficient time for the development of required AFV infrastructure, technology, and market acceptance. However, the major part of AFV penetration would occur in the time period of 2015–2022 when Ontario's network is short of base-load capacity. Transition 2 assumes a fast penetration of AFV during the time periods of 2009–2015 and 2022–2025, with a relatively limited penetration between 2015 and 2022. This transition is appealing as it considers the scarcity of base-load resources between 2015 and 2022; however, it requires a fast development of AFV infrastructure, with about 45% of the 2025 target level of penetration being realized before 2015.

4.6.2 Light-duty Vehicles

Light-duty vehicles are referred to as vehicles with a gross weight below 4.5 tonnes. According to the Canadian Vehicle Survey [145], in a 2005 base, the light-duty vehicle fleet consists of passenger vehicles with a 58% share and light trucks, including sport utility vehicles (SUVs), vans, and pickup trucks with 8%, 16%, and 18% shares, respectively. These shares were considered to be valid for Ontario. Therefore, the passenger vehicles were classified into six types of light-duty vehicles, i.e., compact and midsize sedan (each with 29% share), midsize and full-size SUVs (each with 4% share), vans (16% share), and pickup trucks (18% share).

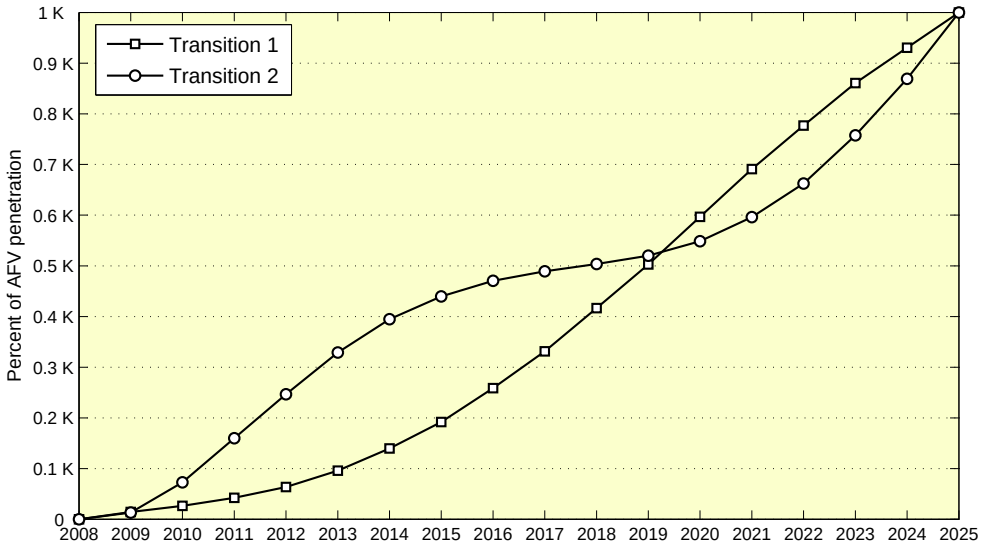

Figure 4.9: Assumed AFVs transitions in Ontario.

As per [69], the approximate fuel economy of these LDVs were calculated. Thus, the fuel economy of compact sedan, mid-size sedan and mid-size SUV were determined as 16.02, 12.28 and 9.43 km/litre, respectively. Also, full-size SUVs, vans and pickup trucks are approximately assigned a similar fuel economy of 7.73 km/litre. Based on these figures, the average fuel economy of a representative gasoline-powered LDV is found to be equal to 11.52 km/litre at the beginning of the planning horizon. Furthermore, in order to not overestimate the environmental credits of FCVs and PHEVs, it is assumed that these fuel economies are 20% improved by the end of the planning horizon.

In order to find Ontario's grid potential for producing hydrogen by HPPs to be used by FCVs or charging the PHEVs, it is first necessary to determine the number of light-duty vehicles during the planning period, which in turn requires the zonal population levels during this period. Therefore, the population of cities and towns of more than 10,000 inhabitants were used to find the population of each zone, considering the geographical location of the zones. The population of each zone was then scaled up such that the sum of zonal populations would equal

the 12,861,940 population estimate for Ontario on January 1, 2008 as per [146]. The annual base-load growth rate for each zone was approximately used to find the zonal population in the study period. The total projected population of Ontario in 2025 estimated in this way (15,663,374) is very similar to what is reported in [147], confirming the adequacy of the assumptions used in this study.

According to 2005 statistics [145], the per capita number of vehicles in Canada ranged from slightly more than 0.1 in Nunavut to 0.85 in Yukon, with a national average of 0.58. The corresponding figure for Ontario, having 6,727,791 vehicles in 2005 was 0.55. This value was considered to be valid during the planning horizon in this study.

4.6.3 Transition to FCVs

Hydrogen Generation

The hydrogen economy, which is considered in this study, is solely based on electrolytic hydrogen production during off-peak hours for transportation purposes. In this work, the operation time of HPPs is impacted by technical considerations as well as by the electricity prices and load levels on the electricity network as discussed in detail below:

- *Technical considerations*: If the plant is switched on (i.e., from a stand-by state), it has to continue operating for a couple of hours, since extended interruptions of current cause damage to the plant due to the shifts of temperature and pressure. For the same reason, both start-up and shut-down of the plant require some time because abrupt changes of operational conditions are not permitted [148].

- *Electricity price and demand*: According to Ontario's IESO, on-peak hours are defined as hours 8 to 23 Monday to Friday with the total of 5×16 hours per week; Hour 8 is 7:00-8:00 and Hour 23 is 22:00-23:00. All remaining

Table 4.3: Average zonal electricity demand of Ontario in different time frames for 2007 [MW]

Average electricity demand [MW]											
Time period	Bruce	West	SW	Niagara	Toronto	East	Ottawa	Essa	NE	NW	Total
Weekdays 23:00-7:00 (8 hours)	71.02	1667.65	2982.16	593.62	5038.52	943.34	1097.99	805.83	1353.97	634.05	15188.15
Weekends 23:00-11:00 (12 hours)	70.49	1578.90	2857.13	552.70	4853.44	938.63	1126.93	820.19	1364.76	629.01	14792.17
Weekends 23:00-13:00 (14 hours)	71.63	1615.37	2915.64	558.82	4995.19	961.15	1156.18	845.11	1375.36	630.44	15124.88
Weekends 23:00-15:00 (16 hours)	72.32	1641.87	2955.29	563.45	5094.71	977.63	1173.75	859.99	1382.06	629.65	15350.72
Weekends 23:00-17:00 (18 hours)	72.95	1665.23	2992.27	568.52	5175.67	993.10	1193.65	874.71	1388.09	628.10	15552.29
Weekends 23:00-19:00 (20 hours)	73.56	1687.07	3030.35	573.60	5254.37	1007.99	1216.93	892.35	1392.99	627.63	15756.84
Weekends 23:00-21:00 (22 hours)	73.95	1703.47	3057.89	577.08	5312.00	1017.58	1232.03	904.62	1397.85	629.62	15906.07
Weekends 23:00-23:00 (24 hours)	73.93	1706.89	3061.19	576.71	5324.42	1018.22	1231.40	905.08	1399.20	631.82	15928.84

hours as well as holidays are defined as off-peak. This gives an indication of the operation time periods when the HPPs could take advantage of the low electricity price and demand in the system for both economic and reliability considerations. Therefore, it is assumed here that the operating time for HPPs is 8 hours (23:00-7:00) during weekdays, and for the weekends, different operation times ranging from 12 to 24 hours were investigated. Based on the data provided in [143], average electricity demand as well as the Hourly Ontario Energy Price (HOEP) for the different time frames considered were calculated and are illustrated in Tables 4.3 and 4.4. It should be noted that for all the demands and prices calculated for the weekdays, the first hour is set to be the last hour of Sundays, i.e., 23:00-24:00. Likewise, for all the demands and prices calculated for the weekends, the first hour is considered to be the last hour of Fridays.

Although more hours of operation during the weekends increase the capacity factor of the HPPs, observe in Tables 4.3 and 4.4 that electricity prices and, in particular, the average zonal demands increase, which in turn limits the possibility of adding extra load in the form of HPPs. Moreover, further hours of operation do not

Table 4.4: Hourly Ontario energy price

Average HOEP [CAD/MWh]						
Time period	**2003**	**2004**	**2005**	**2006**	**2007**	**2008**
Weekdays 23:00-7:00 (8 hours)	38.51	36.31	47.50	33.40	33.18	31.72
Weekends 23:00-11:00 (12 hours)	39.07	36.74	48.14	33.57	32.73	31.35
Weekends 23:00-13:00 (14 hours)	42.34	39.02	51.43	36.02	35.17	34.91
Weekends 23:00-15:00 (16 hours)	43.40	40.10	53.46	37.16	36.41	37.03
Weekends 23:00-17:00 (18 hours)	44.10	40.81	54.91	37.81	37.52	38.68
Weekends 23:00-19:00 (20 hours)	45.49	42.28	57.10	38.86	38.92	40.28
Weekends 23:00-21:00 (22 hours)	46.96	43.27	58.54	39.97	39.90	41.47
Weekends 23:00-23:00 (24 hours)	47.00	43.30	58.33	40.03	39.77	41.26

necessarily bring about significant economic advantages as discussed in detail next.

To further investigate the economic impact of operating hours during the weekends, a literature survey was performed regarding the investment costs for different components of a hydrogen production unit, considering size and economies of scale [14,63,64,116], [149]–[160]. A 300 kW hydrogen production unit is selected in this study; this is the installed power of a unit including a rectifier, electrolyzer and compressor with an overall efficiency of 70%. Based on HHV of hydrogen (39.45 kWh/kg), the hydrogen production rate of this unit is found to be equal to 5.32 kg/h (59.31 Nm^3/h). As per [161], the energy requirement of a multi-stage compressor for the compression of hydrogen up to 400 bar is equal to almost 9% of its HHV. Based on the maximum flow rate of 5.32 kg/h, the maximum demanding power of the multi-stage compressor is found to be equal to almost 19 kW; this tranlates to almost 3.5 kW per kg/h hydrogen flow at high pressure. Consequently, the maximum installed power of the electrolyzer will be equal to 281 kW. The assumed investment cost of an electrolyzer is 65,000 CAD per kg/h hydrogen including electrolyzer stack, gas and water conditioning, power electronics and control systems. Hydrogen storage at 400 bar is sized to hold the average one-day

Table 4.5: Minimum acceptable hydrogen prices for different operating time frames

Operating hours during weekdays	8	8	8	8	8	8	8
Operating hours during weekends	12	14	16	18	20	22	24
Minimum hydrogen selling price [CAD/kg]	6.58	6.40	6.22	6.07	5.93	5.81	5.66

hydrogen production and its investment cost is assumed to be 600 CAD/kg. Total investment cost of hydrogen storage is found based on the assumed operation hours during weekdays and weekends. The investment cost of multi-stage compressor is assumed to be 2,500 CAD/kW or alternatively 8,876 CAD per kg/h of hydrogen. Also, 10% of the total initial investment for the whole unit is assumed to cover the average annual operation and maintenance costs; these costs include labour, insurance, property tax, licensing, maintenance and repair [13, 159]. These figures are used next to determin the minimum prices for selling hydrogen from an electrolytic process, which are justified through an economic analysis.

Note that Table 4.4 shows a general decline in off-peak electricity prices; however, considering the expected price increase during 2016-2021 due to relatively limited base-load generation capacity, the average HOEP in 2008 both on weekdays and weekends have been taken as the expected electricity prices during the lifetime of the plant. Based on these electricity prices and typical discount rates of 8% and a plant lifetime of 20 years (because of low capacity factor), and disregarding the income tax as well as any government support program, the minimum hydrogen selling prices to justify the investment were found for each of the operating time frames considered. The results of these analyses are reflected in Table 4.5. The calculated prices are the minimum hydrogen selling prices that make the net present value (NPV) greater than zero, yielding an 8% internal rate of return (IRR) and a profitability index (PI) greater than unity. Observe in Table 4.5 that each additional 2 hours of operation during the weekends reduces the hydrogen price by almost 0.15 CAD, and the maximum price reduction that can be achieved based on 12 extra hours of operation is only 0.92 CAD. Hence, even if there is no limit

on the load level in the system, a few more hours of operation during the weekends will not be of significant economic importance.

With regard to typical gasoline and electricity prices in Ontario, this analysis also demonstrates the feasibility of hydrogen production during off-peak hours for Ontario's transport sector, considering the typical fuel economies of ICEs and FCVs. Thus, the minimum hydrogen selling price obtained based on 8 and 14 hours of HPP operation during weekdays and weekends, respectively, can be approximately compared to a gasoline price of 1 CAD/litre, assuming the fuel economies of FCVs and ICEs to be 100 km/kg and 11.5 km/litre, respectively, and the cost of hydrogen delivery and dispensing to be 2.5 CAD/kg [110]. This analysis does not factor in any government support; furthermore, no credit is given for the environmental benefit of producing hydrogen through electrolysis versus other more polluting mechanisms such as steam reforming of natural gas.

Notice in Table 4.3 that the 14-hour average demand on weekends (from 23:00-13:00) is closest to the 8-hour average demand on weekdays. Consequently, and based on the aforementioned economic analysis, these 14 hours were selected as the operation time of the hydrogen production plants during the weekends. Thus, along with the 8 hours of operation during the weekdays, a total operation of 68 hours per week are assumed, which yields close to a 40% capacity factor for the hydrogen production plants.

Hydrogen Demand

Based on the average hydrogen demand of a representative FCV (0.55 kg/day), the transition pattern, and the number of LDVs discussed in Section 4.6.2, hydrogen demand can be determined in different zones of Ontario for the planning years. Zonal hydrogen demand for a 1% hydrogen economy penetration by 2025 and following Transition Pattern 1 in Figure 4.9 is depicted in Figure 4.10. Observe in this figure that the total hydrogen demand in Ontario by 2025 will be equal to almost 47 ton/day, of which Toronto, SW and West would be the greatest consumers with

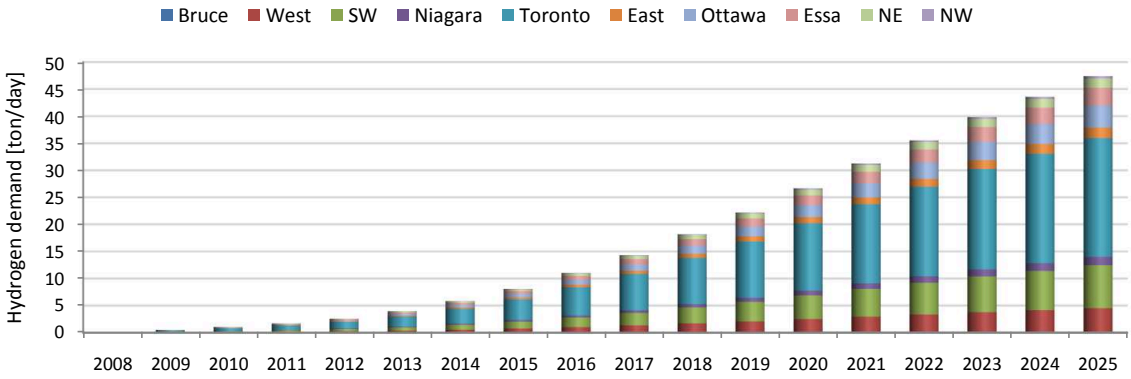

Figure 4.10: Zonal hydrogen demand of fuel cell vehicles for 1% hydrogen economy realization based on Transition Curve 1 in Figure 4.9.

almost a 46%, 17%, and 9% share of the hydrogen demand, respectively.

The zonal hydrogen demand during the planning period allows determining the required capacity of the HPPs, as discussed in Chapter 3. Figure 4.11 illustrates the zonal capacity of HPPs which would need to be developed over time to establish a 1% FCV penetration across Ontario by 2025, assuming a 10% efficiency improvement of the plants by 2025 and following Transition Pattern 1. Observe that almost 250 MW of power is needed by 2025 for a 1% ultimate FCV penetration, with a minimum share in the Bruce zone with less than 540 kW and a maximum share in Toronto with more than 115 MW.

Hydrogen Transportation Costs

The cost of hydrogen transportation based on compressed gas trucks is composed of operation and investment cost components. The investment costs correspond to truck cabs and compressed gas tube trailers, and the operation costs include diesel costs and driver wages, as well as insurance, licensing, maintenance, and repair costs [110, 159, 162]. The corresponding parameters for 2008 which are assumed in this study are illustrated in Table 4.6. Based on the data provided in this table, the operation costs of a compressed gas truck amount to 1.1212 CAD/km for 2008.

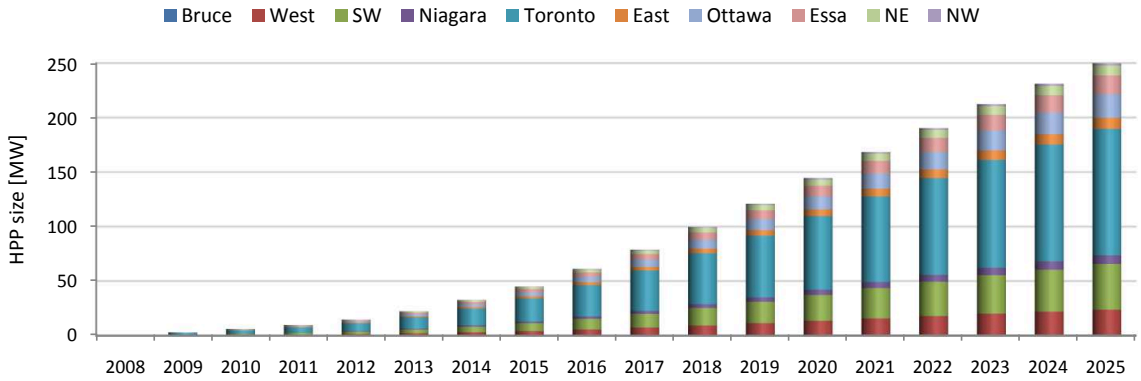

Figure 4.11: Zonal required capacity of electrolytic hydrogen production plants for 1% hydrogen economy realization based on Transition Curve 1 in Figure 4.9.

Table 4.6: Hydrogen transportation cost parameters

Maximum capacity of compressed gas trucks [ton]	0.4
Cab capital cost [CAD]	100,000
Tube trailers capital cost for the maximum capacity of 0.4 ton [CAD]	240,000
Diesel cost [CAD/km]	0.4212
Insurance, licensing, maintenance and repair costs [CAD/km]	0.4
Driver wage [CAD/km]	0.3
Cab lifetime [year]	5
Tube trailers lifetime [year]	20

Based on typical inflation rates in Ontario, it is assumed that this operation costs will increase at 2.5% per year for the following years up to 2025. Finally, assuming that truck cab prices will probably rise due to inflation, but tube trailer prices will likely decrease since nowadays these prices could be considered high, it is assumed that the total investment costs for both combined could be considered to remain approximately constant during the planning years (the uncertainty regarding these investment costs will be investigated in Chapter 6). Also, a maximum limit of 4 ton/day for hydrogen transfer in each route is assumed.

4.6.4 Transition to PHEVs

Charging Demand

PHEV charging is assumed to take place during off-peak hours from 23:00-7:00 in both weekdays and weekends. Moreover, in order to evaluate the PHEVs charging demands on Ontario's grid, the following assumptions are also made:

- A 30-km all-electric average daily trip (referred to as PHEV30km hereinafter and is approximately equivalent to the PHEV20 reference often found in the literature). This covers at least 60% of the average-daily-trip range per LDV in Ontario [145]; in other words, the electric share of vehicle miles traveled is 60%, and the rest is driven by gasoline. This assumption has to do with the time required to charge the PHEV during off-peak hours as explained in more detail below.
- A 70% maximum allowable depth of discharge. Due to life-cycle considerations [74,163,164], at most 70% of the battery's energy is assumed to be used in charge depleting mode.
- A 1.4-kW connection power level (120 V/15 A). This is the capacity of the plug to which the battery is connected and is based on the assumption that little change will take place in the standard Ontario household infrastructure. Note that the continuous rating of a plug circuit is less than its peak capacity [32,34].
- An 85% charging efficiency [165].

It should be pointed out that this study is mainly concerned with generation and transmission-system issues and does not consider distribution-system issues. Nevertheless, keeping in mind that only off-peak demand and base-load generation conditions during the time period of 23:00 to 7:00 are considered, the total demand levels should not be close to on-peak conditions; consequently, technical problems

Table 4.7: Charging requirements for different types of PHEV30km

Vehicle type	Specific energy requirement [kWh/km]	Required useable energy [kWh]	Required battery size [kWh]	Total energy demand [kWh]	Min. charging time [hour]
Compact sedan	0.16	4.8	6.86	5.65	4.03
Mid-size sedan	0.19	5.7	8.14	6.71	4.79
Mid-size SUV	0.24	7.2	10.29	8.47	6.05
Full-size SUV	0.29	8.7	12.43	10.24	7.13
Van	0.29	8.7	12.43	10.24	7.13
Pickup truck	0.29	8.7	12.43	10.24	7.13

such as overloading of distribution feeders and transformers or potential unbalanced conditions is not expected to be a major concern. However, further investigation of this issue is one of the directions for future work.

Based on the previous assumptions and the required specific energy [69, 164, 166], the battery-charging requirements for different types of PHEV30km vehicles shown in Table 4.7 were calculated; full-size SUVs, vans, and pickup trucks are approximately assigned the same energy requirements. Observe that the charging times fit in the assumed 8 h (23:00–7:00) off-peak time periods. It should also be pointed out that a wide variety of PHEV vehicle types and technologies are expected to be introduced; the classifications used in this study simply assume representative vehicle types.

An average hourly power consumption for each type of vehicle was considered in this study from 23:00 to 7:00, assuming that the charger system's controller is capable of providing a smooth charging current and consequently make a uniform charging demand during the whole time period. Based on these averages, total power requirements of PHEV30km vehicles were calculated for the different zones and years of the planning period based on a 100% penetration level by 2025; these results are used to define the zonal-demand constraints in the optimization model developed in Chapter 3. As demonstrated in Figure 4.12, this methodology yields approximately 84 MW of power requirement for a 1% penetration of PHEVs into

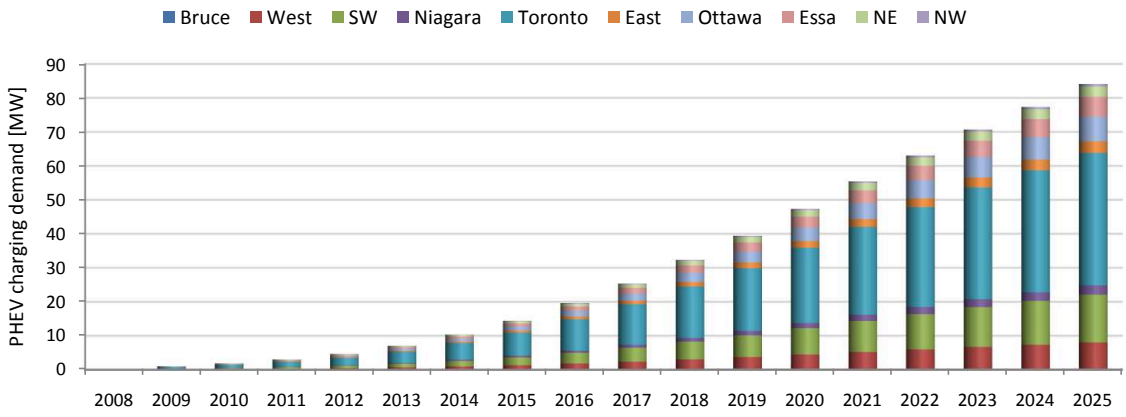

Figure 4.12: Zonal demanding power of PHEVs for a 1% penetration level based on Transition Curve 1 in Figure 4.9.

Ontario's transport sector by 2025. Alternatively, 8.4 GW of power will be needed for a 100% PHEV penetration by 2025, i.e., about 26% for the estimated peak demand in that year. It should also be mentioned that, in Figure 4.12, the presumption is that the maximum possible penetration levels determined by Transition Curve 1 in Figure 4.9 are realized in each year.

Electricity Demand and Price Considerations

In the FCV transition model, the extra load on the system which is imposed by HPPs is constant and uniform during off-peak hours; however, this uniformity of the load cannot be ensured in the PHEV transition model. As discussed in the previous section, it is assumed that the charger's controller can provide a smooth charging current and make a uniform charging demand during off-peak hours. This simplifying assumption, which may not hold in practice at a large scale, may lead to slightly higher PHEV penetration levels. In order to address this issue, the PHEV transition model utilizes the larger winter base-load demands for generating the base-load data during the planning study, as per Figure 4.13, which shows that larger base-load demands occur during the winter season in almost all zones of Ontario except Bruce and Niagara.

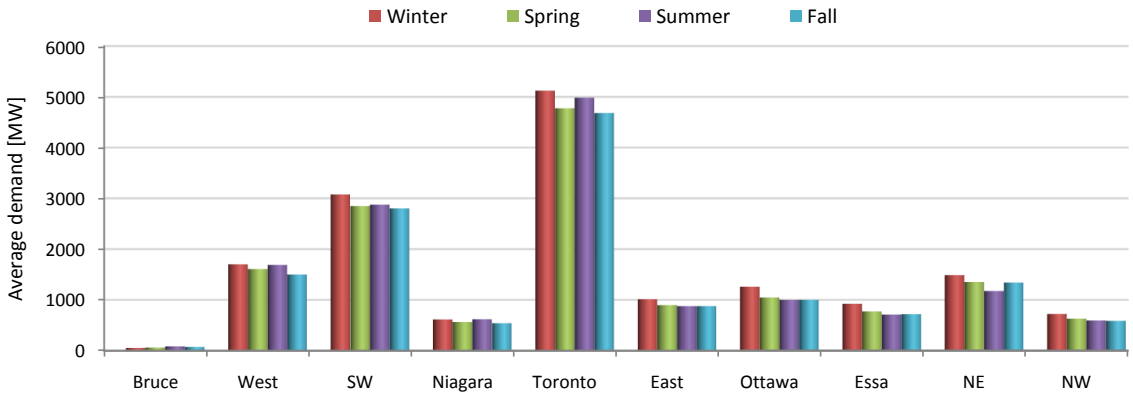

Figure 4.13: Average demands by season during the time period of 23:00 to 7:00 based on 2007 data. Similar patterns can be observed for other years.

Table 4.8: Hourly Ontario energy price

Average HOEP [CAD/MWh]						
Time period	**2003**	**2004**	**2005**	**2006**	**2007**	**2008**
Winter (Dec-Feb)	50.78	38.60	41.71	49.23	34.86	34.14
Spring (Mar-May)	44.04	32.70	44.82	32.47	32.45	30.97
Summer (Jun-Aug)	25.90	29.06	42.44	32.11	27.06	22.89
Fall (Sep-Nov)	34.04	37.78	46.97	29.05	30.67	32.21
Whole year (Jan-Dec)	37.63	35.25	46.06	32.51	31.95	30.09

Table 4.8 shows the calculated average electricity prices in Ontario during the time period of 23:00-7:00 for the whole year as well as in different seasons. Observe that the winter prices have decreased from 49.23 CAD/MWh in 2006 to 34.14 CAD/MWh in 2008. However, similar to the assumption for FCV transition model, the average electricity price in 2008 is deemed as the expected electricity price for all of the planning period. The impact of price uncertainty will be discussed in Chapter 6.

4.7 Summary

In this chapter, appropriate models of Ontario's electricity system and transport sector are developed; these models are required for the application of the proposed optimization models for planning the optimal transition to AFVs in Ontario, Canada. The developed transmission network model is based on major 230 and 500 kV transmission corridors and their possible capacity improvements within a planning horizon starting in 2008 and ending in 2025. The developed model of base-load generation capacity considers the mix of nuclear, wind, hydro, CHP, CDM and coal resources, and specifies the total effective generation capacity which is available in each zone during the planning study to supply base load. The proposed methodology to decompose the annual growth rate of base-load demand of Ontario as a whole into different zones makes it possible to develop zonal base-load demand data during the planning horizon.

This chapter also discusses the issue of power exports and imports in Ontario, proposes transition patterns and develops required data for Ontario's transport sector. Further assumptions regarding the operation of HPPs and charging of PHEVs, in view of Ontario's electricity demand and price are also discussed. An economic assessment of electrolytic hydrogen production in Ontario during off-peak hours is also presented to explore the feasibility of this idea, considering the typical off-peak electricity prices in Ontario as well as the fuel economies of gasoline and fuel cell vehicles.

Chapter 5

Optimal Transition to AFVs in Ontario

5.1 Introduction

This chapter aims to derive the optimal potential penetrations of AFVs into Ontario's transport sector by 2025 based on the optimization planning framework and Ontario's electricity system and transport sector models presented in Chapters 3 and 4, respectively. From these models, Ontario's maximum grid potential for supporting both FCVs and PHEVs are discussed based on the existing and planned Ontario's electric grid, without any additional investment on this infrastructure to specifically accommodate these vehicles in the transport sector. Potential penetration levels and total number of AFVs are determined under both uniform and non-uniform penetration assumptions, considering a variety of scenarios and constraints such as the location of new nuclear units, transition patterns, emission costs of generation, and HPP placement and hydrogen transportation limits.

Table 5.1: FCV transition model statistics

Number of continuous variables	30,576
Number of binary variables	24,224
Number of integer variables	1,673
Number of constraints	85,012
MIP gap (%)	0.5
CPU time (s)	36.155

5.2 Results and Discussion for FCV Transition Model

The proposed model for the transition to FCVs introduced in Chapter 3 along with the models and data discussed in Chapter 4 was formulated using the AMPL modeling language [117], and solved with CPLEX [118] on an IBM eServer xSeries 460 with 8 Intel Xeon 2.8 GHz processors and 3 GB (effective) of RAM. The model statistics are given in Table 5.1; the CPU time reflected in this table corresponds to the case when penetration is uniform and the new nuclear units are developed in Toronto zone. This section presents and discusses the results for the FCV transition model for both uniform and non-uniform penetrations of these vehicles into Ontario's transport sector. Based on the discussion regarding the social cost of emissions presented in Section 3.7 and selecting a sufficiently large value of the social cost of emissions in populated areas, the penetration levels reported in this section represent Ontario's maximum grid potential for supporting FCVs.

5.2.1 Non-uniform FCVs Penetration

Impact of Transition Pattern

Optimal potential FCV penetration levels in different zones of Ontario based on Transition Pattern 1 and neglecting the emission constraints for generation are depicted in Figure 5.1. It is observed that Bruce, SW and Niagara are the zones

most amenable to a hydrogen economy; however, given the electricity prices as well as social costs of CO_2 emission in the population area, the FCV penetration in Niagara is significantly influenced by the location of the new nuclear units. Also, due to the retirement of coal plant in NW and limited base-load resources in this zone, NW is the least susceptible zone to a hydrogen economy. It is also interesting to note that except for Bruce, SW and Niagara (with new nuclear units in the Toronto zone), the improvement in FCV penetrations after 2013 is negligible. Observe that the development of new nuclear units in Bruce instead of Toronto results in lower penetration levels in almost all of the Ontario's zones except Bruce and SW. Also, the total number of supportable FCVs in the entire province by 2025 with new nuclear units in the Toronto and Bruce zones are determined to equal to 684,731 and 263,516, respectively. This shows that the development of new nuclear units in Toronto provides a better opportunity for FCV penetration in Ontario as a whole. Furthermore, with the new nuclear units in Toronto, there is no need for hydrogen transportation between the zones to achieve the FCV penetration levels shown in Figure 5.1; whereas with new nuclear units in Bruce, hydrogen must be transported from Bruce to all zones except NW as well as in the route West-SW during the whole planning horizon with a total cost of 330,258,499 CAD.

The results of a similar study with the consideration of Transition Pattern 2 are depicted in Figure 5.2. Comparing Figures 5.1 and 5.2 shows that similar patterns of FCV penetrations in different zones of Ontario are obtained despite different transition curves. However, it is worth noting that based on Transition Pattern 2, the FCV penetrations in SW and Essa are influenced less by the location of new nuclear units in Ontario, while the FCV penetration in Toronto, which has the largest number of LDVs, is substantially impacted by this factor. Also in this case, the development of new nuclear units in Bruce requires hydrogen transportation from Bruce to all zones except NW as well as in the route Ottawa-SW during the whole planning horizon with a total cost of 319,543,212 CAD.

In order to better illustrate the impact of transition curves, potential FCV penetrations in individual zones of Ontario with different assumptions for the location

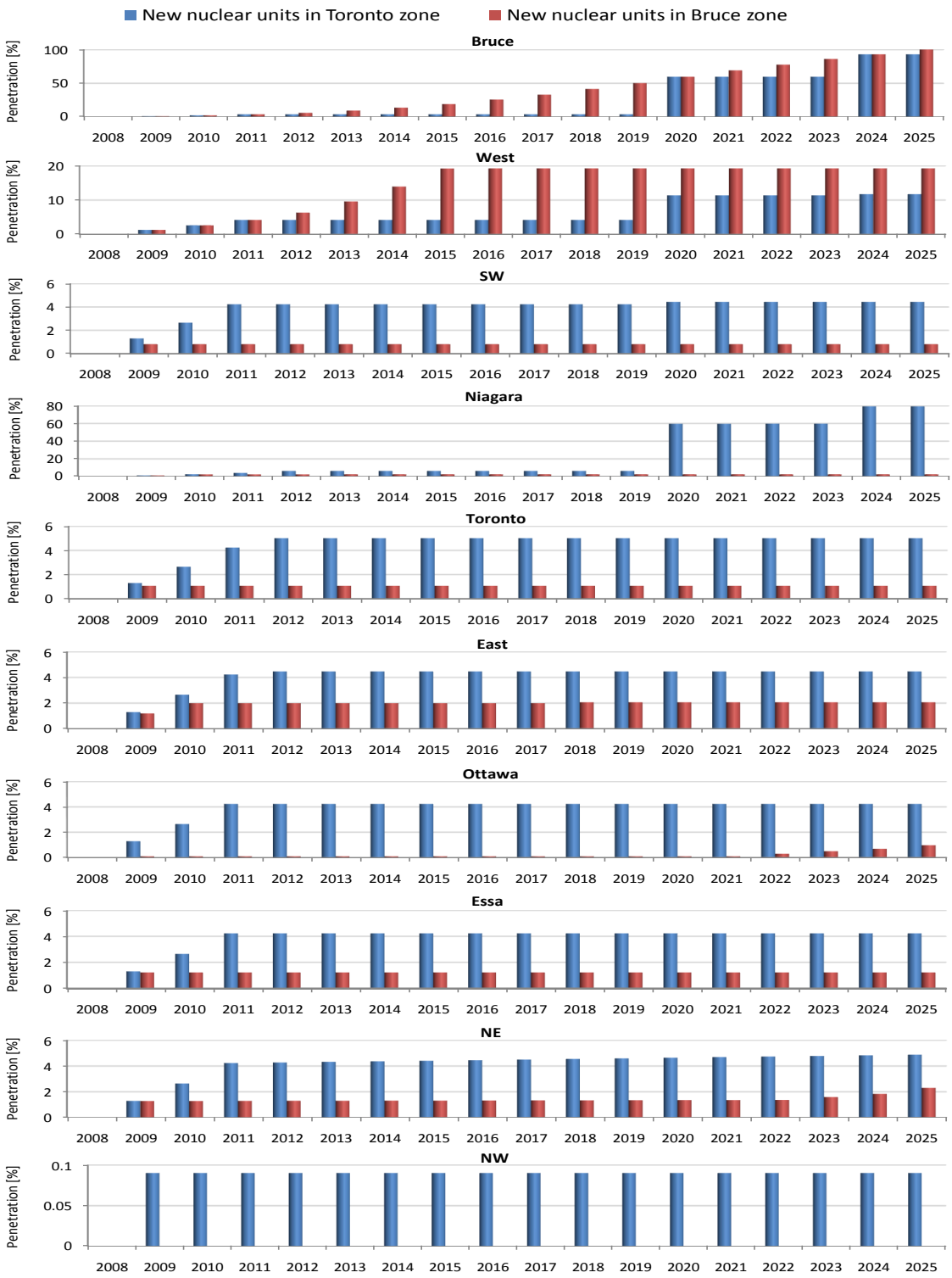

Figure 5.1: Optimal non-uniform hydrogen economy penetration based on Transition Pattern 1.

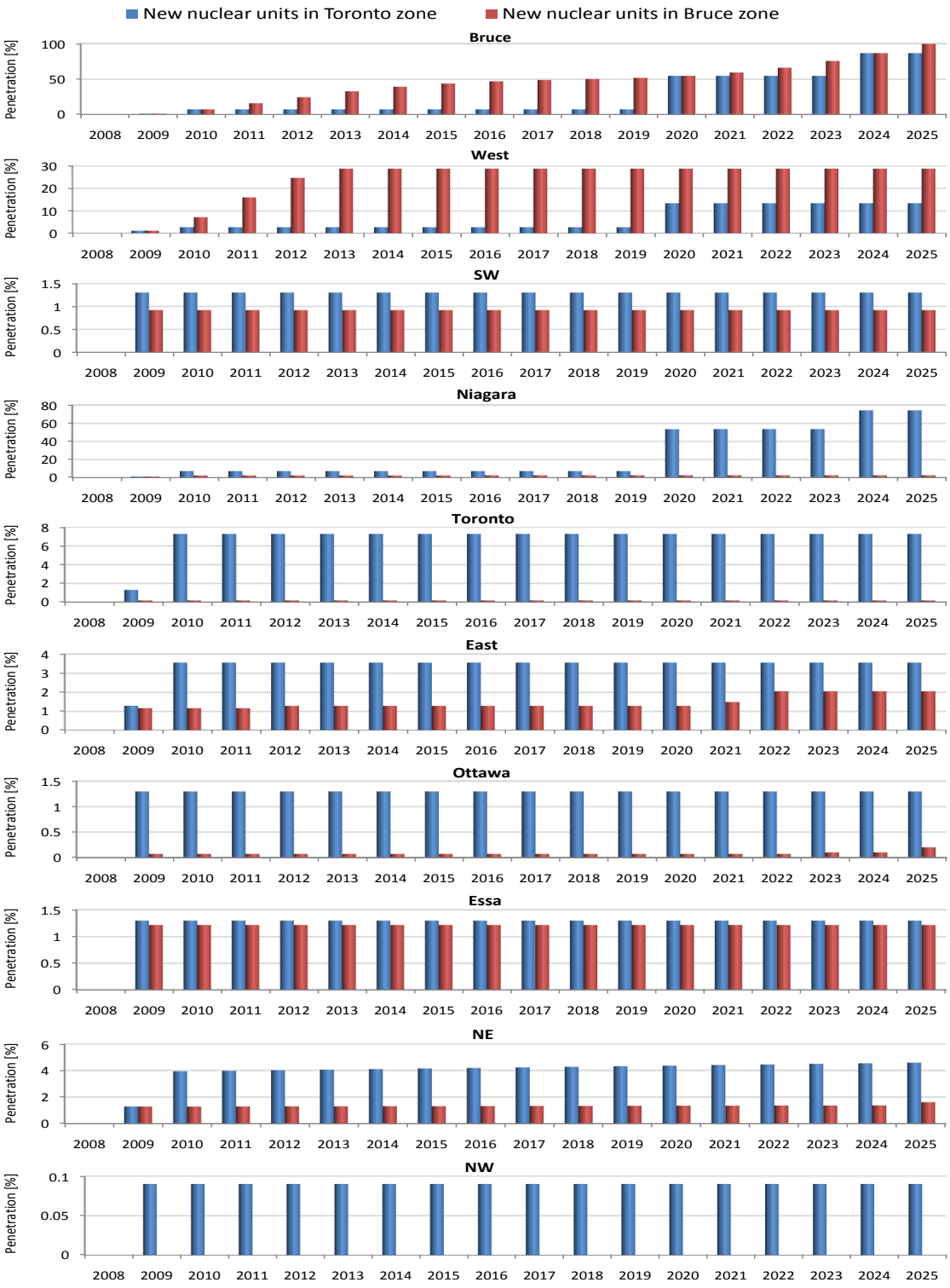

Figure 5.2: Optimal non-uniform hydrogen economy penetration based on Transition Pattern 2.

of new nuclear units are depicted in Figures 5.3 and 5.4. In general, Transition Pattern 2 is found to be more supportive of a hydrogen economy in Ontario than Transition Pattern 1. With the new nuclear units in the Toronto zone, the total number of supportable FCVs by 2025 based on Transition Pattern 2 is found to be equal to 686,261, which is slightly more than that obtained with Transition 1 (684,731). As can be observed in Figure 5.3, this is mainly due to higher penetration levels in the Toronto and West zones, which are the first and third largest populated zones in Ontario, respectively. The advantage of Transition 2 over 1 becomes even more conspicuous with the new nuclear units to be developed in the Bruce zone; in this case, the total number of supportable FCVs by 2025 based on Transition Pattern 2 is determined to equal 297,179, which is 12.77% more than that obtained based on Transition Pattern 1 (263,516). This can be explained by higher penetration levels in SW and in particular West zones; it is observed in Figure 5.4 that the final penetration levels in the West zone based on Transition Patterns 1 and 2 are almost 19% and 29%, respectively. Due to the previously discussed advantages of Transition Pattern 2 and of the development of new nuclear units in the Toronto zone, the studies in the following two sections will be based on these two assumptions.

Impact of Emission Constraints for Generation

The emission constraints for generation have almost no impact on the total number of supportable FCVs by 2025 (which is equal to 686,261); however, Table 5.2 shows that the CO_2 cost of generation is reduced by almost 51% when emission constraints are in place. This is related mainly to the reduction of power generation in SW, which has the largest share of coal plants until 2014, as well as Niagara, West and NE, which have the largest shares of CHP plants. This also justifies the zero revenue for power exports from West and Niagara.

Since emission constraints for generation cause changes in power dispatches within the system, it is expected that the size or pattern of HPP developments in different zones will also be impacted by these constraints. This expectation is con-

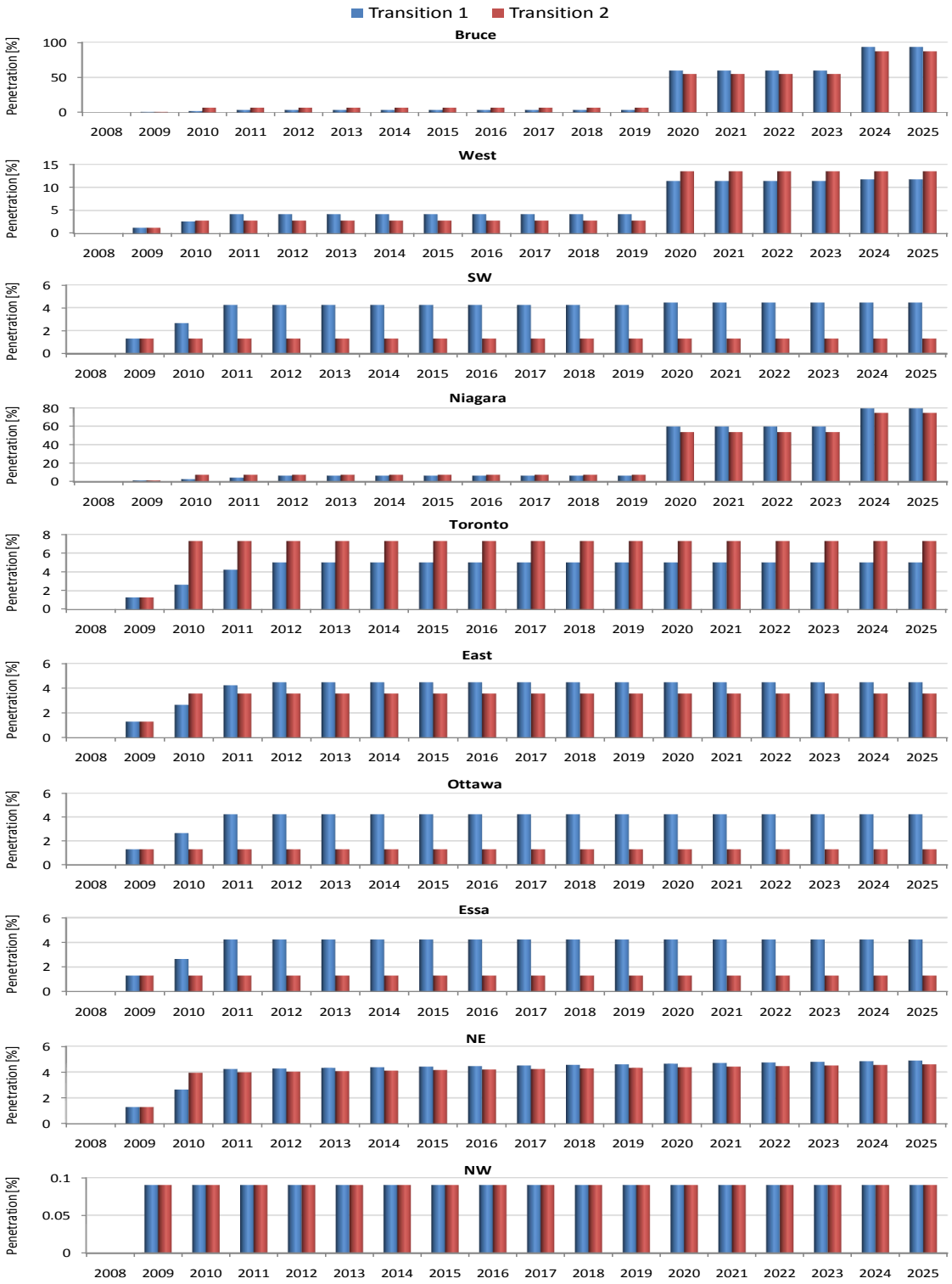

Figure 5.3: Optimal non-uniform FCV penetration with the new nuclear units in the Toronto zone.

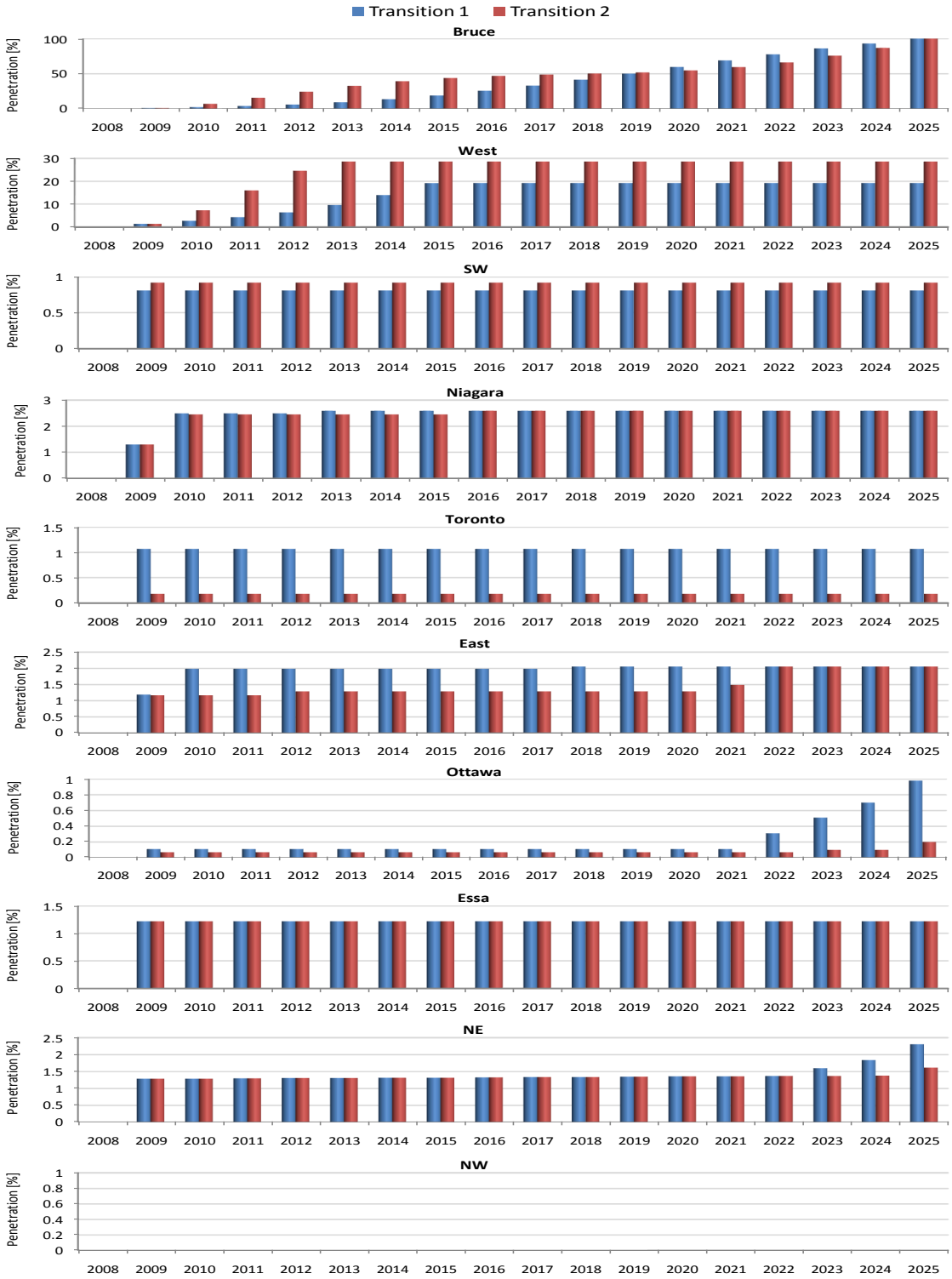

Figure 5.4: Optimal non-uniform FCV penetration with the new nuclear units in the Bruce zone.

Table 5.2: Optimal cost and revenue components (CAD) for non-uniform FCV penetration without and with emission constraints (EC) for generation

Cost/Revenue	without EC	with EC
Power generation	20,675,399,537	19,813,019,950
Power export	-873,136,546	0
Power import	1,279,465,922	1,288,009,105
Hydrogen transportation	0	0
Emission credit in transport sector	-6,004,203,393	-5,995,869,810
Emission cost of generation	1,911,597,561	929,113,192
Total	16,989,123,081	16,034,272,437

firmed by considering Table 5.3 where HPPs developed in different zones with and without the emission constraints are shown. Although the total developed HPPs in all of Ontario remains almost constant, the development of HPPs in the south and southwestern zones are impacted by these constraints, which result in changes in the potential FCV penetrations in these zones. It is also observed in Table 5.4 that final hydrogen economy penetrations by 2025 in almost all zones having high shares of CHP plants are reduced when emission constraints are considered.

Impact of HPP Placement Constraints

From a practical point of view, a maximum of 20 MW annual HPP development in each zone is considered in this section. Thus, based on Transition 2, a hydrogen economy of almost 7.3% can be realized in each zone by the end of 2010. However, due to very large number of LDVs in the Toronto zone (almost 3,400,000 LDVs in 2009 base), the realization of this hydrogen economy requires the development of almost 792 MW of HPPs, which is the capacity of almost 345 of the largest available HPPs [167]. Completing this many HPPs is really infeasible by the end of 2010.

The final number of supportable FCVs in all of Ontario is found to be scarcely affected by this constraint (672,322 compared to 686,587); however, the pattern of

Table 5.3: Optimal HPP development in different zones of Ontario for non-uniform FCV penetrations without (-) and with (+) emission constraints for generation

	Bruce		**West**		**SW**		**Niagara**		**Toronto**		**East**		**Ottawa**		**Essa**		**NE**		**NW**	
	-	+	-	+	-	+	-	+	-	+	-	+	-	+	-	+	-	+	-	+
2009	0.65	0.65	26.05	26.05	45.69	45.69	10.62	10.62	140.5	140.5	12.61	12.61	22.77	22.77	19.22	19.22	13.97	13.97	0.2	0.18
2010	3.01	3.01	31.20	121.2	0.49	0.49	48.81	48.81	649.5	603.6	22.06	0.04	0.29	0.29	0.18	0.18	27.91	0	0	0
2011	0.02	1.31	0.52	1.34	0.50	0.50	0	0	3.28	3.09	0.11	0.04	0.29	0.29	0.18	0.18	0	0	0	0
2012	0.02	0.02	0.53	1.35	0.51	0.51	0	0	3.32	3.13	0.12	0.04	0.3	0.3	0.19	0.19	0	0	0	0
2013	0.02	0.02	0.53	1.37	0.51	0.51	0	0	3.36	3.17	0.12	0.04	0.3	0.3	0.19	0.19	0	0	0	0
2014	0.02	0.02	0.54	1.39	0.52	0.52	0	0	3.40	3.20	0.12	0.04	0.31	0.31	0.19	0.19	0	0	0	0
2015	0.02	0.02	0.55	1.4	0.53	0.53	0	0	3.44	3.24	0.12	0.04	0.31	0.31	0.19	0.19	0	0	0	0
2016	0.02	0.02	0.55	1.42	0.54	0.54	0	0	3.48	3.28	0.12	0.04	0.32	0.32	0.19	0.19	0	0	0	0
2017	0.02	0.02	0.56	1.44	0.54	0.54	0	0	3.52	3.32	0.12	0.05	0.32	0.32	0.20	0.20	0	0	0	0
2018	0.02	0.02	0.57	1.46	0.55	0.55	0	0	3.56	3.36	0.13	0.05	0.33	0.33	0.20	0.20	0	0	0	0
2019	0.02	0.02	0.57	1.48	0.56	0.56	0	0	3.60	3.40	0.13	0.05	0.33	0.33	0.20	0.20	0	0	0	0
2020	25.04	23.71	236.3	7.03	0.57	27.43	376.2	386.2	3.65	197.8	0.13	0.05	0.34	0.34	0.21	0.21	0	0	0	0
2021	0.13	0.13	2.80	1.57	0.57	0.87	0	0	3.69	4.34	0.13	0.05	0.34	0.34	0.21	0.21	0	0	0	0
2022	0.13	0.13	2.84	1.59	0.58	0.88	0	0	3.73	4.39	0.13	0.05	0.35	0.35	0.21	0.21	0	0	0	0
2023	0.13	0.13	2.87	1.61	0.59	0.9	0	0	3.77	4.44	0.13	0.05	0.35	0.35	0.21	0.21	0	0	0	0
2024	17.29	14.47	2.91	27.48	0.6	0.91	168.58	147.01	3.81	4.49	0.13	0.05	0.36	0.36	0.22	0.22	0	0	0	0
2025	0.22	0.2	2.95	1.89	0.61	0.92	0	0	3.85	4.54	0.14	0.05	0.36	0.36	0.22	0.22	0	0	0	0
Total	46.75	43.93	312.8	201	54.45	82.85	604.2	592.7	843.4	993.3	36.55	13.34	27.97	27.97	22.41	22.41	41.88	13.97	0.2	0.18

Table 5.4: Final FCV penetration levels in different zones of Ontario without and with emission constraints for generation

Zone	**Bruce**	**West**	**SW**	**Niagara**	**Toronto**	**East**	**Ottawa**	**Essa**	**NE**	**NW**
without EC	86.89	13.47	1.3	74.48	7.28	3.56	1.3	1.3	4.59	0.09
with EC	81.64	8.65	1.98	73.06	8.58	1.3	1.3	1.3	1.53	0

FCV penetrations are substantially influenced. Thus, as represented in Figure 5.5, a 20 MW HPP placement constraint reduces the FCV penetration in the zones of Toronto and in Niagara (after 2020) zones while increasing the penetration levels in the other zones. Moreover, this constraint makes the hydrogen economy penetrate more evenly with almost no abrupt changes over time in different Ontario zones; this seems to be more harmonious with building and operating considerations.

The pattern of HPP development with and without a 20 MW placement constraint is also demonstrated in Table 5.5. Observe that the substantial developments of HPPs occur only in the Niagara and Toronto zones; thus, in Niagara, there are 386 and 147 MW HPP development in 2020 and 2024, respectively, and in Toronto, there are 604 and 198 MW HPP development in 2010 and 2020, respectively. With a 20 MW HPP placement constraint, such significant HPP developments cannot happen. This reduces the total HPP capacities developed in these two zones which results in lower FCV penetrations, as previously reflected in Figure 5.5. Reduction of the ultimate developed HPPs in the Toronto and Niagara zones provides the opportunity for further HPP development in other zones with the eastern and northern zones having the largest relative change in HPP developments. However, HPP placement constraints cause hydrogen transportation to take place between particular zones. As demonstrated in Figure 5.6, a 20 MW placement constraint makes Bruce as the main hydrogen exporter in Ontario and SW and Toronto as the main hydrogen importers, with the total transportation cost of 58,930,703 CAD during the entire planning cycle. This figure illustrates an integrated hydrogen and electricity system, with the zones acting as energy hubs.

The final number of FCVs by 2025 in different zones of Ontario is also depicted in Figure 5.7. Observe that the differences between the number of FCVs in different zones except for Bruce and NW are not significant; this is due to the 20 MW placement constraint, which reduces the discrepancies between the capacity of HPPs ultimately developed in these zones.

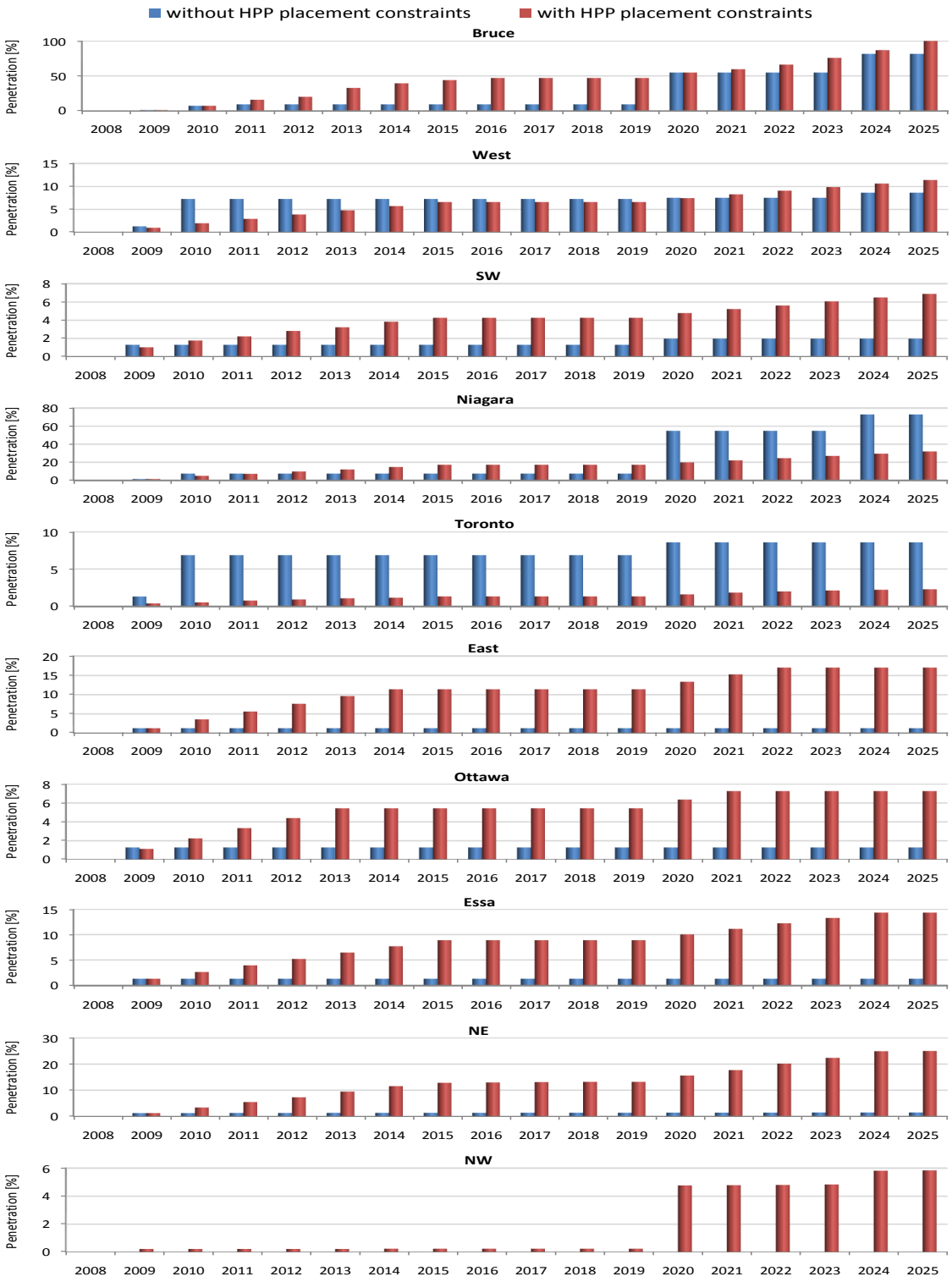

Figure 5.5: Optimal FCV penetrations in different zones of Ontario without and with a 20 MW HPP placement constraints (emission constraints included)

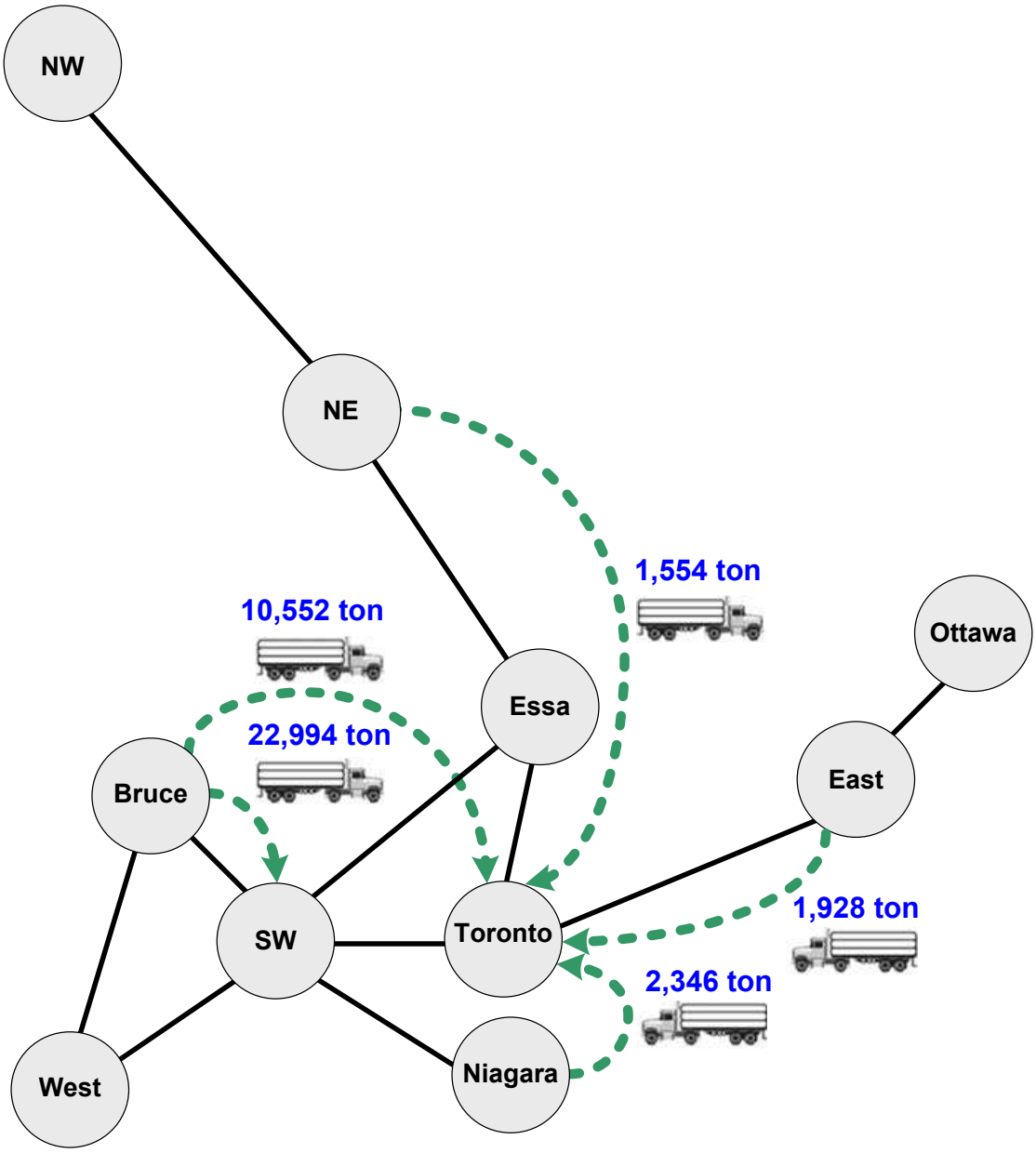

Figure 5.6: Optimal hydrogen transportation routes and total transferred hydrogen during the entire planning horizon with a 20 MW HPP placement constraint (emission constraints included).

Table 5.5: Optimal HPP development in different zones of Ontario for non-uniform FCV penetrations without (-) and with (+) a 20 MW placement constraint (emission constraints included)

	Bruce		West		SW		Niagara		Toronto		East		Ottawa		Essa		NE		NW	
	-	+	-	+	-	+	-	+	-	+	-	+	-	+	-	+	-	+	-	+
2009	0.65	19.11	26.05	20	45.69	20	10.62	19.85	140.5	20	12.61	17.23	22.77	20	19.22	19.22	13.97	18.59	0.18	0.55
2010	3.01	18.96	121.2	20	0.49	20	48.81	20	603.6	20	0.04	20	0.29	20	0.18	20	0	20	0	0
2011	1.31	8.40	1.34	20	0.50	20	0	20	3.09	20	0.04	20	0.29	20	0.18	20	0	20	0	0
2012	0.02	0	1.35	20	0.51	20	0	20	3.13	20	0.04	20	0.30	20	0.19	20	0	20	0	0
2013	0.02	0	1.37	20	0.51	20	0	20	3.17	20	0.04	20	0.30	20	0.19	20	0	20	0	0
2014	0.02	0	1.39	20	0.52	20	0	20	3.2	20	0.04	17.55	0.31	1.28	0.19	20	0	20	0	0
2015	0.02	0	1.40	20	0.53	20	0	20	3.24	20	0.04	0.28	0.31	1.3	0.19	20	0	11.73	0	0
2016	0.02	0	1.42	1.29	0.54	1.86	0	1.39	3.28	1.17	0.04	0	0.32	1.32	0.19	1.33	0	0	0	0
2017	0.02	0	1.44	1.31	0.54	1.89	0	0	3.32	0.99	0.05	0	0.32	1.34	0.20	1.35	0	0	0	0
2018	0.02	0	1.46	1.33	0.55	2.59	0	0	3.36	0	0.05	0	0.33	1.36	0.20	1.37	0	0	0	0
2019	0.02	0	1.48	1.34	0.56	1.64	0	0	3.40	0	0.05	0	0.33	1.38	0.20	1.39	0	0	0	0
2020	23.71	20	7.03	20	27.43	20	386.2	20	197.8	20	0.05	20	0.34	20	0.21	20	0	20	0	9.95
2021	0.13	8.13	1.57	20	0.87	20	0	20	4.34	20	0.05	20	0.34	20	0.21	20	0	20	0	0
2022	0.13	1.63	1.59	20	0.88	20	0	20	4.39	20	0.05	20	0.35	1.93	0.21	20	0	20	0	0
2023	0.13	0	1.61	20	0.90	20	0	20	4.44	20	0.05	0.31	0.35	1.96	0.21	20	0	20	0	0
2024	14.47	0	27.48	20	0.91	20	147	20	4.49	20	0.05	0	0.36	1.99	0.22	20	0	20	0	2.09
2025	0.2	0.78	1.89	20	0.92	20	0	20	4.54	15.29	0.05	0	0.36	2.03	0.22	2.41	0	0	0	0
Total	43.93	77.01	201	265.3	82.85	267.99	592.7	261.2	993.3	257.5	13.34	175.4	27.97	156	22.41	247.1	13.97	230.3	0.18	12.59

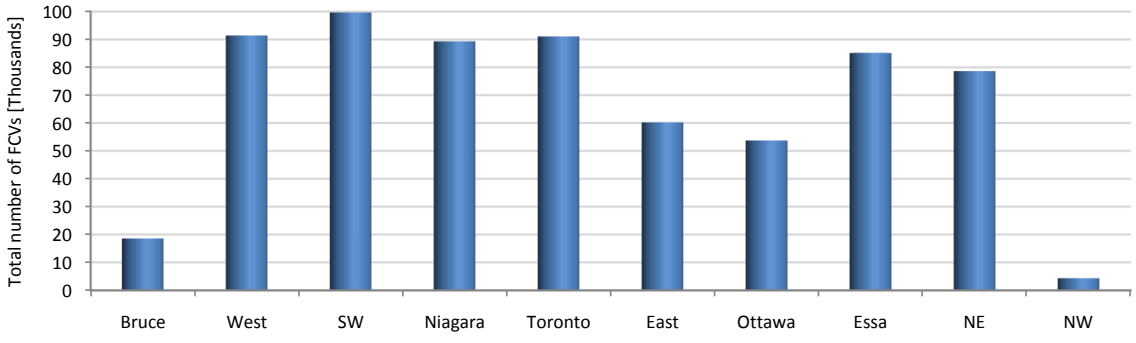

Figure 5.7: Final number of FCVs based on a non-uniform penetration assumption with the consideration of 20 MW placement and emission constraints.

5.2.2 Uniform FCVs Penetration

Impact of Transition Pattern

Optimal FCV penetration levels disregarding the emission constraints and based on different transition patterns and locations for the new nuclear units are depicted in Figure 5.8. Observe in this figure that for a uniform FCV penetration, the type of transition has a negligible impact on the results. Also, similar to the non-uniform penetration study, development of the new nuclear units in the Toronto zone provides a larger FCV penetration in the whole province. Moreover, even the realization of a 1.44% uniform FCV penetration based on the new nuclear units in Bruce requires significant hydrogen transportation between the zones. Thus, total hydrogen transportation costs with the new nuclear units in Toronto and Bruce are found to equal 42,381,547 and 619,012,158 CAD, respectively.

The total number of FCVs by 2025 with the new nuclear units in Toronto and Bruce, are 650,760 and 123,946, respectively. It is interesting to note that with the new nuclear units in Bruce, the total number of FCVs, which is obtained based on a uniform penetration assumption is almost half of that obtained based on non-uniform penetration assumption (123,946 vs. 263,516). This can be explained with the help of electricity and hydrogen constraints. Thus, due to electricity grid limitations, achieving a uniform FCV penetration across all of Ontario requires relatively more hydrogen transportation than that needed for non-uniform penetrations; however, this transportation is restricted by the 4 ton/day limit on hydrogen transfer between any two individual zones. Consequently, a lower number of FCVs is expected.

It should be noted that with the new nuclear units being developed in Toronto, the total number of FCVs is reduced by only 5% compared to the non-uniform case (684,731 vs. 650,760). This is justified by the proximity of generation and major load centers in Ontario in this case. From the results represented in Figure 5.8, one could conclude that the development of new nuclear units in the Toronto zone together with Transition Pattern 2 for a uniform hydrogen economy penetration is

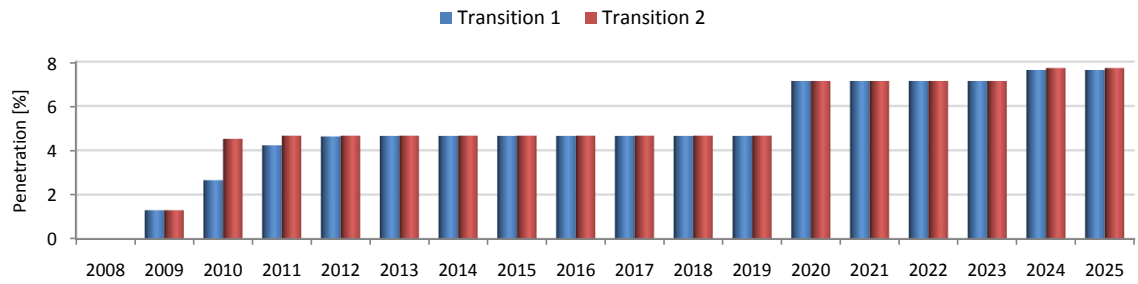

(a) New nuclear units in Toronto zone.

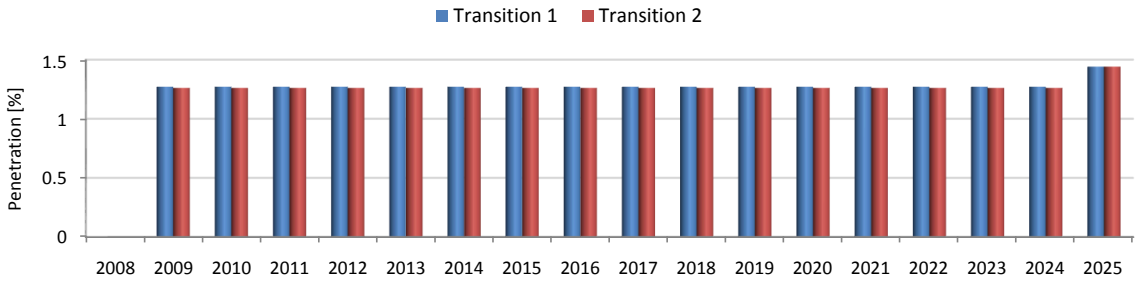

(b) New nuclear units in Bruce zone.

Figure 5.8: Optimal uniform FCV penetration in Ontario based on different transition patterns and location of the new nuclear units.

a superior option; this conclusion is similar to what was observed for non-uniform penetration. The studies in the following two sections will be based on these assumptions.

Impact of Emission Constraints for Generation

It was observed in Section 5.2.1 that for a non-uniform FCV penetration, the size and pattern of HPPs developments in the south and southwestern zones of Ontario are influenced by the emission constraints for generation. However, it is expected that for a uniform FCV penetration, where the rate of load level increases are the same across all zones, the corresponding impact should be comparatively lower. This expectation is verified by considering the results shown in Table 5.6. It is observed that the size of HPPs in Bruce, i.e., the most environmentally-friendly zone of Ontario, is the most influenced by the emission constraints for generation. Also,

Table 5.6: Optimal HPP development in different zones of Ontario for a uniform FCV penetration without (-) and with (+) emission constraints for generation

	Bruce		**West**		**SW**		**Niagara**		**Toronto**		**East**		**Ottawa**		**Essa**		**NE**		**NW**	
	-	+	-	+	-	+	-	+	-	+	-	+	-	+	-	+	-	+	-	+
2009	5.27	10.18	25.47	26.05	46.26	43.08	8.31	8.31	145.1	140.5	8	8	22.77	22.77	19.22	21.53	14.67	14.67	0	0
2010	0.50	0	65.34	63.72	127.6	113.6	27.38	25.63	377.5	371.1	0.65	2.06	57.40	55.99	48.24	54.96	31.94	31.30	0	0
2011	0	0	0.94	5.21	0	6.77	0	2.23	0	7.03	29.98	28.49	3.46	4.88	2.69	0	0	0.64	0	0
2012	0	0	2.64	0.86	0	3.61	0	0	0	0	1.17	0.01	1.07	1.07	0.66	0	0	0	0.57	0.57
2013	0	0	0.11	0.92	0	0	0	0	0	0	0	0	1.11	1.12	0.69	0	0	0	4.64	4.65
2014	0.56	0	0.90	0.89	0	1.25	0	0	0	0	0	0	1.10	1.10	0.68	0	0	0	3.07	3.07
2015	0.46	0	2.32	0.90	0	2.34	0	0.21	0	0	1.83	1.85	1.12	1.12	0.69	0	0	0	0	0
2016	0	0	1.17	0.91	1.64	3.74	0	0	0	0	1.86	0.73	1.13	1.13	0.70	0	0	0	0	0
2017	0	0	0.92	0.92	1.93	1.96	0	0.25	0.07	0	1.83	2.33	1.15	1.15	0.71	0	0	0	0	0
2018	0	0	0.94	0.93	1.96	1.98	0	0	1.76	1.54	0.17	1.09	1.17	1.17	0.72	0	0	0	0	0
2019	1.27	0	0.77	0.95	0	2.01	0.89	0	1.80	1.78	0.17	0.89	1.19	1.19	0.73	0	0	0	0	0
2020	0	0	54.37	55.75	104.5	100	19.18	19.11	288.1	290	22.72	22.90	51.11	51.04	41.38	41.87	24	23.97	0.91	0.90
2021	0	0	3.11	1.48	1.79	3.16	0	0	1.42	1.41	0	0	1.88	1.87	1.14	1.41	1.42	1.42	0	0
2022	0	0	1.43	1.50	3.54	3.20	0	0	2.89	2.88	0	0	1.90	1.90	1.15	1.43	0	0	0	0
2023	0	0	0	1.52	5.04	3.24	0	0	2.94	2.93	0	0	1.93	1.93	1.17	1.45	0	0	0	0
2024	15.16	30.04	16.37	16.54	10.08	15.43	4.65	5.27	71.44	65.02	6.72	9.01	14.17	15.80	10.99	10.71	1.13	1.84	3.24	3.40
2025	4.14	8.27	1.69	2.05	0	0.13	0	0.12	3.06	1.58	0	0	2.15	2.50	1.30	1.57	0	0	0	0
Total	27.35	48.50	178.5	181.1	304.3	305.4	60.41	61.13	896	885.7	75.10	77.36	165.8	167.8	132.9	134.9	73.16	73.85	12.43	12.59

the optimal cost and revenue components in Table 5.7 demonstrate the impacts of these constraints, which particularly result in lower total emission costs and power export revenues in West and Niagara which have the highest shares of CHP plants in Ontario. Larger hydrogen transportation costs, which are obtained when emission constraints are included, mainly correspond to further development of HPPs in Bruce directly increasing the level of hydrogen export from this zone. Comparing the emission credit in the transport sector results illustrates that the ultimate uniform FCV penetration and total number of FCVs is not substantially impacted by emission constraints.

Table 5.7: Optimal cost and revenue components (CAD) for a uniform FCV penetration without and with emission constraints (EC) for generation

Cost/Revenue	without EC	with EC
Power generation	20,674,626,820	19,805,013,754
Power export	-894,355,800	-1,866,518
Power import	1,286,738,017	1,288,070,601
Hydrogen transportation	72,236,670	73,082,980
Emission credit in transport sector	-5,914,859,740	-5,911,545,066
Emission cost of generation	1,907,640,285	927,363,677
Total	17,132,026,252	16,180,119,428

Impact of HPP Placement Constraints

Similar to the non-uniform penetration study, a maximum 20 MW annual HPP development in each zone is also considered here. Optimal FCV penetrations with and without this constraint are depicted in Figure 5.9. It is observed that the 20 MW HPP placement constraint substantially reduces FCV penetrations; moreover, similar to the non-uniform penetration study, it helps the hydrogen economy penetrate more evenly over time. Table 5.8 demonstrates the optimal size of HPPs to be developed in different zones of Ontario to achieve the FCV penetrations shown in Figure 5.9. Observe that the total capacity of HPPs developed by 2025 in all zones are reduced and their total development in all of Ontario is diminished by almost 44%. It is interesting to note that this placement constraint has the largest impact on HPP development in the Toronto zone; this constraint seems to be the main reason for the decline of uniform FCV penetration in Ontario as a whole. Thus, the Toronto zone is not allowed to develop more than 340 MW HPPs by 2025 which is realized by a constant 20 MW development in each year. It would be expected that the deficit of local HPPs in this zone would be partly compensated by further hydrogen imports from other zones; however, total compenstaion is not feasible as the hydrogen transfer is also constrained by a 4 ton/day limit.

Optimal hydrogen transfer routes and total transferred hydrogen during the

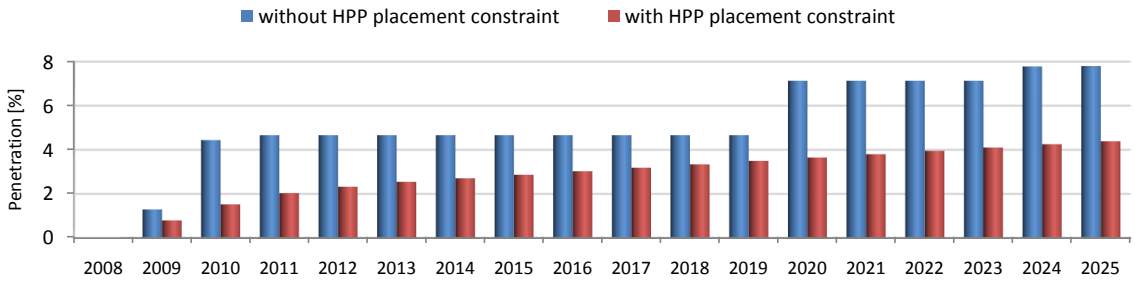

Figure 5.9: Optimal uniform FCV penetration in Ontario without and with a 20 MW HPP placement constraint (emission constraints included).

whole planning period without and with a 20 MW HPP placement constraint are shown in Figures 5.10 and 5.11, respectively. It is observed that the inclusion of the HPP placement constraint causes the transportation of large volumes of hydrogen in Ontario, in particular in the routes ending at Toronto. Optimal cost and revenue components reflected in Table 5.9 show that total hydrogen transportation costs increases by more than five-fold when a HPP placement constraint is considered. Also, comparing the power generation costs in Table 5.9 reveals that there is still unutilized generation capacity in Ontario when the HPP placement constraint is included. However, congestion in hydrogen transportation routes due to a 4 ton/day transfer limit precludes further development of HPPs. It is also interesting to note in Figures 5.10 and 5.11 that similar to the non-uniform penetration study, Bruce has the capability of being the main hydrogen exporter in Ontario. The total number of FCVs in this case is also represented in Figure 5.12. Although a 20 MW placement constraint reduces the significant discrepancies between the developed HPPs in different zones, the uniform penetration assumption results in substantially larger numbers of FCVs in the Toronto zone, which has the largest transport sector in Ontario. Furthermore, the total number of FCVs in this case is almost 56% of the one obtained based on non-uniform penetration assumption. Based on the realistic and practical assumptions made in this section, no more than 378,362 FCVs can be introduced into Ontario's transport sector by 2025.

Table 5.8: Optimal HPP developments in different zones of Ontario for a uniform hydrogen economy penetration without (-) and with (+) a 20 MW placement constraint (emission constraints included)

	Bruce		**West**		**SW**		**Niagara**		**Toronto**		**East**		**Ottawa**		**Essa**		**NE**		**NW**	
	-	+	-	+	-	+	-	+	-	+	-	+	-	+	-	+	-	+	-	+
2009	10.18	20	26.05	20	43.08	20	8.31	20	140.5	20	8	20	22.77	20	21.53	20	14.67	20	0	0.56
2010	0	11.90	63.72	20	113.6	20	25.63	19.56	371.1	20	2.06	17.85	55.99	20	54.96	20	31.30	19.92	0	0
2011	0	0	5.21	20	6.77	20	2.23	10.54	7.03	20	28.49	4.78	4.88	19.29	0	13.40	0.64	8.36	0	0
2012	0	0	0.86	17.38	3.61	19.30	0	0	0	20	0.01	2.84	1.07	5.72	0	4.66	0	1.12	0.57	0
2013	0	0	0.92	0.43	0	19.80	0	0	0	20	0	2.16	1.12	4.55	0	3.66	0	1.71	4.65	2.99
2014	0	0	0.89	3.72	1.25	7.99	0	0.03	0	20	0	1.55	1.10	3.48	0	2.74	0	1.23	3.07	0.35
2015	0	0	0.90	3.77	2.34	8.10	0.21	0	0	20	1.85	1.55	1.12	3.54	0	2.78	0	0.19	0	1.34
2016	0	0	0.91	3.81	3.74	8.19	0	0	0	20	0.73	1.55	1.13	3.61	0	2.81	0	1.49	0	0
2017	0	0	0.92	3.85	1.96	8.28	0.25	0	0	20	2.33	1.55	1.15	3.67	0	2.84	0	1.44	0	0
2018	0	0	0.93	2.24	1.98	8.85	0	1.16	1.54	20	1.09	1.55	1.17	3.73	0	2.87	0	1.39	0	0
2019	0	0	0.95	3.94	2.01	7.33	0	1.11	1.78	20	0.89	1.54	1.19	3.80	0	2.91	0	0.41	0	0.94
2020	0	0	55.75	5.61	100	5.81	19.11	1.10	290	20	22.90	1.54	51.04	3.86	41.87	2.94	23.97	1.31	0.90	0
2021	0	0	1.48	2.40	3.16	9.16	0	1.09	1.41	20	0	1.54	1.87	3.93	1.41	2.97	1.42	1.26	0	0
2022	0	0	1.50	4.06	3.20	7.64	0	1.08	2.88	20	0	1.54	1.90	4	1.43	3.01	0	0.62	0	0.6
2023	0	0	1.52	5.70	3.24	6.14	0	1.07	2.93	20	0	1.54	1.93	4.06	1.45	3.04	0	1.18	0	0
2024	30.04	0	16.54	4.14	15.43	7.85	5.27	1.06	65.02	20	9.01	1.54	15.80	4.13	10.71	3.07	1.84	0.85	3.40	0.29
2025	8.27	0	2.05	4.18	0.13	7.95	0.12	1.05	1.58	20	0	1.54	2.50	4.20	1.57	3.11	0	0.81	0	0.29
Total	48.50	31.90	181.1	125.2	305.4	192.4	61.13	58.83	885.7	340	77.36	66.16	167.8	115.6	134.9	96.80	73.85	63.29	12.59	7.35

Table 5.9: Optimal cost and revenue components (CAD) for a uniform hydrogen economy penetration without and with a 20 MW placement constraint (PC)

Cost/Revenue	**without PC**	**with PC**
Power generation	19,805,013,754	19,252,364,918
Power export	-1,866,518	-4,684,055
Power import	1,288,070,601	1,287,596,262
Hydrogen transportation	73,082,980	380,071,018
Emission credit in transport sector	-5,911,545,066	-3,282,644,537
Emission cost of generation	927,363,677	670,027,214
Total	16,180,119,428	18,302,730,820

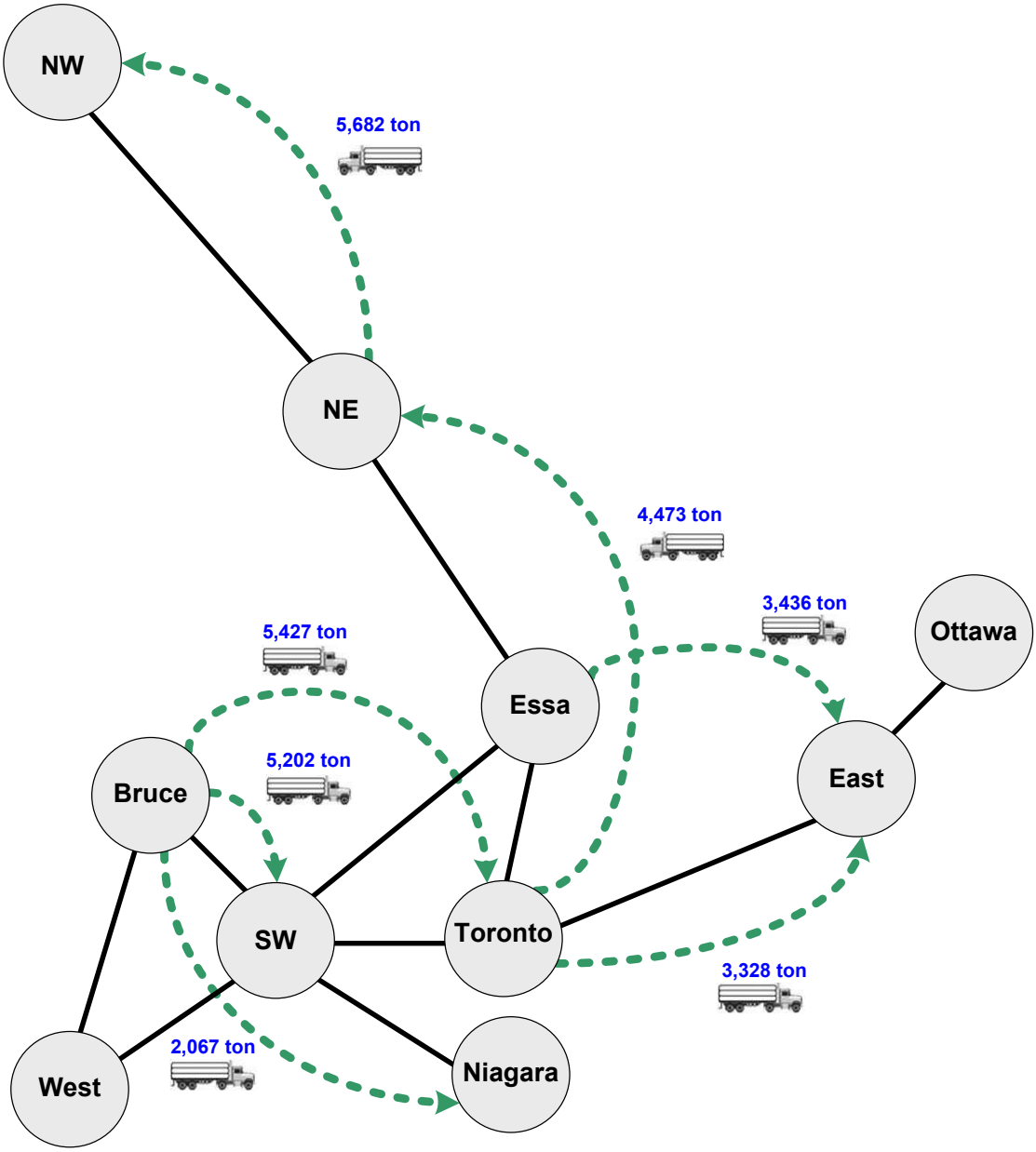

Figure 5.10: Optimal hydrogen transportation for the whole planning horizon based on a uniform hydrogen economy penetration (emission constraints included).

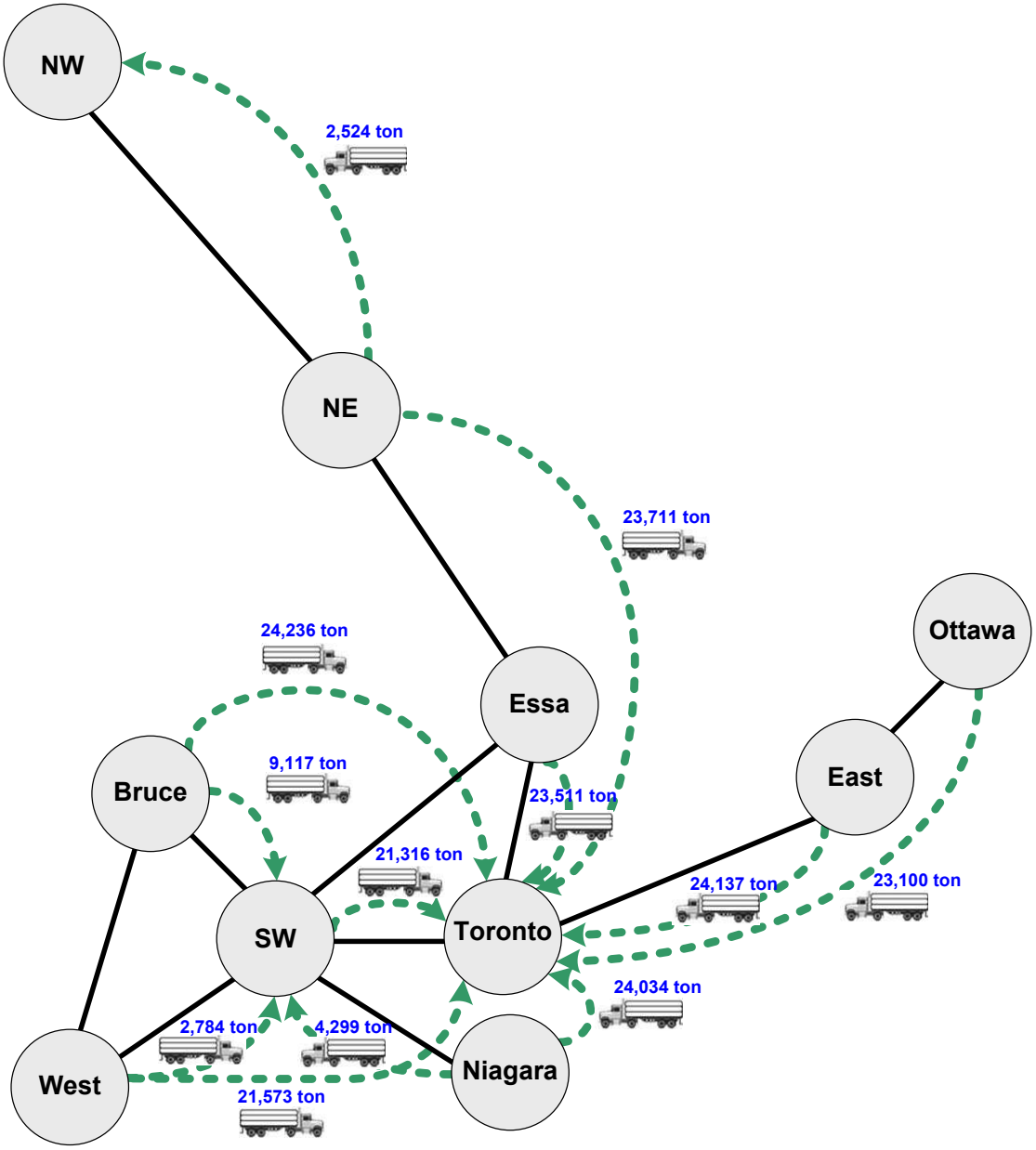

Figure 5.11: Optimal hydrogen transportation for the whole planning horizon based on a uniform hydrogen economy penetration including 20 MW placement and emission constraints.

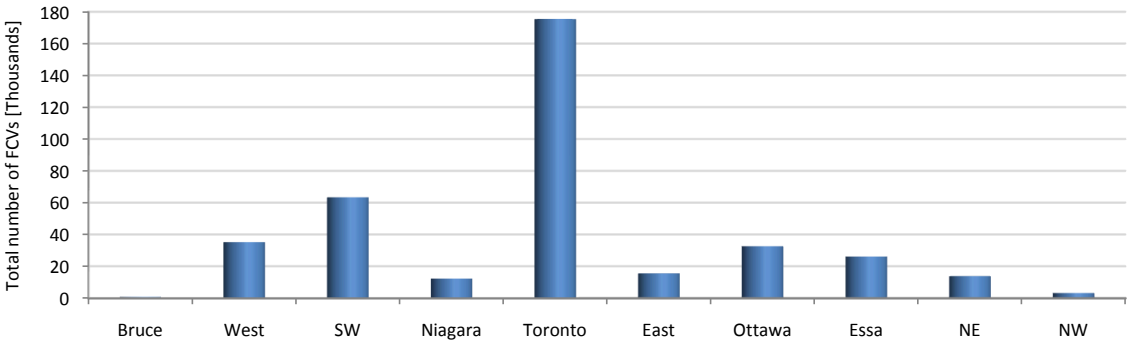

Figure 5.12: Total number of FCVs based on a uniform penetration assumption considering 20 MW placement and emission constraints.

Table 5.10: PHEV transition model statistics

Number of continuous variables	21,684
Number of binary variables	19,993
Number of constraints	62,448
MIP gap (%)	0.02
CPU time (s)	172.292

5.3 Results and Discussion for PHEV Transition Model

The model proposed in Chapter 3 for the transition to PHEVs along with the data discussed in the previous chapter was formulated using the AMPL modeling language [117], and solved with CPLEX [118], on an IBM eServer xSeries 460 with 8 Intel Xeon 2.8 GHz processors and 3 GB (effective) of RAM. The model statistics are given in Table 5.10; the CPU time reflected in this table corresponds to the case when penetration is uniform and the new nuclear units are developed in the Toronto zone. This section presents and discusses the results for the PHEV transition model considering both uniform and non-uniform penetrations of these vehicles into Ontario's transport sector. The penetration levels reported in this section represent Ontario's maximum grid potential for supporting PHEVs.

5.3.1 Non-uniform PHEVs Penetration

Impact of Transition Pattern

The total number of PHEVs based on Transition Patterns 1 and 2 were found to equal 1,037,081 and 1,036,558, respectively. Hence, for a non-uniform PHEV penetration, the type of assumed transition pattern has practically no impact on the total number of supportable PHEVs by the electricity grid in Ontario. However, as observed in Figure 5.13, Transition Pattern 1 facilitates further adoption of PHEVs in the SW, NW and eastern zones, while Transition Pattern 2 provides a better opportunity for penetration of PHEVs into the NE and in particular Toronto's transport sector, which has the largest number of LDVs in Ontario. Similar to FCVs related studies, Bruce and Niagara show the largest PHEV penetration in terms of their percentage of LDVs.

Impact of Emission Constraints for Generation

In Ontario, emission constraints for generation were also found to be of practically no influence on the total number of PHEVs, since the numbers obtained were 1,037,320 and 1,036,555 based on Transition Patterns 1 and 2, respectively. However, optimal cost and revenue components are substantially impacted by these constraints as demonstrated in Table 5.11, where it is shown that power generation is reduced due to the emission constraints; this in turn reduces the total emission cost of generation by almost 27% and hinders power export from the West and Niagara zones.

The minimal impact of emission constraints for generation is also demonstrated in Figure 5.14, where the total number of PHEVs in individual zones of Ontario without and with the consideration of emission constraints and based on different transition patterns are illustrated. Observe in this figure that only the total number of PHEVs in the West and Toronto zones are slightly impacted by the emission constraints based on Transition Pattern 1. Also, in terms of the number of PHEVs

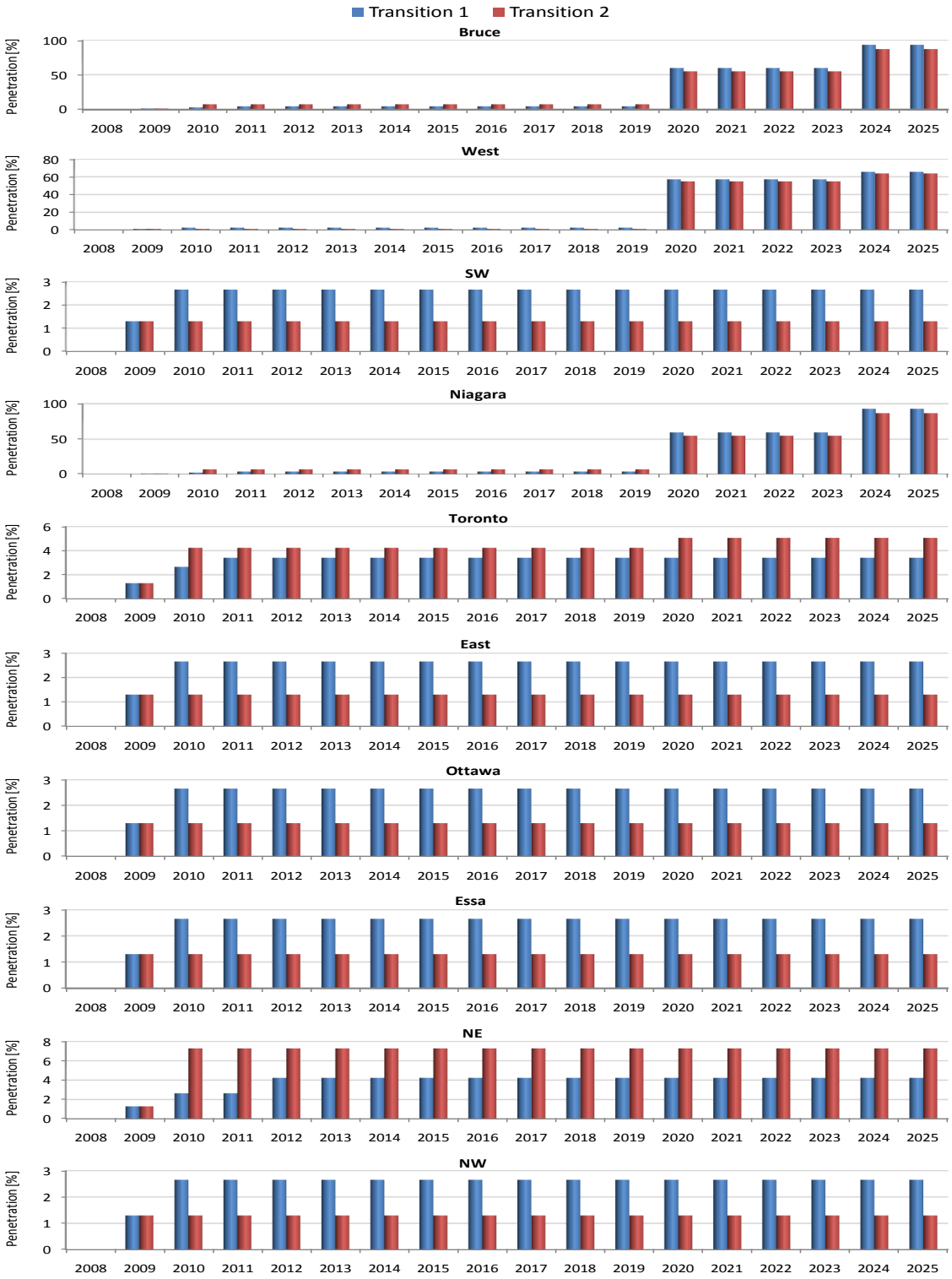

Figure 5.13: Optimal non-uniform PHEV penetration.

Table 5.11: Optimal cost and revenue components (CAD) for a non-uniform PHEV penetration without and with emission constraints (EC) for generation based on Transition Pattern 1

Cost/Revenue	without EC	with EC
Power generation	17,135,825,318	17,030,351,992
Power export	-123,378,869	-1,012,978
Power import	1,096,923,471	1,096,923,471
Emission credit in transport sector	-3,378,790,998	-3,377,231,320
Emission cost of generation	1,285,171,092	932,847,929
Total	16,015,750,014	15,681,879,094

and based on a non-uniform penetration assumption, Ontario's electricity grid has the greatest capability to support PHEVs in the West, Niagara and Toronto zones.

5.3.2 Uniform PHEVs Penetration

Impact of Transition Pattern

Optimal uniform PHEV penetration into Ontario's transport sector based on different transition patterns and without the consideration of emission constraints are depicted in Figure 5.15, where Transition Pattern 2 represents an extremely minor advantage in the year 2020. The total number of supportable PHEVs by 2025 based on both transition patterns are found to equal 912,106; this shows almost a 12% reduction compared to the non-uniform penetration scenario, which can be explained by the increased level of transmission losses. Observe that until 2019 no more than a 3.12% uniform PHEV penetration can be supported by Ontario's grid. It is important to mention that if the feasibility factor FF_{iy} is set the same for all zones (disregarding zone index i), transition curve is scaled down for all zones to keep feasibility; this makes the penetrations of AFVs in different zones follow a similar pattern, but it might underestimate the grid potential for supporting AFVs in the transport sector [168].

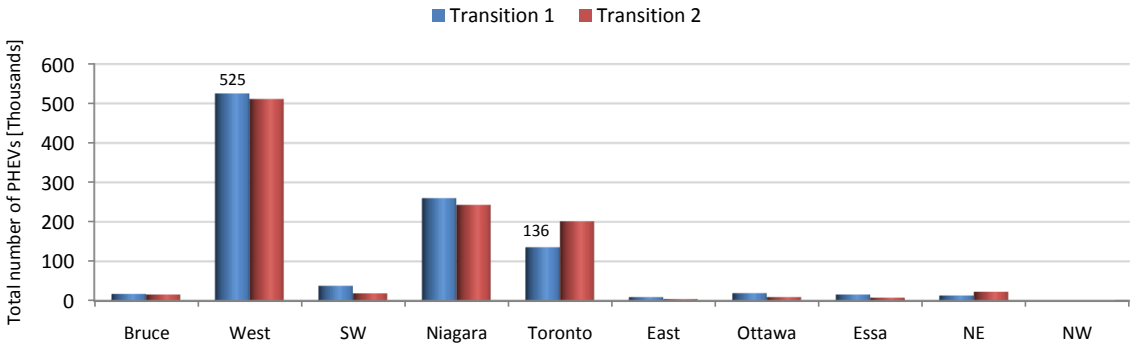

(a) without emission constraints for generation.

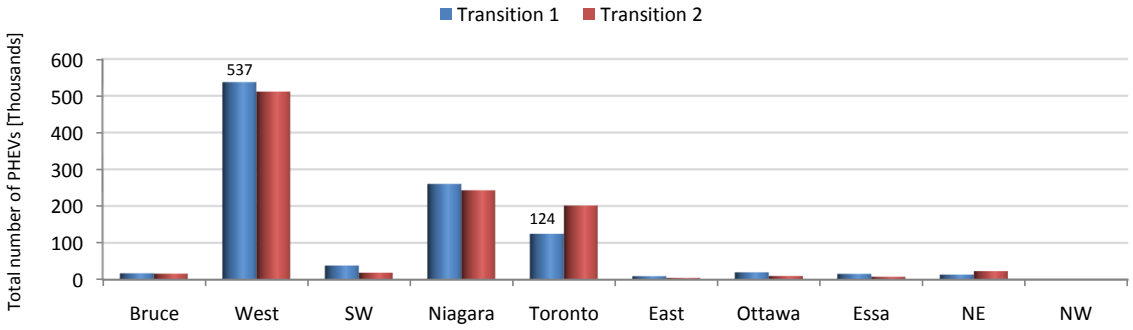

(b) with emission constraints for generation.

Figure 5.14: Total number of PHEVs in different zones of Ontario for a non-uniform penetration.

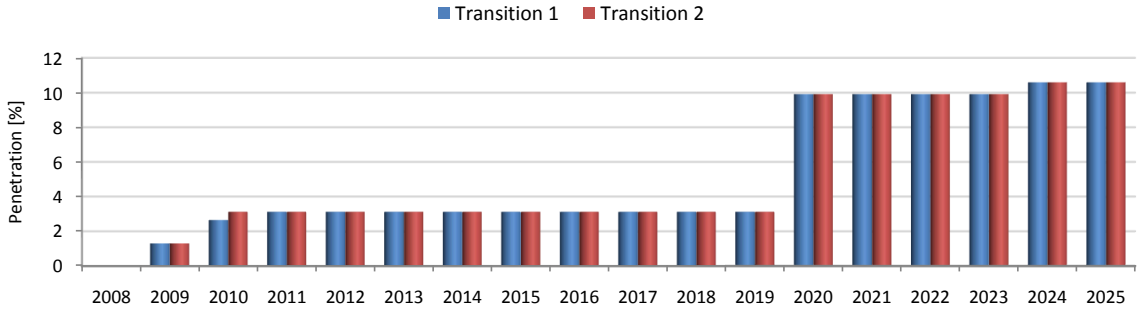

Figure 5.15: Optimal uniform PHEVs penetration into Ontario's transport sector.

Table 5.12: Optimal cost and revenue components (CAD) for a uniform PHEV penetration without and with emission constraints (EC) for generation for Transition Pattern 2

Cost/Revenue	without EC	with EC
Power generation	17,251,370,517	17,028,836,437
Power export	-244,130,997	0
Power import	1,096,923,471	1,096,923,471
Emission credit in transport sector	-3,317,132,123	-3,317,132,123
Emission cost of generation	1,426,569,483	931,936,287
Total	16,213,600,351	15,740,564,072

Impact of Emission Constraints for Generation

For a uniform PHEV penetration, emission constraints have no impact on the number of supportable PHEVs in each individual year during the whole planning horizon, since the penetration levels in this case are exactly the same as the ones depicted in Figure 5.15. However, different cost and revenue components are subject to change. For example, optimal cost and revenue components for PHEV penetration based on Transition Pattern 2, with and without emission constraints for generation are demonstrated in Table 5.12. Observe that in this case, there is no power exports, and the emission cost of generation is significantly reduced by almost 35%.

Figure 5.16 demonstrates the total number of PHEVs supported by Ontario's electricity grid in individual zones of Ontario based on a uniform penetration assumption. As was mentioned earlier, the type of transition pattern and the inclusion of emission constraints for generation do not influence these results. Observe in Figure 5.16 that in terms of the number of PHEVs, Ontario's maximum grid potential is particularly reflected in the Toronto and SW zones.

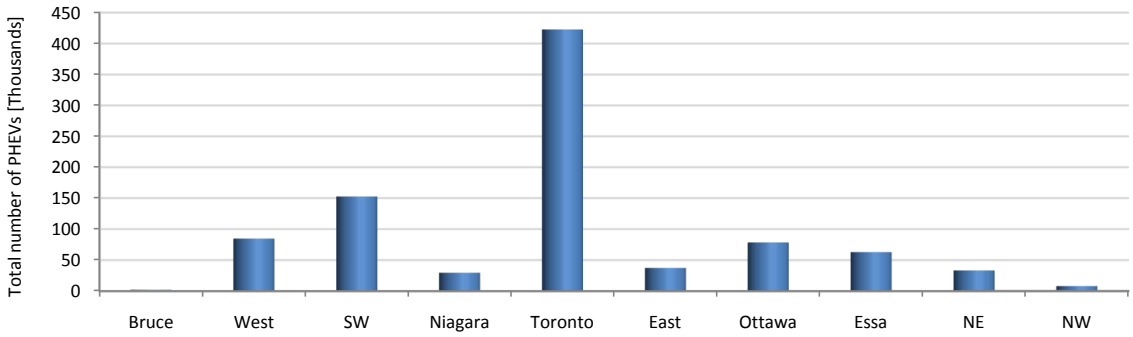

Figure 5.16: Total number of PHEVs in different zones of Ontario for a uniform penetration.

5.4 Summary

This chapter presented and discussed the application of the proposed optimization models for the transition to AFVs to the real case of Ontario, Canada with a planning horizon starting in 2008 and ending in 2025. Maximum Ontario's grid potential for supporting both FCVs and PHEVs were determined under uniform and non-uniform penetration assumptions. The impacts of different constraints and assumptions such as the location of the new nuclear units, transition patterns, the emission cost of generation, and HPP placement and hydrogen transportation limits were also analyzed in detail.

Chapter 6

Optimal Transition to AFVs under Uncertainty

6.1 Introduction

In Chapter 3, comprehensive optimization models were developed for planning the transition to AFVs. Chapter 5 demonstrated the application of these models in Ontario, Canada to determine the maximum grid potential for supporting AFVs in Ontario's transport sector based on the data set and assumptions discussed in Chapter 4. These optimization planning models involve many parameters that must be estimated; however, estimation errors may significantly influence the optimal solution. Therefore, these errors must be taken into account during the optimization process when looking for an optimal solution. One of the approaches in considering these uncertainties during the optimization process is robust optimization, which has received notable attention recently. This chapter proposes the application of robust optimization to deal with parameter uncertainty in planning the transition to AFVs, using the real-case example of Ontario.

In order to identify the influential uncertain parameters, a sensitivity analysis using Monte Carlo simulation is performed first. Once the influential parameters

are determined, the robust optimization approach proposed in [83] is applied to develop robust solutions for the transition to AFVs. A significant advantage of the robust optimization approach used here is that it allows decision makers to adjust the trade-off between optimality and conservatism.

6.2 Sensitivity Analysis

To develop optimal solutions for the optimization models and data discussed in Chapters 3 and 4, one needs to estimate the values of several parameters by relying on historical data and/or making some assumptions. The estimated parameter values, however, may be different from the true values; this disparity might be due to data limitations, biased data, unrealistic assumptions, numerical errors in the estimation process or the nonstationary nature of the data. A common approach to investigate the impact of estimation errors on the optimal solution and the corresponding optimal value is to represent the errors as perturbations to the data in order to perform a sensitivity analysis on the optimal solution [169].

6.2.1 Proposed Methodology

In this section, a sensitivity analysis using Monte Carlo simulation is carried out to find the impact of estimation errors in the parameters of the models developed in Chapter 3. More precisely, given a parameter A in an optimization problem, M perturbations ΔA are generated to represent the estimation errors in the parameter A. It is assumed that the perturbations have independent normal distributions, i.e.,

$$\Delta A = \rho \varepsilon A, \tag{6.1}$$

where parameter $\rho \in (0, 1]$ indicates the size of the relative perturbation and ε is a random parameter, which is assumed to follow a normal distribution with zero mean and unit standard deviation. Throughout this chapter, ρ and M are fixed

at 10% and 1000, respectively; these values were chosen considering a "reasonable" perturbation level of 10%, and 1000 perturbations since satisfactory results are obtained from Monte Carlo simulations for this number. Increasing the number of Monte Carlo simulations beyond 1000 does not yield any significant changes to the final solutions. It is also assumed that only one parameter of the optimization model is perturbed at a time while all other parameters remain at their nominal or expected values.

In this sensitivity analysis, the following three quantities are considered and distinguished [170, 171]:

1. *True optimal value*: It is the value of the objective function (OF) using an unperturbed parameter A at the optimal solution obtained from the unperturbed parameter A; this is denoted by $OF_A\left(X_A\right)$.

2. *Actual optimal value*: It is the value of the objective function using an unperturbed parameter A at the optimal solution obtained from the perturbed parameter $A + \Delta A$; this is denoted by $OF_A\left(X_{A+\Delta A}\right)$.

3. *Estimated optimal value*: It is the value of the objective function using a perturbed parameter $A+\Delta A$ at the optimal solution obtained from the perturbed parameter $A + \Delta A$; this is denoted by $OF_{A+\Delta A}\left(X_{A+\Delta A}\right)$.

In practice, unperturbed or true values of the parameters are unknown to the decision maker at the time of planning; therefore, an optimal solution is obtained from the perturbed or estimated parameters $A + \Delta A$, which are the only available data. During the simulation process, some typical values of the parameters are chosen to represent true values; these assumed true values A are then used to generate perturbations ΔA and to obtain $A + \Delta A$, which represent the estimated value of the parameters. An optimal solution is then found at the estimated parameters, denoted by $X_{A+\Delta A}$. This optimal solution along with the true value of the parameter A, is used to calculate the actual optimal value $OF_A\left(X_{A+\Delta A}\right)$. This actual optimal value determines the performance of the decision made using the estimated

data which is the quantity of interest. Note that the estimated optimal value, i.e., $OF_{A+\Delta A}\left(X_{A+\Delta A}\right)$ might underestimate or overestimate the objective function value and, therefore, is not useful for planning studies.

It is worth mentioning that typical methods used in the literature for sensitivity analysis are valid for small perturbations, allowing to approximately determine the *estimated* optimal value [172, 173]. However, these methods would not be appropriate here to obtain the *actual* optimal value given the larger range of parameter variation considered here.

In order to quantitatively compare the sensitivity of the optimal value to perturbations of different parameters, the following *Average Deviation Index (ADI)* measure is proposed:

$$ADI = \frac{1}{M}\sum_{m=1}^{M}\left|OF_A\left(X_{A+\Delta A_m}\right) - OF_A\left(X_A\right)\right|, \tag{6.2}$$

where $OF_A\left(X_{A+\Delta A_m}\right)$ is the actual optimal value in simulation m. Calculated ADI values for different parameters in each optimization model are ranked to identify the most influential parameters, which are used later in developing the robust counterpart optimization models. The detailed implementation of this method for the previously developed optimization models in Chapter 3 is presented next.

6.2.2 Sensitivity Analysis of the FCV Transition Model

In performing a sensitivity analysis using Monte Carlo simulation of the optimization model for the transition to hydrogen economy, the following assumptions are made:

- *Number of parameters*: In total, 23 single or group parameters are considered which cover the most relevant parameters involved in this optimization model.
- *Type of penetration and transition*: In order to impose a more limiting condition on the electricity grid and the hydrogen transportation network, a uni-

form penetration of FCVs in different zones following the second transition curve is assumed as discussed in Chapter 4 .

- *Hydrogen-related constraints*: To include more realistic construction and operational limits, a 20 MW HPP placement constraint as well as a 4 ton/day limit for transporting hydrogen in each route are in place for all the simulations.

- *Emission constraints for generation*: These are disregarded here because they make the optimization problem much harder to solve, which is certainly an issue when thousands of simulations are required in Monte Carlo simulation approach.

- *Social cost of emissions*: In Chapter 3, the target was to achieve the maximum potential penetration level of AFVs; therefore, the largest reported value for the social cost of emission was used for assigning credit to AFVs in population areas. On the other hand, the value of this parameter, i.e., 125 CAD/ton, considered in this section was chosen as per the following consideration: It should be noted that with regard to typical electricity prices in Ontario, emission costs lower than 125 CAD/ton substantially reduces the potential penetration levels, as shown in Table 6.1. Typical values used for this parameter in the literature for CO_2 emissions are less than 100 CAD/ton; however, the higher 125 CAD/ton value was chosen due to the fact that the environmental benefits of AFVs are not merely limited to the reduction of CO_2 emissions.

  It is also important to highlight that those parameters whose estimation errors are not expected to be larger than 10% are included in the list of uncertain parameters for performing sensitivity analysis or developing the robust models. Since the reported values of the social cost of emissions vary in an extremely wide range and are really unknown in practice, as there is currently no mechansim to precisely price emissions, this parameter is treated here differently from other uncertain parameters; therefore emission costs are

Table 6.1: Optimal uniform FCV penetration for different values of emission costs

Emission cost [CAD/ton]	10	50	75	100	110	125	150	175	200	250	300	400	500	700
FCV penetration [%]	0	0	0	0.06	2.90	2.95	3.02	3.29	3.38	3.79	4.13	4.41	4.43	4.43

not placed in the same category of the other uncertain parameters analyzed in this study.

For this sensitivity analysis, AMPL [117] with a CPLEX [79] solver were used to perform the Monte Carlo simulations and determine the true and actual optimal values; other computational tasks were performed using MATLAB [174]. Also, in order to achieve a high degree of precision, optimality gap was fixed at 0.02% for all the simulations. The results of this analysis for the parameters with non-zero ADIs are depicted in Figures 6.1-6.20; these figures illustrate how the actual optimal value varies with respect to the assumed perturbations in different parameters. The calculated ADI values, together with the ranking of the parameters, are also reflected in Table 6.2. Based on the presented results, annual mileage and fuel economy of fuel cell vehicles are found to be the most influential parameters in this sensitivity analysis. However, hydrogen transfer related parameters have no impact on the optimal solution. This result is expected, since with the chosen value of the social cost of CO_2 emission, hydrogen economy penetration levels are relatively low, which, in turn, requires less hydrogen to be transported between the zones. Also, internal electricity prices in Ontario as well as import and export electricity prices are found to have an average-to-high impact on the optimal solution. Based on these observations and as shown in Table 6.2, all the involved parameters in the optimization model for the transition to hydrogen economy can be classified into three categories based on their relative impact on the optimal solution.

As highlighted in the list of assumptions for the sensitivity analysis, an average 10% deviation for all the parameters is considered. However, given the limitations of the robust optimization technique used here, uncertain parameters such as an-

nual mileage and fuel economy of FCVs which simultaneously appear in multiple constraints and the objective function cannot be handeled by this methodology, hence, to be conservative, the worst-case values of these parameters were used for the robust optimization studies. The most-appealing decision variable in the proposed optimization models for transition to AFVs is the feasibility factor (FF_{iy}), since it translates into penetration levels ($\bar{\mu}_y FF_{iy}$) or total number of AFVs by the end of the planning horizon. To determine the worst-case values for these two parameters, an analysis of their effect on total number of AFVs was performed, as shown in Figures 6.21 and 6.22. From these results, the worst-case value for fuel economy of FCVs is 90% of its nominal or expected value, while the worst-case value of the annual mileage corresponds to 110% of its nominal value. Observe that the other uncertain parameters are basically electricity prices and fuel economy of GVs which only appear on the objective function and can then be studied using the robust optimization method.

6.2.3 Sensitivity Analysis of the PHEV Transition Model

Sensitivity analyses of the optimization model for transition to PHEVs were performed using similar assumptions as employed for the FCV transition model. However, as there are no hydrogen-related parameters and differentiation between weekdays and weekends, 19 sets of parameters were considered in the analysis.

It was observed that the pattern of changes in the actual optimal value with respect to changes in different parameters are very similar to the ones illustrated in Figures 6.3-6.20 for the FCV model. The results of the sensitivity analysis are illustrated in Table 6.3; observe in Table 6.3 that all the parameters in the optimization model for transition to PHEVs are classified into two categories considering their corresponding ADI values and ranking. Based on the discussion in Section 6.2.2 regarding the limitations of the adopted robust optimization approach to handle uncertain parameters, which simultaneously appear in multiple constraints, only electricity prices in the first category are considered here for developing the robust

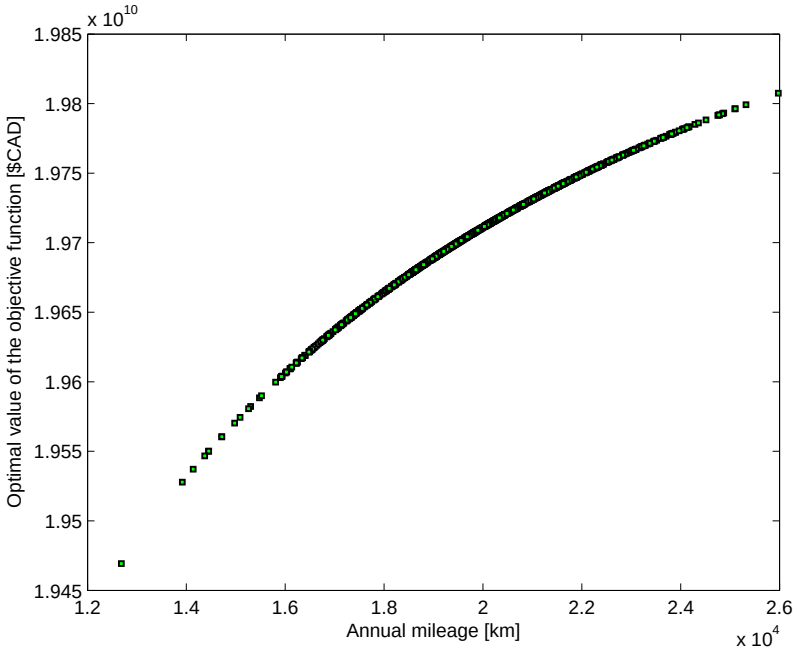

Figure 6.1: Actual optimal value with respect to perturbations in annual mileage.

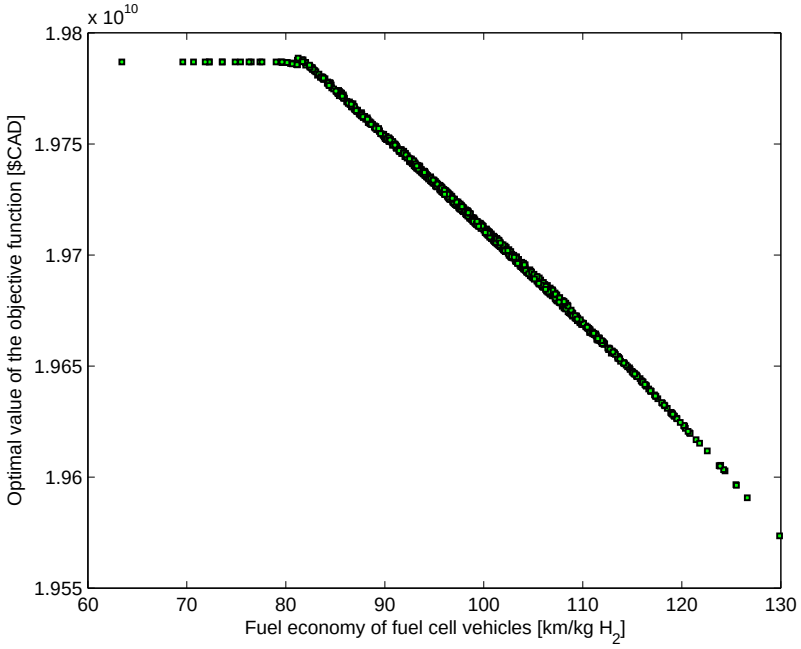

Figure 6.2: Actual optimal value with respect to perturbations in fuel economy of FCVs.

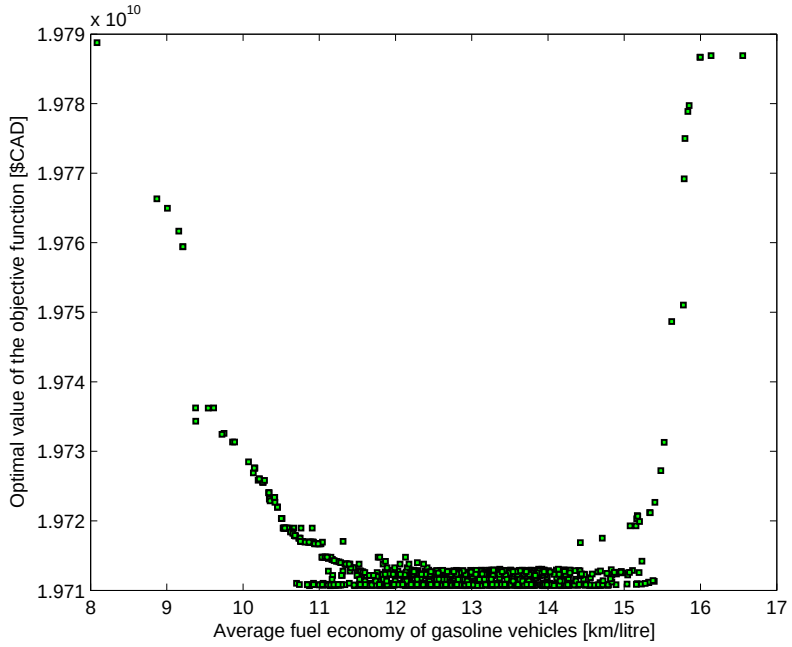

Figure 6.3: Actual optimal value with respect to perturbations in average fuel economy of GVs.

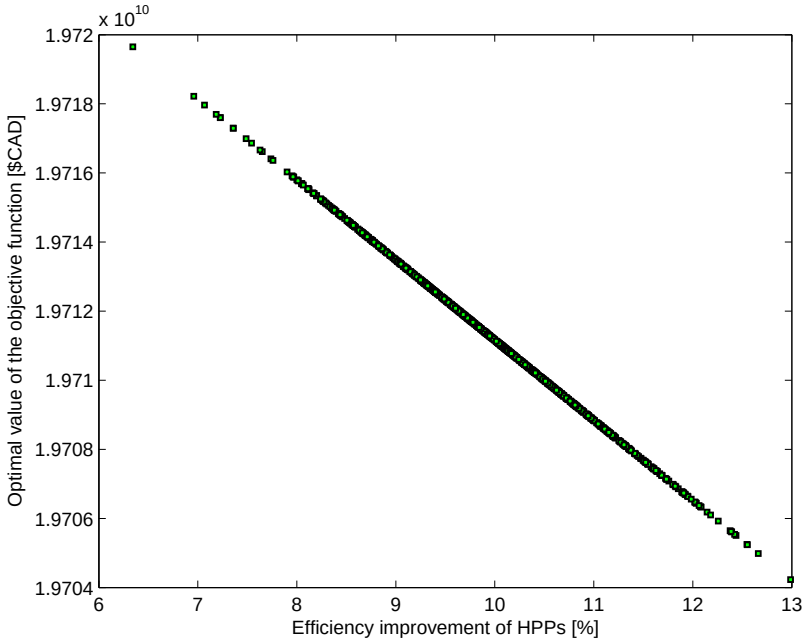

Figure 6.4: Actual optimal value with respect to perturbations in efficiency improvement of HPPs.

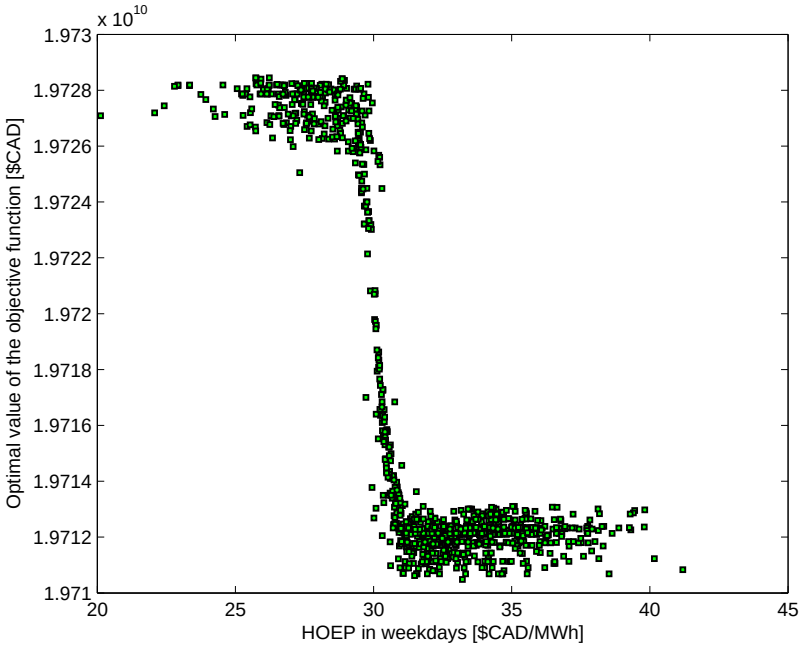

Figure 6.5: Actual optimal value with respect to perturbations in HOEP on weekdays.

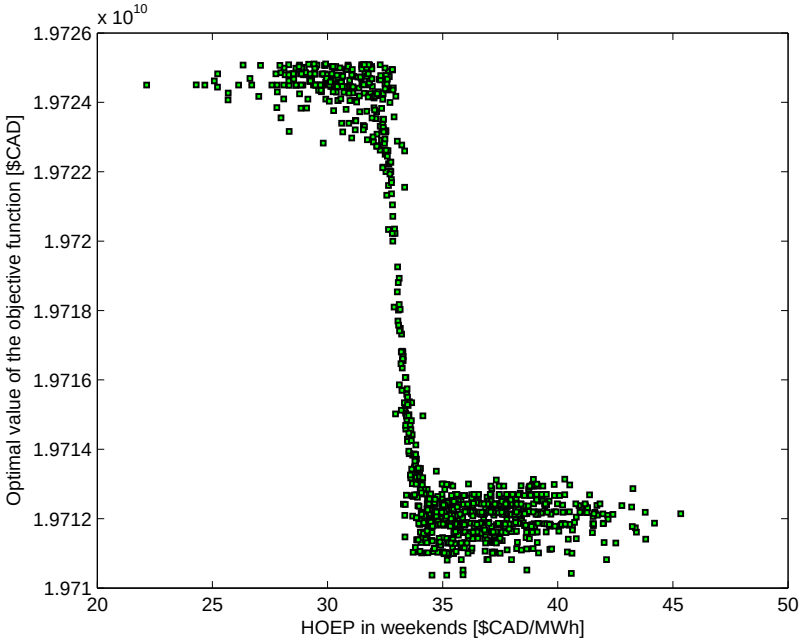

Figure 6.6: Actual optimal value with respect to perturbations in HOEP on weekends.

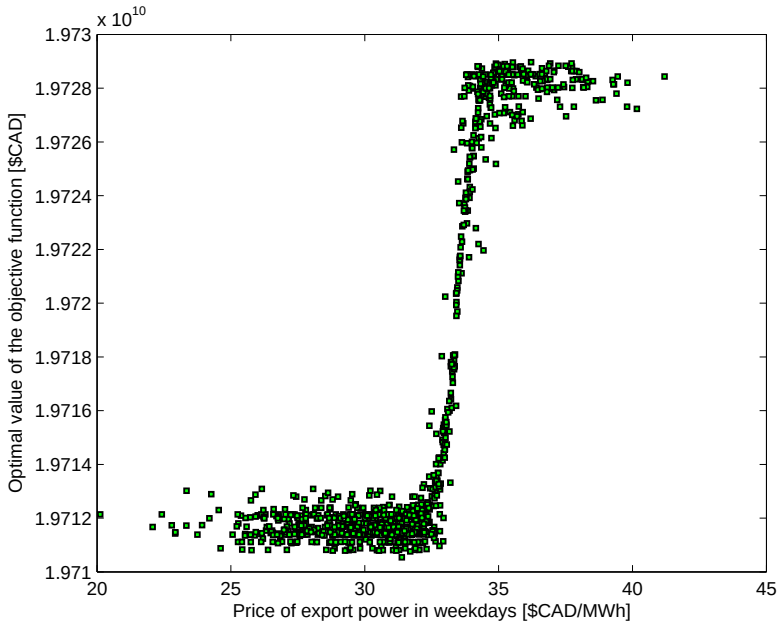

Figure 6.7: Actual optimal value with respect to perturbations in the price of export power on weekdays.

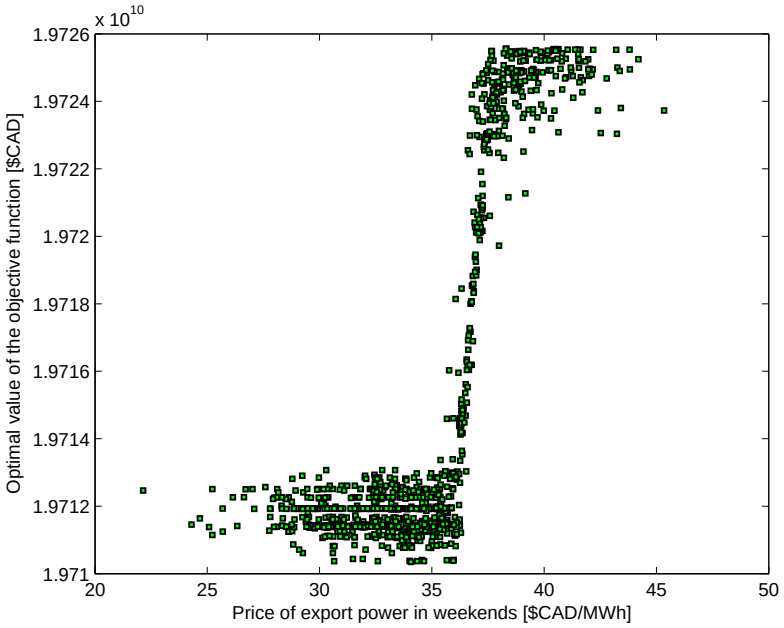

Figure 6.8: Actual optimal value with respect to perturbations in the price of export power on weekends.

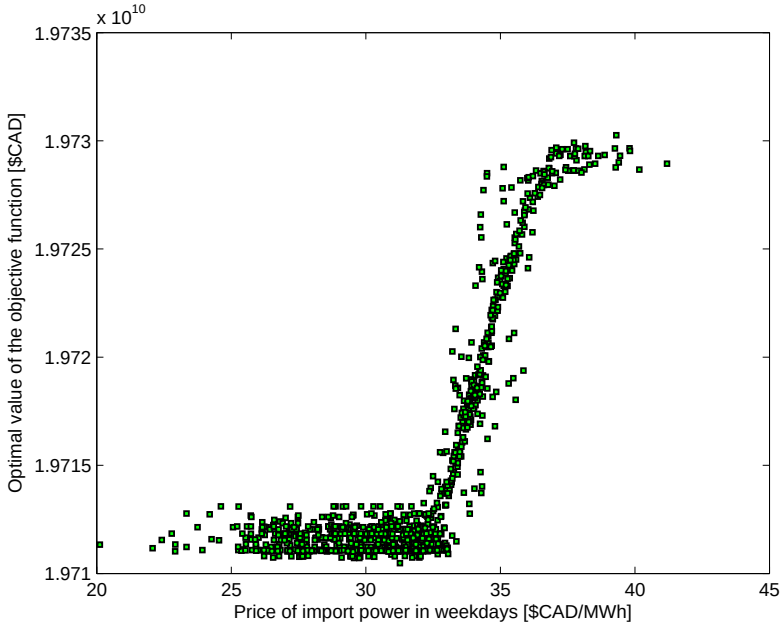

Figure 6.9: Actual optimal value with respect to perturbations in the price of import power on weekdays.

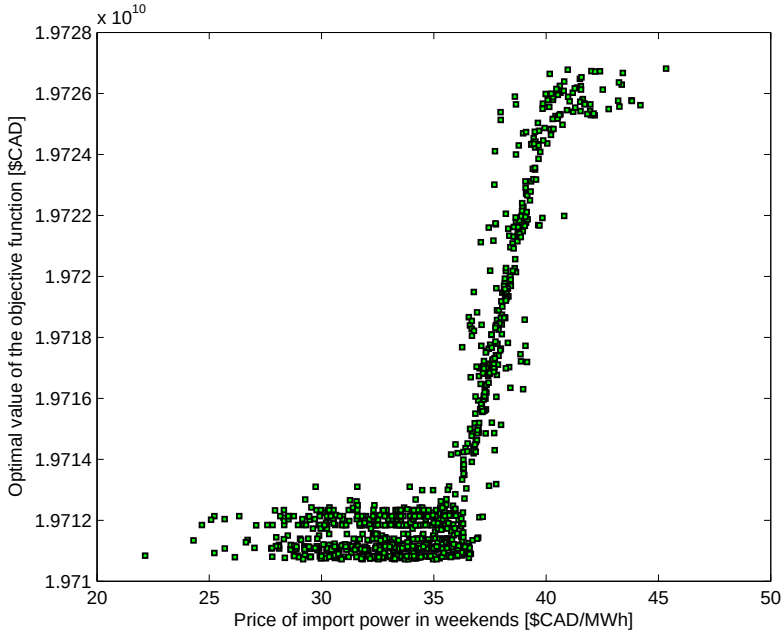

Figure 6.10: Actual optimal value with respect to perturbations in the price of import power on weekends.

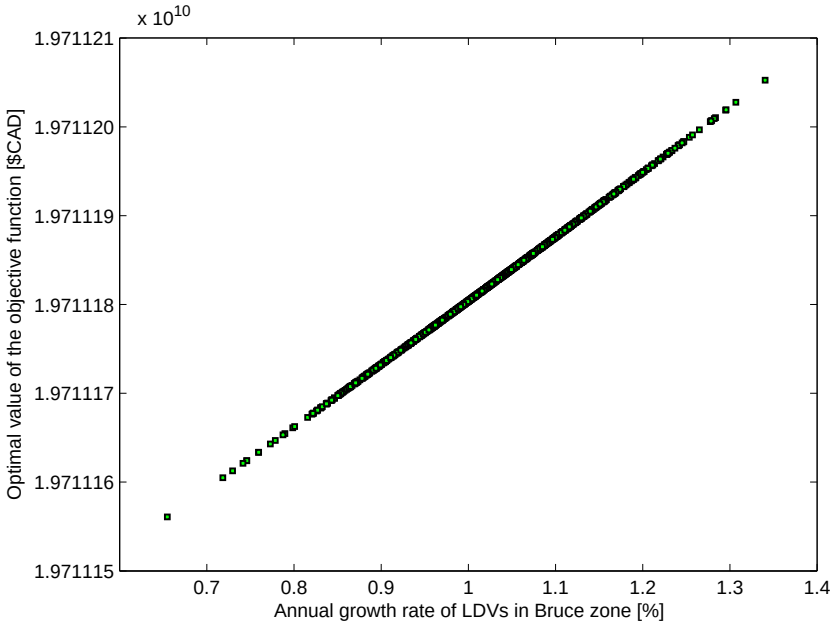

Figure 6.11: Actual optimal value with respect to perturbations in annual growth rate of LVDs in the Bruce zone.

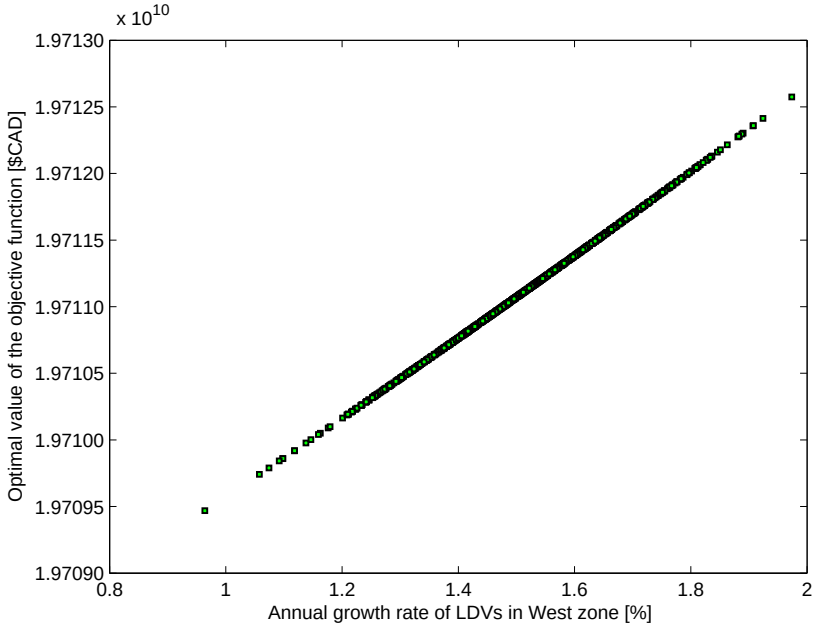

Figure 6.12: Actual optimal value with respect to perturbations in annual growth rate of LVDs in the West zone.

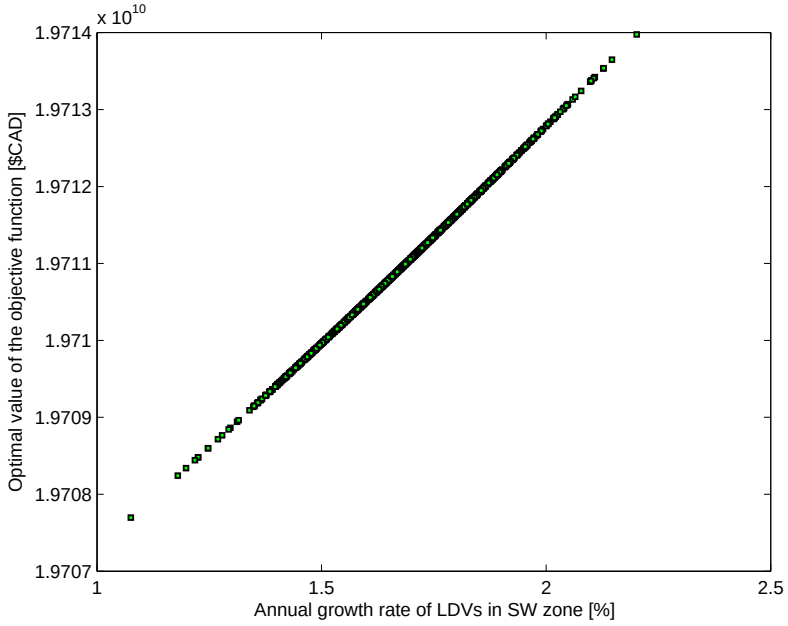

Figure 6.13: Actual optimal value with respect to perturbations in annual growth rate of LVDs in the SW zone.

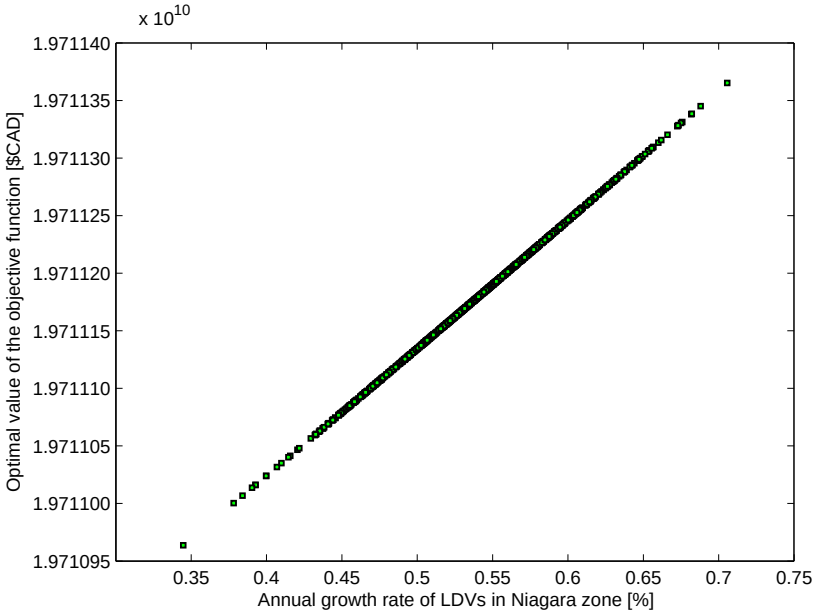

Figure 6.14: Actual optimal value with respect to perturbations in annual growth rate of LVDs in the Niagara zone.

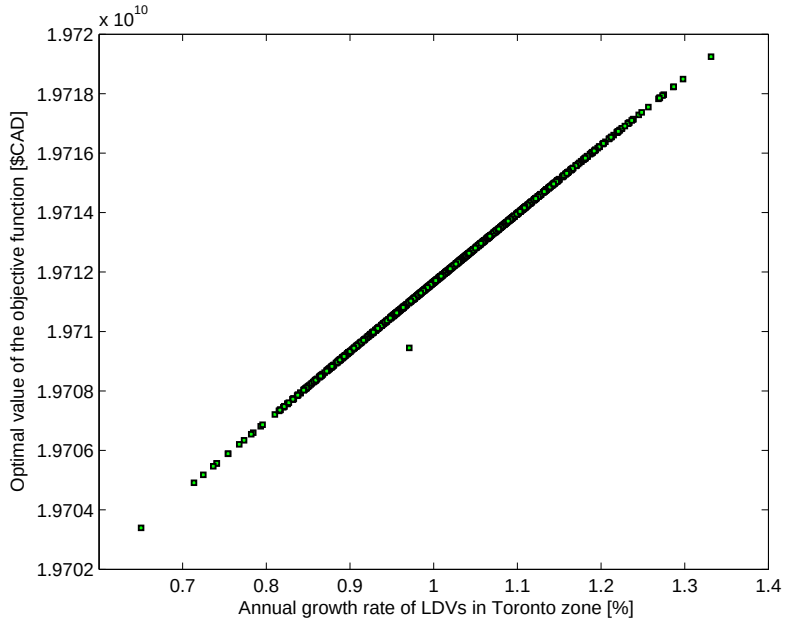

Figure 6.15: Actual optimal value with respect to perturbations in annual growth rate of LVDs in the Toronto zone.

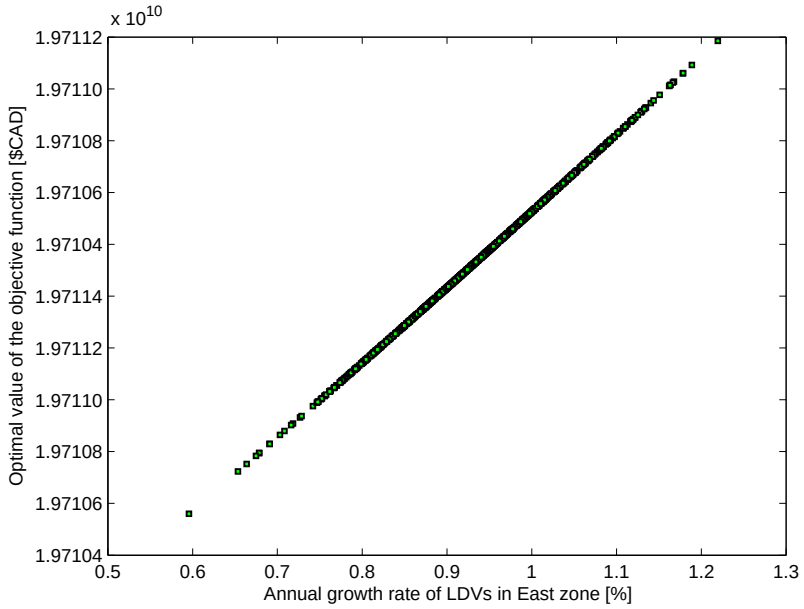

Figure 6.16: Actual optimal value with respect to perturbations in annual growth rate of LVDs in the East zone.

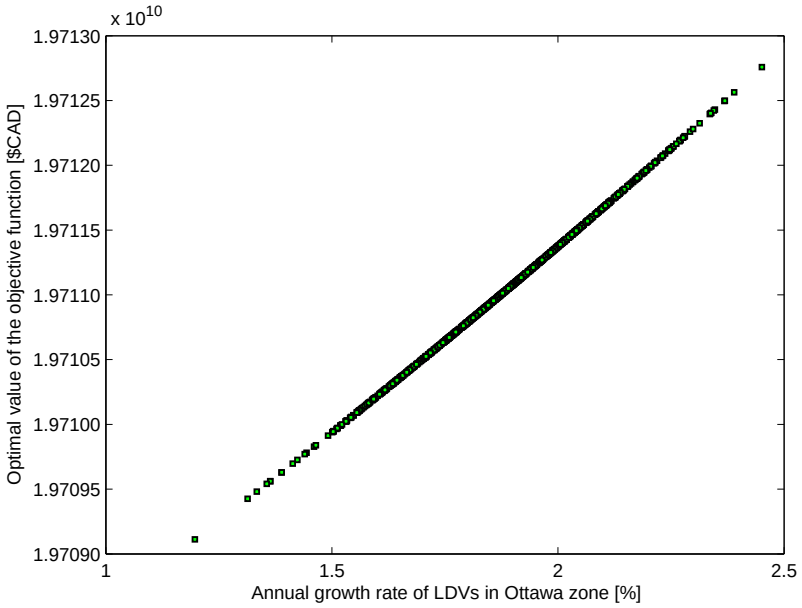

Figure 6.17: Actual optimal value with respect to perturbations in annual growth rate of LVDs in the Ottawa zone.

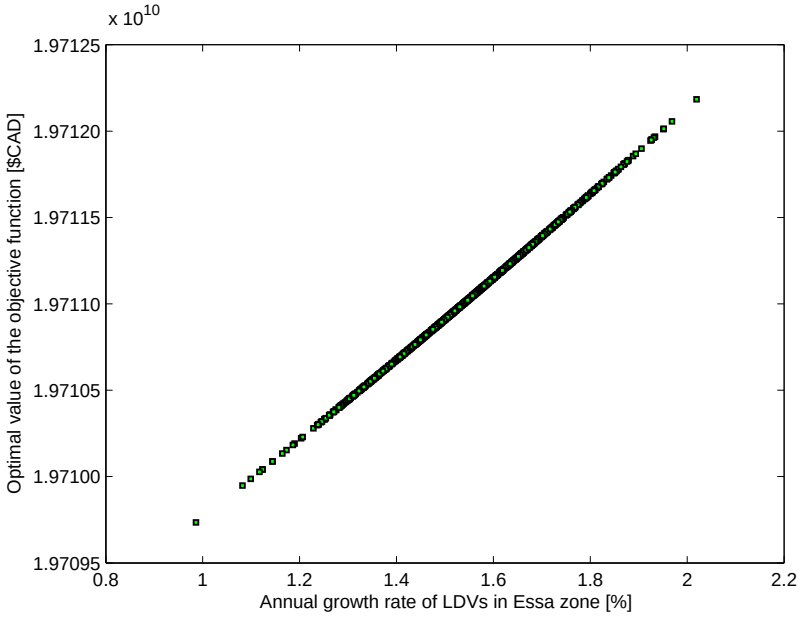

Figure 6.18: Actual optimal value with respect to perturbations in annual growth rate of LVDs in the Essa zone.

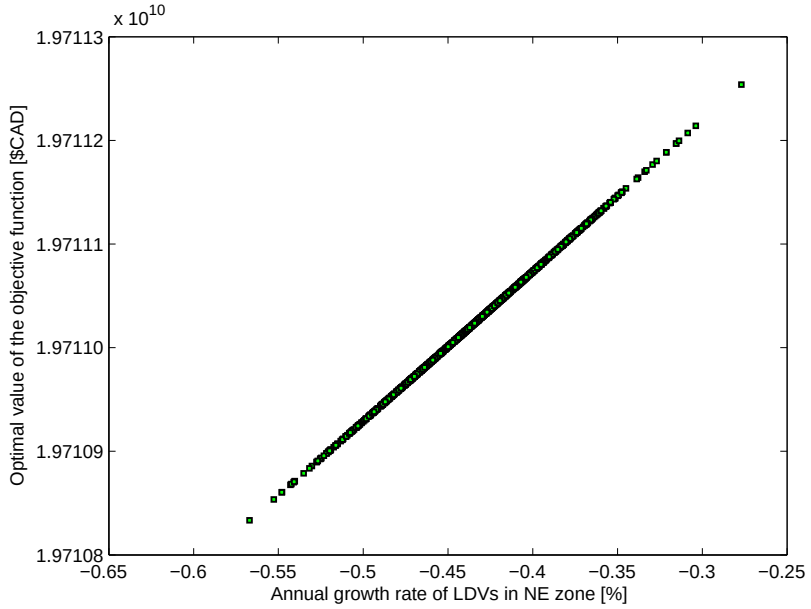

Figure 6.19: Actual optimal value with respect to perturbations in annual growth rate of LVDs in the NE zone.

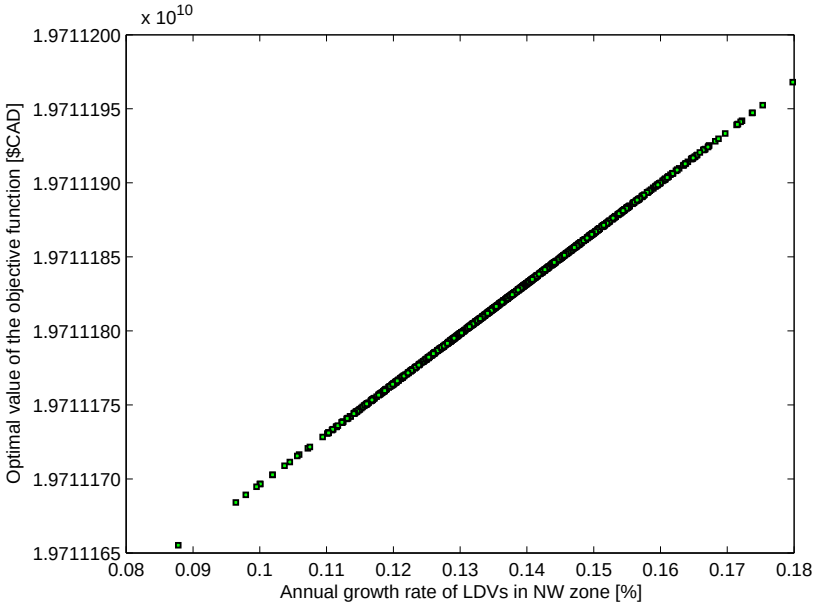

Figure 6.20: Actual optimal value with respect to perturbations in annual growth rate of LVDs in the NW zone.

Table 6.2: Average deviation index of the FCV transition model for different uncertain parameters.

Rank	Uncertain parameter	ADI [CAD]
1	Annual mileage	3.4605e+007
2	Fuel economy of FCVs	3.3263e+007
3	HOEP on weekdays	5.7007e+006
4	Price of export power on weekdays	5.5155e+006
5	HOEP on weekends	4.7217e+006
6	Price of export power on weekends	4.5095e+006
7	Price of import power on weekdays	4.0228e+006
8	Price of import power on weekends	3.2643e+006
9	Average fuel economy of GVs	2.7609e+006
10	Annual growth rate of LDVs in Toronto	2.0736e+006
11	Efficiency improvement of HPPs	1.8587e+006
12	Annual growth rate of LDVs in SW	7.7110e+005
13	Annual growth rate of LDVs in Ottawa	4.5828e+005
14	Annual growth rate of LDVs in West	3.7876e+005
15	Annual growth rate of LDVs in Essa	3.2004e+005
16	Annual growth rate of LDVs in East	2.1949e+005
17	Annual growth rate of LDVs in NE	1.6075e+005
18	Annual growth rate of LDVs in Niagara	4.8479e+004
19	Annual growth rate of LDVs in Bruce	5.9460e+003
20	Annual growth rate of LDVs in NW	3.7698e+003
21	Average operating cost of hydrogen transfer	0
22	Capital cost of tube trailer	0
23	Capital cost of cab	0

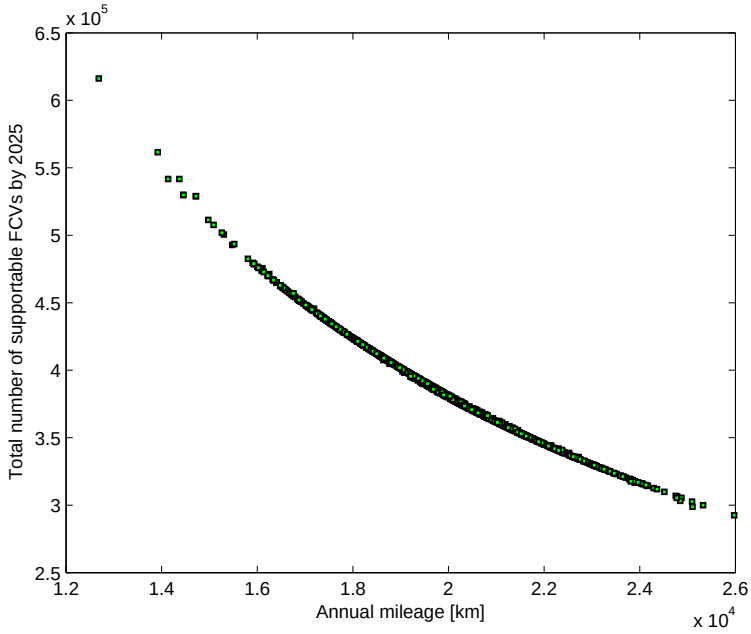

Figure 6.21: Total number of FCVs with respect to annual mileage.

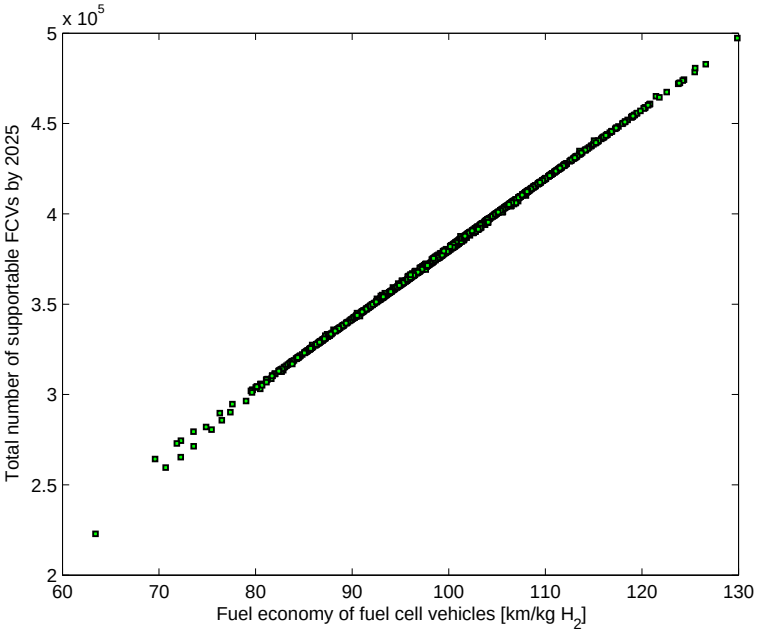

Figure 6.22: Total number of FCVs with respect to fuel economy of fuel cell vehicles.

Table 6.3: Average deviation index of the PHEV transition model for different uncertain parameters.

Rank	Uncertain parameter	ADI [CAD]
1	Price of export power	5.0598e+006
2	HOEP	5.0523e+006
3	Annual growth rate of LDVs in Toronto	3.3158e+006
4	Price of import power	2.4700e+006
5	Annual growth rate of LDVs in SW	2.2047e+006
6	Annual growth rate of LDVs in Ottawa	1.4607e+006
7	Annual growth rate of LDVs in West	1.0384e+006
8	Annual growth rate of LDVs in Essa	8.6978e+005
9	Annual growth rate of LDVs in East	3.2441e+005
10	Annual growth rate of LDVs in NE	1.4591e+005
11	Annual growth rate of LDVs in Niagara	1.4146e+005
12	Annual growth rate of LDVs in Bruce	1.4817e+004
13	Annual growth rate of LDVs in NW	1.1417e+004
14	Average fuel economy of GVs (compact sedan)	0
15	Average fuel economy of GVs (mid-size sedan)	0
16	Average fuel economy of GVs (mid-size SUV)	0
17	Average fuel economy of GVs (full-size SUV)	0
18	Average fuel economy of GVs (van)	0
19	Average fuel economy of GVs (pick-up truck	0

counterpart problem for the PHEV transition model. This assumption can be further justified based on the fact that, in practice, electricity prices are subject to more fluctuations and their forecasting is significantly more challenging compared to other parameters such as annual growth rates of LDVs.

6.3 Robust Optimization Models

This section presents the robust optimization models for the transition to AFVs which are robust with respect to uncertainty in the parameters identified in previous

section. These models are based on the method discussed in Chapter 2 which is capable of adjusting the degree of conservatism. These robust models are developed separately for the transition to FCVs and PHEVs, as discussed in the following sections.

6.3.1 Robust Model for the Transition to FCVs

The optimization problem for the transition to FCVs which was developed and discussed in Chapter 3 can be generally represented as:

$$\begin{aligned} \min \quad & \mathbf{c}'\mathbf{x} \\ \text{s.t.} \quad & \mathbf{A}\mathbf{x} \geq \mathbf{b}, \\ & x \in X, \end{aligned} \tag{6.3}$$

where X includes all mixed integer solutions and the cost vector $\mathbf{c}$ is subject to uncertainty. In order to comply with the robust optimization method, which was discussed in Chapter 2, this problem can be represented as follows, where all the uncertain parameters are in the constraints:

$$\begin{aligned} \min \quad & W \\ \text{s.t.} \quad & W - \mathbf{c}'\mathbf{x} \geq 0, \\ & \mathbf{A}\mathbf{x} \geq \mathbf{b}, \\ & x \in X. \end{aligned} \tag{6.4}$$

For the three sets of electricity prices (internal, import, and export), two time periods (ω_1 and ω_2), one set of fuel economy values for GVs and a planning span of 18 years, problem (6.4) presents 126 uncertain parameters as follows:

$$0.9\widehat{\pi}_y^\tau \leq \widetilde{\pi}_y^\tau \leq 1.1\widehat{\pi}_y^\tau, \quad \Delta\pi_y^\tau = 0.1\widehat{\pi}_y^\tau, \quad \forall y \in Y \wedge \tau \in \Psi \tag{6.5}$$

$$0.9\widehat{\pi}_{m_y}^\tau \leq \widetilde{\pi}_{m_y}^\tau \leq 1.1\widehat{\pi}_{m_y}^\tau, \quad \Delta\pi_{m_y}^\tau = 0.1\widehat{\pi}_{m_y}^\tau, \quad \forall y \in Y \wedge \tau \in \Psi \tag{6.6}$$

$$0.9\widehat{\pi}^{\tau}_{x_y} \leq \widetilde{\pi}^{\tau}_{x_y} \leq 1.1\widehat{\pi}^{\tau}_{x_y}, \quad \Delta\pi^{\tau}_{x_y} = 0.1\widehat{\pi}^{\tau}_{x_y}, \quad \forall y \in Y \wedge \tau \in \Psi \tag{6.7}$$

$$0.9\widehat{FEgv}_y \leq \widetilde{FEgv}_y \leq 1.1\widehat{FEgv}_y, \quad \Delta FEgv_y = 0.1\widehat{FEgv}_y, \quad \forall y \in Y \tag{6.8}$$

where $\widehat{\ }$ and Δ are used to represent nominal values and deviation magnitudes, respectively. Note that in the FCV transition model, disregarding the different types of LDVs, it is assumed that the FCV is replaced by a representative gasoline-powered vehicle with an average fuel economy of $FEgv_y$ as discussed in Section 4.6.2. By defining $EFgv_y = 1/FEgv_y$, constraints in (6.8) can be represented as follows:

$$\frac{1}{1.1\widehat{FEgv}_y} \leq \widetilde{EFgv}_y \leq \frac{1}{0.9\widehat{FEgv}_y}, \quad \Delta EFgv_y \simeq \frac{0.1}{\widehat{FEgv}_y}, \quad \forall y \in Y \tag{6.9}$$

so that (3.22) is linear with regard to this parameter.

In order to develop the robust counterpart problem of (6.4) based on the method discussed in Chapter 2, the following additional variables should be defined:

$$\begin{aligned} & p_e \geq 0, \forall e \in E, \\ & q_{ev} \geq 0, \forall e \in E \wedge v \in V_e, \\ & r_v \geq 0, \forall v \in V, \end{aligned} \tag{6.10}$$

where $E = \{1\}$ and $V_1 = V = \{1, ..., 126\}$ as all the 126 uncertain parameters are in a single constraint. Therefore, the following constraints should be added to the optimization model for the transition to FCVs in Chapter 3:

$$\begin{aligned} W - \sum_{y \in Y} \frac{1}{(1+DR)^{y-y_1}} \Bigg\{ \sum_{i \in Z} \Big\{ & (P^{\omega_1}_{g_{iy}} \widehat{\pi}^{\omega_1}_{y} + P^{\omega_1}_{m_{iy}} \widehat{\pi}^{\omega_1}_{m_y} - P^{\omega_1}_{x_{iy}} \widehat{\pi}^{\omega_1}_{x_y}) \times 8 \times 261 \\ & + (P^{\omega_2}_{g_{iy}} \widehat{\pi}^{\omega_2}_{y} + P^{\omega_2}_{m_{iy}} \widehat{\pi}^{\omega_2}_{m_y} - P^{\omega_2}_{x_{iy}} \widehat{\pi}^{\omega_2}_{x_y}) \times 14 \times 104 \\ & - FF_{iy}.\bar{\mu}_y.Nldv_{iy}.AM.SC_{CO_2}p.Eco_2 \times 10^{-3}/\widehat{FEgv}_y \\ & + \left\{ \begin{array}{c} ER_{chp_i} \left[V^{\omega_1}_{2_{iy}} - K^{\omega_1}_{2_{iy}} \overline{Pga}_{iy} + K^{\omega_1}_{3_{iy}} (\overline{Pgb}_{iy} - \overline{Pga}_{iy}) \right] \\ + ER_{coal_i} (V^{\omega_1}_{3_{iy}} - K^{\omega_1}_{3_{iy}} \overline{Pgb}_{iy}) \end{array} \right\} SC_{CO_2} g \times 8 \times 261 \end{aligned}$$

$$+\left\{\begin{array}{c} ER_{chp_i}\left[V_{2_{iy}}^{\omega_2}-K_{2_{iy}}^{\omega_2}\overline{Pga}_{iy}+K_{3_{iy}}^{\omega_2}(\overline{Pgb}_{iy}-\overline{Pga}_{iy})\right] \\ +ER_{coal_i}(V_{3_{iy}}^{\omega_2}-K_{3_{iy}}^{\omega_2}\overline{Pgb}_{iy}) \end{array}\right\} SC_{CO_2}g\times 14\times 104\ \Big\}$$

$$+PC_y.CCcab(1-Scab_y)+PT_y.CCtube(1-Stube_y)+\sum_{(i,j)\in Z^*}2OC_y.d_{ij}.N_{ijy}\times 365\ \Big\}$$

$$-\Gamma_1 p_1-\sum_{v\in V}q_{1v}\geq 0 \tag{6.11}$$

$$p_1+q_{1v}\geq \Delta a_{1v}r_v,\quad \forall v\in V=V_1=\{1,...,126\}, \tag{6.12}$$

where the deviations of the uncertain parameters are determined to be as follows:

$$\Delta a_{1v}=\begin{cases} \frac{8\times 261}{(1+DR)^{v-1}}\Delta\pi_{y_1+v-1}^{\omega_1}: & \forall v\in\{1,...,18\}, \\ \frac{14\times 104}{(1+DR)^{v-19}}\Delta\pi_{y_1+v-19}^{\omega_2}: & \forall v\in\{19,...,36\}, \\ \frac{8\times 261}{(1+DR)^{v-37}}\Delta\pi_{m_{y_1+v-37}}^{\omega_1}: & \forall v\in\{37,...,54\}, \\ \frac{14\times 104}{(1+DR)^{v-55}}\Delta\pi_{m_{y_1+v-55}}^{\omega_2}: & \forall v\in\{55,...,72\}, \\ \frac{8\times 261}{(1+DR)^{v-73}}\Delta\pi_{x_{y_1+v-73}}^{\omega_1}: & \forall v\in\{73,...,90\}, \\ \frac{14\times 104}{(1+DR)^{v-91}}\Delta\pi_{x_{y_1+v-91}}^{\omega_2}: & \forall v\in\{91,...,108\}, \\ \frac{\bar{\mu}_{y_1+v-109}.AM.SC_{CO_2}p.E_{CO_2}\times 10^{-3}}{(1+DR)^{v-109}}\Delta EFgv_{y_1+v-109}: & \forall v\in\{109,...,126\}. \end{cases}$$

$$-r_v\leq\sum_{i\in Z}P_{g_{i,y_1+v-1}}^{\omega_1}\leq r_v,\quad \forall v\in\{1,...,18\} \tag{6.13}$$

$$-r_v\leq\sum_{i\in Z}P_{g_{i,y_1+v-19}}^{\omega_2}\leq r_v,\quad \forall v\in\{19,...,36\} \tag{6.14}$$

$$-r_v\leq\sum_{i\in Z}P_{m_{i,y_1+v-37}}^{\omega_1}\leq r_v,\quad \forall v\in\{37,...,54\} \tag{6.15}$$

$$-r_v \leq \sum_{i \in Z} P^{\omega_2}_{m_{i,y_1+v-55}} \leq r_v, \quad \forall v \in \{55, ..., 72\} \tag{6.16}$$

$$-r_v \leq \sum_{i \in Z} P^{\omega_1}_{x_{i,y_1+v-73}} \leq r_v, \quad \forall v \in \{73, ..., 90\} \tag{6.17}$$

$$-r_v \leq \sum_{i \in Z} P^{\omega_2}_{x_{i,y_1+v-91}} \leq r_v, \quad \forall v \in \{91, ..., 108\} \tag{6.18}$$

$$-r_v \leq \sum_{i \in Z} (Nldv_{i,y_1+v-109}.FF_{i,y_1+v-109}) \leq r_v, \quad \forall v \in \{109, ..., 126\} \tag{6.19}$$

6.3.2 Robust Model for Transition to PHEVs

Based on the discussions in Section 6.2.3, the robustness of the PHEV transition model is investigated here with respect to perturbations in electricity prices. As HOEP, export and import electricity prices are defined for each individual year of the planning span, there are in total 54 parameters whose uncertainties can significantly influence the optimal value. These parameters can be expressed as follows:

$$0.9\widehat{\pi}^{\omega}_{y} \leq \widetilde{\pi}^{\omega}_{y} \leq 1.1\widehat{\pi}^{\omega}_{y}, \quad \Delta\pi^{\omega}_{y} = 0.1\widehat{\pi}^{\omega}_{y}, \quad \forall y \in Y \tag{6.20}$$

$$0.9\widehat{\pi}^{\omega}_{m_y} \leq \widetilde{\pi}^{\omega}_{m_y} \leq 1.1\widehat{\pi}^{\omega}_{m_y}, \quad \Delta\pi^{\omega}_{m_y} = 0.1\widehat{\pi}^{\omega}_{m_y}, \quad \forall y \in Y \tag{6.21}$$

$$0.9\widehat{\pi}^{\omega}_{x_y} \leq \widetilde{\pi}^{\omega}_{x_y} \leq 1.1\widehat{\pi}^{\omega}_{x_y}, \quad \Delta\pi^{\omega}_{x_y} = 0.1\widehat{\pi}^{\omega}_{x_y}, \quad \forall y \in Y \tag{6.22}$$

In this case, based on (6.4), the following constraints should be added to those of the PHEV transition model in Chapter 3:

$$\begin{aligned} W - \sum_{y \in Y} \frac{1}{(1+DR)^{y-y_1}} \Bigg\{ \sum_{i \in Z} \Big\{ & (P^{\omega}_{g_{iy}} \widehat{\pi}^{\omega}_{y} + P^{\omega}_{m_{iy}} \widehat{\pi}^{\omega}_{m_y} - P^{\omega}_{x_{iy}} \widehat{\pi}^{\omega}_{x_y}) \times 8 \times 365 \\ & - FF_{iy}.\bar{\mu}_y.Nldv_{iy}.DT.SC_{CO_2}p.Eco_2 \times 0.365 \sum_{c \in VT} \left(\frac{VS_c}{FEgv_{cy}} \right) \\ & + \left\{ \begin{array}{c} ER_{chp_i} \left[V^{\omega}_{2_{iy}} - K^{\omega}_{2_{iy}} \overline{Pga}_{iy} + K^{\omega}_{3_{iy}} (\overline{Pgb}_{iy} - \overline{Pga}_{iy}) \right] \\ + ER_{coal_i} (V^{\omega}_{3_{iy}} - K^{\omega}_{3_{iy}} \overline{Pgb}_{iy}) \end{array} \right\} SC_{CO_2}g \times 8 \times 365 \Big\} \Bigg\} \end{aligned}$$

$$-\Gamma_1 p_1 - \sum_{v \in V} q_{1v} \geq 0 \tag{6.23}$$

$$p_1 + q_{1v} \geq \Delta a_{1v} r_v, \quad \forall v \in V = V_1 = \{1, ..., 54\}, \tag{6.24}$$

where the deviations of the uncertain parameters are determined to be as follows:

$$\Delta a_{1v} = \begin{cases} \frac{8\times365}{(1+DR)^{v-1}} \Delta\pi^{\omega}_{y_1+v-1} : & \forall v \in \{1, ..., 18\}, \\ \frac{8\times365}{(1+DR)^{v-19}} \Delta\pi^{\omega}_{m_{y_1+v-19}} : & \forall v \in \{19, ..., 36\}, \\ \frac{8\times365}{(1+DR)^{v-37}} \Delta\pi^{\omega}_{x_{y_1+v-37}} : & \forall v \in \{37, ..., 54\}. \end{cases}$$

$$-r_v \leq \sum_{i \in Z} P^{\omega}_{g_{i,y_1+v-1}} \leq r_v, \quad \forall v \in \{1, ..., 18\} \tag{6.25}$$

$$-r_v \leq \sum_{i \in Z} P^{\omega}_{m_{i,y_1+v-19}} \leq r_v, \quad \forall v \in \{19, ..., 36\} \tag{6.26}$$

$$-r_v \leq \sum_{i \in Z} P^{\omega}_{x_{i,y_1+v-37}} \leq r_v, \quad \forall v \in \{37, ..., 54\} \tag{6.27}$$

6.3.3 Robust Optimization Results and Discussion

The robust models developed for the transition to both FCVs and PHEVs were formulated using AMPL [117] modeling language and solved with CPLEX [79] with 0.02% optimality gap, on an IBM eServer xSeries 460 with 8 Intel Xeon 2.8 GHz processors and 3 GB (effective) of RAM. This section presents and discusses numerical results, which are obtained using the same assumptions made for the sensitivity analysis in Section 6.2. For the assumed social cost of emissions of 125 CAD/ton in the population area, the corresponding emission cost of generation is 10 CAD/ton; this value is used in the emission constraints for generation in the models. Note that in this case there is no need to neglect emission constraints for generation due to computational restrictions as in the case of Monte Carlo simulation analysis. This allows to analyze the effect of emission constraints for

generation in the robust optimization results, as shown next.

Robust Results for Transition to FCVs

The performance of the robust solution as a function of the protection level (Γ) is illustrated in Figure 6.23, which demonstrates how optimality is affected as the budget of uncertainty or protection level of the constraint with uncertain parameters increases. The trade-off between optimality and robustness is also illustrated in Figure 6.24; observe that lower losses of optimality correspond to higher probabilities of constraint violation, as expected. Note that by allowing an 8% loss of optimality, it is possible to make the probability of constraint violation less than 1% when emission constraints for generation are considered. It is also interesting to note that the impact of emission constraints for generation becomes more conspicuous for lower violation probabilities. Hence, for a certain low level of violation probability (e.g., less than 5%), the loss of optimality is lower if emission constraints for generation are considered.

Samples of the objective function values and the probability bounds of constraint violation are presented in Table 6.4. Observe that under zero ($\Gamma = 0$) and under full protection ($\Gamma = 126$) of the constraint with uncertain parameters, the optimal value is increased by 0.21% and 10.42%, respectively; hence reducing the chance of constraint violation to zero can be realized at the cost of losing 10.21% optimality. If the decision maker accepts a maximum of 4.53% chance of constraint violation, the budget of uncertainty must be at least 20, i.e., it is sufficient to protect the constraint against only 16% of the uncertain parameters taking their worst-case values at the same time.

It is interesting to note that even setting the budget of uncertainty at $\Gamma = 20$, i.e., assuming 20 out of 126 uncertain parameters take their worst-case values at the same time, results in a significantly low value of violation probability (4.53%) or a high probability of constraint protection against uncertainty (95.47%). In this case, the optimal value is increased by 6.98% but there is very little effect on the

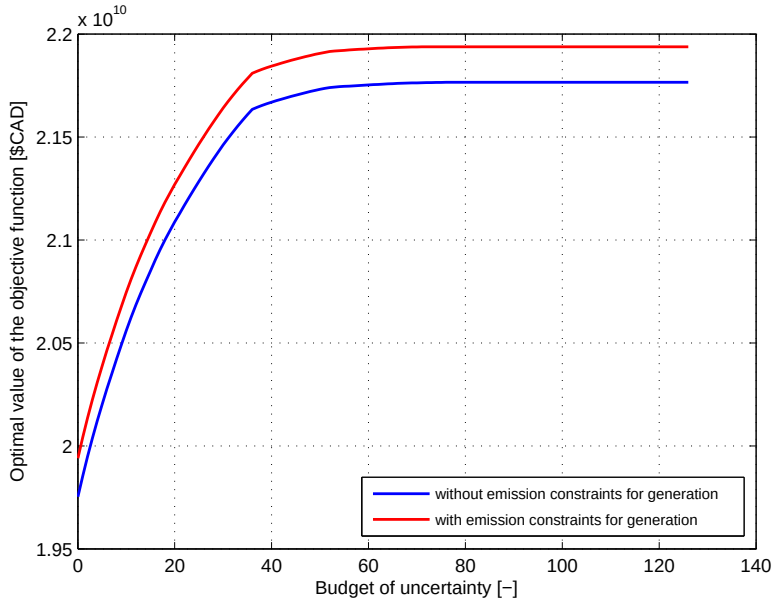

Figure 6.23: Impact of the budget of uncertainty Γ on the optimal value of the robust FCV transition model.

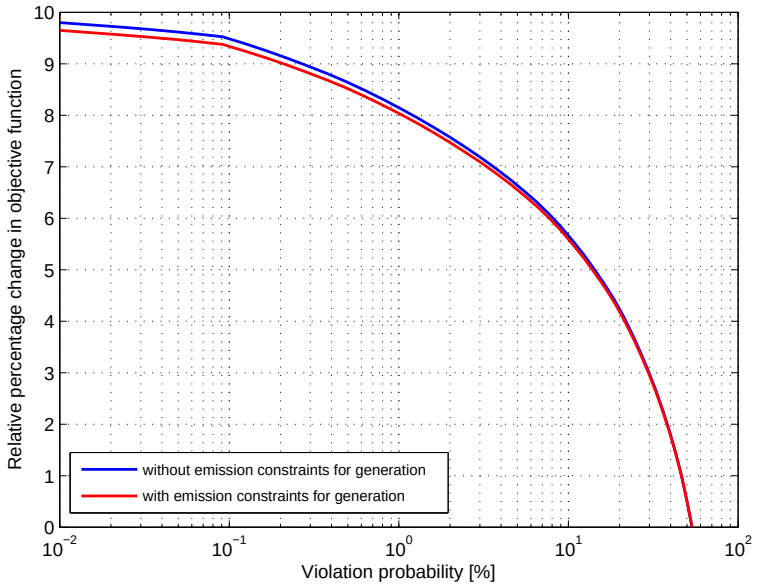

Figure 6.24: Relative change in optimal value of the robust FCV transition model with respect to the probability bound of constraint violation.

Table 6.4: Sample results of deterministic and robust FCV transition models disregarding emission constraints for generation. (DM: deterministic model; RM: robust model.)

	Γ [-]	Violation probability [%]	Optimal value [CAD]	Change [%]	Uniform penetration [%]	# of FCVs by 2025
DM	-	-	19,711,182,690	0	2.95	253,799
RM	0	53.55	19,752,896,295	0.21	2.41	207,654
	10	21.13	20,560,656,476	4.31	2.41	207,654
	20	4.53	21,087,436,480	6.98	2.41	207,654
	30	0.49	21,462,267,255	8.88	2.39	205,776
	40	0.03	21,669,378,711	9.93	1.22	104,948
	50	6.3484e-004	21,731,799,724	10.25	1.22	104,948
	60	7.3556e-006	21,753,277,418	10.36	0.76	65,649
	70	3.9479e-008	21,763,392,764	10.41	0.30	25,899
	126	0	21,766,013,701	10.42	0	0

Table 6.5: Sample results of deterministic and robust FCV transition models including emission constraints for generation.

	Γ [-]	Violation probability [%]	Optimal value [CAD]	Change [%]	Uniform penetration [%]	# of FCVs by 2025
DM	-	-	19,898,614,370	0	2.95	253,799
RM	0	53.55	19,939,908,389	0.21	2.05	176,795
	10	21.13	20,746,054,029	4.26	2.05	176,795
	20	4.53	21,269,710,333	6.89	2.05	176,795
	30	0.49	21,641,324,147	8.76	1.21	104,155
	40	0.03	21,844,474,815	9.78	0	0
	50	6.3484e-004	21,906,895,830	10.09	0	0
	60	7.3556e-006	21,928,751,579	10.20	0	0
	70	3.9479e-008	21,937,865,105	10.25	0	0
	126	0	21,938,722,324	10.25	0	0

FCV penetration level and the corresponding number of FCVs, since it results in uniform FCV penetration of 2.39%, and an optimal number of FCVs by the end of the planning horizon in all of Ontario of 207,654.

Table 6.5 presents similar results for the case of considering emission constraints

for generation. Observe that setting the budget of uncertainty at Γ=20 results in a reasonable trade-off between optimality and conservatism, since it does not affect significantly the optimal penetration level and the corresponding number of FCVs, while the constraint with uncertain parameters is protected with the probability of 95.47% at the cost of losing 6.89% of optimality. In this case, the optimal uniform FCV penetration and the optimal number of FCVs by 2025 in all of Ontario will be equal to 2.05% and 176,795, respectively. These figures represent almost 50% of the Ontario's maximum grid potential as obtained and discussed in Chapter 5, reflecting the effect of uncertainty.

It should also be noted that for an extremely large number of uncertain parameters, the theoretical violation probability for Γ=0 must be equal to 50%; the slightly higher values in the first rows of Tables 6.4 and 6.5 are due to relatively limited number of uncertain parameters.

Robust Results for Transition to PHEVs

Robust optimization results for the transition to PHEVs are illustrated in Figures 6.25 and 6.26. Observe in Figure 6.25 that increasing the protection level above $\Gamma = 30$ has negligible impact on loss of optimality, showing that almost 56% of the uncertain parameters in the PHEV transition model are highly influential on the optimal solution. Based on Figure 6.26, it can be concluded that the PHEV model compared to the FCV model is more susceptible to the loss of optimality for a certain level of violation probability. In other words, if the constraint is to be protected against uncertainty with a certain probability, the decision maker should accept more losses of optimality for the PHEV model.

Sample results of the PHEV robust model are reflected in Tables 6.6 and 6.7. Observe that, in spite of the loss of optimality with the increase of the budget of uncertainty, uniform PHEV penetration and, consequently, total number of PHEVs by 2025 is not impacted by the constraint protection level.

It is interesting to investigate whether the uniform PHEV penetrations remain

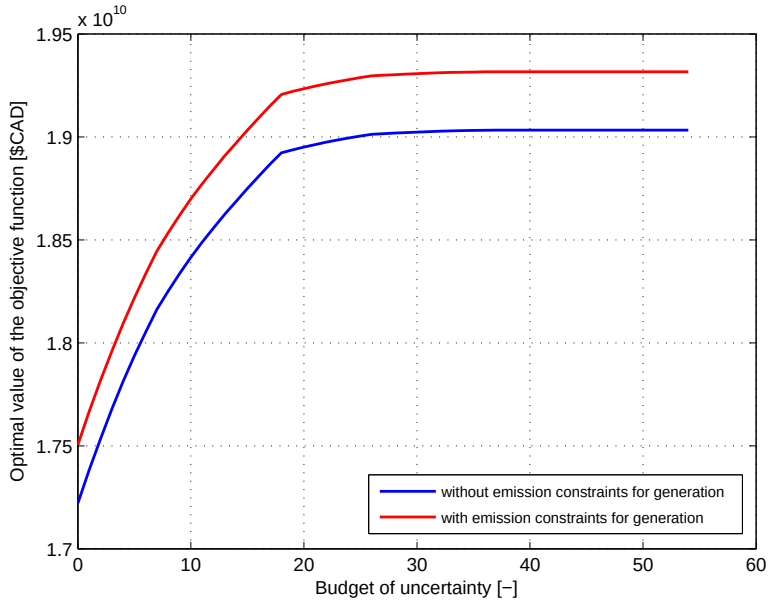

Figure 6.25: Impact of the budget of uncertainty Γ on the optimal value of the robust PHEVs transition model.

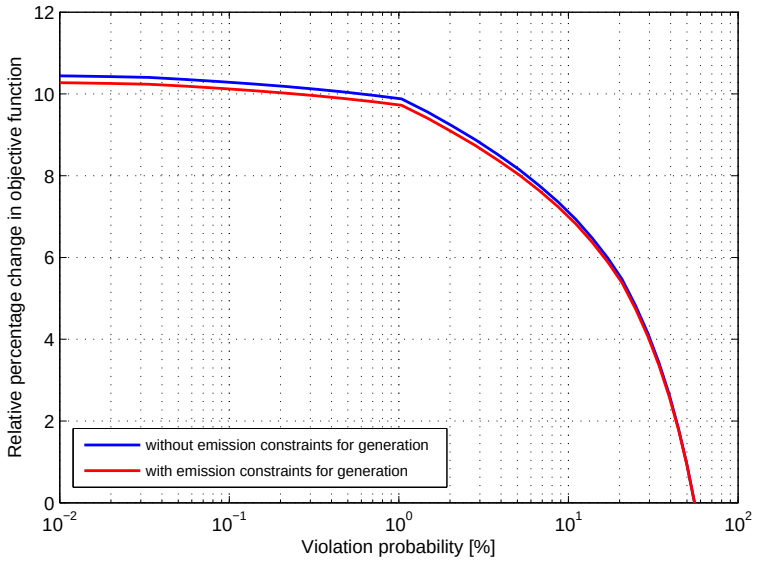

Figure 6.26: Relative change in optimal value of the robust PHEV transition model with respect to the probability bound of constraint violation.

Table 6.6: Sample results of deterministic and robust PHEV transition models disregarding emission constraints for generation. (DM: deterministic model; RM: robust model.)

	Γ [-]	Violation probability [%]	Optimal value [CAD]	Change [%]	Uniform penetration [%]	# of PHEVs by 2025
DM	-	-	17,221,538,686	0	10.59	912,106
RM	0	55.41	17,221,538,686	0	10.59	912,106
	5	29.31	17,937,023,950	4.15	10.59	912,106
	10	11.03	18,415,602,507	6.93	10.59	912,106
	14	3.84	18,687,421,196	8.51	10.59	912,106
	24	0.09	18,995,591,558	10.30	10.59	912,106
	34	3.5490e-004	19,030,056,581	10.51	10.59	912,106
	54	2.7489e-0011	19,033,322,863	10.52	10.59	912,106

Table 6.7: Sample results of deterministic and robust PHEV transition models including emission constraints for generation.

	Γ [-]	Violation probability [%]	Optimal value [CAD]	Change [%]	Uniform penetration [%]	# of PHEVs by 2025
DM	-	-	17,504,918,805	0	10.59	912,106
RM	0	55.41	17,504,918,805	0	10.59	912,106
	5	29.31	18,218,390,702	4.08	10.59	912,106
	10	11.03	18,699,206,394	6.82	10.59	912,106
	14	3.84	18,971,100,492	8.38	10.59	912,106
	24	0.09	19,279,362,145	10.14	10.59	912,106
	34	3.5490e-004	19,314,768,622	10.34	10.59	912,106
	54	2.7489e-0011	19,316,448,570	10.35	10.59	912,106

independent of the budget of uncertainty for lower emission costs or not. In order to do so, further robust analysis was performed using different values of the social cost of emissions in the population area. These studies reveal that the independence of the uniform PHEV penetration from the budget of uncertainty holds for even relatively large deviations (about 50%) of the social cost of emissions with regard to the initially assumed 125 CAD/ton. However, larger than 50% reductions of the social cost of emissions causes the budget of uncertainty to greatly influence the uniform PHEV penetration. This is demonstrated in Tables 6.8 and 6.9, where the robust results are found based on a social cost of emission equal to 50 CAD/ton. In this case, by accepting almost a 96% protection level of the constraints against uncertainty and 8% loss of optimality, at least 1.55% uniform PHEV penetration can be obtained at the social cost of emission of 50 CAD/ton and 10 CAD/ton in population areas and generation facilities, respectively; this translates into at least 133,548 PHEVs that can be introduced into Ontario's transport sector by 2025.

6.4 Summary

In this chapter, the application of a robust optimization approach for planning the transition to AFVs was proposed. A comprehensive sensitivity analysis using Monte Carlo simulation was performed for the optimization models for transition to FCVs and PHEVs in Ontario, Canada. Based on the proposed Average Deviation Index (ADI), different parameters in each model were ranked with respect to their impact on actual optimal values. The high-ranking parameters were then used to develop the robust counterpart models. The main advantage of these robust models is that the policy makers can choose the level of risk and establish a balance between optimality and conservatism/risk.

The findings of this chapter demonstrate that with a reasonable trade-off between optimality and conservatism/risk, more than 170,000 FCVs or 900,000 PHEVs can be supported by the Ontario's grid by 2025 at the social cost of CO_2 emissions equal to 125 CAD/ton and 10 CAD/ton in population areas and generation facili-

Table 6.8: Sample results of deterministic and robust PHEV transition models with SC_{CO_2p}=50 CAD/ton, disregarding emission constraints for generation. (DM: deterministic model; RM: robust model.)

	Γ [-]	Violation probability [%]	Optimal value [CAD]	Change [%]	Uniform penetration [%]	# of PHEVs by 2025
DM	-	-	17,749,875,901	0	9.91	853,397
RM	0	55.41	17,749,875,901	0	9.91	853,397
	5	29.31	18,462,420,204	4.01	9.91	853,397
	10	11.03	18,942,348,114	6.72	9.91	853,397
	14	3.84	19,213,595,806	8.25	9.61	827,938
	24	0.09	19,513,035,695	9.93	0.68	58,284
	34	3.5490e-004	19,548,443,500	10.13	0.68	58,284
	54	2.7489e-0011	19,550,124,730	10.14	0.68	58,284

Table 6.9: Sample results of deterministic and robust PHEV transition models with SC_{CO_2p}=50 CAD/ton, including emission constraints for generation.

	Γ [-]	Violation probability [%]	Optimal value [CAD]	Change [%]	Uniform penetration [%]	# of PHEVs by 2025
DM	-	-	18,024,967,839	0	7.93	682,994
RM	0	55.41	18,024,967,839	0	7.93	682,994
	5	29.31	18,732,050,321	3.92	7.93	682,994
	10	11.03	19,208,575,792	6.57	7.93	682,994
	14	3.84	19,475,404,857	8.05	1.55	133,548
	24	0.09	19,772,818,146	9.70	0	0
	34	3.5490e-004	19,808,225,951	9.89	0	0
	54	2.7489e-0011	19,809,907,181	9.90	0	0

ties, respectively. The robust results obtained for the FCV model is almost 50% of Ontario's maximum grid potential, as obtained and discussed in Chapter 5. However, based on the PHEV robust model, the total number of PHEVs is found to be insensitive to the level of conservatism/risk. Sufficiently low values of the social cost of CO_2 emissions, e.g., 50 CAD/ton, make the PHEV model sensitive to the level of conservatism/risk and substantially limits the number of PHEVs.

Chapter 7

Conclusions

7.1 Summary

This thesis has concentrated on the analysis of electricity and transport sectors within a single integrated framework and presents the capabilities of this integrated approach to realize an environmentally and economically sustainable transport sector based on AFVs. Comprehensive optimization planning models for the transition to FCVs and PHEVs were developed to determine the optimal electricity grid potential to support these types of AFVs in the transport sector within a planning horizon. A simple 3-zone test system was developed to better understand and interpret the results, to assess the impact of different constraints and, consequently, to evaluate different aspects of the proposed models. These models were then applied to the real case of Ontario, Canada for a planning horizon from 2008 to 2025. The relevant components of Ontario's electricity system and transport sector were properly modelled, including the transmission network, the zonal pattern of base-load generation capacity, and the resulting zonal base-load demand based on data for Ontario's transport sector.

The issue of parameter uncertainty was also incorporated into the models. Thus, a methodology based on Monte Carlo simulation was used to identify the most

influential parameters on the optimal solution. Using these uncertain parameters, a robust optimization approach that provides the possibility of making a trade-off between optimality and conservatism was finally applied to derive robust solutions for the transition to AFVs.

The following summarizes the main content and conclusions of this thesis:

- Chapter 3 presented a novel MILP optimization framework for planning the transition to AFVs considering relevant electricity grid constraints in generation and transmission levels. This optimization framework, which is based on zonal representation of the region under study considering the main power generation and load centers, allows to determine the optimal potential penetration of AFVs into the transport sector for each zone for the planning horizon. For the FCV transition model, this was achieved by finding the optimal size and location of HPPs as well as the optimal hydrogen production and hydrogen transportation routes. In order to better understand and interpret the results and evaluate the impact of different constraints, a small 3-zone test system was developed to study the transition to FCVs. The results of this study showed how the environmental issues as well as operational limitations, such as maximum annual development of HPPs or congestion in electricity or hydrogen networks, can influence the optimal FCV penetration levels.

- Chapter 4 studied the application of the proposed optimization framework to the real of Ontario, Canada. This was accomplished by first developing appropriate models and data for Ontario's electricity system and transport sector for a 2008-2025 planning horizon. Thus, a model of Ontario's transmission network was developed by representing the main transmission corridors and their possible capacity improvements. Furthermore, a zonal pattern of base-load generation capacity was developed to specify the total effective generation capacity available in each zone to supply base load. Also, the required base-load demand data, was obtained by decomposing the annual growth rate of base-load demand in the whole of Ontario into different zones. This chapter

discussed as well power exports and imports in Ontario, transition patterns, and further assumptions made regarding the operation of HPPs and charging of PHEVs in view of Ontario's electricity demand and price. An economic analysis of electrolytic hydrogen production in Ontario during off-peak hours was also presented.

- Chapter 5 presented and discussed the application of the proposed optimization framework to Ontario, Canada under a variety of scenarios. This chapter studied Ontario's maximum grid potential for supporting both FCVs and PHEVs under uniform and non-uniform penetration assumptions. Different constraints and limitations, such as the location of the new nuclear units, transition patterns, the emission costs of generation, and HPP placement and hydrogen transportation limits were shown to influence the number of AFVs within the Ontario's transport sector by 2025. The following are the main conclusions that can be derived from the studies performed in this chapter:
  - The proposed Transition Pattern 2, which considers the scarcity of baseload resources in Ontario from 2015-2022, was found to be more supportive of both FCVs and PHEVs penetrations than Transition Pattern 1. However, this transition pattern necessitates the rapid development of required infrastructure in the early years.
  - In general, development of new nuclear units in the Toronto zone yielded higher penetration levels of both FCVs and PHEVs. Having the new nuclear units developed in the Bruce zone yielded significant hydrogen export from this zone and larger transmission losses for the FCV and PHEV transition models, respectively. However, the studies performed demonstrate the capability of the Bruce zone to act as the main hydrogen exporter in Ontario.
  - Considering emission constraints for generation influences the patterns of power dispatches and exports in the system and consequently AFV penetration levels in different zones. However, the maximum number of

AFVs in all of Ontario, which was determined based on a sufficiently large value of the social cost of emissions is shown to be almost immune to these constraints under both uniform and non-uniform penetration assumptions.

- Based on the non-uniform penetration assumption, HPP placement constraints are shown to impact the patterns of HPP development and FCV penetrations in different zones of Ontario. However, the maximum number of FCVs in the whole of Ontario is scarcely impacted.
- Uniform FCV penetration levels are shown to be substantially affected by HPP placement constraints. This result is mainly related to the reduction of HPP developments in the Toronto zone, requiring large hydrogen transportation, especially in routes ending at Toronto.
- The maximum number of PHEVs that can be supported by Ontario's grid by 2025 under the uniform penetration assumption was found to be less than that obtained based on non-uniform penetration assumption. This disparity is due to increased level of transmission losses.
- Based on realistic and practical assumptions, it was found that almost 378,000 FCVs or 912,000 PHEVs (almost 4.4% and 10.6% of Ontario's vehicles fleet, respectively) can be introduced into Ontario's transport sector by 2025, neglecting the issue of parameter uncertainty. These values reflect Ontario's maximum grid potential to support AFVs.

- Chapter 6 addressed the issue of parameter uncertainty and proposed the application of robust optimization for planning the transition to AFVs. Thus, a sensitivity analysis using Monte Carlo simulation was carried out to find the impact of estimation errors in the parameters of the models developed in Chapter 3. In order to quantitatively compare the sensitivity of the optimal value to perturbations in different parameters, a measure labeled Average Deviation Index (ADI) was proposed and calculated for different parameters of each optimization model. Ranking of the ADI values revealed the most

influential uncertain parameters, which were then used for developing the robust counterpart problems of the optimization models. The main advantage of these robust models is that they allow decision makers to adjust the trade-off between optimality and conservatism/risk. The following conclusions are derived from the analyses performed in this chapter, for chosen values of the social costs of emissions for population areas and generation facilities, respectively:

- In general, electricity prices are found to be among the most influential parameters on the optimal value in both FCV and PHEV transition models.
- The robust FCV transition model is influenced by the emission constraints for generation. This impact is even more conspicuous for high probability levels of constraint protection against uncertainty.
- With a reasonable trade-off between optimality and conservatism/risk, more than 176,000 FCVs (almost 2% of Ontario's vehicles fleet) can be supported by Ontario's grid by 2025.
- It was found that the PHEV transition model is more susceptible to loss of optimality for a certain level of violation probability, compared to the FCV transition model.
- The robust PHEV transition model was shown not to be influenced by the emission constraints for generation. Moreover, decreasing the constraints violation probability, despite increasing the loss of optimality, had no impact on the total number of PHEVs by 2025 which is almost 912,000 (10.6% of Ontario's vehicles fleet).
- Based on sufficiently low values of the social cost of emissions in population areas, the PHEV transition model was shown to become sensitive to both emission constraints for generation and constraints violation probability.

7.2 Contributions

The following are the main contributions of the research presented in this thesis:

1. A comprehensive zone-based optimization framework for planning the transition to a hydrogen economy to support FCVs in the transport sector has been developed. This model, which requires the development of an adequate sub-model for hydrogen transportation between the zones, determines the optimal grid potential to accommodate FCVs during a planning horizon. This is achieved through finding the optimal size and location of HPPs as well as optimal hydrogen transportation routes.
2. The planning model developed for the transition to a hydrogen economy has been extended to derive optimal penetrations of PHEVs into the transport sector.
3. Environmental costs/credits associated with adding extra load in the system for both population areas and generation facilities have been incorporated in the proposed transition models. This is accomplished by developing an emission cost model that penalizes the objective function depending on the value of zonal generation and the social cost of emissions in generation power plants, and assigning social credits for AFVs which cut emissions in population areas.
4. The proposed optimization planning models have been applied to the real case of Ontario, Canada, where optimal penetration levels of AFVs are derived for a variety of scenarios for a 2008-2025 planning horizon. This is accomplished by first developing appropriate models for Ontario's electricity system and transport sector.
5. A methodology based on Monte Carlo simulation has been proposed and implemented to study the issue of parameter uncertainty in the developed optimization planning models, and to derive the most influential parameter uncertainties based on their impacts on the optimal value.

6. A robust optimization approach has been applied to develop robust counterpart problems of the planning models, and consequently derive robust optimal penetration levels of AFVs into the transport sector, with application to Ontario.

Parts of the proposed models and corresponding results presented in this thesis have been published in a number of journals and conference proceedings [66, 67, 105, 168, 175].

7.3 Future Work

Based on the work reported in this thesis, future research may be pursued in the following directions:

1. In this thesis, a fixed value for the daily drive was assumed in the FCV transition model. This value is based on average figures in the real case of Ontario, Canada; however, driving behaviors may change in different jurisdictions and may be different on weekdays and weekends. Therefore, the impact of drive cycle behavior could be investigated.
2. The target in this thesis was to find the optimal potential penetrations of AFVs into the transport sector without any additional grid investment. However, the problem can be looked at the other way around; thus, a stochastic optimization model could be developed to determine the optimal required capacity of the different types of generation resources based on uncertain penetrations of AFVs into the market. Such a model could provide valuable inputs for policy makers and system planners in the electricity sector, so that the existing plans could be modified based on the economic benefits accrued due to the introduction of these AFVs into the system.
3. In this thesis, impact assessment of PHEVs is performed at the transmission level. This study could be extended to account for the constraints of

distribution systems which is a more challenging task. Thus, due to the spatial and temporal diversity of these vehicles, different feeders may experience different levels of PHEV adoption. Consequently, the problem is stochastic in nature and hence requires adequate analysis tools.

4. The integration of PHEVs into the transport sector would be facilitated under a smart grid framework, where there are interactive communications between the utilities and their customers. How the proposed PHEVs transition model can be reformulated in this framework, and how the optimal penetration levels can be influenced need to be examined.

5. Finding the optimal penetrations of PHEVs with the consideration of the vehicle-to-grid (V2G) operation and uncontrolled charging is another area for future research.

Appendices

Appendix A

3-zone System Data

This appendix provides additional data for the 3-zone test system shown in Figure 3.3. Table A.1 represents the data of the transmission system in 2008, which change during the planning horizon as per the discussion in Section 3.6.2, and Table A.2 shows the data for the zonal effective generation capacity including the capacity factors.

Table A.1: Transmission data for 3-zone test system

From Zone i	To Zone j	R_{ij} [p.u.]	X_{ij} [p.u.]	$\overline{Pd}_{ij}$ [MW]	$\overline{Pr}_{ijy}$ [MW]
1	2	.001904	.0221	2560	9999
1	3	.003024	.0351	1940	9999
2	3	.002352	.0273	1560	1560

Table A.2: Zonal effective generation capacity contributing to base-load demand (MW)

Nuclear																		
	2008	2009	2010	2011	2012	2013	2014	2015	2016	2017	2018	2019	2020	2021	2022	2023	2024	2025
Zone 1	3000	3000	3000	3000	3000	4500	4500	4500	4500	4500	4500	3000	3000	3000	3000	3750	3750	3750
Zone 2	0	0	0	0	0	0	0	0	0	0	0	0	0	0	0	0	0	0
Zone 3	0	0	0	0	0	0	0	0	0	0	0	0	0	0	0	0	0	0
Wind																		
	2008	2009	2010	2011	2012	2013	2014	2015	2016	2017	2018	2019	2020	2021	2022	2023	2024	2025
Zone 1	20	70	75	75	75	145	210	225	300	310	350	365	375	375	375	375	375	375
Zone 2	35	110	200	235	240	240	250	260	260	260	265	270	275	275	275	275	275	275
Zone 3	30	30	60	95	115	120	125	135	140	150	165	180	180	180	180	180	180	180
Hydro																		
	2008	2009	2010	2011	2012	2013	2014	2015	2016	2017	2018	2019	2020	2021	2022	2023	2024	2025
Zone 1	0	0	0	0	4	4	6	6	6	6	6	6	6	6	6	6	6	6
Zone 2	15	15	15	30	50	60	60	65	65	72	72	72	78	81	81	81	89	89
Zone 3	5	5	5	10	15	20	25	40	50	50	50	50	55	55	55	55	55	55
CHP																		
	2008	2009	2010	2011	2012	2013	2014	2015	2016	2017	2018	2019	2020	2021	2022	2023	2024	2025
Zone 1	0	0	0	0	0	0	0	0	0	0	0	0	0	0	0	0	0	0
Zone 2	10	10	10	10	10	100	100	100	100	100	100	100	100	100	100	100	100	100
Zone 3	10	100	100	100	100	180	180	180	180	180	280	280	280	280	280	280	280	280
Coal																		
	2008	2009	2010	2011	2012	2013	2014	2015	2016	2017	2018	2019	2020	2021	2022	2023	2024	2025
Zone 1	0	0	0	0	0	0	0	0	0	0	0	0	0	0	0	0	0	0
Zone 2	1000	1000	1000	750	500	500	500	0	0	0	0	0	0	0	0	0	0	0
Zone 3	2000	2000	2000	2000	2000	1750	1500	1500	1500	1500	1500	1500	1500	1500	1500	1500	1500	1500

Appendix B

10-zone Ontario's System Data

This appendix provides additional data for the 10-zone simplified model of Ontario's electricity system depicted in Figure 4.1. Table B.1 shows the data for the transmission system at the beginning of the planning horizon, which change with the reinforcement of the grid based on the assumptions illustrated in Table 4.1, while Tables B.2-B.8 illustrate the data for the zonal effective generation capacity including the capacity factors.

Table B.1: Transmission data for 10-zone Ontario's system

From Zone i	To Zone j	R_{ij} [p.u.]	X_{ij} [p.u.]	$\overline{Pd}_{ij}$ [MW]	$\overline{Pr}_{ijy}$ [MW]
1	2	.003024	.0351	1940	9999
1	3	.001904	.0221	2560	9999
2	3	.002352	.0273	1560	1560
3	4	.002352	.0273	9999	1750
3	5	.002352	.0273	3212	9999
3	8	.003584	.0416	2488	9999
5	6	.003808	.0442	9999	9999
5	8	.002352	.0273	2000	1000
6	7	.00112	.013	1900	9999
8	9	.004032	.0468	1900	1400
9	10	.051985	.50737	350	325

Table B.2: Nuclear power capacity contributing to base-load demand (Scenario 1) (MW)

	2008	2009	2010	2011	2012	2013	2014	2015	2016	2017	2018	2019	2020	2021	2022	2023	2024	2025
Bruce	4720	4720	4720	4720	4720	6220	6220	6220	6220	6220	4720	3220	3220	3220	3220	4720	6220	6220
Toronto	6645	6645	6645	6645	6645	6645	5615	4580	3699	3699	5199	6229	7259	7259	8140	8140	7259	7259

Table B.3: Nuclear power capacity contributing to base-load demand (Scenario 2) (MW)

	2008	2009	2010	2011	2012	2013	2014	2015	2016	2017	2018	2019	2020	2021	2022	2023	2024	2025
Bruce	4720	4720	4720	4720	4720	6220	6220	6220	6220	6220	6220	4720	4720	4720	4720	6220	7720	7720
Toronto	6645	6645	6645	6645	6645	6645	5615	4580	3699	3699	3699	4729	5759	5759	6640	6640	5759	5759

Table B.4: Effective coal power capacity contributing to base-load demand (MW)

	2008	2009	2010	2011	2012	2013	2014	2015	2016	2017	2018	2019	2020	2021	2022	2023	2024	2025
West	974	974	974	792.5	475.5	475.5	475.5	0	0	0	0	0	0	0	0	0	0	0
SW	1910	1910	1910	1554.5	932.5	932.5	932.5	0	0	0	0	0	0	0	0	0	0	0
NW	258.5	258.5	258.5	153	92	92	92	0	0	0	0	0	0	0	0	0	0	0

Table B.5: Effective wind power capacity contributing to base-load demand (MW)

	2008	2009	2010	2011	2012	2013	2014	2015	2016	2017	2018	2019	2020	2021	2022	2023	2024	2025
Bruce	22.8	66.68	75.63	75.63	75.63	143.58	211.83	223	299	310	354.3	365.6	376	376	376	376	376	376
West	29.7	30.4	57.9	94.9	112.4	119.4	126.5	133.5	140.5	147.5	165.9	173	180	180	180	180	180	180
SW	32.4	109.8	201.5	235.9	240.3	244.8	249.2	253.7	258.1	262.5	267	271.4	275.9	275.9	275.9	275.9	275.9	275.9
Niagara	0	0	0	0.7	1.3	2	2.6	3.3	4	4.6	5.3	5.9	6.6	6.6	6.6	6.6	6.6	6.6
Toronto	0	0	0	0.7	1.4	2.1	2.8	3.5	4.1	4.8	5.5	6.2	6.9	6.9	6.9	6.9	6.9	6.9
East	0	30	52.8	56.6	60.5	64.3	148.2	152	155.8	159.6	163.4	167.2	171	171	171	171	171	171
Ottawa	0	0	0	0	0	0	0	0	0	0	0	0	0	0	0	0	0	0
Essa	0	0	0	3.8	7.5	56.3	60	63.8	67.5	71.3	75	78.8	82.5	82.5	82.5	82.5	82.5	82.5
NE	56.7	56.7	106	109.6	113.3	116.9	120.5	124.2	127.8	131.4	135.1	198.7	292.3	292.3	292.3	292.3	292.3	292.3
NW	0	0	0	1.4	2.9	4.3	5.8	7.2	8.6	10.1	11.5	13	14.4	14.4	14.4	14.4	14.4	14.4

Table B.6: Effective hydro power capacity contributing to base-load demand (MW)

	2008	2009	2010	2011	2012	2013	2014	2015	2016	2017	2018	2019	2020	2021	2022	2023	2024	2025
Bruce	0	0	0	0	0	0	0	0	0	0	0	0	0	0	0	0	0	0
West	0	0	0	0	0	0	0	0	0	0	0	0	0	0	0	0	0	0
SW	0	0	0	0	0	0	0	0	0	0	0	0	0	0	0	0	0	0
Niagara	1651	1654	1659	1668	1670	1674	1677	1680	1682	1685	1685	1685	1685	1685	1685	1685	1685	1685
Toronto	0	0	0	0	0	0	0	0	0	0	0	0	0	0	0	0	0	0
East	815.1	818.1	818.1	821.1	821.6	821.6	821.6	824.1	824.1	824.1	824.1	824.1	824.1	824.1	824.1	824.1	824.1	824.1
Ottawa	1	1	1	4.5	10	10	10	12	12	12	12	12	12	12	12	12	12	12
Essa	0	0	0	0	4	4	5.5	5.5	5.5	5.5	5.5	5.5	5.5	5.5	5.5	5.5	5.5	5.5
NE	16.4	16.4	21.4	27.9	51.4	57.4	58.4	64.4	65.4	72.4	72.4	72.4	77.4	80.9	80.9	80.9	88.4	88.4
NW	5	7	8	9.5	16.5	22	26	38.5	46.5	46.5	50	50	54.5	54.5	54.5	54.5	54.5	54.5

Table B.7: CHP capacity contributing to base-load demand (MW)

	2008	2009	2010	2011	2012	2013	2014	2015	2016	2017	2018	2019	2020	2021	2022	2023	2024	2025
Bruce	0	0	0	0	0	0	0	0	0	0	0	0	0	0	0	0	0	0
West	11.5	95.5	95.5	95.5	95.5	179	179	179	179	179	179	179	179	179	179	179	179	179
SW	12	12	12	12	12	96	96	96	96	96	96	96	96	96	96	96	96	96
Niagara	0	0	236	236	236	319	319	319	319	319	319	319	319	319	319	319	319	319
Toronto	7.3	7.3	7.3	7.3	7.3	91	91	91	91	91	91	91	91	91	91	91	91	91
East	0	0	0	0	0	84	84	84	84	84	84	84	84	84	84	84	84	84
Ottawa	0	0	0	0	0	84	84	84	84	84	84	84	84	84	84	84	84	84
Essa	0	0	0	0	0	0	0	0	0	0	0	0	0	0	0	0	0	0
NE	0	63	63	63	63	147	147	147	147	147	147	147	147	147	147	147	147	147
NW	0	0	0	0	0	0	0	0	0	0	0	0	0	0	0	0	0	0

Table B.8: CDM released capacity contributing to base-load demand (MW)

	2008	2009	2010	2011	2012	2013	2014	2015	2016	2017	2018	2019	2020	2021	2022	2023	2024	2025
Bruce	1.7	2.4	3.6	4.2	4.7	5.3	5.9	6.5	6.9	7.3	7.7	8	8.3	8.6	8.9	9.1	9.3	9.5
West	41.1	56.2	84.8	99.3	113.8	128.5	143.3	158	168.4	178.8	189.4	199.4	208.5	216.1	223.4	230.6	238.1	244
SW	73.7	100.9	152.4	178.8	205.3	232.2	259.4	286.5	305.9	325.4	345.1	364	381.3	395.8	410.1	424	438.5	450
Niagara	14.5	19.6	29.3	34	38.6	43.2	47.7	52.1	55	57.8	60.6	63.2	65.5	67.2	68.8	70.3	71.9	73
Toronto	123.6	168.2	252.5	294.2	335.5	377.1	418.5	459.2	487	514.6	542.2	568	591.1	609.6	627.4	644.4	662	675
East	23.1	31.4	47.1	54.9	62.6	70.2	77.9	85.4	90.5	95.5	100.6	105.3	109.5	112.8	116	119	122.1	124.5
Ottawa	27.2	37.3	56.4	66.3	76.3	86.5	96.8	107.1	114.5	122.1	129.7	137.1	143.9	149.6	155.3	160.9	166.7	171.4
Essa	19.9	27.2	41	48.1	55.1	62.2	69.4	76.6	81.6	86.7	91.8	96.7	101.2	104.9	108.5	112.1	115.7	118.6
NE	32.7	43.9	64.9	74.6	83.8	92.8	101.6	109.8	114.8	119.5	124.1	128.2	131.4	133.6	135.5	137.2	138.9	139.5
NW	15.4	20.8	30.9	35.7	40.4	45	49.5	53.9	56.6	59.3	61.9	64.3	66.3	67.8	69.2	70.4	71.7	72.5

Bibliography

[1] International Energy Agency, Key world energy statistics 2006. [Online]. Available: http://www.iea.org/

[2] World Energy Outlook. [Online]. Available: http://www.worldenergyoutlook.org/

[3] Transport Canada. [Online]. Available: http://www.tc.gc.ca/environment/menu.htm#climatechange

[4] R. S. M. Arico, "Measuring the oil vulnerability of canadian cities," Master's thesis, Simon Fraser University, 2007. [Online]. Available: http://ir.lib.sfu.ca/bitstream/1892/4211/1/etd2765.pdf

[5] B. S. Reddy and J. K. Parikh, "Economic and environmental impacts of demand side management programmes," *Energy Policy*, vol. 25, no. 3, pp. 349–356, February 1997.

[6] Distributed Generation, Education Module. [Online]. Available: http://www.dg.history.vt.edu/index.html

[7] M. H. Didden and W. D. D'haeseleer, "Demand side management in a competitive european market: Who should be responsible for its implementation?" *Energy Policy*, vol. 31, no. 13, pp. 1307–1314, October 2003.

[8] G. Pepermansa, J. Driesen, D. Haeseldonckxc, R. Belmansc, and W. D'haeseleer, "Distributed generation: definition, benefits and issues," *Energy Policy*, vol. 33, no. 6, pp. 787–798, April 2005.

[9] J. A. Turner, "A realizable renewable energy future," *Science*, vol. 285, no. 5428, pp. 687–689, July 1999.

[10] J. Ogden, "Hydrogen- The fuel of the future?" *Physics Today*, vol. 55, no. 4, pp. 69–75, 2002.

[11] *The Hydrogen Economy: Opportunities, Costs, Barriers, and R&D Needs*. Washington, D.C.: The National Academies Press, 2004. [Online]. Available: http://www.nap.edu

[12] W. McDowall and M. Eames, "Towards a sustainable hydrogen economy: A multi-criteria sustainability appraisal of competing hydrogen futures," *International Journal of Hydrogen Energy*, vol. 32, no. 18, pp. 4611–4626, 2007.

[13] S. Prince-Richard, M. Whale, and N. Djilali, "A techno-economic analysis of decentralized electrolytic hydrogen production for fuel cell vehicles," *International Journal of Hydrogen Energy*, vol. 30, no. 11, pp. 1159–1179, 2005.

[14] P. Floch, S. Gabriel, C. Mansilla, and F. Werkoff, "On the production of hydrogen via alkaline electrolysis during off-peak periods," *International Journal of Hydrogen Energy*, vol. 32, no. 18, pp. 4641–4647, 2007.

[15] J. Vidueira, A. Contreras, and T. Veziroglu, "PV autonomous installation to produce hydrogen via electrolysis, and its use in FC buses," *International Journal of Hydrogen Energy*, vol. 28, no. 9, pp. 927–937, 2003.

[16] A. González, E. McKeogh, and B. Gallachoir, "The role of hydrogen in high wind energy penetration electricity systems: The Irish case," *Renewable Energy*, vol. 29, no. 4, pp. 471–489, 2004.

[17] C. Greiner, M. Korps, and A. Holen, "A Norwegian case study on the production of hydrogen from wind power," *International Journal of Hydrogen Energy*, vol. 32, no. 10-11, pp. 1500–1507, 2007.

[18] K. Martin and S. Grasman, "An assessment of wind-hydrogen systems for light duty vehicles," *International Journal of Hydrogen Energy*, vol. 34, no. 16, pp. 6581–6588, 2009.

[19] J. Ramirez-Salgado and A. Estrada-Martinez, "Roadmap towards a sustainable hydrogen economy in Mexico," *Journal of Power Sources*, vol. 129, no. 2, pp. 255–263, 2004.

[20] S. Milciuviene, D. Milcius, and B. Praneviciene, "Towards hydrogen economy in Lithuania," *International Journal of Hydrogen Energy*, vol. 31, no. 7, pp. 861–866, 2006.

[21] J. Brey, R. Brey, A. Carazo, I. Contreras, A. Hernández-Díaz, and A. Castro, "Planning the transition to a hydrogen economy in Spain," *International Journal of Hydrogen Energy*, vol. 32, no. 10-11, pp. 1339–1346, 2007.

[22] M. Ball, M. Wietschel, and O. Rentz, "Integration of a hydrogen economy into the German energy system: an optimising modelling approach," *International Journal of Hydrogen Energy*, vol. 32, no. 10-11, pp. 1355–1368, 2007.

[23] R. Smit, M. Weeda, and A. de Groot, "Hydrogen infrastructure development in The Netherlands," *International Journal of Hydrogen Energy*, vol. 32, no. 10-11, pp. 1387–1395, 2007.

[24] M. L. Murray, E. Hugo Seymour, and R. Pimenta, "Towards a hydrogen economy in Portugal," *International Journal of Hydrogen Energy*, vol. 32, no. 15, pp. 3223–3229, 2007.

[25] E. Tzimas, P. Castello, and S. Peteves, "The evolution of size and cost of a hydrogen delivery infrastructure in Europe in the medium and long term," *International Journal of Hydrogen Energy*, vol. 32, no. 10-11, pp. 1369–1380, 2007.

[26] M. L. Murray, E. Hugo Seymour, J. Rogut, and S. W. Zechowska, "Stakeholder perceptions towards the transition to a hydrogen econ-

omy in Poland," *International Journal of Hydrogen Energy*, vol. 33, no. 1, pp. 20–27, 2008.

[27] M. Contaldi, F. Gracceva, and A. Mattucci, "Hydrogen perspectives in Italy: Analysis of possible deployment scenarios," *International Journal of Hydrogen Energy*, vol. 33, no. 6, pp. 1630–1642, 2008.

[28] Z. Lin, C. W. Chen, J. Ogden, and Y. Fan, "The least-cost hydrogen for Southern California," *International Journal of Hydrogen Energy*, vol. 33, no. 12, pp. 3009–3014, 2008.

[29] A. Ajanovic, "On the economics of hydrogen from renewable energy sources as an alternative fuel in transport sector in Austria," *International Journal of Hydrogen Energy*, 2008.

[30] R. Boudries and R. Dizene, "Potentialities of hydrogen production in Algeria," *International Journal of Hydrogen Energy*, vol. 33, no. 17, pp. 4476–4487, 2008.

[31] D. H. Lee, S. S. Hsu, C. T. Tso, A. Su, and D. J. Lee, "An economy-wide analysis of hydrogen economy in Taiwan," *Renewable Energy*, vol. 34, no. 8, pp. 1947–1954, 2009.

[32] P. Denholm and W. Short, "An evaluation of utility system impacts and benefits of optimally dispatched plug-in hybrid electric vehicles," National Renewable Energy Laboratory, Golden, CO, Tech. Rep. NREL/TP-620-40293, October 2006.

[33] K. Parks, P. Denholm, and T. Markel, "Costs and emissions associated with plug-in hybrid electric vehicle charging in the xcel energy colorado service territory," National Renewable Energy Laboratory, Golden, CO, Tech. Rep. NREL/TP-640-41410, May 2007.

[34] S. W. Hadley, "Evaluating the impact of plug-in hybrid vehicles on regional electricity supplies," in *Proc. Bulk Power System Dynamics and Control VII Symposium, IREP*, Charleston, South Carolina, August 2007.

[35] M. Kintner-Meyer, K. Schneider, and R. Pratt, "Impacts assessment of plug-in hybrid vehicles on electric utilities and regional us power grids part 1: Technical analysis," *Pacific Northwest National Laboratory*, 2007.

[36] M. D. Galus and G. Andersson, "Demand management of grid connected plug-in hybrid electric vehicles," in *Proc. IEEE Conference on Global Sustainable Energy Infrastructure (Energy 2030)*, Atlanta, GA, USA, 2008.

[37] X. Yu, "Impacts assessment of PHEV charge profiles on generation expansion using national energy modeling system," in *Proc. IEEE Power and Energy Society General Meeting*, Pittsburg, Pensylvania, USA, 2008.

[38] B. Bakken, M. Fossum, and M. Belsnes, "Small-scale hybrid plant integrated with municipal energy supply system," in *Proc. of third International Energy Symposium*, Ossiach, Austria, 2001.

[39] M. Geidl, "Integrated modeling and optimization of multi-carrier energy systems," Ph.D. dissertation, Power Systems Laboratory, ETH Zurich, 2007. [Online]. Available: http://e-collection.ethbib.ethz.ch/cgi-bin/show.pl?type=diss\&nr=17141

[40] M. Geidl, G. Koeppel, P. Favre-Perrod, B. Klöckl, G. Andersson, and K. Fröhlich, "Energy hubs for the future," *IEEE Power & Energy Magazine*, vol. 5, no. 1, 2007.

[41] ——, "The energy hub – a powerful concept for future energy systems," in *Third Annual Carnegie Mellon Conference on the Electricity Industry*, Linkoping, Sweden, March 2007.

[42] P. Favre-Perrod, M. Geidl, B. Klockl, and G. Koeppel, "A vision of future energy networks," in *Inaugural IEEE PES 2005 Conference and Exposition in Africa*, Durban, South Africa, July 2005, pp. 13–17.

[43] M. Geidl, P. Favre-Perrod, B. Klockl, and G. Koeppel, "A greenfield approach for future of power systems," in *Proc. of Cigre General Session 41*, Paris, France, 2006.

[44] J. Rifkin, *The Hydrogen Economy: The Creation of the Worldwide Energy Web and the Redistribution of Power on Earth.* Penguin Putnam, New York, 2002.

[45] M. L. Wald, "Questions about a hydrogen economy," *Scientific American*, pp. 40–47, May 2004.

[46] A. Benthem, G. Kramera, and R. Ramerb, "An options approach to investment in a hydrogen infrastructure," *Energy Policy*, vol. 34, pp. 2949–2963, 2006.

[47] S. Ramesohl and F. Merten, "Energy system aspects of hydrogen as an alternative fuel in transport," *Energy Policy*, vol. 34, pp. 1251–1259, 2006.

[48] K. Adamson, "Hydrogen from renewable resources—the hundred year commitment," *Energy Policy*, vol. 32, pp. 1231–1242, 2004.

[49] US Department of Energy, Carbon Sequestration. [Online]. Available: http://www.energy.gov/sciencetech/carbonsequestration.htm

[50] E. Tzimas and S. D. Peteves, "The impact of carbon sequestration on the production cost of electricity and hydrogen from coal and natural-gas technologies in europe in the medium term," *Energy*, vol. 30, pp. 2672–2689, 2005.

[51] B. Johnston, M. C. Mayo, and A. Khare, "Hydrogen: the energy source for the 21st century," *Technovation*, vol. 25, no. 6, pp. 569–585, June 2005.

[52] A. B. Lovins, "Twenty hydrogen myths," Rocky Mountain Institute, June 2003. [Online]. Available: http://www.rmi.org/images/other/Energy/E03-05-20HydrogenMyths.pdf

[53] G. W. Crabtree, M. S. Dresselhaus, and M. V. Buchanan, "The hydrogen economy," *Physics Today*, vol. 57, no. 12, pp. 39–44, 2004.

[54] D. B. Barber, "Nuclear energy and the future; the hydrogen economy or the electricity economy?" March 2005. [Online]. Available: http://www.iags.org/barber.pdf

[55] R. Hammerschlaga and P. Mazzab, "Questioning hydrogen," *Energy Policy*, vol. 33, pp. 2039–2043, 2005.

[56] U. Bossel, "Does a hydrogen economy make sense?" in *Proc. IEEE: Special Issue on the Hydrogen Economy*, vol. 94, no. 10, October 2006, pp. 1826–1837.

[57] W. W. Clark and J. Rifkin, "A green hydrogen economy," *Energy Policy*, vol. 34, pp. 2630–2639, 2006.

[58] W. McDowall and M. Eames, "Forecasts, scenarios, visions, backcasts and roadmaps to the hydrogen economy: A review of the hydrogen futures literature," *Energy Policy*, vol. 34, pp. 1236–1250, 2006.

[59] W. H. Vanderburg, "The hydrogen economy as technological bluff," *Bulletin of Science, Technology & Society*, pp. 299–302, August 2006. [Online]. Available: http://bst.sagepub.com/cgi/reprint/26/4/299.pdf

[60] C. J. Andrews, "Formulating and implementing public policy for new energy carriers," in *Proc. IEEE: Special Issue on the Hydrogen Economy*, vol. 94, no. 10, October 2006, pp. 1852–1863.

[61] S. Cole, D. V. Hertem, L. Meeus, and R. Belmans, "Energy storage on production and transmission level: a SWOT analysis." [Online]. Available: http://www.esat.kuleuven.be/electa/publications/fulltexts/pub-1515.pdf

[62] V. S. Budhraja, "Harmonizing electricity markets with the physics of electricity," *The Electricity Journal*, vol. 16, no. 3, 2003.

[63] G. Taljan, C. A. Cañizares, M. W. Fowler, and G. Verbic, "The feasibility of hydrogen storage for mixed wind-nuclear power plants," *IEEE Transactions on Power Systems*, vol. 23, no. 3, pp. 1507–1518, 2008.

[64] G. Taljan, M. W. Fowler, C. A. Cañizares, and G. Verbič, "Hydrogen storage for mixed wind–nuclear power plants in the context of a hydrogen economy," *International Journal of Hydrogen Energy*, vol. 33, no. 17, pp. 4463–4475, 2008.

[65] F. A. Felder and A. Hajos, "Using restructured electricity markets in the hydrogen transition: The PJM case," in *Proc. IEEE: Special Issue on the Hydrogen Economy*, vol. 94, no. 10, October 2006, pp. 1864–1879.

[66] A. Hajimiragha, C. A. Cañizares, M. W. Fowler, M. Geidl, and G. Andersson, "Optimal energy flow of integrated energy systems with hydrogen economy considerations," in *Proc. Bulk Power Systems Dynamics and Control VII Symposium, IREP*, Charleston, South Carolina, August 2007.

[67] A. Hajimiragha, M. W. Fowler, and C. A. Cañizares, "Hydrogen economy impact on optimal planning and operation of integrated energy systems," in *Proc. International Conference & Workshop on Micro-Cogeneration Technologies & Applications*, Ottawa, Canada, April 2008.

[68] D. Hermance and S. Sasaki, "Hybrid electric vehicles take to the streets," *IEEE Spectrum*, vol. 35, no. 11, pp. 48–52, 1998.

[69] M. Duvall, "Comparing the benefits and impacts of hybrid electric vehicle options for compact sedan and sport utility vehicles," Electric Power Research Institute (EPRI), Palo Alto, CA, Tech. Rep., 2002.

[70] A. Emadi, Y. Lee, and K. Rajashekara, "Power electronics and motor drives in electric, hybrid electric, and plug-in hybrid electric vehicles," *IEEE Transactions on Industrial Electronics*, vol. 55, no. 6, pp. 2237–2245, 2008.

[71] L. Sanna, "Driving the solution—the plug-in hybrid vehicle," *EPRI Journal*, pp. 8–17, 2005. [Online]. Available: http://mydocs.epri.com/docs/public/000000000001012885.pdf

[72] A. Simpson, "Cost-benefit analysis of plug-in hybrid vehicle technology," in *Proc. 22nd International Battery, Hybrid and Fuel Cell Electric Vehicle Symposium and Exhibition*, Yokohama, Japan, Oct. 23-28, 2006.

[73] T. Markel and A. Simpson, "Energy storage system considerations for grid-charged hybrid vehicles," in *Proc. SAE Future Transportation Technology and IEEE Vehicle Power and Propulsion Joint Conference*, Chicago, IL, September 7-9, 2006.

[74] ——, "Plug-in hybrid electric vehicle energy storage system design,," in *Proc. Advanced Automotive Battery Conference*, Baltimore, MD, May 17-19, 2006.

[75] C. A. Floudas, *Nonlinear and Mixed-Integer Programming - Fundamentals and Applications*. Oxford University Press, 1995.

[76] E. Balas, S. Ceria, and G. Cornuéjols, "A lift-and-project cutting plane algorithm for mixed 0–1 programs," *Mathematical Programming*, vol. 58, no. 1, pp. 295–324, 1993.

[77] C. Barnhart, E. L. Johnson, G. L. Nemhauser, M. W. P. Savelsbergh, and P. H. Vance, "Branch-and-price: Column generation for solving huge integer programs," *Operations Research*, vol. 46, no. 3, pp. 316–329, 1998.

[78] E. L. Johnson, G. L. Nemhauser, and M. W. P. Savelsbergh, "Progress in linear programming-based algorithms for integer programming: An exposition," *INFORMS Journal on Computing*, vol. 12, no. 1, pp. 2–23, 2000.

[79] *IBM ILOG AMPL version 12.1 User's Guide*, June 2009.

[80] A. Lodi, "Mixed integer programming computation," in *50 Years of Integer Programming 1958-2008*, M. Junger, T. M. Liebling, D. Naddef, G. L. Nemhauser, W. R. Pulleyblank, G. Reinelt, G. Rinaldi, and L. A. Wolsey, Eds. Springer-Verlag, 2009, pp. 619–645.

[81] A. Mahajan, "On selecting disjunctions for solving mixed integer programming problems," Ph.D. dissertation, Lehigh University, May 2009.

[82] R. Bixby and E. Rothberg, "Progress in computational mixed integer programming—a look back from the other side of the tipping point," *Annals of Operations Research*, vol. 149, no. 1, pp. 37–41, 2007.

[83] D. Bertsimas and M. Sim, "The price of robustness," *Operations Research*, vol. 52, no. 1, pp. 35–53, 2004.

[84] D. Bertsimas and A. Thiele, "Robust and data-driven optimization: modern decision-making under uncertainty," *INFORMS Tutorials in Operations Research: Models, Methods, and Applications for Innovative Decision Making*, 2006.

[85] P. Kall and S. W. Wallace, *Stochastic Programming*. Chichester: John Wiley & Sons, 1994.

[86] J. Mulvey, R. Vanderbei, and S. Zenios, "Robust optimization of large-scale systems," *Operations Research*, pp. 264–281, 1995.

[87] A. J. Kleywegt and A. Shapiro, *Handbook of Industrial Engineering*, 3rd ed. New York: John Wiley and Sons, 2001, ch. 102 Stochastic Optimization, pp. 2625–2650.

[88] N. Sahinidis, "Optimization under uncertainty: state-of-the-art and opportunities," *Computers and Chemical Engineering*, vol. 28, no. 6-7, pp. 971–983, 2004.

[89] R. Y. Rubinstein and D. P. Kroese, *Simulation and the Monte Carlo Method*, 2nd ed. New York: Wiley, 2007.

[90] S. Moazeni, "Flexible robustness in linear optimization," Master's thesis, University of Waterloo, 2006.

[91] M. Sim, "Robust optimization," Ph.D. dissertation, Massachusetts Institute of Technology, 2004.

[92] A. Thiele, "Robust stochastic programming with uncertain probabilities," *IMA Journal of Management Mathematics*, vol. 19, no. 3, p. 289, 2008.

[93] H. Beyer and B. Sendhoff, "Robust optimization–a comprehensive survey," *Computer methods in applied mechanics and engineering*, vol. 196, no. 33-34, pp. 3190–3218, 2007.

[94] A. Ben-Tal, L. El Ghaoui, and A. Nemirovski, *Robust Optimization*. Princeton, NJ: Princeton University Press, 2009.

[95] L. El-Ghaoui and H. Lebret, "Robust solutions to least-square problems to uncertain data matrices," *SIAM J. Matrix Anal. Appl*, vol. 18, pp. 1035–1064.

[96] L. El Ghaoui, F. Oustry, and H. Lebret, "Robust solutions to uncertain semidefinite programs," *SIAM journal of optimization*, vol. 9, pp. 33–52, 1998.

[97] A. Ben-Tal and A. Nemirovski, "Robust convex optimization," *Mathematics of Operations Research*, vol. 23, pp. 769–805, 1998.

[98] ——, "Robust solutions to uncertain programs," *Oper. Res. Lett*, vol. 25, no. 1–13, 1999.

[99] ——, "Robust solutions of linear programming problems contaminated with uncertain data," *Mathematical Programming*, vol. 88, no. 3, pp. 411–424, 2000.

[100] D. Bertsimas and M. Sim, "Robust discrete optimization and network flows," *Mathematical Programming*, vol. 98, no. 1, pp. 49–71, 2003.

[101] D. Pearce, "The social cost of carbon and its policy implications," *Oxford Review of Economic Policy*, vol. 19, no. 3, p. 362, 2003.

[102] G. W. Yohe, R. D. Lasco, Q. K. Ahmad, N. W. Arnell, S. J. Cohen, C. Hope, A. C. Janetos, and R. T. Perez, "Perspectives on climate

change and sustainability," in *Climate Change 2007: Impacts, Adaptation and Vulnerability. Contribution of Working Group II to the Fourth Assessment Report of the Intergovernmental Panel on Climate Change*, M. L. Parry, O. F. Canziani, J. P. Palutikof, P. J. van der Linden, and C. E. Hanson, Eds. Cambridge, UK: Cambridge University Press, 2007, pp. 811–841.

[103] R. S. J. Tol, "The marginal damage costs of carbon dioxide emissions: an assessment of the uncertainties," *Energy policy*, vol. 33, no. 16, pp. 2064–2074, 2005.

[104] M. Duvall and E. Knipping, "Environmental assessment of plug-in hybrid electric vehicles," EPRI, Palo Alto, CA, Tech. Rep., 2007.

[105] I. Kantor, M. W. Fowler, A. Hajimiragha, and A. Elkamel, "Air quality and environmental impacts of alternative vehicle technologies in Ontario, Canada," *International Journal of Hyrdogen Energy*, in press, 2010.

[106] Ontario Medical Association, *The illness costs of air pollution: 2005–2026 health and economic damage estimates,* June 2009. [Online]. Available: http://www.oma.org/health/smog/report/icap2005_report.pdf

[107] M. Jacobson, "Enhancement of Local Air Pollution by Urban CO_2 Domes," *Environmental Science & Technology*, vol. 44, no. 7, pp. 2497–2502, 2010.

[108] J. L. R. Proops, P. W. Gay, S. Speck, and T. Schröder, "The lifetime pollution implications of various types of electricity generation: An input-output analysis," *Energy Policy*, vol. 24, no. 3, pp. 229–237, 1996.

[109] S. Andseta, M. J. Thompson, J. P. Jarrel, and D. R. Pendergast, "Candu reactors and greenhouse gas emissions," in *Proc. 19th Annual*

Conference, Canadian Nuclear Society, Toronto, ON, Canada, October 1998.

[110] C. Yang and J. Ogden, "Determining the lowest-cost hydrogen delivery mode," *International Journal of Hydrogen Energy*, vol. 32, no. 2, pp. 268–286, 2007.

[111] A. J. Wood and B. F. Wollenberg, *Power Generation, Operation, and Control*, 2nd ed. New York: Wiley, 1996.

[112] K. Y. Lee and M. A. El-Sharkawi, *Modern Heuristic Optimization Techniques: Theory and Applications to Power Systems.* New York: Wiley-IEEE Press, 2008, pp. 285–335.

[113] A. Gomez-Exposito, A. J. Conejo, and C. A. Cañizares, Eds., *Electric Energy Systems: Analysis and Operation.* CRC Press, 2008.

[114] A. L. Motto, F. D. Galiana, A. J. Conejo, and J. M. Arroyo, "Network-constrained multiperiod auction for a pool-based electricity market," *IEEE Trans. on Power Systems*, vol. 17, no. 3, pp. 646–653, 2002.

[115] U. Diwekar, *Introduction to Applied Optimization.* Norwell, MA: Kluwer, 2003.

[116] J. Ivy, "Summary of electrolytic hydrogen production, milestone completion report," National Renewable Energy Laboratory, Tech. Rep., Sept. 2004.

[117] R. Fourer, D. M. Gay, and B. W. Kernighan, *AMPL: A Modeling Language for Mathematical Programming*, 2nd ed. Pacific Grove, CA: Duxbury Press, 2002.

[118] *ILOG CPLEX Version 11.2 User's Guide*, ILOG, 2008.

[119] Independent Electricity System Operator (IESO), *Ontario Transmission System,* June 2006. [Online]. Available: http://www.theimo.com/imoweb/pubs/marketReports/OntTxSystem_2006jun.pdf

[120] P. Kundur, *Power System Stability and Control.* McGraw Hill, 1994.

[121] Ontario Power Authority (OPA), *Ontario's Integrated Power System Plan; Scope and Overview,* June 2006. [Online]. Available: http://www.powerauthority.on.ca/Storage/24/1922_OPA_-_IPSP_Scope_and_Overview.pdf

[122] Ontario Power Authority (OPA), *ElectrON: Planning ONtario's Electricity System,* June 2006. [Online]. Available: http://www.powerauthority.on.ca/electron/

[123] Ministry of Energy and Infrastructure, Ontario, Canada. [Online]. Available: http://www.mei.gov.on.ca/en/energy/electricity/?page=nuclear-ontario-plants

[124] Independent Electricity System Operator (IESO), *Monthly Generator Disclosure Report.* [Online]. Available: http://www.ieso.ca/imoweb/marketdata/genDisclosure.asp

[125] Ontario Power Authority (OPA), *Nuclear Resources for Base-Load,* Toronto, ON, Canada, 2007. Submission to the Ontario Energy Board (EB-2007-0707, Exhibit D, Tab 6, Schedule 1). [Online]. Available: http://www.powerauthority.on.ca/Storage/53/4873_D-6-1_corrected_071019.pdf

[126] Ontario Power Authority (OPA), *Determining resource requirements,* Toronto, ON, Canada, 2007. Submission to the Ontario Energy Board (EB-2007-0707, Exhibit D, Tab 3, Schedule 1). [Online]. Available: http://www.powerauthority.on.ca/Storage/53/4867_D-3-1_corrected_071019.pdf

[127] Ontario Power Authority (OPA), *Supply-Renewable resources,* Toronto, ON, Canada, 2007. Submission to the Ontario Energy Board (EB-2007-0707, Exhibit D, Tab 5, Schedule 1). [Online]. Available: http://www.powerauthority.on.ca/Storage/69/6444_D-5-1_corrected_080505__mm_.pdf

[128] Ontario Power Authority (OPA), *Calculation of capacity contribution of wind and hydro,* Toronto, ON, Canada, 2007. Submission to the Ontario Energy Board (EB-2007-0707, Exhibit D, Tab 5, Schedule 1, Attachment 4). [Online]. Available: http://www.powerauthority.on.ca/Storage/53/4871_D-5-1_Att_4_corrected_071019.pdf

[129] Ontario Power Authority (OPA), *Ontario's Integrated Power System Plan, Discussion Paper 7: Integrating the Elements-A Preliminary Plan,* Toronto,ON, Canada, 2007. Submission to the Ontario Energy Board (EB-2007-0707, Exhibit C-11-1).

[130] Helimax Energy, Inc., *Analysis of future wind farm development in Ontario,* A report to the Ontario Power Authority, March 2006.

[131] AWS Truewind *Wind generation data,* A report to the Ontario Power Authority, April 2007. [Online]. Available: http://www.powerauthority.on.ca/Storage/50/4537_D-5-1_Att_3.pdf

[132] Ontario Power Authority (OPA), *Feed-in Tariff Program,* ver. 1.1, September 2009. [Online]. Available: http://fit.powerauthority.on.ca/Storage/97/10759_FIT-Program-Overview_v1.1.pdf

[133] Ministry of Energy and Infrastructure, *Green Energy and Green Economy Act,* Ontario, Canada, 2009. [Online]. Available: http://www.ontla.on.ca/web/bills/bills_detail.do?locale=en&BillID=2145

[134] Ontario Power Authority (OPA), *Generation procurement.* [Online]. Available: http://www.powerauthority.on.ca/gp/Page.asp

[135] A. Shalaby, *Renewable energy projects; overview of integrated power system plan,* April 2007. [Online]. Available: http://www.powerauthority.on.ca/Storage/41/3706_Renewable_Energy_Forum_PSP_2007-04-17_final.pdf

[136] R. A. Geyer, *A Global Warming Forum: Scientific, Economic, and Legal Overview.* Boca Raton, FL: CRC press, 1993.

[137] R. E. H. Sims, H. H. Rogner, and K. Gregory, "Carbon emission and mitigation cost comparisons between fossil fuel, nuclear and renewable energy resources for electricity generation," *Energy Policy*, vol. 31, no. 13, pp. 1315–1326, 2003.

[138] R. E. Uhrig, "Greenhouse gas emissions: Gasoline, hybrid-electric, and hydrogen-fuelled vehicles," in *Encyclopedia of Energy Engineering and Technology*, B. L. Capehart, Ed. Boca Raton, FL: CRC press, 2007.

[139] Ontario Power Generation (OPG), *Sustainable Development Report 2007,* Toronto, ON, Canada. [Online]. Available: http://www.opg.com/pdf/Sustainable%20Development%20Reports/Sustainable%20Development%20Report%202007.pdf

[140] Ontario Power Authority (OPA), *Supply Mix Analysis Report,* vol. 2*,* December 2005. [Online]. Available: http://www.powerauthority.on.ca/Page.asp?PageID=122&ContentID=1141&SiteNodeID=127

[141] Ontario Power Authority (OPA), *Pollution Probe Interrogatory 94,* Toronto, ON, Canada, June 2008. Submission to the Ontario Energy Board (EB-2007-0707, Exhibit I, Tab 31, Schedule 94), p. 213. [Online]. Available: http://www.powerauthority.on.ca/Storage/116/16360_7307_Tab_31_OPA_IRR_I-31_Pollution_Probe_20080702original.pdf

[142] Independent Electricity System Operator (IESO), *10 year outlook: Ontario demand forecast,* July 2005. [Online]. Available: http://www.ontla.on.ca/library/repository/ser/259652/200601-201512.pdf

[143] Independent Electricity System Operator (IESO), *Market data*. [Online]. Available: http://www.ieso.ca/imoweb/marketdata/marketData.asp

[144] Independent Electricity System Operator (IESO), *Ontario Transmission System,* November 2009. [Online]. Available: http://ieso.com/imoweb/pubs/marketReports/OntTxSystem_2009nov.pdf

[145] Natural Resources Canada, *Canadian Vehicle Survey, Summary Report,* May 2007. [Online]. Available: http://www.oee.nrcan.gc.ca/Publications/statistics/cvs05/pdf/cvs05.pdf

[146] Statistics Canada. [Online]. Available: http://www.statcan.ca/Daily/English/080327/d080327d.htm

[147] Ministry of Finance, Ontario, Canada, *Ontario Population Projections Update,* Spring 2008. [Online]. Available: http://www.fin.gov.on.ca/en/economy/demographics/projections/demog08.pdf

[148] A. Latella, "Shortcircuiting system for use in monopolar and bipolar electrolyzers," US Patent 5 431 796, 1995.

[149] H. Wendt and G. Imarisio, "Nine years of research and development on advanced water electrolysis. A review of the research programme of the Commission of the European Communities," *Journal of Applied Electrochemistry*, vol. 18, no. 1, pp. 1–14, 1988.

[150] N. Ouellette, H. H. Rogner, and D. S. Scott, "Hydrogen from remote excess hydroelectricity. part i: Production plant capacity and production costs," *International Journal of Hydrogen Energy*, vol. 20, no. 11, pp. 865–871, 1995.

[151] A. G. Dutton, H. Dienhart, W. Hug, and A. J. Ruddell, "The economics of autonomous wind-powered hydrogen production systems,," in *Proc. European wind energy Conference (EWEC'97)*, Dublin, 1997.

[152] W. Amos, "Cost of storing and transporting hydrogen," National Renewable Energy Laboratory, Golden, CO, Tech. Rep. NREL/TP-570-25106, November 1998.

[153] A. G. Dutton, J. A. M. Bleijs, H. Dienhart, M. Falchetta, W. Hug, D. Prischich, and A. J. Ruddell, "Experience in the design, sizing, economics, and implementation of autonomous wind-powered hydrogen production systems," *International Journal of Hydrogen Energy*, vol. 25, no. 8, pp. 705–722, 2000.

[154] C. E. Thomas, J. P. Reardon, F. D. Lomax, J. Pinyan, and I. F. Kuhn, "Distributed hydrogen fueling systems analysis," in *Proc. of the 2001 DOE hydrogen program review*, 2001, p. 83. [Online]. Available: http://www.ecosoul.org/files/knowledge/downloads/30535bk.pdf

[155] D. Simbeck and E. Chang, "Hydrogen supply: cost estimate for hydrogen pathways-scoping analysis," National Renewable Energy Laboratory, Golden, CO, Tech. Rep. NREL/SR-540-32525, January 2002.

[156] D. Mignard, M. Sahibzada, J. M. Duthie, and H. W. Whittington, "Methanol synthesis from flue-gas CO_2 and renewable electricity: a feasibility study," *International Journal of Hydrogen Energy*, vol. 28, no. 4, pp. 455–464, 2003.

[157] T. E. Lipman and J. X. Weinert. (2006) An assessment of the near-term costs of hydrogen refueling stations and station components. UC Davis: Institute of Transportation Studies. [Online]. Available: http://repositories.cdlib.org/itsdavis/UCD-ITS-RR-06-03

[158] M. Sjardin, K. J. Damen, and A. P. C. Faaij, "Techno-economic prospects of small scale membrane reactors in a future hydrogen fuelled transportation sector," *Energy*, vol. 31, no. 14, pp. 2523–2555, 2006.

[159] N. Parker. (2007) Optimizing the design of biomass hydrogen supply chains using real-world spatial distributions: A case study using California rice straw. UC Davis: Institute of Transportation Studies. [Online]. Available: http://repositories.cdlib.org/itsdavis/UCD-ITS-RR-07-13

[160] G. Saur, "Wind-to-hydrogen project: electrolyzer capital cost study," National Renewable Energy Laboratory, Golden, CO, Tech. Rep. NREL/TP-550-44103, December 2008.

[161] U. Bossel, B. Eliasson, and G. Taylor, "The future of the hydrogen economy: bright or bleak?" *Cogeneration and Distributed Generation*

Journal, vol. 18, no. 3, pp. 29–70, 2003. [Online]. Available: http://www.efcf.com/reports/E08.pdf

[162] Logistic solution builders Inc., *Operating costs of trucks in Canada,* 2005. [Online]. Available: http://www.tc.gc.ca/policy/report/acg/operatingcost2005/2005-e.htm

[163] C. Rosenkranz, "Deep cycle batteries for plug-in hybrid application," in *Proc. Plug-in Hybrid Vehicle Workshop, 20th International Electric Vehicle Symposium*, Long Beach, CA, 2003.

[164] M. Duvall, "Advanced batteries for electric-drive vehicles," Electric Power Research Institute (EPRI), Palo Alto, CA, Tech. Rep., May 2004.

[165] W. Short and P. Denholm, "A preliminary assessment of plug-in hybrid electric vehicles on wind energy markets," National Renewable Energy Laboratory, Golden, CO, Tech. Rep. NREL/TP-620-39729, April 2006.

[166] M. Duvall, "Electricity as an alternative fuel: Rethinking off-peak charging," in *Proc. Plug-in HEV Workshop*, 2003.

[167] K. Verfondern, *Nuclear Energy for Hydrogen Production.* Forschungszentrum Jülich, 2007. [Online]. Available: http://juwel.fz-juelich.de:8080/dspace/bitstream/2128/2518/1/Energietechnik_58.pdf

[168] A. Hajimiragha, C. Cañizares, M. W. Fowler, and A. Elkamel, "Optimal Transition to Plug-in Hybrid Electric Vehicles in Ontario-Canada Considering the Electricity Grid Limitations," *IEEE Trans Ind Electron*, vol. 57, no. 2, pp. 690–701, 2010.

[169] B. Bank, J. Guddat, D. Klatte, B. Kummer, and K. Tammer, *Non-linear parametric optimization.* Birkhäuser Berlin, 1983.

[170] M. Broadie, "Computing efficient frontiers using estimated parameters," *Annals of Operations Research*, vol. 45, no. 1, pp. 21–58, 1993.

[171] S. Moazeni, T. F. Coleman, and L. Yuying, "Optimal portfolio execution strategies and sensitivity to price impact parameters," *SIAM J. Optimization*, vol. 20, no. 3, pp. 1620–1654, 2010.

[172] R. M. Freund, "Postoptimal analysis of a linear program under simultaneous changes in matrix coefficients," *Mathematical Programming Study*, vol. 24, pp. 1–13, 1985.

[173] A. J. Conejo, E. Castillo, R. Minguez, and R. Garcia-Bertrand, *Decomposition techniques in Mathematical Programming*. Springer-Verlag, 2006, ch. 8 Local sensitivity analysis, pp. 304–346.

[174] *MATLAB version 7.9*, MathWorks Inc. [Online]. Available: http://www.mathworks.com/

[175] A. Hajimiragha, M. W. Fowler, and C. A. Cañizares, "Hydrogen economy transition in Ontario–Canada considering the electricity grid constraints," *International Journal of Hydrogen Energy*, vol. 34, no. 13, pp. 5275–5293, 2009.